ASSESSMENT OF SIDESTREAM AND MAINSTREAM ANAMMOX-BASED SYSTEMS USING EXPERIMENTAL AND MATHEMATICAL MODELLING TOOLS

PARIN IZADI

A DISSERTATION SUBMITTED TO
THE FACULTY OF GRADUATE STUDIES
IN PARTIAL FULFILLMENT OF THE REQUIREMENTS
FOR THE DEGREE OF DOCTOR OF PHILOSOPHY

GRADUATE PROGRAM IN CIVIL ENGINEERING

YORK UNIVERSITY
TORONTO, ONTARIO

JULY 2021

Abstract

Anaerobic Ammonium Oxidation (ANAMMOX) process is an innovative alternative which is carried out by an entirely autotrophic method for shortcut N-removal in nitrogen cycle, in addition this technological advancement results in less aeration demand, decline in organic matter addition as well as nitrite reduction. Compared to conventional biological nitrogen removal processes, an ANAMMOX-based process can potentially save energy since it reduces oxygen requirement by around 60%, organic carbon utilization by 100%, and sludge production by approximately 90%. Due to low growth rates and cellular yields of autotrophic ammonia removal bacterial communities and their sensitivity to adverse environmental conditions, ANAMMOX reactor startup from conventional returned activated sludge has become a major challenge. This comprehensive study aimed to understand the engineering aspects and practical applications of ANAMMOX-based autotrophic nitrogen removal processes and overcome the current challenges. Fast start-up using micro-granular development of ANAMMOX reactor was investigated to evaluate ANAMMOX activity, population dynamics and core community members as well as the potential start-up options for mainstream municipal ANAMMOX process, in an upflow anaerobic sludge blanket (UASB) reactor seeded with municipal returned activated sludge (RAS). The micro-granular UASB reactor has been operated under steady-state conditions with average nitrogen loading rate ranging from 1.2 to 0.18 KgN /m^3/day and the average SRT of the reactor ranged from 36 to 72 days. Subsequently, a set of manometric batch experiments to evaluate ANAMMOX performance efficiency in different conditions with a distinct emphasis on high-temperature mainstream conditions. To better assess the response and overall performance of the ANAMMOX system in a long-term operation period and to evaluate the possibility of using mathematical modelling for process prediction, intended for potential future scale-ups, a BioWin model was adapted. The

results of this study, provide an alternative and efficient configuration for ANAMMOX cultivation and demonstrate the effectiveness and high performance efficiency of micro-sized granules in both sidestream and mainstream ANAMMOX processes. The section of the research focusing on mainstream processes highlights the factors monitoring and promoting the growth of ANAMMOX bacteria in mainstream wastewater treatment which can potentially guide the future implementation of ANAMMOX-based technologies. This study also confirms the reliability of ANAMMOX-based process modeling and high predictive ability with BioWin, being a valuable in enhancing the efficiency of UASB-ANAMMOX practical operation in an industrial scale.

Dedication

To my amazing parents; My extraordinary Mom and Dad.

To Parnian; My best friend since day one.

To Ardavan: My best companion.

Acknowledgement

First and foremost, I wish to thank my supervisor, Professor **Ahmed Eldyasti**. He has been supportive since the days I began working on my project. He helped me come up with the thesis topic and guided me over the four years of research development. And during the most difficult times when developing the project and writing this thesis, he gave me the moral support and the freedom I needed to move on.

I would like to thank **Dr. Magdalena Krol** and **Dr. Usman Khan** for the time they dedicated to this research and for their constant support through my PhD program.

I would like to thank my friends, lab mates, colleagues and IWATER research team – **Ahmed Alsayed, Moomen Soliman, Ahmed Fergala, Rana Salem, Danelle Bishoff**, for a cherished time spent together in the lab, and in social settings.

I would also like to thank my incredible sister/colleague/best friend, **Parnian**, whom without this would have not been possible. You have been my best friend all my life and I love you dearly. Thank you for all your advice and support!

I would like to express my gratitude to my **Parents**. Without their tremendous understanding and encouragement in the past few years, it would be impossible for me to complete my study.

I also thank my **F.r.i.e.n.d.s** and **Family** (too many to list here but you know who you are!) for providing support and friendship that I needed.

The last one is for you **Ardavan**! You have been a true and great supporter and have unconditionally loved me during my good and bad times. I truly thank you for sticking by my side and being a constant source of support and encouragement during the challenges of graduate school and life. I am truly thankful for having you in my life.

TABLE OF CONTENTS

LIST OF TABLES

LIST OF FIGURES

CHAPTER 1

Background and research objectives

1.1. Background

1.1.1. Introduction

Wastewater treatment plants are studied as a well-defined industry with highly regulated end products. Wastewater features are reasonably predictable and the plant design supports a practical function in specific flows and loads. There is an increasing demand for a more comprehensive understanding of different wastewater characteristics to enhance the treatment systems operation (Water Environment Federation, 2005). Nitrogenous compounds are one of the most important groups of elements present in wastewater streams. Nitrogen-based compounds detected in wastewater streams are sourced back to fertilizer and food production lines since they are vastly utilized in the synthesis of proteins, nucleic acids, and different cell components (Winkler and Straka, 2019). Moreover, different forms of nitrogen present in wastewater vary from ammonia, nitrite, and nitrate to organic molecules such as amino acids (Wiesmann, 1994). Nitrogen detected in wastewater streams is mainly present as ammonia (total ammonia, or NH_4^+ and NH_3) (Winkler and Straka, 2019). The total nitrogen content of raw municipal wastewater is approximately 30 to 100 mgN/L which is 65-75% ammonium and 25-35% organic nitrogen (Water Environment Federation, 2005). There are a series of severe problems caused by the introduction of substantial fluxes of reactive nitrogen to receiving waters including, decrease in dissolved oxygen concentration, toxicity to aqua-life, algae growth stimulation and eutrophication, severe health concerns as well as carcinogenic and mutagenic effects linked to consumption of untreated drinking water (EPA US, 2011). As a result of the detrimental health and environmental effects of untreated wastewater release to water bodies, the legislation has adapted more stringent effluent standards for discharged nitrogen concentrations, demanding an increase in wastewater treatment processes (Komorowska-Kaufman et al., 2006).

The microbial nitrogen cycle and the metabolism of inorganic nitrogen compounds are the principal basis of a wide variety of biological processes and technologies responsible for developing and implementing of nitrogen removal from wastewater streams (Zhu et al., 2008). One principal strategy for removing nitrogen from wastewater and its conversion to dinitrogen gas is based on conventional biological nitrogen removal (BNR), carried out by the nitrification-denitrification process (Metcalf et al., 2003). Nitrification is a two-step biological process carried out by autotrophic bacteria in which ammonia is converted to nitrite and nitrate through oxidation (Liu and Wang, 2012). As illustrated in Equation 1-1 and Equation 1-2, the two sequential steps of oxidation involved in the nitrification process are: (i) conversion of ammonia to nitrite (nitritation) by ammonia-oxidizing organisms (AOB) and (ii) oxidation of nitrite to nitrate (nitratation) by nitrite-oxidizing organisms (NOB) (Henze et al., 2008).

$$55\ NH_4^+ + 76O_2 + 109\ HCO_3^- \rightarrow C_5H_7NO_2 + 54\ NO_2^- + 57\ H_2O + 104\ H_2CO_3$$

Equation 1-1

$$1.0\ NO_2^- + 0.473\ O_2 + 0.005\ NH_4^+ + 0.02\ CO_2 + 0.005\ HCO_3 + 0.005\ H_2O \rightarrow 1.0\ NO_3^- + 0.005\ C_5H_7O_2N$$

Equation 1-2

$$NH_4^+ + 1.83\ O_2 + 1.98\ HCO_3^- \rightarrow 0.021\ C_5H_7NO_2 + 1.041\ H_2O + 0.98\ NO_3^- + 1.88\ H_2CO_3$$

Equation 1-3

According to growth yields of 0.08 $gVSS/gNH_4^+$-N and 0.05 $gVSS/gNO_2^-$-N for ammonium oxidizer and nitrite oxidizer organisms respectively, the overall reaction for complete nitrification can be written as Equation 1-3 (Lin et al., 2009). Biological reduction of nitrate/nitrite to dinitrogen gas with the absence of oxygen and the presence of organic carbon as an electron donor is the fundamental definition of denitrification process (Metcalf et al., 2003).

Although the conventional nitrification-denitrification scheme is effective, there is a considerable performance limitation associated with the denitrification step because of organic matter requirements and significant aeration costs related to the nitrification process (Kallistova et al., 2016). BNR increases the energy use for aeration, pumping ,and solids handling by 30 to 50%, contributes to greenhouse gas emissions by N_2O production ,and affects the operational costs due to organic carbon addition (Metcalf et al., 2003) (Winkler and Straka, 2019). These issues put forward the need to increase the economic appeal of conventional nitrogen removal processes by reducing organic matter and oxygen supplementation to the system (Kallistova et al., 2016). Anaerobic Ammonium Oxidation (ANAMMOX) process is an innovative alternative which is carried out by an entirely autotrophic method for shortcut N-removal in the nitrogen cycle, in addition, this technological advancement results in less aeration demand, a decline in organic matter addition as well as nitrite reduction (Kallistova et al., 2016) (Henze et al., 2008).

Compared to conventional BNR, an ANAMMOX-based process can save energy by reducing oxygen requirement by around 60%, organic carbon utilization by 100%, and sludge production by approximately 90% (X. Li et al., 2018). There was a radical modification in wastewater treatment technologies when ANAMMOX was discovered. In this process, ammonium is directly oxidized to nitrogen gas using nitrite as the electron acceptor under anaerobic environments with carbon dioxide as the carbon source (Henze et al., 2008). This process discovery led the biotechnological advances in wastewater to a new path, which changed the views towards the nitrogen cycle. This innovative concept resulted in substantial modification of the ecosystem and flow ratios concepts, forming a thought-provoking subject for further study and experimentation.

1.1.2. Problem statement

From the time ANAMMOX was discovered, an extensive amount of research has focused on developing ANAMMOX-based technologies. Although there are operational sidestream ANAMMOX-based systems worldwide, there are still a number of challenges in practical applications of ANAMMOX-based processes, including extended start-up times, the accumulation of inhibition factors in nitrogen-rich wastewater streams, poor effluent qualities ,and issues with mainstream process operation (Ali and Okabe, 2015). The main barrier in ANAMMOX application is the low bacterial growth rates (doubling time between 7 to 14 days), affecting the start-up of the process at full-scale (Oshiki et al., 2011). Due to low growth rates and cellular yields of autotrophic ammonia removal bacterial communities and their sensitivity to adverse environmental conditions, ANAMMOX reactor startup from conventional returned activated sludge has become a significant challenge (Van Hulle et al., 2010). Additionally, the ANAMMOX process has been mainly operated for ammonium-rich wastewater (500 mgN/L, 25-30 °C) treatment including sludge digester effluent, and there is still a lack of comprehension on mainstream domestic wastewater treatment, potentially because of elevated carbon to nitrogen ratio, reduced temperature levels and poor effluent water quality (Ali and Okabe, 2015). Further studies and technology development are vital to resolve problems including long start-up periods, ineffective retention and accumulation of ANAMMOX bacterial biomass, significant washing outs, substrate inhibitions, mainstream process start-up ,and performance.

1.1.3. Objectives

To understand the engineering aspects and practical applications of the ANAMMOX-based autotrophic nitrogen removal process and overcome the current challenges, the specific objectives of this research were :

- Investigate the ANAMMOX process from a fundamental standpoint and build a principal perception of ANAMMOX microbiology and metabolism fundamentals
- Improve the operational factors for syntrophic micro-granular ANAMMOX consortium cultivation in a laboratory-scale UASB reactor from solely activated sludge without any bioaugmentation from a previously enriched ANAMMOX biomass to overcome the issues related to seed availability as well as sludge retention and growth in newly started ANAMMOX reactors
- Investigate the dynamic response of micro-granular ANAMMOX consortium in presence of either inhibition or stimulation factors and identifying the intermediate-based recovery opportunities in high loading rates at sidestream level
- Evaluate the possibility of using Biowin for process prediction, intended for potential future scale-ups, Asses the results with the aid of statistical analysis methods
- Explore the potential start-up options for mainstream municipal ANAMMOX process

1.1.4. Thesis layout

This dissertation consists of NINE chapters.

Chapter 1: Background and Research Objectives

Chapter 2: Introduction and Literature Review

Chapter 3: Review: Holistic Insights into Extracellular Polymeric Substance (EPS) in ANAMMOX Bacterial Matrix and the Potential Sustainable Biopolymer Recovery

Chapter 4: Review: Towards mainstream deammonification: Comprehensive review on potential mainstream applications and developed sidestream technologiesChapter 5: Influence of microbial population dynamics on accelerated development of

ANAMMOX micro-granular consortium

Chapter 6: Development of Long-Term Dynamic BioWin Model Simulation for ANAMMOX UASB Micro-Granular Process

Chapter 7: Evaluation of Nitrogen Loading Rate Impact on ANAMMOX Activity and Potential Contribution of Intermediates in Inhibition-Recovery Dynamics

Chapter 8: Perspectives of Developing and Sustaining Mainstream ANAMMOX in UASB Systems

Chapter 9: Conclusion

1.1.5. Thesis contribution

ANAMMOX-based systems are innovative technologies within the wastewater treatment industry that can result in optimum removal of nitrogen. ANAMMOX-based processes demand fewer resources, including oxygen, energy, external carbon sources ,and equipment. Moreover, if ANAMMOX balance and ecology are maintained, it can be a profitable replacement for conventional nitrification-denitrification processes. The main challenges observed in full-scale sidestream applications of the ANAMMOX process is potentially because of bacteria's prolonged growth rate and insufficiency in developed sludge. Thus, in this research studies the enrichment process of ANAMMOX biomass from conventional returned activated sludge with no bio-augmentation. The first goal of this research was to improve the operational factors for syntrophic micro-granular ANAMMOX consortium cultivation in a laboratory-scale UASB reactor from

solely activated sludge without any bioaugmentation from a previously enriched ANAMMOX biomass, to overcome the issues related to seed availability as well as sludge retention and growth in newly started ANAMMOX reactors. The results of the first stage of the study provide an alternative and efficient configuration for ANAMMOX cultivation and demonstrate the effectiveness and high-performance efficiency of micro-sized granules in the ANAMMOX process.

After successful sidestream ANAMMOX process development, a comprehensive evaluation of the dynamic response of micro-granular ANAMMOX consortium when either inhibition or stimulation factors including the primary process substrates and intermediates are introduced was completed. The main goal of this research was to uncover a potential solution for the existing key challenges associated with mainstream ANAMMOX process implementation. In this stage, we initially reported on the dynamic response of a micro-granular ANAMMOX biomass to the introduction of high ammonium and nitrite concentrations and supplementation of hydroxylamine to understand the process functional factors. This stage of the research focuses on identifying the intermediate-based recovery opportunities in harsh loading rates at sidestream levels and links the potential stimulatory effects of hydroxylamine to mainstream applications. The urging idea that placing the impact of hydroxylamine on microbial activity and granular structure in warm-mainstream conditions can elevate the process applicability, presented a reliable foundation for studying intermediates as ANAMMOX-accelerating factors.

Regardless of the tremendous technical and financial appeal of ANAMMOX, the process of commercialization of this novel technology has been introduced only in recent years. There are significant restrictions introduced due to the low growth rate of ANAMMOX bacteria and the high sensitivity of the microorganisms to a broad scope of external elements, obstructing the cultivation

process and the analysis of physiological characteristics. To review the capability of the ANAMMOX process and assess its chances for biotechnology implementation, conducting physical and mathematical modeling is vital. An imperative step to facilitate the scale-up of such complicated and poorly comprehended systems is developing a process model at dynamic conditions and completing process calibration and validation. Hence, the purpose of this stage of the research is to establish a BioWin model to illustrate the long-term dynamic behavior of a lab-scale UASB performing single-stage micro-granular-based ANAMMOX process. This study confirms the reliability of ANAMMOX-based process modeling and high predictive ability with BioWin, and the presented simulation constants and modeling outline can be engaged in full-scale applications design and development. Results of this study will be valuable in enhancing the efficiency of UASB-ANAMMOX's practical operation on an industrial scale.

Countless efforts have targeted mainstream ANAMMOX-based technologies in recent decades to deduce the prospective energy costs and move towards energy positive plants . Despite all attempts and activities, there are still a number of challenges linked to mainstream ANAMMOX application including, low nitrogen removal rates, reduced nitrogen concentrations and inconsistent loads, lowered temperatures, presence of chemical oxygen demand (COD), competition with other bacterial communities, strict effluent qualities and long-term process stability. The main purpose of this study was to explore the potential start-up options for the mainstream municipal ANAMMOX process. The UASB configuration can potentially overcome the issues related to seed availability and sludge retention and growth. This section of the research highlights the factors monitoring and promoting the growth of ANAMMOX bacteria in mainstream wastewater treatment, which can potentially guide the future implementation of ANAMMOX-based technologies.

CHAPTER 2

Introduction and literature review

Abstract

ANAMMOX, an innovative and sustainable alternative to the conventional nitrification-denitrification process, has the advantage of higher nitrogen removal rates with lower operational costs and smaller space requirements. Recent studies indicate that ANAMMOX bacteria endure in different artificial and natural environments with oxygen-depleted zones and available NO_x, such as marine ecologies, terrestrial ecosystems, freshwater environments, and wastewater treatment systems. ANAMMOX bacteria are coccoid-shaped with a mean diameter fluctuating from 800 to 1100 nm. This bacterial population are strict anaerobic chemolithoautotrophs, consequently, they are physiologically different from other identified *Planctomycetes*. ANAMMOX microorganisms consume nitrite as the electron acceptor to generate nitrogen gas as the ultimate reaction product. The impact of ANAMMOX bacteria in the environment and the growing implication in wastewater treatment lead to them being an essential subject of recent and future studies. This chapter addresses the fundamentals of ANAMMOX bacteria from their discovery to metabolism, growth, inhibition, and activity.

Keywords: ANAMMOX; Nitrification-Denitrification; Nitrogen cycle; Wastewater treatment; Metabolism and growth; Inhibition factors

2.1. Introduction

There is an increasing interest in new innovative nitrogen removal processes due to the binding obligations on wastewater treatments to lower the N-loading before discharging it into natural waters (Ward, 2008). The conventional nitrogen removal process, nitrification and denitrification, are ecologically irreconcilable processes mainly because nitrification necessitates aerobic conditions and denitrification is only induced under anoxic states. Because of the two completely different environments, it is common to implicate two separate steps in conventional N-removal

in wastewater treatments wherein the first aerobic phase NH_4 is converted to NO_3, and in the following anoxic step, NO_3 is transformed into N_2. The presence of an organism that would be able to combine the two steps could potentially save enormous amounts of time, energy, and money (Ward, 2008). Anaerobic Ammonia Oxidation or ANAMMOX process converts nitrite and ammonium directly into dinitrogen gas under anaerobic conditions: $NH_4^+ + NO_2^- \rightarrow N_2 + 2H_2O$ (Jeannotte, 2014). ANAMMOX was originally detected in a wastewater treatment plant in the Netherlands in 1995, yet subsequently, it has been discovered in numerous environments, including freshwater and marine sediments and anaerobic water columns (Zheng et al., 2019). Simultaneous analysis of nitrogen balances in a highly stratified fjord, led to an unsolved ammonia loss (Tchobanoglous et al., 2003). Based on the Gibbs free energy calculations, nitrate and nitrite can be the essential bacterial electron acceptor, comparable to oxygen (Kallistova et al., 2016). For the first time, Arnold Mulder from Gist Brocades fermentation company in Delft Netherlands realized a noticeable reduction in ammonium concentration by nitrate consumption and a clear rise in nitrogen gas generation in a denitrification pilot plant system (Mulder, 1989) (Kallistova et al., 2016). After N-labelled ammonium introduction to the biological reactor by Astrid Van Graaf, a mixed labeled nitrogen gas production was observed, which was the first trigger of process discovery and further potentials for implication (Kuenen, 2008a)(van de Graaf et al., 1997). N-removal from wastewater streams by ANAMMOX-based processes has been identified as an adequate, economical, low-energy substitute for the established nitrification-denitrification processes (Ali and Okabe, 2015).

ANAMMOX bacteria are cocci-shaped microorganisms with less than 1 µm diameter. These bacterial groups are strict anaerobes whose residues of oxygen (more than 2µM) can potentially hinder their metabolism (Kallistova et al., 2016). ANAMMOX bacteria's doubling time ranges

between 10 to 30 days resulting in them being described as slow growers, nevertheless as indicated in Figure 2-1, *Ca*. "Brocadia" sp. has the quickest doubling time of around 3.3 days, though this quantity can increase up to 32 days for *Ca*. "Anammoxomic robium moscowii" (Niftrik et al., 2004). The initial estimates of the ANAMMOX bacterial growth rate in the order of 10 days doubling time showed a specific growth rate of 0.0027 h^{-1}. Based on preliminary measurements, the microorganism's yield was 0.066 C-mol/mol of NH_4^+ and a maximum ammonium consumption rate of 45 nmol/mg protein/min was detected (Kuenen, 2020). Monophyletic order of discovered ANAMMOX bacterial groups belongs to *Brocadiales*, a larger group; *Planctomycetes* (Kuenen, 2020). Recent advancements succeeded to describe at least 25 ANAMMOX species from mixed consortia within six different ANAMMOX genera as *Candidatus* (well characterized but not studied in pure culture) with a range of 87-99% for 16s RNA species characteristics (Kallistova et al., 2016) (Ding et al., 2020). They are linked to the orders Brocadiales (genera '*Candidatus* Anammoxoglobus', '*Ca*. Brocadia', '*Ca*. Jettenia', '*Ca*. Kuenenia', '*Ca*. Scalindua', all within the family Brocadiaceae) or Planctomycetales (genus '*Ca*. Anammoximicrobium') (Ding et al., 2020). 80% of the genera were developed from activated sludge, leaving the outstanding 20% for natural habitats, more precisely in marine sediments and zones with low oxygen concentrations (Jetten et al., 2009) (Gao et al., 2018). The four genera developed from activated sludge are *Candidatus* "Kuenenia", *Ca*. "Brocadia", *Ca*. "Anammoxoglobus", and *Ca*. "Jettenia" while the fifth ANAMMOX genus discovered in natural habitations and low-oxygen marine regions was, *Ca*. "Scalindua" (Kallistova et al., 2016). Discovery of a novel genus of ANAMMOX bacteria, *Ca*. "Anammoxomicrobium," was reported in 2013 (Khramenkov et al., 2013). Most *Planctomycetes* are aerobic chemoorganoheterotrophs, containing intracytoplasmic membrane constructing a central cell compartment (Niftrik et al.,

2004). Despite being a member of *Plactomycetes*, ANAMMOX bacteria are physiologically divergent from others, as they are anaerobic chemolithoautotrophs (Jetten et al., 2009) (Cohen-Bazire et al., 1964).

As illustrated in Figure 2-1, the optimal growth temperature for *Ca*. "Brocadia Anammoxidans" ranges between 20-43 °C, while *Ca*. "Scalindus" sp. has the most favorable growth condition in considerably lower temperatures ranging from 10 to 30 °C (Cho et al., 2019). Microbial community shifts from specific ANAMMOX genera or species to another were frequently validated in different studies. ANAMMOX bacteria geographic distributions signify the prospect of developing species-specific habitations (Sonthiphand et al., 2014), in which growth kinetics (Figure 2-1) is one of the basic parameters for comprehension of the role diversity of ANAMMOX bacteria. Park et al., 2010, demonstrated the population shift from "*Ca*. B. fulgida" to "*Ca*. B. sp.40", while a shift from "*Ca*. B. fulgida" to "*Ca*. K.stuttgartiensis" was reported by Park, Sundar, Ma, & Chandran, 2015. Different analytical findings indicate that population alterations in ANAMMOX communities are mainly transformed by numerous selective pressure factors, such as; seeding inoculum, salinity levels and potential tolerance, organic acids presence for nitrate reduction, different affinities to substrates, and DO levels (Ali et al., 2018).

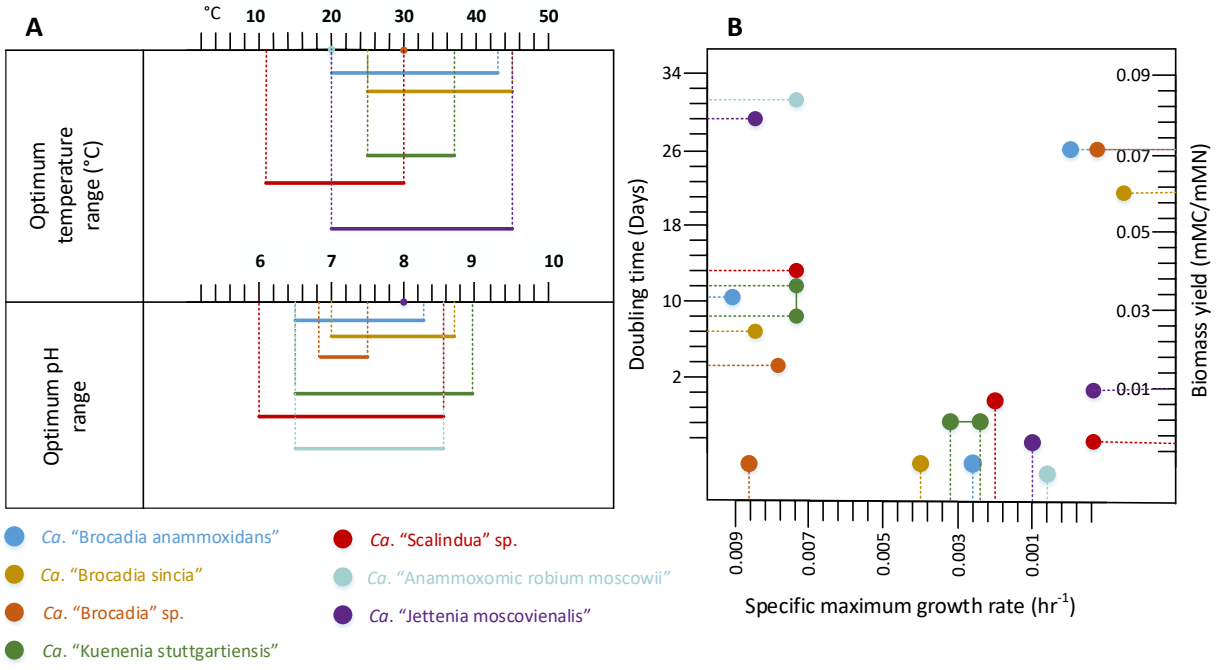

Figure 2-1 Optimal range of pH and temperature B) average range of growth parameters, for seven ANAMMOX genera ((Sonthiphand et al., 2014), (Cho et al., 2019), (Park et al., 2010))

2.2. ANAMMOX intracellular structural composition

ANAMMOXOSOME hypothesized as the inner compartment where ANAMMOX reactions occur and as the leading site for energy production (Niftrik et al., 2004) (Kuenen, 2020), is comparable to mitochondria's function in eukaryotic cells (Van Niftrik, 2013). This presumption was based on immunogold localization of process key enzymes; hydroxylamine oxidoreductase (HAO). The result of a study on HAO-like enzymes demonstrated the presence of HAO in ANAMMOXOSOME (Jetten et al., 2009). The genome encoding of "*Candidatus* Kuenenia stuttgartiensis" resulted in ten HAO-like octaheme proteins, of which 60% were vastly disclosed in proteome and transcriptome (Kallistova et al., 2016). Based on results of a study on the genome, conveying Western blot analysis as well as immunofluorescence and immunogold localization, cytochrome c proteins were detected within 150 nm of the inside of the ANAMMOXOSOME membrane, indicating that cytochromes participation in electron transport chain is inside the

ANAMMOXOSOME membrane (van Teeseling et al., 2013). Additional evidence for ANAMMOXOSOME being the site for energy metabolism is within the folded membrane structure, which intensifies the necessary surface for enzymatic catabolism similar to critae (inner membrane) in mitochondria (Kallistova et al., 2016).

Equivalent to the entire existing microorganisms, glycerolipid bilayers are the main structure of membranes in ANAMMOX bacteria (de Almeida et al., 2016). Lipid structure encompasses fatty acids residues and glycerol moieties accompanying ester bonds in bacteria and eukarya; however the bond transforms to ether binding in archaea. ANAMMOX lipids merge both ether and ester bonds in their structure (Figure 2-2) (van Niftrik and Jetten, 2012). This rare lipid configuration involves hydrocarbon chains containing 3 or 5 linear integrated cyclobutane rings, in which the 3-ladderanes are connected to a cyclohexane ring as illustrated in Figure 2-2 (de Almeida et al., 2016) (Boumann et al., 2009).

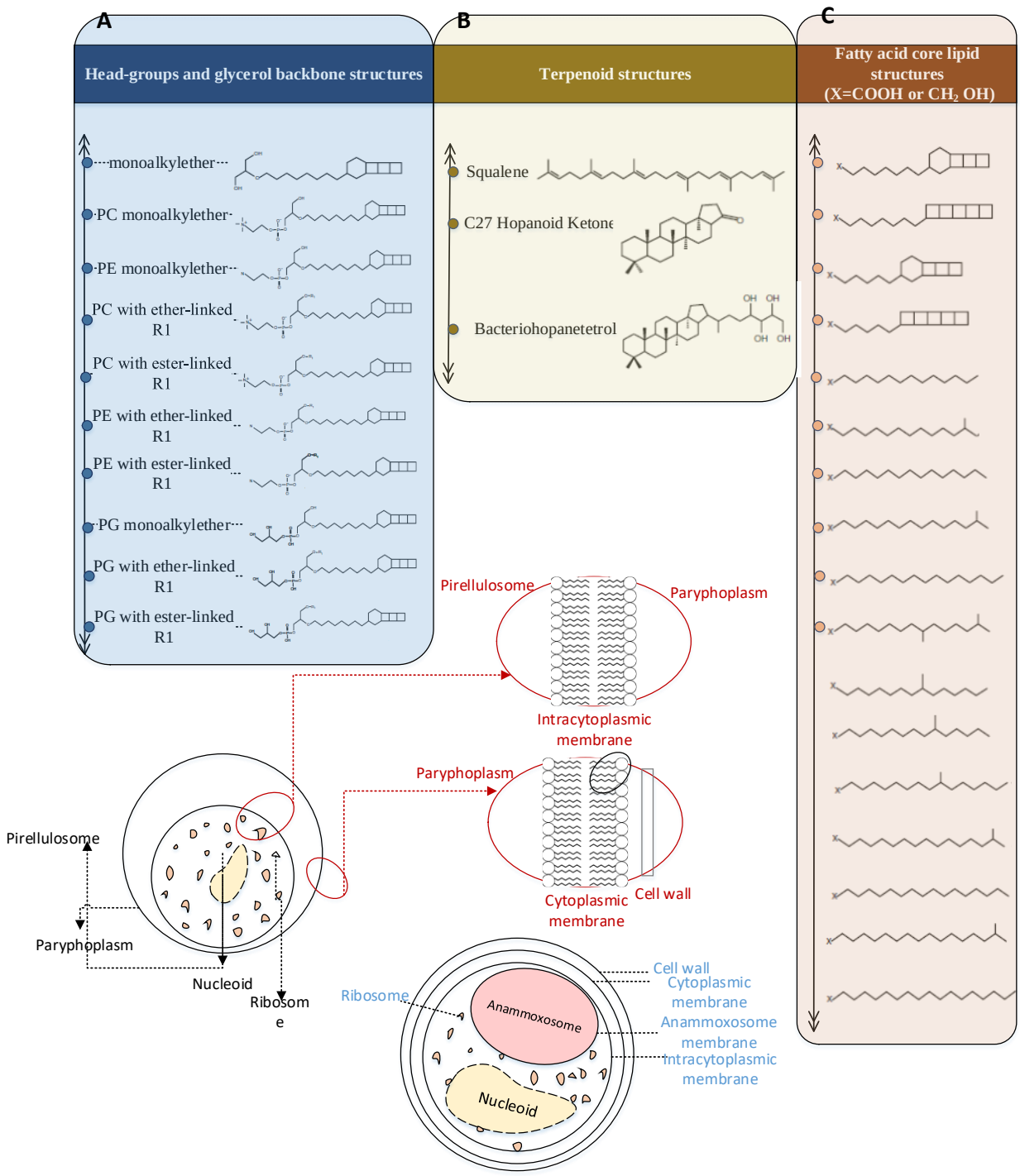

Figure 2-2 Major phospholipids present in ANAMMOX bacteria A) Head-groups and glycerol backbone structures, B) Terpenoid structures and C) Fatty acid core lipid structures (X=COOH or CH_2OH)(PC, Phosphocholine; PE, Phosphoethanolamine; PG, Phosphoglycerol) ((Rattray et al., 2008), (de Almeida et al., 2016), (Boumann et al., 2009))

The general structures of the PC, PE and PG diether and the ether–ester lipids of PC, PE and PG, are indicated in Figure 2-2 A (Rattray et al., 2008). The R1 hydrocarbon chains indicated in Figure 2-2 C are: C18- [3]-ladderane, C18- [5]-ladderane, C20- [3]-ladderane, C20- [5]- ladderane, C22- [3]-ladderane, C22- [5]-ladderane, pentadecane, 14-methylpentadecane, hexadecane, 9,14-dimethylpentadecane, 10-methylhexadecane, 15-methylhexadecane, with X=COOH or CH_3OH. In the stated structures, 3-ladderane has three cyclobutane moieties and one cyclohexane moiety, bound with ether bonding consuming ultimate carbon atom to the glycerol unit (Niftrik et al., 2004). The other structure holds five linear cyclobutane rings containing methyl ester moiety at the ultimate carbon atom (Rattray et al., 2009). The ring structure mentioned above, joined by a cis-ring junction, creates a ladder-shaped arrangement named ladderane (van Niftrik and Jetten, 2012). Afterward it was suggested that the main head group moieties of ladderane lipids are phosphocholine and phosphoethanolamine (de Almeida et al., 2016). In addition, the main ANAMMOX molecular diversity factor is the different lipid species varying in hydrocarbon tails of the glycerol backbone (Boumann et al., 2009). Based on cell fractionation, up to 34% of the overall lipids of certain ANAMMOX species contain ladderane moieties from the stated groups (de Almeida et al., 2016)(Boumann et al., 2009)(Niftrik et al., 2004).

2.3. Metabolism, Growth, and Activity

Through transcriptome and proteome data analysis, there was an indication of nitrite reductase enzyme (cd1 NirS) being responsible for nitrite reduction to nitric oxide (Figure 2-3) (de Almeida et al., 2016). Based on several inhibition and functional studies, NO was shown to have a critical intermediary role in ANAMMOX metabolism (Gao et al., 2018). The present model for ANAMMOX metabolism is established on the genomic, proteomic, transcriptomic, and physiological experimental studies (de Almeida et al., 2016). ANAMMOX is the one-to-one

mixture of ammonium and nitrite, resulting in dinitrogen gas as the key product and nitrate as reducing equivalent for carbon fixation (Kuenen, 2020) (Jetten et al., 2009). Figure 2-3 demonstrates a complete synopsis of processes contributing to the ANAMMOX reactions, ATP synthesis and carbon fixation in *K. stuttgartiensis.* ACS shown in Figure 2-3 is, Acetyl-CoA synthase/CO dehydrogenase, which signifies carbon fixation by the reductive Acetyl-CoA (de Almeida et al., 2016).

Studies on the gene coding illustrate a match for the reductive acetyl-coA (Wood- Ljungdahl) pathway. Other carbon fixation pathways are missing or incomplete based on the reports on key enzyme activities (Kartal et al., 2008). In the wood-Ljungdahl pathway, acetyl coA is generated by reducing two carbon dioxide molecules, binding to coenzyme A (HS-coA). Acetyl-coA is the substrate for all cells beginning with gluconeogenesis/glycolysis path and tricarboxylic acid cycle as transitional routes (Strous et al., 2006). Entire genes of the mentioned pathway are discovered in the genome, not including the gene coding for ATP citrate lyase (Kartal et al., 2008) (Strous et al., 2006).

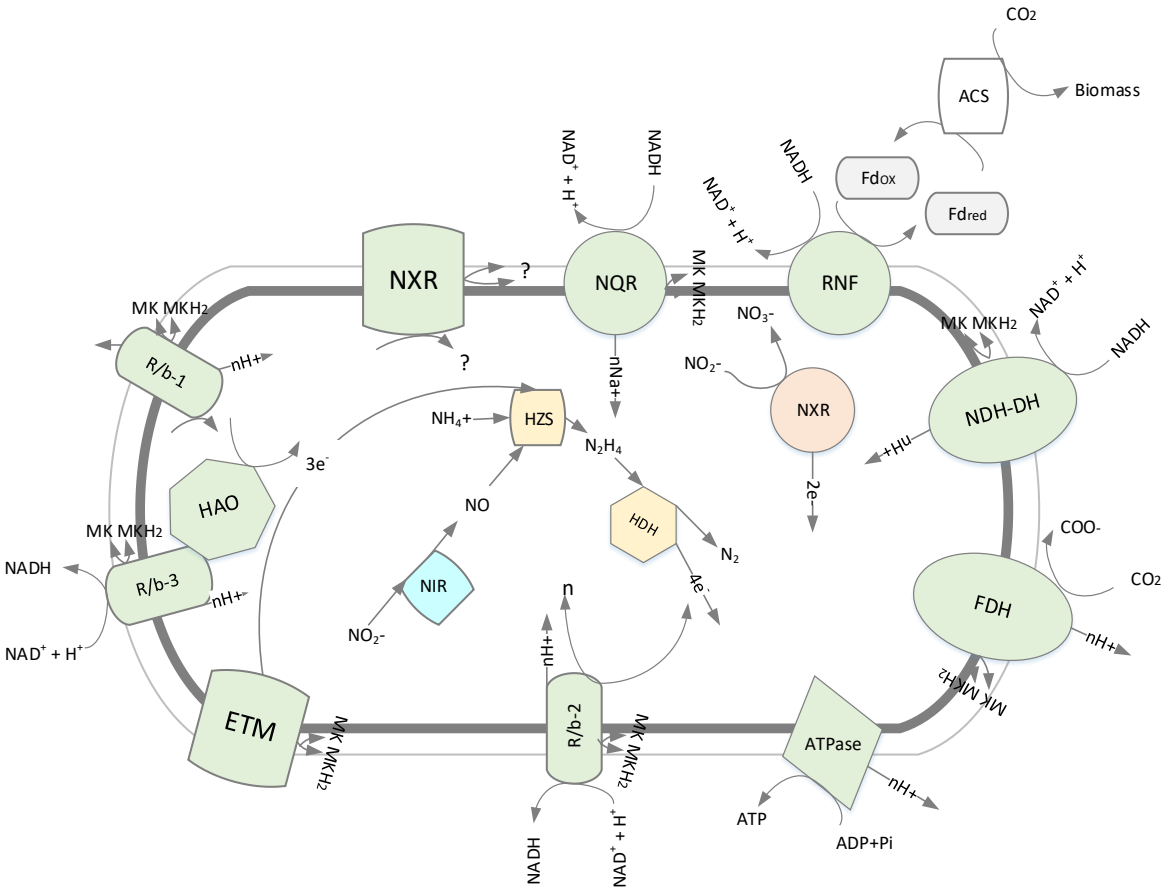

Figure 2-3 Microbial pathway in ANAMMOX bacteria within the ANAMMOXOSOME membrane in the center of the cell; ATPase, ATP synthase; ETM, electron transfer module from the Q-pool to HZS; FDH, putative membrane-bound formate dehydrogenase/CO2 reductase; HDH, hydrazine dehydrogenase; HZS, hydrazine synthase; NADH-DH, NADH dehydrogenase; Nir, nitrite reductase; NXR, nitrite:nitrate oxidoreductase; NXR, membrane-bound complex of the nxr gene cluster. R/b: Rieske/cytochrome b complexes. ((Jetten et al., 2009), (Strous et al., 2006), (Kuenen, 2020))

Studies show a lack of two reaction steps: initially, the reaction in which ammonium is combined with nitric oxide resulting in hydrazine (hydrazine hydrolase) and subsequently the reaction where nitrite is reduced to produce ammonium dimer (Jetten et al., 2009). Full apprehension of the second reaction is essential, since, the ANAMMOX bacteria's potential for production of dinitrogen gas from nitrate in the absence of ammonium through the utilization of organic acids as their only electron source is abundantly included in this step (Strous et al., 2006). ANAMMOX bacteria can

generate nitrogen gas from nitrate, wherein this pathway nitrate is reduced to ammonium by dissimilatory nitrite reductase (NrfA) and pentaheme cytochrome c, forming a dimer (Jetten et al., 2009)(Klotz and Stein, 2008). There is no apparent orthologue for NefA in the genome. Candidate genes for the two mentioned missing steps were identified by focusing on domains instead of genes (Jetten et al., 2009). The genes encompassing the domains generally coded for small proteins are involved in electron transfer not catalysis. The key genetic uniqueness covering both electron transfer and catalysis could be identified in three operons (Jetten et al., 2009). Every single one of these codes are for a candidate complex containing two pentaheme and one decaheme cytochrome c proteins. Even though these genes are not orthologous to a dissimilatory nitrite reductase (NrfA), the existence of five or ten heme-c binding locations creates complexity as the presumable candidate to code for a functional homologue of NrfA in *K. stuttgartiensis* (Strous et al., 2006). The other two complexes are the potential nominees as of hydrazine hydrolase (HH). The primary candidate operon proposes that the biological development of hydrazine from ammonium and nitric oxide is catalyzed using a beta-propellor protein, for instance, nitrous oxide reductase, with the assistance of a quino-cofactor, which is likewise used in methylamine oxidation by methylotrophic bacteria (Jetten et al., 2009). The subsequent candidate operon recognized was suggested for an innovative multicopper oxidase (such as the nitrite reductase, NirK), a Flavin comprising amine oxidase, and numerous fundamental membrane proteins (Jetten et al., 2009).

Based on several N-labelled substrate experiments, accumulation of hydrazine (N_2H_4) was identified as a result of hydroxylamine (NH_2OH) addition to the cells (Kartal et al., 2008) (Gao et al., 2018). Hydrazine's synthesis, with hydrazine being the most powerful reductant in nature, is unique to ANAMMOX bacterial pathway (van de Graaf et al., 1997). Based on the results of this study, it was suggested that both mentioned nitrogenous compounds could be the process

intermediates; this is when the genome sequence indicates an intermediary role for nitric oxide (NO) instead (Strous et al., 2006) (Wouter R L van der Star et al., 2008). The genomic study shows a lack of nitrite: hydroxylamine reductase and the presence of cd1 nitrite: nitric oxide oxidoreductase (NirS) (Kostera et al., 2008). The current hypothesis for the pathway involves three different redox reactions: [1] Nitrite reduction to nitric oxide: $NO_2^- + 2H^+ + e \rightarrow NO + H_2O$ ($E_\circ$'= +0.38 V), [2] Combination of nitric oxide and ammonia, generating hydrazine: $NO + NH_4^+ + 2H^+ + 3e \rightarrow N_2H_4 + H_2O$ ($E_\circ$'= +0.34 V), [3] Hydrazine oxidation to nitrogen gas: $N_2H_4 \rightarrow N_2 + 4H^+ + 4e$ ($E_\circ$'= -0.75 V) (Figure 2-4) (Kartal et al., 2008) (Sliekers et al., 2002).

As shown in Figure 2-4, the hypothetical catabolism pathway involves oxidation of ammonium, using nitrite as the electron acceptor to generate proton motive force (PMF) in ANAMMOXOSOME (J.Y. Jung et al., 2007). As indicated in step [1], nitrite (NO_2^-) is reduced to nitric oxide (NO) via utilizing one low-energy electron. In the second step [2], ammonia (NH_4^+) and NO combine to produce hydrazine with the uptake of three low energy electrons (C.-J. Tang et al., 2010a). In the final step [3], hydrazine oxidation to nitrogen results in the production of four high-energy electrons (Sliekers et al., 2002) (Ahn, 2006).

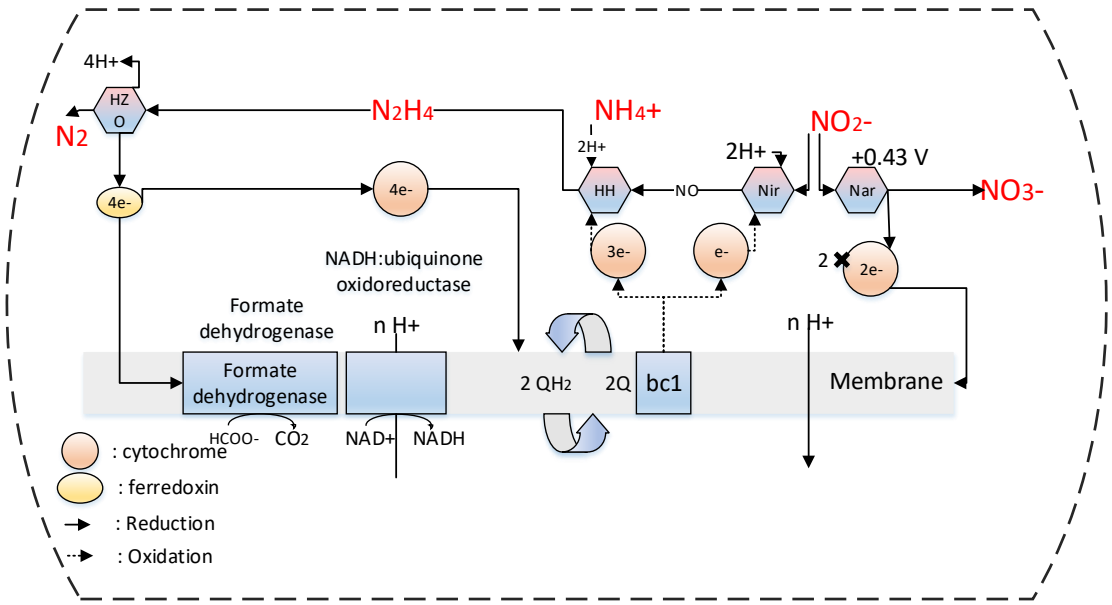

Figure 2-4 hypothetical catabolism pathway (oxidation of ammonium, using nitrite as an electron acceptor to produce proton motive force)((Kuenen, 2008a), (Kuenen, 2020))

The mentioned electrons, will flow through the Quinone pool (Q) and cytochrome bc1 complex, producing PMF (Kuenen, 2008a). Cytochrome bc1 is in charge of [a] electron transport to nitrite reduction and hydrazine production as shown in steps [1] and [2] respectively, [b] couple with electron transmission, translocate protons across membrane system and generate PMF (Jetten et al., 2009). The generated motive force is then used as a source of energy for ATPase proton translocation and production of ATP in the riboplasm. The electron transport in the central catabolism is combined with nitrate (NO_3^-) reductase for the production of ferredoxin to reduce carbon dioxide in the acetyl-CoA pathway (Kuenen, 2020). Although, as previously stated, hydrazine oxidation in step [3] can donate four electrons to ferredoxin, they are not recycled back to the system, so this brings up the important role of nitrite oxidation to nitrate by nitrate reductase (Nar) (Niftrik et al., 2004). This oxidation path produces four low-energy electrons that must drift through the membrane, be energized by the PMF, and be fed back to the ANAMMOX pathway (Kuenen, 2008a). Acetyl CoA pathway requires input of low redox potential electrons for NAD+

reduction (-0.32 V), carbon dioxide reduction to formate (-0.44 V) and acetyl CoA synthesis (-0.5) (Kuenen, 2020). This is when nitrite only delivers +0.43 V, showing the requirement of energy-driven reversed electron transport. Since hydrazine has a unique reducing power, a portion of the electrons resulting from the oxidation reaction is moved to NAD+ and carbon dioxide reduction to withstand carbon fixation. So, hydrazine needs to be recycled which necessitates inverted transport of electrons from nitrite oxidation to the level of bc1 complex (J.Y. Jung et al., 2007) (Chen, Zheng, Shen, 2011). Several indications support this hypothetical pathway; step [1] is catalyzed by NirS, which exists in the K. *stuttgartiensis* genome. HZO (Gao et al., 2018), as shown in Figure 2-4, responsible for catalyzing hydrazine, has been purified from ANAMMOX strain KSU-1 (Shimamura et al., 2006). Dual copies of dimeric octaheme enzyme are richly present in the *Kuenenia* genome. It still needs to be fully confirmed whether or not there is a potential for the third step [3] of the mechanism to take place (Kartal et al., 2008) (Shimamura et al., 2006).

2.4. Inhibition and environmental factors

The inhibition effects on the ANAMMOX process by different components can be explained through the proposed pathways; the first mechanism highlights the potential for a competition between the heterotrophs and autotrophic ANAMMOX microorganisms (Waki et al., 2007) (C. Tang et al., 2010). Since heterotrophic bacteria have higher growth rates, they would outcompete the ANAMMOX bacteria and reduce the nitrogen removal capability (Kimura et al., 2010), (Dapena-Mora et al., 2007a). The subsequent scheme focuses on metabolic diversity, where the ANAMMOX bacteria utilizes the present organic matter in preference to ammonium and nitrite as the substrate for growth, energy production, and cell synthesis (Fernández et al., 2012), (Strous et al., 1999), (Isaka et al., 2007), (Oshiki et al., 2011) (Jin et al., 2012).

Table 2-1 Inhibition factors (Free ammonia) for ANAMMOX bacteria

Inhibition factor	Experiment operational mode	Exposure range	Additional information
Free Ammonia (FA)	Batch tests	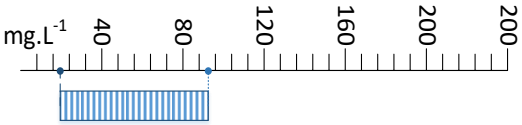	Toxicity to ANAMMOX organisms
	Continuous tests	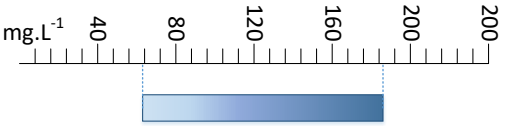	Inhibitory for ANAMMOX bacteria
	Batch tests and Continuous tests	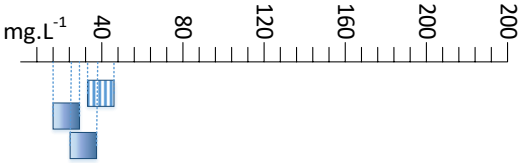	Short-term tests: Decrease in specific ANAMMOX activity, Long-term tests: Performance instability and unstable and zero removal efficiency
	Continuous tests	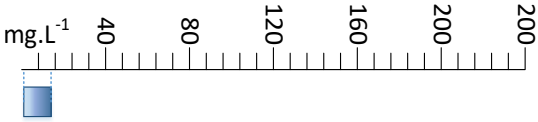	Lowest FA toxicity threshold (1.7mg/l)

**References: (Waki et al., 2007) (C. Tang et al., 2010) (Fernández et al., 2012) (J.Y. Jung et al., 2007)*

Other studies signified ANAMMOX inhibition resulting from ammonium concentrations over 1gN/L; however studies confirm ANAMMOX destruction by high levels of ammonia concentrations (Error! Reference source not found.) (Waki et al., 2007). As a result of several trials, it has been indicated that the actual inhibitor of the process is free ammonia instead of ammonium, which has been broadly studied for anaerobic digestion and nitrification process (Jin et al., 2012). Studies on the effects of ammonium concentration on the ANAMMOX process showed a 50% decrease in specific ANAMMOX activity in 38 mg/L concentration of free ammonia-nitrogen (FA-N) in a short-term batch test (Error! Reference source not found.). Tests were done in sequencing batch reactors studying the long-term effects, resulting in performance instability for FA-N concentrations over 20-25 mg/L (Fernández et al., 2012). Increasing the

concentrations over 20-25 mg/L in the long-term process caused extensive instability and efficiency reduction, down to zero. The optimal FA-N concentration in order to maintain a stable ANAMMOX performance is below 20-25 mg/L (Jin et al., 2012) (Fernández et al., 2012) (Waki et al., 2007).

Table 2-2 Inhibition factors (Nitrite) for ANAMMOX bacteria

Inhibition factor	Experiment operational mode	Exposure range	Additional information
Nitrite	Batch tests	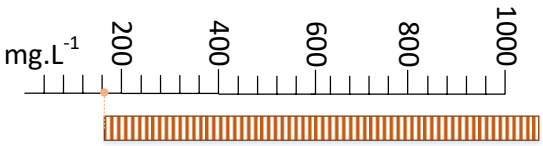	Serum Bottles, ANAMMOX sludge, Biomass inactivation
	Continuous tests	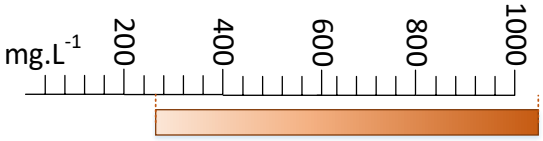	Continuous flow ABF reactor, Process inhibition
	Batch tests	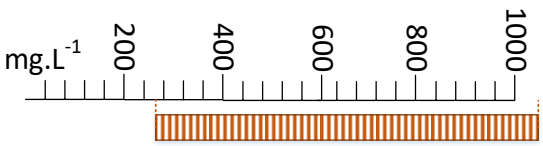	Monode batch test tubes, Process inhibition
	Continuous tests	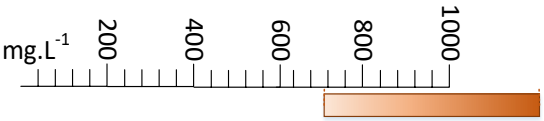	Continuous cylindrical reactor, Process inhibition
	Sequential batch tests	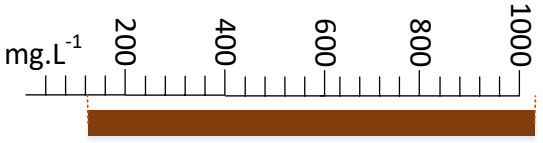	Sequential batch reactor, Process inhibition
	Continuous tests	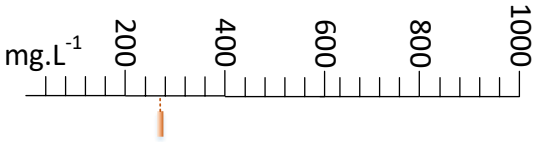	UBF continuous reactor inoculated with anaerobic granular sludge, -31% TN removal efficiency
	Continuous tests	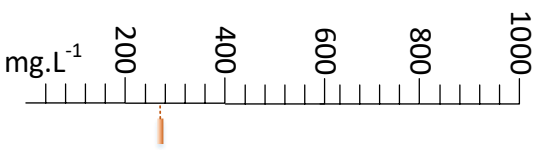	UBF continuous reactor inoculated with denitrifying flocculent sludge, -85% TN removal efficiency

	Batch tests	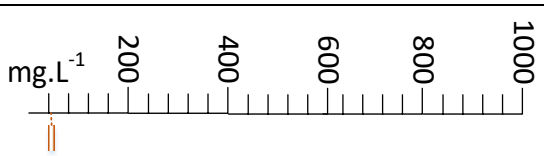	Closed batch vials inoculated with ANAMMOX biofilm sludge, 70% inhibition in biofilm and 100% inhibition in floc TN removal efficiency
	Sequential batch tests	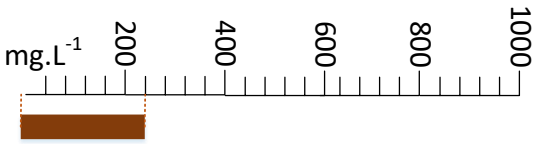	Continuous flow SBR inoculated with ANAMMOX biofilm sludge, No inhibition
	Sequential batch tests	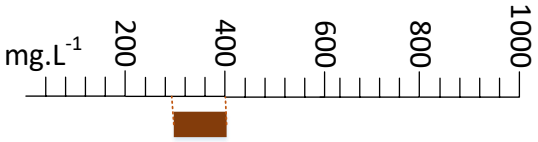	Continuous flow SBR inoculated with ANAMMOX biofilm sludge, Process inhibition
	Continuous tests	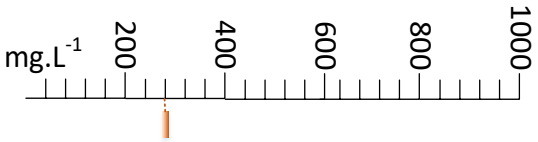	Continuous flow UASB, inoculated with ANAMMOX granular sludge, -12% TN removal efficiency
	Batch tests	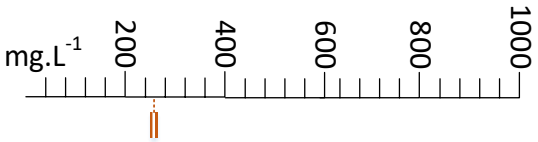	Batch vials, inoculated with ANAMMOX biofilm sludge, -50% TN removal efficiency
	Continuous tests	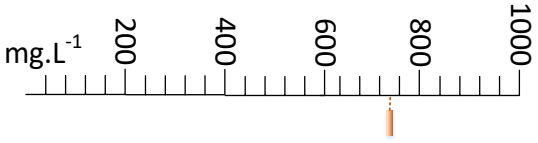	Continuous flow EGSB, inoculated with ANAMMOX granular sludge, -24% TN removal efficiency

**References: (Chen et al., 2011) (Oshiki et al., 2011) (C. Tang et al., 2010) (Fernández et al., 2012) (Strous et al., 1999) (Kimura et al., 2010) (Isaka et al., 2007)*

High concentrations of nitrite have detrimental effects on a number of microorganisms (Jin et al., 2012). Although nitrite is an essential substrate for the ANAMMOX process, excessive concentrations of this substance can result in process suppression (Table 2-2). Studies indicate that ANAMMOX bacteria is more sensitive to high nitrite concentration than ammonia inhibition levels (Jin et al., 2012). Results of the analysis, confirmed the critical effect of nitrite concentration on the ANAMMOX process, but the reported threshold ranges significantly from 5 to 280 mgN/L

(Kimura et al., 2010) (Fernández et al., 2012) with various operational and environmental conditions (Jin et al., 2012) (Anthonisen et al., 1976). Chemoautotrophic microorganisms comprising ANAMMOX bacteria, use CO_2 as their sole carbon source; therefore influent bicarbonate concentration is a fundamental factor for ANAMMOX cultivation and growth (MOLINUEVO et al., 2009). Studies on effects of nontoxic organic matters, as shown in Table 2-3, on the ANAMMOX process indicate an inhibition factor caused by high concentrations of organic matters, however, no specific negative impact was observed with low concentrations of organic matters (van de Graaf et al., 1996) (MOLINUEVO et al., 2009).

Table 2-3 Inhibition factors (Organic matter) for ANAMMOX bacteria

Inhibition factor	Experiment operational mode	Exposure range	Additional information
Organic matter	Continuous tests, Glucose	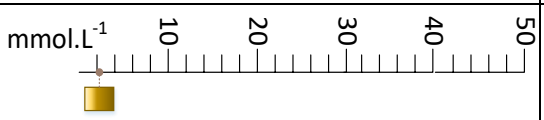	Continuous FBR reactor, -12% decrease in TN removal efficiency
	Batch tests, Glucose	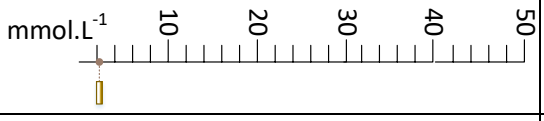	Batch vial reactors, 5% increase in TN removal efficiency
	Batch tests, Acetate	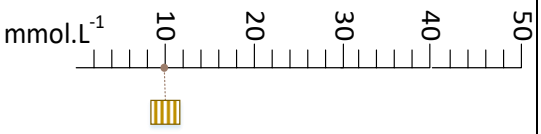	Batch vial reactors, No significant effect
	Batch tests, Acetate	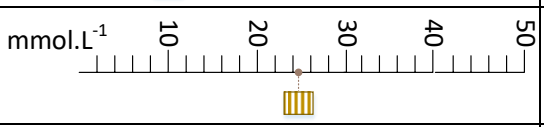	Batch vial reactors, -22% decrease in TN removal efficiency
	Batch tests, Acetate	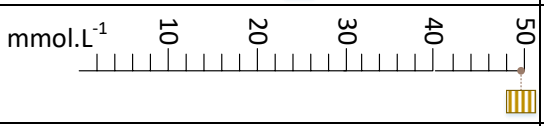	Batch vial reactors, -70% decrease in TN removal efficiency
	Batch tests, Acetate	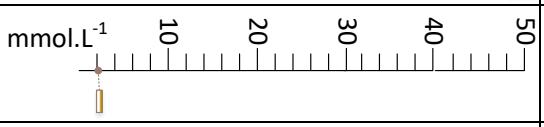	Batch vial reactors, -2% decrease in TN removal efficiency
	Batch tests, Propionate	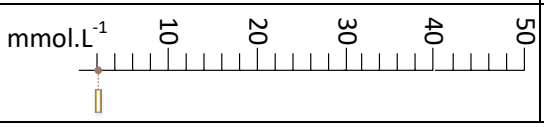	Batch vial reactors, -1% decrease in TN removal efficiency

	Continuous tests, Sucrose (COD)	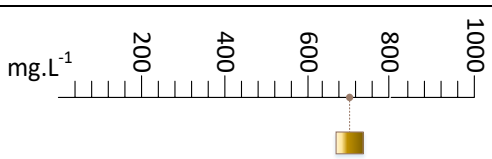	Continuous UASB reactor, -45% to -98% decrease in TN removal efficiency
	Continuous tests, Pig manure effluent after UASB post digestion (COD)	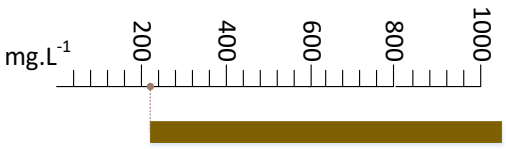	Semi-Continuous UASB reactor, with COD load of 112 mg/L.d, -100% decrease in TN removal efficiency, complete inhibition
	Continuous tests, Pig manure effluent after UASB post digestion (COD)	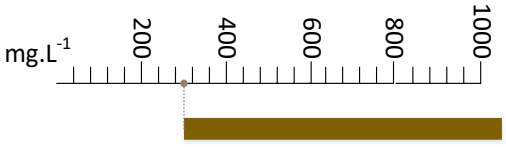	Semi-Continuous UASB reactor, with COD load of 136 mg/L.d, -100% decrease in TN removal efficiency, complete inhibition

**References: (Molinuevo et al., 2009) (C. Tang et al., 2010) (Oshiki et al., 2011) (Dapena-Mora et al., 2007a)*

2.5. Conclusion

The ANAMMOX process discovered in the early 1990s has the potential unique capacity to combine nitrite and ammonia to form nitrogen gas. ANAMMOX is a lithoautotrophic biological transformation method completed by a group of *Planctomycete* bacteria with slow growth rates and low bacterial yields. As a result of the reduced energy costs associated with aeration, no need for a carbon source and alkali, and the decreased production of excess sludge, ANAMMOX has been widely examined as a replacement for the conventional nitrification-denitrification method for biological nitrogen removal from wastewater streams. Compared to the conventional processes, ANAMMOX-based methods seem to offer more sustainable biotechnology for ammonia removal in a fully autotrophic bioprocess. However, the ANAMMOX process struggles with low biomass yields, low microbial growth, rate and extended doubling times, creating significant challenges to process startup and application. As a result of the stated issues, there is an increasing demand to investigate this innovative nitrogen removal process from microbial and engineering perspectives.

CHAPTER 3

Parin Izadi[a] , Parnian Izadi[a] , Ahmed Eldyasti*[a]

[a] Civil Engineering, Lassonde School of Engineering, York University, 4700 Keele Street, Toronto, ON, Canada , M3J 1P3

* Corresponding author

Authors' contributions All authors contributed to the study conception and design. Material preparation, data collection and analysis were performed by Parin Izadi and Parnian Izadi. The first draft of the manuscript was written by Parin Izadi and all authors commented on previous versions of the manuscript. Dr. Ahmed Eldyasti drafted and critically revised the work. All authors read and approved the final manuscript.

Review: Holistic Insights into Extracellular Polymeric Substance (EPS) in ANAMMOX Bacterial Matrix and the Potential Sustainable Biopolymer Recovery[1]

Abstract

The anaerobic ammonia oxidation (ANAMMOX) process has been proven to be a good and innovative process for treating nitrogen-rich wastewater due to decreased oxygen and carbon requirements at very high nitrogen loading rates. The ANAMMOX process is mainly operated through biofilm or granular sludge structures; as for such slow-growing microorganisms, high settling velocity of granules allows for adequate biomass retention and loweres the potential risk of washouts. The stability of granular sludge biomass is highly critical, yet the formation mechanism is poorly understood. There is number of essential functions linked to Extracellular Polymeric Substance (EPS) in the ANAMMOX bacterial matrix, such as; structural stability, aggregation promotion, maintenance of physical structure in the granules, water preserving, and protective cell barrier. There is an increasing demand for accurate methods for proper EPS extraction and characterization to expand the perception of ANAMMOX granule stability and potential resource recovery. Analyzing EPS focusing on various (mechanical and physical) properties can lead to biopolymer production from granular sludge. Biopolymers such as EPS are attractive alternatives substituting the conventional chemical polymers furthermore, their recovery from the waste sludge and the potential applications in industrial sectors leads to a radical enhancement of both environmental and economic sustainability, accelerating the circular economy advancements. Here, this study aims to overview the newest understanding of

[1] A version of this Chapter has been published in the Chemosphere Journal, Volume 274, February 2021, https://doi.org/10.1016/j.chemosphere.2021.129703

ANAMMOX sludge EPS structure obtained recently, and assess the potential challenges and prospects to identify the knowledge gaps towards constructing an inclusive ANAMMOX EPS recovery and characterization procedure.

Keywords: Biological Treatment, ANAMMOX, Extracellular Polymeric Substance, Resource Recovery, Biopolymer

3.1. Introduction

Before the ANAMMOX process, it was assumed that anaerobic ammonium oxidation is not practicable due to ammonium being a chemical inert, plus oxygen and mixed-function oxygenase requirements for the oxidation path. In 1977, the feasibility of anaerobic ammonium oxidation was predicted by Broda, through thermodynamic calculations, who believed "two kinds of lithotrophs are missing in nature" (Broda, 1977). In the initial stoichiometry for the missing lithotrophic pathways, ammonium acts as an electron donor and nitrite as the acceptor for the process (Wen et al., 2020) (Broda, 1977). Based on isotopic experimentations, nitrite is an oxidizing agent in the ammonium oxidation reaction (Du et al., 2019) (Ye et al., 2020). The essential energy source for bacterial growth is the 1:1 chemolithotrophic conversion of ammonium and nitrite to dinitrogen gas (Kallistova et al., 2016). ANAMMOX bacteria are cocci-shaped microorganisms with less than one µM diameter. These bacterial groups are restricted anaerobes which traces of oxygen (more than two µM) obstruct their metabolism (Kallistova et al., 2016). The doubling time associated with ANAMMOX bacteria is between 10 to 30 days, resulting in them being defined as slow growers (Kuenen, 2020).

The slow growth rate of the ANAMMOX bacterial population demands for extended sludge retention as a principal prerequisite for process operation (Zhao et al., 2018), and as a result, the ANAMMOX consortium is commonly cultured in either granular sludge form or in membrane

bioreactors (Wouter R.L. van der Star et al., 2008). The microbial community and biomass granulation are primarily affected by the reactor configuration, operational modes, and influent characteristics (Izadi et al., 2020a). The use of a continuously stirred tank reactor (CSTR) may sacrifice high cell density and proper biomass retention. Yet, it can theoretically promote the culture homogeneity, being appropriate for physiological characterization and a homogenous source for further batch cultivation and ANAMMOX organism's isolation (Ding et al., 2018). In CSTR system design, the process substrates are constantly supplied while being instantly blended with all reactor contents. CSTR hydrodynamics results in the homogenization of the ANAMMOX activity across the system (Reino et al., 2018), and so there will be no activity/concentration gradient change with position.

On the other hand, the occurrence of ANAMMOX granules/biofilm biomass have been identified in different bioreactor configurations comprising of upflow anaerobic sludge blanket reactor (UASB), sequential batch reactor (SBR), moving bed biofilm reactor (MBBR), dynamic membrane bioreactor (DMBR), and rotating biological contactor (RBC) (Xu et al., 2015a) (Izadi et al., 2020b). Development of various system configurations with distinct biomass retention schemes, has been focused on sustaining the slow-growing microbial community in the reactor (Gilbert et al., 2015a). For instance, in the UASB reactor, efficient biomass accumulation is accomplished because of the successful sludge granulation procedure (Jin et al., 2007). Granulation has been perceived as a critical element in the ANAMMOX process (Bagchi et al., 2010). UASB reactor design elements demonstrate certain qualities such as the capacity to cope with extreme influent substrate loadings, the ability to perform under decreased hydraulic retention times (HRT), and contain significant volumes of granular biomass. When comparing UASB reactor configuration with flocculent sludge-based systems, good settling ability and resistance to

fluctuating operating conditions are two of the most highlighted elements (Xing et al., 2014). As a result of high shear forces in upflow systems, the granules are physically broken into smaller-sized aggregates with enhanced mass transfer. ANAMMOX bacteria form robust microcolonies, similar to other slow-growing communities, balancing the microbial ecology and nutrient removal from wastewater (Izadi et al., 2020a).

Compared to other biofilms/granular sludge types, ANAMMOX bacteria are restrained in a self-generated matrix containing a convoluted assortment of elements, denoted as extracellular polymeric substances (EPS). EPS matrix has a significant impact on elucidating the bacterial aggregation aptitude (Zhao et al., 2018). Given that, ANAMMOX consortium has a high tendency to grow in aggregated forms, comprehension of the physical and chemical properties of the aggregates, which is entirely dependent on EPS composition, is of great importance (Flemming and Wuertz, 2019). EPS presence becomes critical for stable ANAMMOX reactor operation, as EPS has an immense drive to mediate dense biofilm and granule formation (Boleij et al., 2019). Moreover, understanding the EPS composition can aid in production stimulation for further biopolymer extraction. EPS are adhesive hydrated substances, produced through microbial cell secretion in straining circumstances, disintegration of cells, and adsorption of molecules from bulk liquid (Sheng et al., 2010).

EPS assist the aggregation progression by linking bacteria with other bacteria or inert particulates. EPS is detected to be one of the most prevalent elements of ANAMMOX sludge, and so it is potentially an influential aspect in ANAMMOX biofilm or granule development (Wang et al., 2019). On top of the significant contributions in ANAMMOX granulation, the extracellular matrix is primarily responsible for ANAMMOX granules' architectural structure and mechanical stability. Highly-enriched ANAMMOX granules have higher EPS contents, which lead to high resource

recovery potential. In most of studied systems, comprehension of the precise EPS configuration and creating a connection to the role of each distinct element is yet to be determined (Boleij et al., 2018). Information deficiency on the chemical and physical characteristics of EPS in ANAMMOX-based processes constrains the prospective to engineer biofilm systems reasonably (Seviour et al., 2019). Considering the rapid development of ANAMMOX biofilm-based technology implementations, EPS remains an unexploited resource thus far, which can potentially be the driving force to shift the current wastewater treatment scheme towards wastewater bio-refineries (Lotti et al., 2019a). Extracting EPS from ANAMMOX is a possible imminent product recovery path, which can generate a valuable outcome. Despite numerous valuable studies broadening the wastewater resource recovery, so far, there are no reviews available that deliver a complete overview of EPS-based biopolymer recovery from ANAMMOX-based systems. Biopolymers are reflected as a possible substitute for customary chemical polymers owing to the simplicity of biodegradability, high proficiency, non-harmfulness, and non-secondary contamination. However, the knowledge on the potential EPS applications are discrete. There is a lack of a unified document to give a broad overview of existing state-of-the-art information concerning the ANAMMOX bacterial EPS and the environmental applications.

Recent studies indicate that the scope of promising EPS applications, as a complex or as a raw substance, is enormous. Nevertheless, their broad span of appealing characteristics is still not entirely recognized. There is a need to advance the comprehension of EPS characterization from biofilms comprising of organisms known as prominent advocates of crucial water and wastewater functions, including the ANAMMOX process. This paper aims to fill the gaps by presenting a broad outline of ANAMMOX sludge EPS, with the final aim is to urge for more sustainable development through perceiving wastewater as a resource.. This critical review proposes that

identifying methods for accurate characterization and extraction of functional ANAMMOX biofilm EPS is the critical path to address crtitical questions in EPS-based biopolymer production technical uncertainties and the expected future roles as a resource, allowing for an enhanced circular economy.

3.2. General characteristics of EPS

EPS has a significant impact on the properties and performance of the sludge, yet there is a poor understanding of the mechanisms and definite roles of specific structural elements (Yu, 2020). EPS composition primarily involves proteins, polysaccharides, uronic acids, nucleic acids, lipids along with inorganic constituents, however, additional macromolecules are contributing to the structure, consisting of glycoproteins or proteoglycans (Bourven et al., 2015). Carbohydrates and proteins are typically discovered as the key elements of EPS; moreover humic constituents (just about one-fifth of the total amount) can play a major role in EPS produced in the sludge of biological wastewater treatment reactors (Sheng et al., 2010). Furthermore, uronic acids, nucleic acids, lipids, and particular inorganic elements were detected in EPS from different environments depending on the extraction methods and sludge origin (Sheng et al., 2010). As the main elements of EPS, proteins and polysaccharides make up for 1-60% and 40-95% of the total EPS components, correspondingly (Y. Zhang et al., 2016). Chained amino acids mainly form proteins, and as a result, the genome from databases can facilitate untying protein sequences, yet, proteins post-translational adjustments (including glycosylation, methylation, sulfation) cannot be simply projected. Polysaccharides follow a similar scenario; wherein assorted arrangements expose various properties and functionalities (Michael T. et al., 2008).

Nutrients play an essential part in the microbial production and secretion of EPS. Undoubtedly, the inducement of EPS expression in biofilms/granules is altered by environmental factors

(xenobiotics, high/low pH, oxidants, shear forces) and the availability of nutrients (Ashraf et al., 2016). EPS matrix can potentially guard the biofilm/granule structure and divide distinct population or bacterial groups in the environment. In cultures with one single species, the width of the biofilm and the EPS profusion have been directly linked to the capacity of the biofilm/granule to preserve signals for quorum sensing (QS) initiation under flow conditions (Tan et al., 2020). Additionally, EPS elements were a major impact factor, manipulating the interaction among aggregates within the biofilm structure (Flemming et al., 2016). QS is a bacterial interaction structure that depends on the generation, excretion, and perception of small diffusible signaling molecules (Papenfort and Bassler, 2016). The accepted model for bacterial biofilm generation proposes that: primarily, bacterial population growth on exteriors is an accretive process including adhesion, growth, motility, and EPS formation; and subsequently, QS-mediated regulatory signals are engaged as biofilm progress controllers in a strictly structured segregation procedure (Kjelleberg and Molin, 2002). In the case of ANAMMOX bacteria, they have an excellent aggregation capacity, anywhere the cell density is more significant than 10^{10}–10^{11} per liter, ANAMMOX bioactivity occurs, indicating the possible incidence of quorum sensing. As soon as the signal molecules levels in the environs reach a limit, QS bacteria will initiate controlling the manifestation of associated genes and activate consequent actions involving biofilm formation (Q. Zhang et al., 2020). There is still a significant knowledge gap on how the extracellular matrix affects the QS signaling and how the spatial allocation and arrangement separated by EPS matrix may impact the results of biofilm community's transmissions (Dilanji et al., 2012). The studies indicating that the EPS matrix captivates signals from the surrounding environment offer a systematic perception of how aggregates successfully execute QS, even at highly subtle signal levels (Tan et al., 2014).

EPS can presumably be divided to bound EPS (B-EPS) forms plus soluble EPS (S-EPS) arrangements. B-EPS is tightly attached to cells and linked to the conglomerate physiognomies, including; shear force, surface charge, dewaterability, settling velocity, and hydrophilicity/hydrophobicity features (Hou et al., 2015). In the two-layer EPS structure paradigm, the interior layer with a thicker and more condensed arrangement, firmly bound to the cell is classified as tightly-bound EPS (TB-EPS) (X. Guo et al., 2016), while the outer layer with a more dispersible and less condensed configuration is acknowledged to be loosely-bound EPS (LB-EPS). (Y. Zhang et al., 2016). Hypothetically, EPS can be connected to the cell exterior as marginal capsules (TB- EPS), or else discard to the adjacent bio-network being a more disorganized (amorphous) slime (LB-EPS) (Basuvaraj et al., 2015). Several studies have proven that TB-EPS retains a more significant sum of proteins however, LB-EPS held a greater extent of polysaccharides. Furthermore, protein is principally pinpointed in the central area of granular flocs in sections where the cells are mostly densely arranged, yet, pin flocs potentially contain higher quantities of polysaccharides, and cells are loosely bundled (Basuvaraj et al., 2015).

It has been proven that EPS supplies considerable volumes of hydrophobic amino acid groups to assist hydrophobic contacts, which potentially accelerate ANAMMOX EPS aggregation (Wong et al., 2019). As one of the major organic compounds in EPS, proteins are stated to systematize the internal structure through electrostatic, hydrophobic, and hydrogen bonds with additional biological elements (Mayer et al., 1999). In addition, by examining numerous sodium dodecyl sulfate- polyacrylamide gel electrophoresis (SDS-PAGE) bands utilizing tryptic digestion of in-gel proteins for mass spectrometry analysis, a number of bacterial proteins and sewage-originated polypeptides were detected (Bourven et al., 2015). Based on a report from Jorand et al. 1998, hetero-polymers including glycoproteins and lipoproteins, are the main constituents of activated

sludge originated EPS. Haemag- glutination analyses of lectin from activated sludge EPS, illustrate the presence of lectins and glycoproteins, being the set of proteins implanted in the linked system structure (Park and Novak, 2009). Isabelle Bourven et al. 2015, characterized the protein fraction of EPS obtained from two anaerobic granular sludge samples, wherein the results indicated glycoproteins containing α-D-mannosyl and/or α-D-glucosyl and with N-acetyl-β-D-glucosamine remainders in the bound-EPS.

In the recent decade, the rise in environmental awareness and fossil fuel restrictions have led to the introduction and development of renewable biopolymers. There is a potential for growing demand for bacterial EPS production from wastewater sludge, customized for environmental purposes (T T More et al., 2014). However, although an increasing trend in studies on EPS role in wastewater has been observed, there are still many discrepancies and ambiguities on EPS functions and inadequate perception of the primary compositional and structural characteristics. EPS is still a dark matter for most wastewater treatment sludge, creating challenges for gaining in-depth insight and proper maneuvering for enhanced performance (Yu, 2020).

3.3. ANAMMOX EPS molecular composition and structure

To accomplish adequate retention, one important element in ANAMMOX-based processes development is restraining granular or biofilm-based ANAMMOX bacteria (Abma et al., 2007). Apart from the ANAMMOX intracellular structure significance, cells arrangement within granules or biofilm matrix is of great importance, mainly because of its strong tendency to grow in aggregated forms (Boleij, 2020). Cells within biofilms are enclosed by EPS, which represents the direct surroundings of the bacterial cells (Flemming and Wingender, 2010). Biofilm’s EPS are an intricate assortment of interlinked biopolymers (Seviour et al., 2019). EPS' presence can be beneficial and detrimental since it has the propensity to form dense ANAMMOX biofilms, aiding

in reaching a more stable process, while it can also impair the cell biology characterization process (Boleij et al., 2019). Although there have been several advancements in ANAMMOX identification, including; population, cell structure, kinetics, etc., there is a limited perception of the EPS concept in the ANAMMOX process (Boleij et al., 2019). The tructure and maintenance of multicellular microbial communities strongly depend on the production rate and amount of EPS in the system (Ian W Sutherland, 2001). Biofilm's form of life is influenced by EPS concentration, distinct EPS constituents, charge, consistency, sorption capacity, and the three-dimensional architecture of the matrix (Flemming and Wingender, 2010). A full compositional and structural characterization of the EPS produced in the ANAMMOX process is of great significance for improving bioprocesses and recovery/reuse purposes. Reaching a complete perception of detailed ANAMMOX EPS composition is yet to be obtained, and the current literature is still controversial due to the lack of effective analytic techniques and biased results from non-standardized extraction protocols. (Lotti et al., 2019a).

A comprehensive summary of numerous studies on ANAMMOX EPS composition is presented in Table 3-1. The quantities and specific components of EPS may perhaps act on diverse physical and biological circumstances, but the majority of the existing procedures lack an adequate comprehension of the accurate EPS composition and fail to connect to the role of the specific constituents (Boleij et al., 2018).

Table 3-1 A comprehensive summary of several studies on ANAMMOX EPS structural composition in comparison to activated sludge EPS composition

ANAMMOX granular sludge	
Study #1 (Boleij et al., 2018)	
EPS composition	**Content (mg/g EPS)**
Proteins	599 ± 4
Carbohydrates	49.0 ± 2

Elemental composition	**Content (weight %)**		
Carbon	40.5		
Hydrogen	6.6		
Nitrogen	9.0		
Oxygen	35.7		
Sulfur	1.4		
Study #2 (Wang et al., 2019)			
EPS composition	**Content (Relative abundance %)**		
	S-EPS	LB-EPS	TB-EPS
α-helix (1650< <1660 cm^{-1})	24.2 ± 3.5	29.2 ± 11.0	23.3 ± 6.2
β-sheet (1610<<1642, 1680< <1695 cm^{-1})	55.1 ± 6.8	48.7 ± 9.9	42.5 ± 9.3
β-turn (1660< <1680 cm^{-1})	20.7 ± 3.3	22.1 ± 1.1	24.8 ± 2.1
random coil (1642< <1650 cm^{-1})	0	0	9.5 ± 13.4
Study #3 (Wong et al., 2020)			
EPS composition	**Monosaccharides (μg/g)**		
Rhamnose	~ 480		
Arabinose	~ 1550		
Ribose	~ 150		
Fucose	~ 400		
Xylose	~ 200		
Galactose	~ 500		
Mannose	~ 400		
Glucose	~ 1000		
Study #4 (X. Yin et al., 2015)			
EPS composition	**Content (mg/g VSS)**		
Proteins	63.8-307		
Polysaccharides	151-287		
Protein: polysaccharide	0.34-1.07		
Study #5 (Ni et al., 2015)			
EPS composition	**Content (mg/g VSS)**		
Proteins	55.6 ± 3.2		
Polysaccharides	70.8 ± 6.5		
Protein: polysaccharide	0.8		
Study #6 (C.-J. Tang et al., 2010b)			
EPS composition	**Content (mg/g VSS)**		
Proteins	164.4 ± 9.3		
Polysaccharides	71.8 ± 2.3		
Protein: polysaccharide	2.29		

Study #7 (C. Yin et al., 2015)	
EPS composition	**Content (mg/g VSS)**
Proteins	79.51 ± 3.61
Polysaccharides	30.12 ± 1.52
Protein: polysaccharide	2.64 ± 0.12
Study #8 (Y. Zhang et al., 2016)	
EPS composition	**Content (mg/g VSS)**
Proteins	46.2 ± 24.9
Polysaccharides	10.8 ± 2.6
Protein: polysaccharide	5.4 ± 2.1
Study #9 (C.-J. Tang et al., 2010b)	
EPS composition	**Content (mg/g VSS)**
Proteins	298.2 ± 8.7
Carbohydrates	112.1 ± 2.8
Protein: polysaccharide	2.66
Study #10 (Ni et al., 2010)	
EPS composition	**Content (mg/g VSS)**
Proteins	42.7 ± 6.5
Carbohydrates	83.2 ± 7.9
Protein: polysaccharide	0.51
Study #11 (Li et al., 2014)	
EPS composition	**Content (mg/g VSS)**
Proteins	34.9
Carbohydrates	9.8
Protein: polysaccharide	3.54
Study #12 (Hou et al., 2015)	
EPS composition	**Content (mg/g VSS)**
Proteins	67.9
Carbohydrates	25.3
Protein: polysaccharide	2.7
Study #13 (Ni et al., 2015)	
EPS composition	**Content (mg/g VSS)**
Proteins	55.6 ± 3.2, 75.3 ± 9.4
Carbohydrates	70.8 ± 6.5, 36.0 ± 4.1

Protein: polysaccharide		0.8, 2.1		
ANAMMOX biofilm sludge				
Study #1' (Y. Zhang et al., 2016)				
EPS composition		**Content (mg/g VSS)**		
Proteins		21.1 ± 8.7		
Polysaccharides		10.2 ± 0.3		
Protein: polysaccharide		2.6 ± 1.4		
Study #2' (Ali et al., 2018)				
1	**EPS composition**	**Content (mg/g VSS)/ *Ca*.B. sinica**		
	Proteins	~ 53		
	Carbohydrates	~ 35		
	Protein: carbohydrates	~ 1.5		
2	**EPS composition**	**Content (mg/g VSS)/ *Ca*.J. caeni**		
	Proteins	~ 28		
	Carbohydrates	~ 46		
	Protein: carbohydrates	~ 0.6		
3	**EPS composition**	**Content (mg/g VSS)/ *Ca*.B. sapporoensis**		
	Proteins	~ 15		
	Carbohydrates	~ 35		
	Protein: carbohydrates	~ 0.42		
4	**Quantitative analysis of different element C**	**Content (%)**		
		Ca.B. sinica	*Ca*.J. caeni	*Ca*.B. sapporoensis
	C-(C/H)	62.8	43.9	52.0
	C-OH	26.6	19.4	26.9
	C=O	10.6	24.2	19.0
	O-C=O	0	12.4	2.1
Study #3' (Miao et al., 2018)				
EPS composition		**Content (mg/g VSS)**		
		LB-EPS	TB-EPS	
Proteins		1.69-19.41	40.49-132.05	
Carbohydrates		7.25-85.24	41.30-106.32	

ANAMMOX sludge (flocs, biofilm and granules)			
Study #1" (Jia et al., 2017)			
EPS composition	**Content (Relative abundance %)**		
Slime	15.61 ± 9.92		
LB-EPS	6.46 ± 3.02		
TB-EPS	77.93 ± 10.3		
Ratios			
Protein: polysaccharide	2.10 ± 1.07		
Protein: DNA	6.38 ± 7.88		
Protein: humic acid	1.48 ± 0.57		
Study #2" (Miao et al., 2018)			
EPS composition	**Content (mg/g VSS)**		
	LB-EPS	TB-EPS	
Proteins	1.41-7.71	10.23-50.82	
Carbohydrates	0.45-27.96	16.69-32.07	
Activated sludge			
Study #1* (X. Guo et al., 2016)			
EPS composition	**Content (mg/g MLVSS)**		
	S-EPS	LB-EPS	TB-EPS
Proteins	4.4	18.6	86.7
Polysaccharides	11.2	25.7	50.6
Humic substances	0.6	5.1	15.6
Total	16.1	49.4	152.9
Fraction (%)	7.4	22.6	70.0

Extensive classification of glycoproteins originating from ANAMMOX granular sludge for a better understanding of ANAMMOX EPS structure was established by Boleij, Pabst, Neu, Van Loosdrecht, & Lin, 2018. The elemental composition of the extracted EPS was analyzed in an ANAMMOX granular sludge with "*Ca*.Brocadia sp" as the dominant species **(Study #1)** (Boleij et al., 2018). The protein and carbohydrate content analysis from the extracted EPS are as

following; proteins mg/g EPS and the carbohydrates mg/g EPS were 599±4 and 49.0±2, respectively. The elemental analysis shows a composition of (weight-%) 40.4, 6.6, 9.0, 35.7, and 1.4 for carbon, hydrogen, nitrogen, oxygen, and Sulphur (Boleij et al., 2018). The results of a different study shown in Table 3-1 **Study #2** (Wang et al., 2019) confirms the presence of proteins, polysaccharides, and humic acids as the main components in the EPS of ANAMMOX granules. The primary substance of the extracted TB-EPS, was proteins. 67±5% of the total EPS was TB-EPS, and S-EPS and LB-EPS were present in 3±0.6 and 30±5%, respectively (Wang et al., 2019). The total and the individual concentrations of proteins, polysaccharides, and humic acids increased significantly from S-EPS to LB-EPS and from LB-EPS to TB-EPS ($p < 0.05$). Proteins, polysaccharides and humic acids were mainly found in TB-EPS with fractions of 64±5%, 82±3% and, 70±8% of the total amounts in the EPS. Similar studies (Wu et al., 2019) noted that, protein was the main constituent in all EPS sub-fractions (C. Yin et al., 2015), with 65±17, 82±5 and, 68±2% of the total EPS in S-EPS, LB-EPS, and TB-EPS, correspondingly. Humic acid's amount in the sub-fractions was comparable with polysaccharide's quantity, which indicates the importance of humic acids in ANAMMOX granular EPS development (Wang et al., 2019).

As indicated in Table 3-1 **Study #1"**, Jia et al., 2017, studied various ANAMMOX-dominated biomass samples collected from lab-scale and pilot-scale systems using multivariate statistical analysis. It was found that the major component of the total EPS was TB-EPS with 77.93%, while LB-EPS and slime only contributed to 6.46 and 15.61 % of the total present elements (Jia et al., 2017). The most broadly dispersed constituents in the slime were, polysaccharide and humic acid. The most predominant substances in LB-EPS and TB-EPS were humic acid and protein respectively. The ratios of protein to polysaccharides, protein to DNA and protein to humic acid were 2.10 ± 1.07, 6.38 ± 7.88, and 1.48 ± 0.57, respectively (Jia et al., 2017). Based on specific

studies (Study #1'), both the EPS composition and concentration have considerable influence on the sludge's particle size, structure, strength, and settlibility (Y. Zhang et al., 2016). Based on this perception, verifying the ideal EPS component empowers the advancement of the granulation and increases aggregates' strength to prevent cell dewatering and destruction due to toxic substances, using a massive netting configuration with enough water (Ian W Sutherland, 2001).

As presented in Table 3-1, the EPS composition content (mg/gVSS) varies significantly in different studies. The dynamics regulating the bacterial metabolism extensively affect the excretion of EPS from cells in their growth conditions. Some of these factors include incubation conditions, culture’s growth conditions, genotype, pH, carbon to nitrogen ratio in the system, temperature and, etc., all of which are different from one study to another (T T More et al., 2014). Comparing studies #4 and #5 in the granular ANAMMOX section of Table 3-1 indicates a noticeable difference in proteins and polysaccharides concentrations as main EPS elements. In Study #4 conducted by X. Yin et al., (2015), effects of electrochemical technologies on ANAMMOX sludge were investigated, where the results show a significant EPS secretion (proteins: 307 mg/gVSS and polysaccharides: 287 mg/gVSS) stimulation in reactors with the electric potential application. The system was operated in 35 °C and a pH of 7.0, while the EPS was extracted by centrifugation and the protein content was measured using the Bradford procedure bovine serum albumin. Study #5 completed by Ni et al., (2015), was conducted in a pilot-scale upflow anaerobic sludge blanket reactor at 37 °C and a pH of 7.5. The EPS were extracted by cation exchange resin, and the protein and polysaccharide contents were analyzed thru Bradford protein assay with bovine serum albumin and Anthrone method with glucose, respectively. A similar pattern is detected in all studies indicated in Table 3-1, wherein the EPS composition and content notably fluctuate in different studies. Besides different experimental

conditions, the varied extraction and characterization methods result in qualitative and quantitative differences (Comte et al., 2007).

The information on EPS composition can be valuable as it potentially affects the method development process and ultimately facilitates controlling EPS production. However, EPS is poorly characterized due to extraction limitations as well as deficient analytical methods. Proteins and polysaccharides' characterization has been mainly restricted to colorimetric assays with comparatively low specificity and potential over or underestimating the specific elements (Le and Stuckey, 2016). Moreover, colorimetric methods can only characterize separate classes of molecules, and there is a lack of perception of the macromolecules structures (Jorand et al., 1998). In addition to proteins and polysaccharide's presence in EPS structure, a number of studies proposed the existence of glycoconjugates, which are a long way from being well-understood due to the complexity and substantial variety (Boleij et al., 2018) (van Teeseling et al., 2016) (Orner et al., 2003). Based on a recent study by Boleij et al., 2018, glycoproteins and acidic glycoconjugates were detected through staining experiments. This study found a high abundance of glycoproteins, which were heavily glycosylated with heterogeneous O-glycan. Glycoprotein identified in the samples could have potentially been an impenetrable protein from a "*Ca*. Brocadia" species, as robust indications have been present for solo amino acid polymorphism in the corresponding sequence zones, also several additional fragments of the sequence were incompatible, whatsoever (Boleij et al., 2018). 250 kDa S-layer glycoprotein Kustd1514, has been newly detected in two ANAMMOX species, "*Ca*. Kuenenia stuttgartiensis" and "*Ca*. Brocadia sapporoensis" (Boleij et al., 2018) (van Teeseling et al., 2016). The novelty of this experimentation was the investigation of glycoproteins, while most studies only study proteins and polysaccharides separately (Boleij et al., 2018).

Although there have been fast advancements in molecular characterization and biomolecular identification techniques, yet lack of an inclusive standardized extraction and characterization protocol for ANAMMOX EPS led to confounded property discovery and accurate role allocation. Spectroscopic methods such as Fourier-transform infrared spectroscopy and Raman spectroscopy (Table 3-2) are prevailing approaches equipped for characterizing partial functional groups however, they are incapable of providing a broad structural overview because of major signal overlapping and low resolutions. As a result, most existing studies (Table 3-1) have failed to characterize glycoconjugates containing covalently coupled oligosaccharides with proteins in ANAMMOX sludge EPS. Integrating spectral analysis with additional molecular characterization procedures, for instance, chromatography and mass spectrometry can aid in identifying important glycoconjugates in granular sludge. Liquid chromatography combined with tandem mass spectrometry can potentially provide information on chemical modifications, relevant for protein functions. On the other hand, although a number of techniques are developed for high throughput protein identification, there is a lack of equivalent progresses for extracellular polysaccharide analysis due to the structural diversity of carbohydrates, resulting in impaired and non-representative polysaccharide quantification by colorimetric methods (Seviour et al., 2018) (Yu, 2020).

3.4. EPS Polysaccharides bacterial biosynthesis

Although recently, there has been a considerable knowledge gain on ANAMMOX kinetics and metabolism, the EPS bacterial biosynthesis is possibly the least comprehended feature of ANAMMOX communities (Boleij et al., 2019). The restrictive factor in EPS analysis is poor solubility and heterogeneity of the substances, which results in a major challenge in EPS characterization and linking the composition to the function and synthesis process (Seviour et al.,

2019). The characteristics of EPS accountable for the formation and role of biofilms are inadequately recognized; moreover there is increasing attention towards clarifying the biosynthetic and genetic mechanisms of bacterial polysaccharides (Ates, 2015). Even though ANAMMOX sludge EPS have been the focus of recent critical studies in the environmental area, the current comprehension is largely based on fractionalized EPS elements such as polysaccharides. Polysaccharides are the most abundant fraction of sludge EPS, with extremely high compositional diversity and variability (Yu, 2020). Secreted polysaccharides represent the most extensively studied component of the EPS matrix and are often assumed to be the most abundant EPS component in biofilms (Starkey et al., 2014). So far, experiments on EPS biosynthesis pathways are mainly focused on polysaccharides, and the fundamental understanding of biochemistry for environment-provoked regulation of EPS production is inadequate (Starkey et al., 2014) (An et al., 2016).

There is a critical need to understand the interactions among metabolic paths and EPS biosynthesis mechanisms to direct and improve the potential bacterial biopolymer production (Schmid and Sieber, 2015). In this section of the review, a brief description of the microbial EPS polysaccharides and the potential biosynthesis mechanisms, are critically discussed. Exopolysaccharides are either synthesized extracellularly or intracellularly. The genes involved in EPS formation are in charge of encoding, control, chain-size indication, repeat-unit compilation, polymerization, in addition to transmit (Péant et al., 2005). The majority of exogenous microbial layers include neutral carbohydrates such as mainly-hexose and seldom-pentose along with uronic acids. Acetate esters, pyruvates, formats, plus succinates are some of the most conventional extracellular carbohydrates components (Sleytr, 1997). Polypeptides' existence in exopolysaccharides matrix is a common characteristic in a very limited number of gram-positive

bacterial cell structures (Ian W. Sutherland, 2001). Polysaccharides and proteins are the most well-studied constituents of EPS configuration (Czaczyk and Myszka, 2006). Bacterial exopolysaccharides can consist of both homopolysaccharides or heteropolysaccharides (Monsan et al., 2001). Bacterial polysaccharides are generally produced inside the cells and transferred to the extracellular ecosystem, emitting homopolysaccharides, such as; dextran, levan, and mutan, which are originally generated out of the cells through the activity of discharged enzymes shifting the substrate into polymeric substances (Ates, 2015).

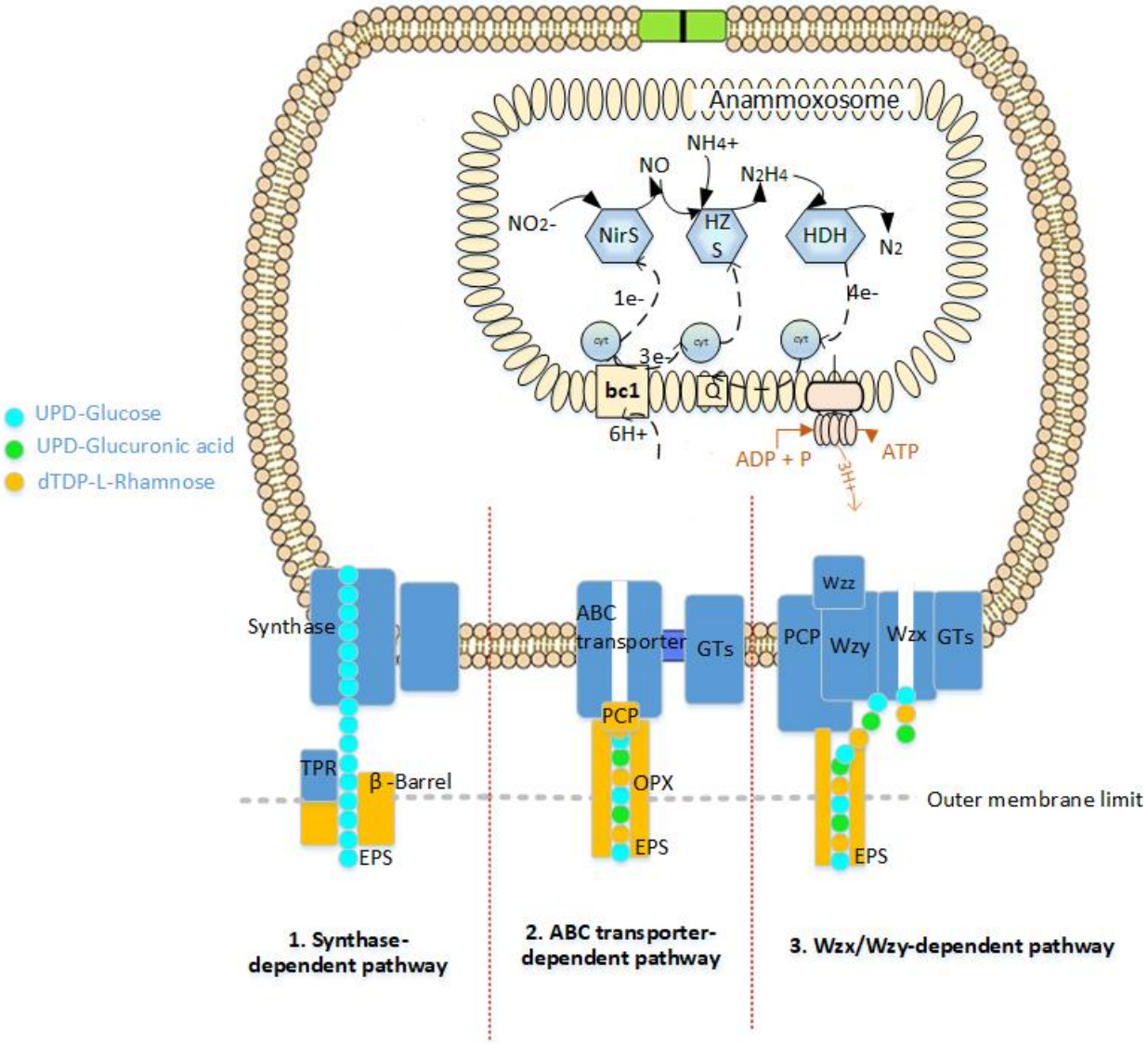

*Figure 3-1 Broad synopsis of distinct intracellular exopolysaccharides biosynthesis routes; 1. Synthase dependent; comprehends the polymerization coupled with passage via the synthase compound, covering whole cell envelope, containing tetratricopeptide repeat (TPR) proteins, 2. ABC transporter dependent route compiles polysaccharide chain attached on the poly-kdo-linker, consequently conveyed through the membranes and cell wall through the contribution of PCP plus OPX proteins. 3. Demonstrate the Wzx/Wzy dependent approach including the repeating unit built using several Glycosyltransferases (GT's) at the C55-lipid linker and the succeeding translocation headed for the periplasm by Wzx flippase.((*Schmid et al., 2015)*, (Ates, 2015))*

As a general rule of thumb, bacterial biosynthetic pathways encompass substrate usage, central metabolite pathway, and polysaccharide synthesis (Freitas et al., 2011). In general, the exopolysaccharides synthesis enzymes are located in various regions of the cell structure (Vu et al., 2009) and are mainly categorized into four different sections. The first category belongs to intracellular enzymes involved in the phosphorylation of glucose to glucose-6-phosphate, such as hexokinase (Ates, 2015). The next group is essential for catalyzing the change of sugar nucleotides. Uridine-5′-diphosphate-glucose pyrophosphorylase involved in the transforing glucose-1-phosphate to Uridine-5′-diphosphate-glucose is one of the most significant molecules in exopolysaccharides amalgamation and is an illustration for this group of enzymes (Rehm, 2010). The last group, glycosyltransferases, located in the cell periplasmic membrane, are possibly engaged in macromolecules polymerization besides being located in the exterior of the cell membrane and the cell wall (Suresh Kumar et al., 2007). The common bio-procedures of polysaccharide assembly in bacterial cells include Wzx/Wzy-dependent pathway, the ATP-binding cassette (ABC) transporter-dependent pathway, the synthase-dependent pathway, plus the synthesis occurring outside the cell using a sole sucrase protein, as shown in Figure 3-1 (Schmid and Sieber, 2015). Excretion of exopolysaccharides is a complicated activity for the bacteria, wherein hydrophilic, high molecular weight polymers accumulated inside the cytoplasm pass across the cell membrane, creating no issue for the critical barrier characteristics (Cuthbertson et al., 2009). Unlike the broad multiplicity of the molecular structures in exopolysaccharides, the biosynthesis pathways and exporting process in most gram-negative bacteria follow one of two mechanisms stated; the Wzx–Wzy-dependent pathway, in which the polymer repeat unit, is

compiled at the internal border of the cytoplasmic membrane and polymerized at the periplasm, along with the ABC transporter-dependent path, where polymerizing occurs on the interior layer cytoplasmic region (Freitas et al., 2011).

As briefly illustrated in Figure 3-1, stimulated sugars are networked in a particular arrangement to lipid transporter by an enzyme set called glycosyltransferases (GTFs), situated in the periplasmic membrane, in the Wzx/Wzy-dependent pathway, up to the point where repeating units are produced. The polymerization process transpires in the inner membrane cytoplasmic region (Freitas et al., 2011). Polymerization genes are known to be wza (indoctrinating external-membrane protein), wzb (encrypting acid phosphatase), and wzc (coding internal tyrosine autokinase) (Ates, 2015). During the synthase-dependent pathway, the exopolysaccharides excretion can appear either in the presence or absence of a lipid acceptor molecule, producing full polymer threads among the membranes along with the cell wall, and is unrelated to a flippase for translocating repeat units. Concerning this specific method, the translocation and polymerization are completed concurrently by a distinct synthase protein (Schmid and Sieber, 2015).

The extracellular synthesis involves a polymerization reaction, which continues to execute the transmission of monosaccharides from a disaccharide to a developing polysaccharide sequence in the external ecosystem (Ates, 2015). This exopolysaccharides assembly pathway is straightforward, as it is separate from the fundamental carbon metabolic reactions, and there is a narrow structure discrepancy likelihood. The extracellular polysaccharides production can take place for homopolysaccharides thru extracellular GTFs (Finore et al., 2014). The intracellular production of both homo- and heteropolysaccharides is reflected as a crucial growth factor, as asymmetrical repeating unit formation from sugar nucleotide predecessors is also implicated in the bioproduction of numerous cell wall elements (Li and Wang, 2012). Intermediates of the central

carbon metabolism have the potential to produce explicit originators for bacterial polysaccharides biosynthesis intracellularly. Sugar nucleotides are the originators and donor monomers in the biosynthesis of a good number of the repeating units (Barreto et al., 2005). Some of the sugar nucleotides include; nucleoside diphosphate sugars (for example ADP-glucose), nucleoside diphosphate sugar acids (including GDP-mannuronic acid), in addition to nucleoside diphosphate sugar byproducts [for instance UDP-glucose, UDP-N-acetyl glucosamine, UDP-galactose, plus deoxythymidine diphosphate (dTDP)-rhamnose] (Ates, 2015). The three vital transportation pathways for these sugars are; ATP hydrolysis combined with sugar translocation by the use of a sugar carrying ATPase, introduction together with convey of ions and further solutes, and passage thru the phosphoenolpyruvate (PEP) transport system (PTS) (Péant et al., 2005).

The stated polysaccharides are potentially in full synchronization with proteinaceous constituents, which might be a key foundation of the high concentrated glycoproteins detected in ANAMMOX sludge EPS (Boleij et al., 2018). More specifically Sulfated glycosaminoglycans have been isolated from the EPS matrix of ANAMMOX granules, which may result from Sulfo groups' integration in sugar residues of polysaccharides (Boleij et al., 2020). Although multiple enzymatic EPS-modifying reactions and integration processes may occur, the glycoconjugates biosynthesis is less foreseeable, and the specified regulation pathways and contributing genes are still vague (Yu, 2020). EPS biosynthesis and secretion pathways are greatly controlled and structured by a complicated system of signaling networks (Blanco et al., 2019). EPS Biosynthesis is generally originated in the cytoplasm, transforming monosaccharides into sugar nucleotides in advance to them being passed on by exclusive glycosyltransferases to transporter molecules placed in the plasma membrane. Countless proteins engaged in such activities are an element of the typical metabolism determining the EPS composition. The following stages of polymerization,

construction, and dissemination are commonly somewhat preserved, adhering to one of three principal procedures, the Wzy-, ABC transporter- or Synthase-dependent routes, explained comprehensively (Pereira et al., 2015).

3.5. Physiological Elements of EPS Biosynthesis

The effects of external factors on bacterial EPS production are variable. Based on different studies, EPS production can be the result of both stress conditions and media enrichment process configuration; on the other hand it is proven that microbial EPS is yielded at the highest rate, in the course of the stationary stage of bacteriological development (Sengupta et al., 2018). Linkage amongst EPS assembly and the microbial growth phase is dependent on specific bacterial genera. Some of the influential factors affecting EPS production are; variation in carbon source and nitrogen source (Degeest and De Vuyst L, 1999), oxygen concentration, pH, temperature, presence of enzymes and ions, stress along with fermentation conditions (Sandhya and Ali, 2015) (Sengupta et al., 2018). Stress is a potential contributor to EPS production stimulation, which triggers bacterial communities to enhance EPS assembly and to facilitate durability in such stress factors (Sandhya and Ali, 2015). Consequently, further EPS production in stress conditions signifies EPS' unique part in tension forbearance and water retaining aptitude for the bacteria (Sengupta et al., 2018).

3.5.1. Temperature and pH

Temperature is known to be one of the most significant elements affecting EPS production in microbial cells. The ideal temperature necessary for suitable EPS production is primarily controlled by the bacterial strain and natural bacterial ecosystem temperature (T T More et al., 2014). Reminiscent of temperature, the pH of the bacterial culture can greatly impel the EPS production, yet the pH impact is different in various microorganisms, operating settings, and

medium constituents (Shu and Lung, 2004). Temperature and pH necessary for optimum growth of the bacterial community are primarily different from the required range for optimum EPS production (Sengupta et al., 2018), as these parameters determine the morphological adjustments in the bacterial cell structures (Lindsay et al., 2000). Similar to other factors, components and characteristics of EPS rely on the category of substrate consumed, bacterial growth phase, microbial species composition and pH and temperature (Tomaszewski et al., 2017b). The influence of temperature and pH on ANAMMOX bacteria has been reviewed comprehensively (Tomaszewski et al., 2017a), yet, there is a lack of knowledge on the effect of these significant parameters on EPS composition and structure.

Based on a study by Jin, Ma, and Yu (2013), the EPS concentration lessened during a temperature increase in the range of 8.7-28.3 °C, and contrariwise. One other research on the link between temperature and EPS confirmed the results from (Jin et al., 2013), indicating that mainly polysaccharides are responsible for the change in the range of 2.5-31.2 °C (Guo et al., 2015). A similar confirmation was observed from a study wherein the performance of partial nitritation-ANAMMOX process under a temperature gradient from 20 to 10 °C in four different reactors was studied (Gilbert et al., 2015a). Zhang et al., (2020) study on the ANAMMOX biofilm system at low temperatures showed an interesting increasing EPS production trend when the system's temperature decreased from 25.8 to 13.7 °C. The study was conducted in a sequencing batch biofilm reactor in three different phases with temperature adjustments in each reaction stage. The potential reason behind detecting more EPS in lower temperatures could be the bacteria struggling to protect themselves from external threats. EPS content expansion can hypothetically offer additional extracellular nutrients and enzymes, enhancing the system stability (Flemming and Wingender, 2010). More specifically, TB-EPS with abundant protein was isolated at reduced

temperature, which may guard the bacteria encountering unpleasant situations (Jianhua Zhang et al., 2019). Guo et al. (2015), study demonstrated the contents of S-EPS and B-EPS under natural seasonal temperature variations. The results illustrated that in stages where the temperature dropped, the polysaccharide content in EPS elevated to shield the biomass from distressing factors, enhancing the robustness and consistency of the ANAMMOX granules.

ANAMMOX-based systems are pH-dependent, and as a result, pH can either have a direct or an indirect effect on the process (He et al., 2015a). The studies show that the optimal pH range for ANAMMOX is between 7.5 to 8.0 however, there is limited research on the effect of transient pH shocks on ANAMMOX granule structure and EPS production (He et al., 2016). Jing Zhang et al., (2019) study on the effects of pH on ANAMMOX granule properties indicated that once pH declined from 7 to 6, the high biomass density granules could discharge elevated amounts N-acyl-homoserine lactone, stimulating the EPS excretion from the cells. The study results show that at pH 6, the EPS constituent of ANAMMOX granules was around 124 mg/gVSS, which is approximately 70% higher than pH 7. The protein content boosted drastically, although the polysaccharide content stayed unaffected, leading to a 98% rise in protein: polysaccharide. During particularly acidic (pH ~ 5.5) plus alkaline circumstances (pH ~ 7.5 to 9.0), the structure of granules was damaged, corresponding to EPS contents diminution (Jing Zhang et al., 2019).

3.5.2 Salinity

Distinctive physicochemical aspects, including osmotic stress, which potentially constrain the cellular actions, can improve the microbial EPS assembly (Bemal and Anil, 2018). In salinity stress circumstances, cells begin to enhance EPS production rate by reducing the bacterial growth rate. This process results from bacterial populations devoting more energy towards endurance rather than reproduction (Bemal and Anil, 2018). Augmented EPS coating is capable of defending the

cells against dehydration via forming a contiguous microenvironment around the cell wall, which acts as a barrier towards the osmotic disequilibrium within the cell membrane and delivers a source for water along with reducing the ion influx in the hypersaline state (Sheng et al., 2006). The salinity effect on sludge characteristics is a critical factor in achieving good retention of the biomass in ANAMMOX systems. Dapena-Mora et al., 2010, reported that salinity could trigger the transition from flocculent sludge to granular sludge and decrease the sludge volume index in the ANAMMOX consortium. Increased cell density in saline environments enhances the robustness of gene expression, which results in elevated bacterial activities (Tan et al., 2013). The reason behind the promising outcomes observed regarding improved sludge settling in ANAMMOX microbial population in the presence of specific salt concentrations lies within the Derjaguin-Landau-Verwey-Overbeek (DLVO) theory (J. Li et al., 2018). This theory indicates that, rise in salinity concentration can potentially lessen electrostatic repulsion using compacting double layer and, consequently, improve the granulation process.

Up to date, several researchers concentrated on understanding salinity impacts on EPS formation and its configuration within the granular sludge and the potential linkage to granule stability (Corsino et al., 2017). The addition of salt has been reported to be a stimulating factor to improve the EPS production in ANAMMOX bacteria (Wang et al., 2013). Elevated salt levels may boost the osmotic pressure, which can trigger a reverse diffusion of the intracellular water out of the cell. Furthermore, EPS could have a critical influence on osmotic acclimatization in ANAMMOX bacteria (J. Li et al., 2018). Thus far, limited studies have focused on salt-in strategy in ANAMMOX bacteria, and based on previous studies, there are promising and favorable effects on osmoregulation under high saline conditions (J. Li et al., 2018). Speth et al., 2017, reported the survival of ANAMMOX bacteria in high salinity environments via salt-in strategy. Based on this

study, "*Ca*. S. aprofunda" and "*Ca*. S. brodae" possibly employ salt-in strategy to acclimatize with saline environments, while "*Ca*. S. rubra" depend on harmonious solute to tackle elevated salinity levels (Speth et al., 2017). Since the metabolic variety of ANAMMOX species are very complicated, more study is necessary (J. Li et al., 2018). Fang et al. 2018, investigated the adaptation of ANAMMOX granular sludge bacterial community, surface characteristics at various salinities, and the prospective connection with sludge granulation. The study results indicated that salinity provoked the microorganisms to adjust the EPS conformation to survive under salt stress, yet the changes in EPS structure were in opposition to the ANAMMOX aggregation. Salinity resulted in inhibition of the hydrophobic protein secondary structures, in addition to initiation of hydrophobic functional groups, causing a considerable diminution of hydrophobicity of cell surface (Fang et al., 2018). In an analysis done by Engelbrecht et al. 2019 the impacts of various NaCl concentrations on the effectiveness of acclimatized and non-adapted ANAMMOX biofilms were assessed. The outcome of the study shows that attributable to the impulsive stress, the non-adapted biomass might begin to generate EPS which intensifies the accessible amount of total organic carbon, and as a consequence, denitrification is stimulated in the system (Engelbrecht et al., 2019). Studies regarding the influence of salinity on growth and EPS production in the ANAMMOX bacterial community are limited, and this narrow understanding results in a barrier towards defining the fate of these strains.

3.5.3. Carbon and nitrogen sources

EPS' qualitative and quantitative yield is strongly dependent on the carbon supply existing in the bacterial medium (Molina-Ramírez et al., 2017). Several studies suggest the connection of microbial EPS to the carbon source consumed being the bacterial growth substrate, yet the bacterial enzymes have a substantial effect on the breakdown of the complex carbon sources (Audy et al.,

2010). In a study conducted by Li et al. (2015), the effect of COD disturbance on ANAMMOX granulation was investigated. The results of the study indicated that the organic intrusion greatly altered EPS dissemination and bacterial configuration. As a result of glucose addition, EPS distribution of polysaccharide and protein improved, wherein the protein content had a more significant escalation. More specifically, by rising the COD concentration from 0 to 200 mg/L, the total EPS concentration proliferated from 33 mg/gVSS to 181 mg/gVSS, yet increasing the COD to 300 mg/L resulted in a drop in EPS concentration to 155 mg/gVSS (Li et al., 2015). The results of different studies show that the introduction of an appropriate concentration of COD can potentially increase the EPS content, promoting a denser and more robust ANAMMOX granule which allows for a better bacterial accumulation.

Similar to carbon source, nitrogen sources present in the bacterial medium have been proven to have a major part in the assembly and improvement of bacterial EPS (Degeest and De Vuyst L, 1999). There is a vital requirement to adjust the nitrogenous compounds in the media to support the EPS production, wherein the effect of nitrogen products similar to aspartic acid, sodium nitrate, urea, yeast extract, amino acids as glycine, glutamic acid, ammonium sulfate and phenylalanine in the enrichment environment, and the potential impacts on production of EPS turned out to be fundamentally important (Sengupta et al., 2018). The presence of appropriate sources of both carbon and nitrogen in the growth media for metabolite assembly is of great importance, so eventually, obtaining an optimum concentration of each is crucial (Farrés et al., 1997). In a study done by Zhang et al. (2016), impacts of substrate shock on EPS secretion and characteristics were investigated in an ANAMMOX biofilm system. A transitory (24 hours) high substrate concentration of 2500 mgN/L, resulted in EPS exertion stimulation and ultimately deterioration of ANAMMOX granules. With a substrate total nitrogen upsurge from 600 to 1250 mgN/L, the mean

EPS concentration increased by approximately 50%. Nitrogen loading rate's increase from 4.8 to 10.0 gN/L. d, resulted in a boost in the mean EPS level, from 22.3 ± 3.2 to 35.2 ± 7.3 mg/gVSS, specifying EPS excretion being provoked by substrate feeding (Y. Zhang et al., 2016).

Identification of bacterial genes accountable for EPS production that promote different subordinate functional characteristics to the bacteria is extremely critical. Developing a solid perception of diverse influential aspects liable for better production of bacterial EPS requires comprehensive expertise on the impact of genes and their manipulation. This comprehension is better strengthened by understanding the corresponding impact of physical and chemical factors in charge of qualitatively enhanced and quantitatively boosted yield of the expected EPS (Sengupta et al., 2018).

3.6. EPS recovery and analysis methods

3.6.1. Extraction methods

EPS extraction approaches can be categorized into physical and chemical methods (T. T. More et al., 2014). Figure 3-2 provides a comprehensive overview of both physical and chemical extraction methods. In physical extraction approaches, external forces promote EPS separation from the cell and further dissolution in the mixture. Alternatively, chemical compounds act as a disruption agent in chemical methods to attack the bonds linking EPS and the cell to enhance EPS's dissolution. Typically, the extraction efficacy of physical methods is lower than chemical approaches (Sheng et al., 2010), yet there is a potential for EPS contamination by chemical extractants in chemical procedures (Comte et al., 2007). As indicated in Figure 3-2, some of the most common physical EPS extraction methods include centrifugation (Dignac et al., 1998), cation exchange resin (CER) (Frølund et al., 1996), plus heating (Morgan et al., 1990), and sonication (Comte et al., 2007). On the other hand, a few of the chemical procedures used for EPS extraction from wastewater sludge

are: trichloroacetic acid, crown ether, ethanol, enzymes, glutaraldehyde, sulfide, ethylenediaminetetraacetic acid (EDTA) (Liu and Fang, 2002), alkaline NaOH (Frølund et al., 1996), boiling benzene and acid-H_2SO_4 (T. T. More et al., 2014) (Figure 3-2). There is also a potential to apply both physical and chemical extraction methods, a couple of them being: CER and sonication, alkaline and heating, formaldehyde and heating plus ion exchange and stirring (Sheng et al., 2010).

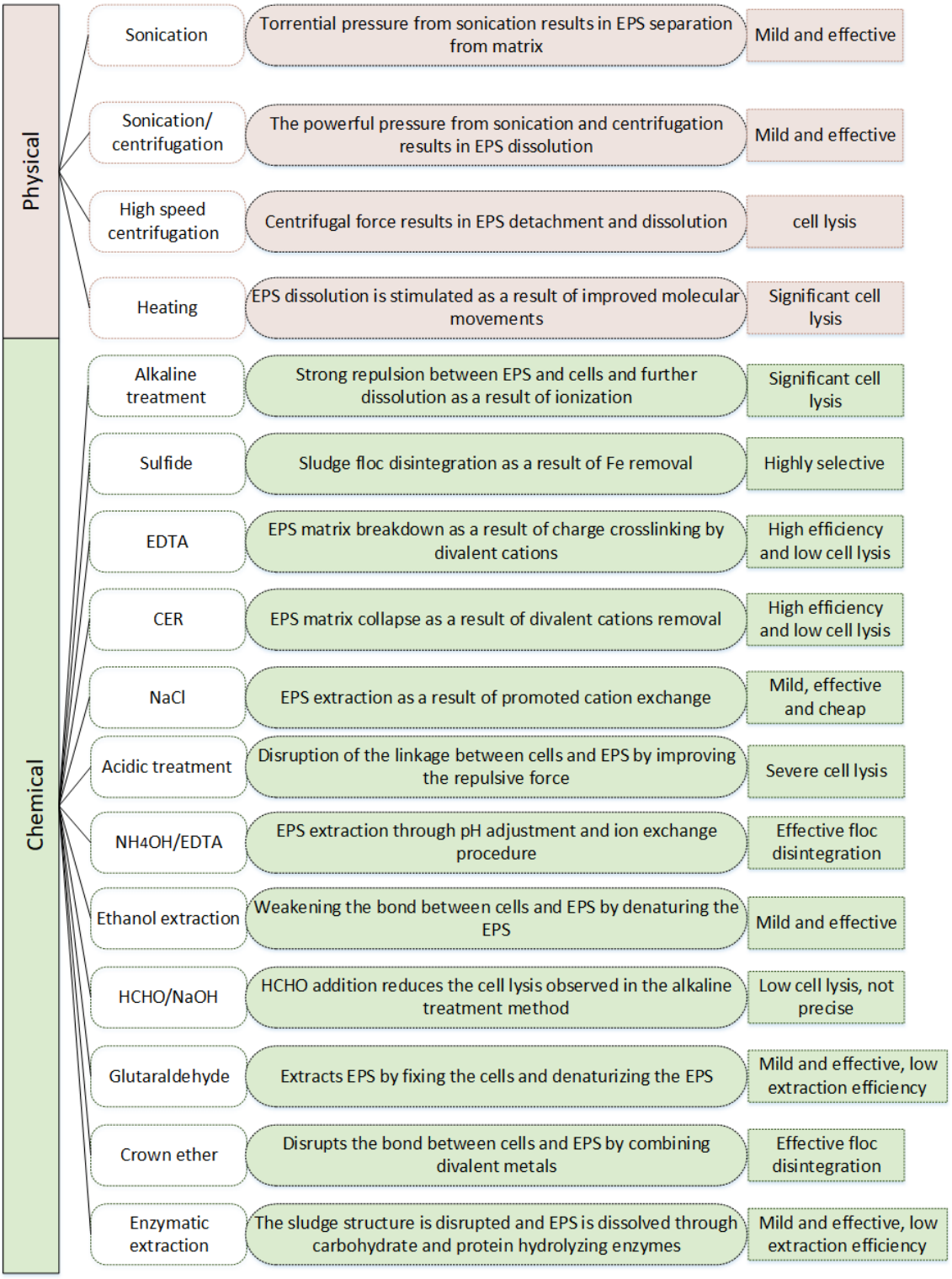

Figure 3-2 Different EPS extraction methods

The efficacy of EPS extraction techniques is analyzed based on the extent of cell lysis and intrusion for EPS structure (Frølund et al., 1996), which substantially varies from one method to another (Sheng et al., 2010). Different reports indicate that boiling and alkaline treatments have the potential to cause a severe macromolecular EPS composition disruption, which theoretically alters the polymer composition and disulfides the bindings present in glycoproteins (Frølund et al., 1996). As illustrated in Figure 3-2, applying chemical methods such as EDTA and alkaline NaOH can result in EPS contamination and further interference with protein determination and critical cell damage and macromolecules disorder, respectively (Sheng et al., 2005) (Liu and Fang, 2002). CER technique is the most acknowledged EPS extraction method, given that it has high efficiency with low cell lysis, and because the resin can be simply removed there is a reduced chance for chemical pollution (Frolund et al., 1996) (Sheng et al., 2010). Since there are no general methods available for quantitative EPS extraction, there is a need to select an optimized method for each case.

3.6.2. Characterization and analytical methods

As a consequence of EPS's intricacy, heterogeneity and sludge inconsistency, the characterization process is complex and problematical (Yu, 2020). Despite identifying a few classes of glycoconjugates and proteinaceous elements, there is still a poor understanding of macromolecules types in EPS structure. Moreover, there is a lack of information on specific molecular structures, dissemination, and roles of different EPS components in wastewater sludge (Sheng et al., 2010). An inclusive overview of the new EPS analysis and characterization methods is presented in Table 3-2. Conventional methods such as scanning electron microscopy (SEM) and transmission electron microscopy (TEM) require an initial step of dewatering and fixation for the bacterial granules, which potentially results in a shift in the fundamental composition of the sludge EPS. In contrast,

procedures such as environmental scanning electron microscopy (ESEM) (Beech et al., 1996), atomic force microscopy (AFM) (Li and Logan, 2004) and confocal laser scanning microscopy (CLSM) (Zhang and Fang, 2001), can demonstrate the primary forms and structures of EPS (Sheng et al., 2010) (Table 3-2).

Table 3-2 Comprehensive summary of new EPS analytical methods

Analytical methods	Descriptions and remarks	Schematic descriptions of the methods
Gas Chromatography (GC)	Monosaccharides and amino acids qualitative and quantitative analysis after hydrolysis	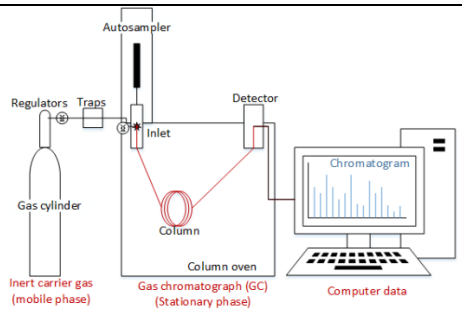
Gas chromatography-mass spectrometry (GC-MS)		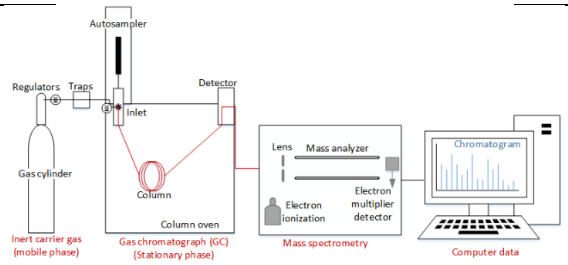
High-performance liquid chromatography (HPLC)		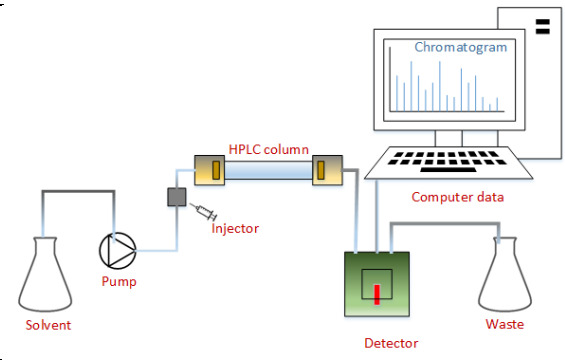

Quartz crystal microbalance (QCM)	In-situ and real-time analysis of kinetics of EPS adsorption/adhesion to cell or material surfaces	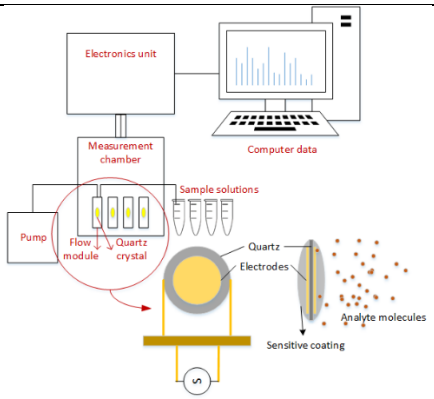
Nuclear magnetic resonance (NMR)	Molecular structure of carbohydrates and proteins and the link between EPS and metals can be determined	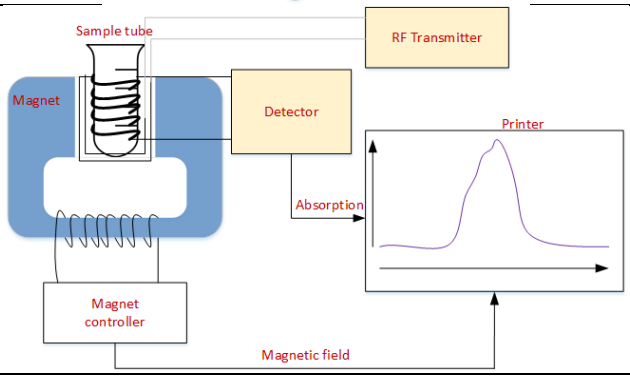
Scanning electron microscopy (SEM) and Transmission electron microscopy (TEM) Environmental scanning electron Technique (ESEM)	EPS microbial microstructures can be detected after fixation and dewatering	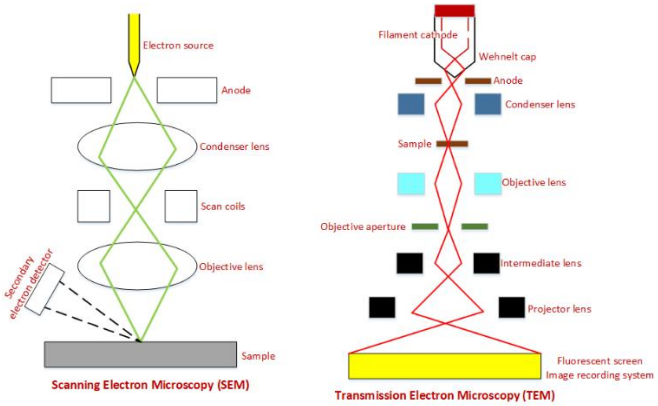
Confocal laser scanning microscopy (CLSM)	Structure of fully hydrated samples can be detected. The spatial distribution and content of EPS can be analyzed	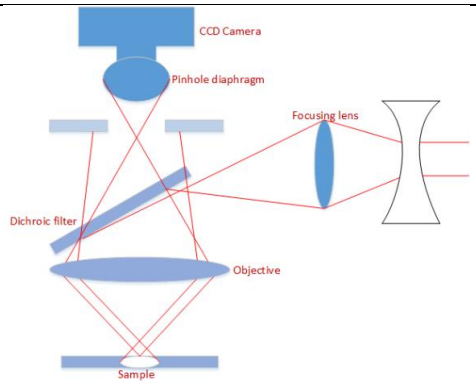

Fourier transform infrared Spectroscopy (FTIR)	Detects functional groups and linked EPS, can detect microbial adhesion (in-situ)	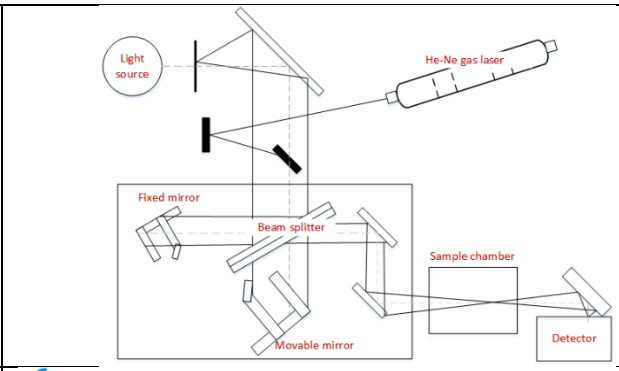
X-ray photoelectron spectroscopy (XPS)	Detects EPS's surface functional groups and EPS interaction with metals, analyzes EPS's role in microbial adhesion	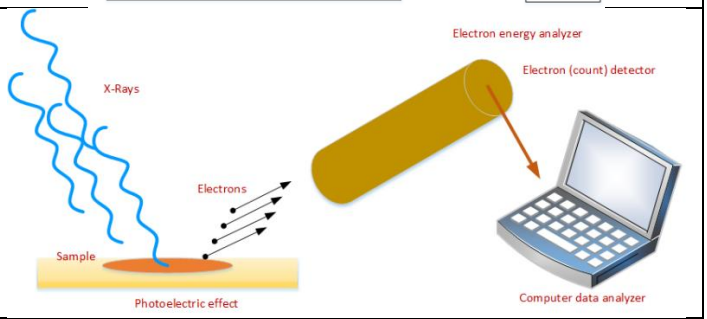
Raman spectroscopy 3-Dimensional excitation–emission matrix spectroscopy (3D-EEM)	A sensitive and selective method to analyze EPS chemical structure (in-situ)	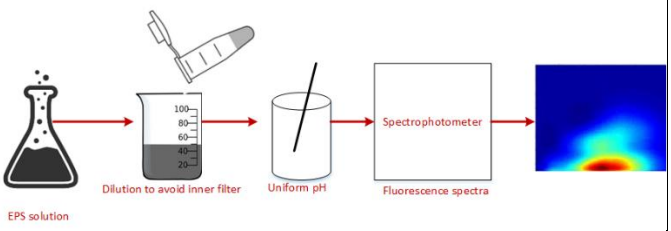
Atomic force microscopy (AFM)	Can detect the spatial EPS distribution	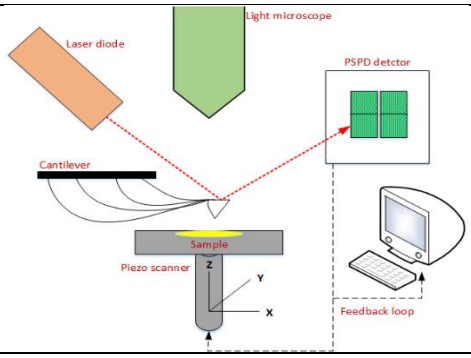

**References: (Sheng et al., 2010) (Beech et al., 1996) (Can Der Aa and Dufrêne, 2002) (Esparza-Soto and Westerhoff, 2001) (Wagner et al., 2009) (Ortega-Morales et al., 2007) (Omoike and Chorover, 2004) (Allen et al., 2004) (Sheng and Yu, 2006) (Kawaguchi and Decho, 2002) (Staudt et al., 2004) (Bura et al., 1998) (MacLeod et al., 1995) (Beech et al., 1996) (Manca et al., 1996) (Lattner et al., 2003) (Kwon et al., 2006) (Zhu et al., 2009) (Dignac et al., 1998) (Ortega-Morales et al., 2007)*

As a result of the significant shortcomings of conventional methods and their inefficiency in classifying chemically unstable or nonextractable elements and the discharged intracellular matrix (Chen et al., 2018). Some of the spectroscopy-based methods comprising X-ray photoelectron

spectroscopy (XPS) (Ortega-Morales et al., 2007), 3-dimensional excitation-emission matrix fluorescence spectroscopy (3D-EEM) (Esparza-Soto and Westerhoff, 2001), Fourier-transform infrared (ATR-FTIR) spectroscopy (Omoike and Chorover, 2004), Raman spectroscopy and nuclear magnetic resonance (NMR) (Lattner et al., 2003) (Table 3-2), can be employed for in-situ analysis of sludge EPS, to determine the functional groups and elemental conformations in EPS or bacterial masses (Sheng et al., 2010) (Yu, 2020). The most commonly used method for sludge characterization and analysis is fluorescence spectroscopy (Neu and Kuhlicke, 2017), which concedes for molecular structure detection and EPS spatial distribution visualization (Yu, 2020). The intricacy, heterogeneity, and inconsistency of ANAMMOX sludge EPS result in problematic characterization pathways. Thus, there is still an urgent need for innovative practices considering the precise perception of EPS configuration at the molecular level and a detailed classification of their three-dimensional disseminations and functions. Correspondingly, the in situ spectroscopic methods and high-resolution molecular characterization procedures play a key role.

3.7. Case studies of the recently established methods for EPS extraction and characterization in ANAMMOX sludge samples

One of the important factors in developed ANAMMOX processes designed for satisfactory biomass retention is bacterial immobilization through aggregation or biofilm formation (Aqeel et al., 2019). EPS production accelerates the biofilm development and granulation procedure and plays a key role in achieving a stable ANAMMOX reactor operation (Boleij et al., 2018). There has been an intensive increase in a number of studies on EPS extracted from ANAMMOX systems, aiming to substantiate a link between reactor performance and EPS physio-chemical characteristics (Ding, 2016). The reason for the high investment in EPS production in the ANAMMOX process was due to its role as a cell aggregation facilitator, significant impact on intracellular distance and substrate diffusivity as well as characteristics showing high correlation with process performance

and efficiency, but the literature assertions on the issue are yet debatable (Lotti et al., 2019b). The stated inconsistencies are foreseeable given that the ANAMMOX EPS extraction practices employed in the number of studies in the literature have been primarily established for other categories of biomass, with significantly different mechanical characteristics (Lotti et al., 2019b) (Lin et al., 2018) (Ding, 2016). Given the insufficiency of ANAMMOX sludge, in addition to its slow growth, EPS extraction and characterization practices ought to vary from other conventional sludge (Ding, 2016). It is of great significance to primarily establish a new extraction scheme which is entirely distinctive for the biomass being analyzed rather than implementing practices that are created in former frameworks as presented in most existing literature articles.

Table 3-3 is a comprehensive summary of the recent extraction and characterization methods developed for ANAMMOX bacterial populations. In a recent study done by Boleij et al., 2019, two individual extraction means; alkaline (NaOH) (Boleij et al., 2018) and ionic liquid extraction (Wong et al., 2019) were evaluated, and the retrieved polymers were scrutinized to assess the impact of diverse extraction practices, improving the conception on the principal extraction mechanisms (Table 3-3). In this study the ANAMMOX granular sludge was collected from three full scale plants and one lab-system. A live/dead staining was performed on the sample after alkaline (NaOH) extraction, and ionic liquid extraction treatments were conducted to have a clear image of the cell viability in the samples. Additionally, FTIR of the extracted EPS was recorded, and excitation-emission matrix was performed. As illustrated in Table 3-3, the extracted EPS were evaluated by SDS-PAGE (sodium dodecyl sulfate e polyacrylamide gel electrophoresis), furthermore, mass spectrometry (MS) analysis was completed. Exponentially Modified Protein Abundance Index (emPAI) analysis was also implemented, to properly estimate the protein abundance in the samples (Boleij et al., 2019). This study was able to link the EPS characteristics

to the dominant species found in the reactor consortium, discounting the reactor configuration and operational conditions. Both extraction methods were able to solubilize the ANAMMOX granules, and a range of proteins and glycosylated proteins were recovered. More great molecular weight acidic glycoconjugates were present in the NaOH extraction method rather than the ionic liquid extraction (Boleij et al., 2019). A comprehensive comparison between the two extraction methods indicated that both methods have a tendency to instigate substantial damage to the cells, and when the granules have dense and robust structures, cell damage is inevitable during EPS extraction (Boleij et al., 2019).

Table 3-3 Summary of several recent studies on EPS characterization and extraction methods

Sludge/ System	**Main Objectives**	**Summary of extraction/characterization method**
Granular sludge/ three full scale plants in Netherlands and one lab-scale in Singapore	• Compare two extraction methods, on different sludge with an emphasis on proteins	**EPS Extraction**: Alkaline (NaOH) extraction, Ionic liquid extraction, **Other analysis**: FTIR of the extracted EPS, Excitation-emission matrix, SDS-PAGE, MS, emPAI analysis
Granular sludge/ Full-scale ANAMMOX reactor in Dokhaven, Rotterdam	• Comprehensive assessment of glycoproteins • Better understand the EPS structure	**EPS Extraction**: Freeze-drying, centrifugation, precipitation, lyophilization **EPS composition**: Purge and trap chromatograph + ion chromatograph, Bicinchoninic acid method, Phenol sulfuric acid assays

Granular sludge/ parent lab-scale reactor	• Exact role of stratified EPS in the early adhesion of ANAMMOX consortia	**EPS Extraction**: Modified heat method, **Other analysis**: 3-D EEM fluorescence spectra measured using a FluoroMax-4 spectrophotometer, FTIR spectrometer, QCM-D technique (Q-Sense Analyzer, Sweden), Aggregation assays
Granular sludge/ Full-scale ANAMMOX reactor in Rotterdam	• Development of a robust chemical method for the extraction of large amount of EPS • Production of a hydrogel composed of ANAMMOX EPS • Evaluation of filming properties of EPS	**EPS Extraction**: biofilm matrix solubilization in 0.1 M NaOH, centrifugation, acidification with 1M HCl, precipitation, demineralization, dialyzing against milli-Q water and freeze drying **Other analysis**: Oscillatory shear measurement, differential scanning calorimetry, TEM, atomic force microscopy, small-angle X-ray scattering in addition to water and grease resistance of EPS-based coatings
Granular sludge/ Full-scale ANAMMOX reactor in Rotterdam	• Develop a strong and Replicable EPS extraction method special for ANAMMOX biofilms	**EPS Extraction**: Incubation for 4 h in 0.1M NaOH, breakdown of granular initial structures, centrifugation, alkaline pellet development by microorganisms, acidification with 1M HCl, precipitation, freeze drying, dialyzing against milli-Q water and repeated freeze drying

	• Maximize the overall EPS extraction yield • Minimize cell lysis • Extract the structural components	**Other analysis**: phenol-sulfuric acid assay, bicinchoninic acid, the Lowry and Modified-Lowry methods, DLS, UV–Vis, CD, FTIR spectra
Flocs, biofilm and granular sludge /18 different lab and pilot-scale reactors	• Elucidate the relationship between the properties of stratified EPS and the properties of ANAMMOX biomass	**EPS Extraction**: Modified slime and LB-EPS methods **Other analysis**: EEM Fluorescence Spectroscopy and PARAFAC Analysis, Quantitative Real-Time PCR Assay, FTIR,
Lab-scale sequential batch reactor	• Examining ammonium, nitrite and hydrazine addition impacts	**EPS Extraction**: biomass transfer to micro-tube, centrifugation, uniforming of sediments, repetition of centrifugation, repetition of uniforming of sediments **Other analysis**: BCA method, phenol-sulfuric acid method
Granular sludge/ 4-liter lab-scale reactor	• Address the challenge of processing ANAMMOX EPS,	**EPS Extraction**: freeze drying of granules, addition of EMIM-Ac/N,N dimethylacetamide (DMAc) mixture, incubation in water bath, ionic liquid-soluble fraction (IL-Sol) captured by

	• Demonstrate how to subsequently isolate a potentially conserved ANAMMOX extracellular protein	precipitation with ethanol, centrifugation, cleaned by dialysis, and lyophilized **Other analysis**: Nuclear magnetic resonance spectroscopy of acid-digested granules, P NMR analysis of soluble EPS, Staining and microscopy, Sodium dodecyl sulfate-polyacrylamide gel electrophoresis analysis of the soluble EPS, Liquid chromatography with tandem mass spectroscopy analysis of gel bands, immunoblot analysis, Size exclusion chromatography analysis with fluorescence detector, Global protein analysis of Ca. B. sinica-enriched granules and Carbohydrate analysis
Biofilm sludge/5-liter lab-scale reactor	• Expand the perception on the major features of EPS in attached bioflm ANAMMOX granules • Content variation and concentration evaluation of EPS • Study of granular shear strength	**EPS Extraction**: Modification of cation exchange resin (CER) approach **Other analysis**: Lowry method with bovine serum albumin, phenol-sulfuric acid procedure with glucose, size distribution, settling velocity and shear strength, SEM, shear strength analysis, integrity coefficient analysis

Granular sludge/ lab-scale UASB reactors	• Investigation of effects of five different sludge EPS on ANAMMOX bacteria activity	**EPS Extraction**: Heat technique procedure **Other analysis**: Polysaccharides content of EPS measured by anthrone-H_2SO_4 method using glucose as benchmark, protein substance of EPS measured by the BSA

**References: (Jianbo Guo et al., 2016) (Y. Zhang et al., 2016) (Wong et al., 2020) (Ganesan and Vadivelu, 2019) (Jia et al., 2017) (Lotti et al., 2019b) (Lotti et al., 2019a) (Wang et al., 2019) (Boleij et al., 2018) (Boleij et al., 2019)*

Boleij et al. (2018) explored EPS extraction from granular biomass originated from a full-scale ANAMMOX plant. This study presents in detail the classification of ANAMMOX glycoproteins to better understand the EPS structure. For EPS extraction, the freeze-dried ANAMMOX granules were cultivated in 0.1 M NaOH (50 mg/ml) for 5 hours, agitated with a magnetic stirrer at 400 rpm. Following the 20 minutes' centrifugation in 4000 rpm at 4°C, the pellets were removed. Supernatant polymers were precipitated by reducing the pH to 5 with 1 M HCl. Polymers were then accumulated by centrifugation at 4000 rpm for 20 minutes at 4°C then lyophilized (Table 3-3). The elemental composition of the extracted EPS was analyzed by a purge and trap chromatograph combined with an ion chromatograph. The proteins were measured in the role of Bovine Serum Albumin equivalents using the bicinchoninic acid approach (Boleij et al., 2018). Carbohydrates were determined as glucose equivalent employing phenol sulfuric acid assays. The results of the study proved that *Ca*. Brocadia sp was the principal species in ANAMMOX granular sludge samples, and the protein and carbohydrate content analysis from the extracted EPS were 599±4 and 49.0±2 mg/g EPS, respectively. Boleij et al., (2018), concluded that, since the EPS has a complicated system, no distinct approach can extract the entire EPS constituents.

Given that EPS is acidic by nature, the breaking down process may decrease the pH, so elevated concentrations of NaOH were necessary to sustain an elevated pH throughout the experiment..

Glycoproteins and acidic glycoconjugates were detected through staining experiments. This study found a high abundance of glycoprotein, which was heavily glycosylated with heterogeneous O-glycan. The novelty of this specific study was investigating the glycoproteins, while most studies only study proteins and polysaccharides separately (Boleij et al., 2018).

Further review of the results indicates that glycoprotein is an S-layer protein mainly detected as the cell surface structure of prokaryotes (Sleytr et al., 2014). It would be of significance to examine the share of S-layers in granules matrix structure. The most significant approach to distinguish S-layers is by microscopy, envisioning their particular arrangement on the cell surface (Boleij et al., 2018). Nevertheless, due to the compressed EPS surrounding the cells, it is further problematic to perceive the S-layer proteins in mature granules compared to the suspended biomass from lab systems. Presently the extracellular matrix of biofilms is acknowledged as an extremely complicated and systematized arrangement and even reflected to be equivalent to the extracellular matrix of multicellular organisms. Outstandingly, a high number of the prokaryotic protein glycosylation with advanced intricacy has been linked with bacterial pathogenic features (Sleytr et al., 2014); on the other hand, they were hardly ever illustrated in natural biofilm populations (Boleij et al., 2018). Understanding the prospective function of the acknowledged glycoprotein in ANAMMOX granules requires detailed analyses on the protein localization reviewing the potential if it is appended to the exterior of the cell wall or incorporated in the interior matrix.

In a recent study by Wang et al. (2019), and as indicated in Table 3-3**,** the exact role of stratified EPS in the early adhesion of ANAMMOX consortia was examined. Various studies focused on investigating the role and properties of EPS in ANAMMOX bacteria aggregation (Z. Chen et al., 2019) and dissimilarity among ANAMMOX bacteria EPS and other microbial communities (Hou et al., 2015). Yet adhesion properties of ANAMMOX bacteria with or without the EPS has been

neglected. The extended DLVO theory was utilized to differentiate diverse repulsion and attraction forces among microbes however, the adhesion of microbes to abiotic surfaces was ignored (Hou et al., 2015). In this study, the principal mechanism of stratified EPS on the preliminary establishment of ANAMMOX biofilms is deliberated, and the results are anticipated to assist in the cultivation of ANAMMOX biofilms and the full-scale employment of ANAMMOX biofilm processes (Wong et al., 2019). The ANAMMOX sludge used in the study was brought in from a parent lab-reactor. A modified heat practice was employed to extract EPS, S-EPS, LB-EPS and, TB-EPS (Li and Yang, 2007), while the role of stratified EPS sub-fractions in the adhesion of ANAMMOX consortia was analyzed using aggregation assays. The adherence and adsorption properties of the extracted stratified EPS sub-fractions and ANAMMOX sludge samples on abiotic surfaces were analyzed using the QCM-D technique (Q-Sense Analyzer, Sweden) with gold-coated sensor chips to mimic the abiotic surface (Wang et al., 2019). The study results confirm the presence of proteins, polysaccharides, and humic acids as the main components in the EPS of ANAMMOX granules. The total and individual concentrations of proteins, polysaccharides and humic acids increased significantly from S-EPS to LB-EPS and from LB-EPS to TB-EPS ($p < 0.05$). This study showed that the proteins to polysaccharides ratio in LB-EPS was higher than S-EPS and TB-EPS, and as a result, LB-EPS has the most unfavorable effect on the granular strength factor. The composition analysis and the 3D-EEM showed that TB-EPS was the most abundant EPS sub-fraction. The results indicated that the stability (ability to resist aggregation and remain in a uniformly dispersed state in the solutions) of ANAMMOX consortia weakened after each EPS sub-fraction extraction (Wang et al., 2019).

All studies presented in Table 3-3, have a comparable objective of stipulating a proficient method for ANAMMOX EPS extraction and characterization. Yet, there is a lack of a specific extraction

method for ANAMMOX EPS in biofilms which incorporates the structural fraction, the necessity for evocative assessments of ANAMMOX EPS and the structural components. There is a need for a robust and reproducible method to extract structural EPS with elevated effectiveness and fill in the current gaps. The main targets of future studies should focus on increasing the inclusive EPS extraction with reduced preferential extraction of particular components, a comprehensive evaluation of cell lysis to potentially lessen the rate, and extract the structural components accountable for the mechanical assets of the biofilm. An expressive evaluation of ANAMMOX EPS can lead to additional innovation towards the potential modification from the existing treatment schemes to a circular economy perspective.

3.8. Gaps in ANAMMOX EPS extraction and characterization methods

Due to ANAMMOX bacteria's high tendency to grow in either granules or biofilms, the physical and chemical properties of the aggregated structure, which is mainly dependent on the EPS composition, is of great importance (Cirpus et al., 2006). Characterization of the extracellular matrix composition is vital for understanding the formation and stability of granular sludge (Flemming and Wuertz, 2019). EPS matrix composition, structure, and function are poorly studied in ANAMMOX granular sludge or other aggregated forms. Comprehension of EPS physical and chemical properties and the composition and formation in ANAMMOX can aid in stimulating the bacterial aggregation process and reduce the enrichment time requirements. A full understanding of the matrix composition leads to morphology adjustments based on process need and paving the way towards biopolymer production from granular sludge (Boleij, 2020). Sorting out the critical elements of biopolymers, including the interrelation and constitution of ANAMMOX granules principally relies on the extraction methods implemented for EPS and components characterization

(Feng et al., 2019). Nevertheless, there is yet a deficiency of standard techniques for EPS characterization and extraction.

In terms of EPS component characterization, the analysis of proteins and polysaccharides is inaccurate because of high discrepancies. Protein sequencing is done by translation of DNA, and as a result, there are significant struggles in post-translational modifications of the proteins such as; glycosylation, methylation and sulfation (Boleij, 2020). Comparably, polysaccharides encompass several monosaccharides linked by glycosidic bonds, and due to the enormous variety of the monomers and glycosidic bonds, identifying the polysaccharide's structure becomes a challenge (Michael T. et al., 2008). Existing EPS analyses methods are typically inadequate and can only assess the general quantification of polysaccharides and proteins by colorimetric approaches. These traditional colorimetric methods are only proficient for classifying separate classes of molecules, and there is a major gap in the provision of the macromolecular structure of the components however, there are a number of studies indicating the presence of glycoconjugates in the EPS (Boleij et al., 2018) (Tan et al., 2015) (Boleij, 2020). Prokaryotes glycoproteins are poorly studied, and there is a significant scarcity due to the complexity and vast diversity of glycosylation (Tan et al., 2015). As a result, a comprehensive analysis of the protein glycosylation in a pure environmental granular sludge sample is significant. Previous research mainly proposed colocalization and orthogonal staining experiments for glycoprotein characterization in EPS, yet there is a lack of broad parallel molecular classification to dictate evidence for the glycosylated proteins in EPS (Boleij et al., 2018). These examinations are not capable of indicating the actual composition of EPS, and a more specific characterization plus definite objectives are essential for a better understanding of the EPS structural functions in ANAMMOX (Boleij, 2020).

Several EPS characterization techniques are available to investigate the configuration and the potential contribution in natural living systems. Quantitative approaches introduce the overall level of proteins, nucleic acids, humic-like constituents, uronic acids, polysaccharides, etc. To identify the comprehensive characteristics of EPS molecules, diverse qualitative techniques are established (Table 3-2). These methods include; UV detection, confocal laser scanning microscopy (CLSM), gas chromatography, size exclusion chromatography (SEC), 3-dimensional excitation-emission matrix fluorescence spectroscopy (3D-EEM), Fourier transform infrared spectroscopy (FT-IR), and so on (Sheng et al., 2010). Based on the results of different studies, 3D-EEM was known to be a simple and accurate approach for organic compound identification (Kunacheva and Stuckey, 2014). SEC method delivers qualitative data regarding the EPS distribution in evident molecular weight from sludge samples (Comte et al., 2007), while in the UV detection method, wavelengths of 210 nm, 254 nm, and 280 nm are presumed to resemble diverse elements of EPS molecules (Bhatia et al., 2013). Correspondingly, hydrophobicity is an imperative factor in EPS characterization. Hydrophobic interaction is significant for sludge settling, flocculation, in addition to granulation. Comprehension of hydrophobicity is accomplished through contact angle determination or XAD resin fractionation (Hou et al., 2015).

Cation exchange resins have developed to be the most broadly used system because of high efficiencies, lessened cell death, and ease of solid/liquid separation meant for EPS withdrawal from floccules and granules (Sheng et al., 2010). Based on a study done by (Bourven et al., 2013), characteristics of EPS extricated by divergent physical and chemical approaches on various categories of sludge following by partition by SEC columns were studied. The study results indicated that physical approaches merely alter the comparative absorbance, whereas chemical

procedures manipulate the physiognomies of EPS fragments as suggested by the atypical peaks that existed on the chromatograms (Bourven et al., 2013).

One other important issue with EPS research is the ineffectiveness of extraction methods (Figure 3-2), resulting from limited information on EPS composition and a lack of specific targets (Neu and Lawrence, 1999). In granular sludge, EPS is directly involved in physical structure formation (Felz et al., 2016). A critical step in EPS extraction from granular biomass, is solubilization of the polymers, and as a result, if the granules remain integral and undamaged through the course of extraction, structural polymers are not recovered (Felz et al., 2016). Since different bacterial communities have different EPS polymeric structures, the solubilization method varies case by case (Boleij et al., 2019). There are no regulated or standardized extraction and characterization method for EPS in the ANAMMOX process (Boleij et al., 2019). A number of conventional EPS extraction approaches focus on the prevention of cell lysis, but as a result, there is limited structural polymer solubilizing associated with the methods, and the polymers in the biofilm and granules are not analyzed. Several physical and chemical extraction techniques or a mixture of both and enzyme digestion are used (Neu and Lawrence, 1999) (Figure 3-2). A few of the physical methods employed in the literature consist of centrifugation, sonication, and heat treatments plus chemical processes including extraction drivers such as bases, EDTA, acids, cation exchange resins, plus organic solvents. Two other previously proposed extraction methods which are capable of solubilizing and recovering EPS from ANAMMOX granular sludge are alkaline (NaOH) extraction (Boleij et al., 2018) and ionic liquid extraction (Wong et al., 2019). However, there has been no direct comparison to comprehend whether the two methods lead to comparable extracted EPS or not. The selection of procedures varies based on the sludge source in addition to the factors being evaluated. Lack of target for EPS extraction and variable extraction conditions, imposes a

major issue in comparing different studies results (Boleij, 2020). Even though numerous methods have been established for ANAMMOX EPS extraction, stated approaches can either be damaging or have inadequate matrix solubilization (Wong et al., 2020).

Electing an applicable extraction method for extracellular polymeric substances is fundamental, as it dramatically influences the yield, configuration, and properties of the EPS. A standard EPS extraction scheme is supposed to be efficient, trigger minimum cell lysis, and not distress the EPS structure. As highlighted in Figure 3-2, numerous procedures have been established and employed to extract EPS from ANAMMOX cultures however, none of these methods can extract all the EPS solely from ANAMMOX microbial aggregates. Since there is still a lack of a collective extraction scheme for quantitative extraction of EPS from ANAMMOX microbial aggregates, an inclusive system must be designated and optimized. Method designs require numerous EPS extraction techniques to be evaluated then the most suitable method should be selected. An integrated extraction is needed to aim various EPS elements, and repeated extractions are constantly required to attain a high extraction proficiency. Moreover, cell lysis factors should be assessed thoroughly for the combined and repeated extractions.

3.9. Potential applications of ANAMMOX EPS

Bacteria are capable of synthesizing a broad scope of biopolymers that provide a variety of different biological applications, and the produced materials are appropriate for several industrial and medical practices (Rehm, 2010). Additional knowledge on the genome of the EPS creator microbes will lead to the progression of novel approaches so that adequate enrichment of EPS is possible. It will potentially increase the EPS production rate and the development of engineering strategies for improved biopolymer properties. A boosted comprehension of the fundamental processes focused on EPS biosynthesis coupled with the adjustment of these procedures is vital

for potential genetic, metabolic, and protein-engineering methodologies to generate biological-based polymers (Schmid et al., 2015). Regardless of the growing attraction of bacterial EPS, the comprehension of the particular routes initiating its production is highly restricted. Therefore, it is critical to classify genes/proteins associated with the final phases of EPS generation and assess the bacterial distribution. Conducting a phylogenomic examination concentrating on the representative genes/proteins of the main methods of microbial EPS building and transfer can potentially aid in reaching this goal.

The extent of the existing information on EPS' environmental uses is still inadequate, resulting in major ambiguity of various sides, from EPS production and recovery to its role in pollution control applications (T. T. More et al., 2014). As indicated in Figure 3-3, EPS can be utilized in a mixture with multivalent cations as a flocculant to remove suspended solids and natural organic matters from wastewater streams, to improve the effluent quality (Nontembiso et al., 2011) (Gong et al., 2008). Studies have shown promising results on the effectiveness of EPS for dye removal (caused by untreated textile industrial wastewater) (Buthelezi, 2008) as well as metal removal/recovery (Guibaud et al., 2003) from wastewater effluents (Figure 3-3). Generally, significant amounts of chemical polymers are utilized to complete mechanical sludge dewatering, resulting in a costly process for the plant; however lately, EPS has been considered a potential bioflocculant material in sludge dewatering (More et al., 2010). EPS can eliminate toxic organic complexes present in diverse types of wastewater, sludge, and soils (Zhang et al., 2011). Another potential application of bacterial EPS is their usage in leachate treatment instead of conventional chemical coagulants and flocculants (Zouboulis et al., 2004) (Kaur et al., 2019). The majority of the reviews on environmental EPS applications in wastewater treatment and toxic organic compound removal were completed in lab-scale, yet conducting pilot-scale experiments could shed light upon the

realistic usages of EPS. Besides the potential environmental applications, as determined in Figure 3-3, microbial EPS can make an enormous impact on food (van den Berg et al., 1995) (Lindgren and Dobrogosz, 1990), pharmaceutical (Okutani, 1985) (Vanhooren and Vandamme, 2000), biomedical, wastewater treatment, bioremediation and, etc. fields (Kumar Singha, 2012) (Iyer et al., 2006). A few recent studies have focused on the potential contribution of bacteria-derived biopolymers as drug carriers attaining extended circulation period, lessening toxicity and shielding from enzymatic destruction, improving antitumor competence, and monitoring drug discharge (Mokhtarzadeh et al., 2016).

In a specific study conducted by Lotti et al. (2019a), the hydrogel was generated from ANAMMOX EPS recovered from waste ANAMMOX granular sludge, leading to an opportunity towards potential application of EPS-based substances as an economical and sustainable substitute for regularly implemented paper coatings. The described characteristics of EPS-based materials can pave the way towards assessing its prospective uses as a resource in the future of the circular economy.

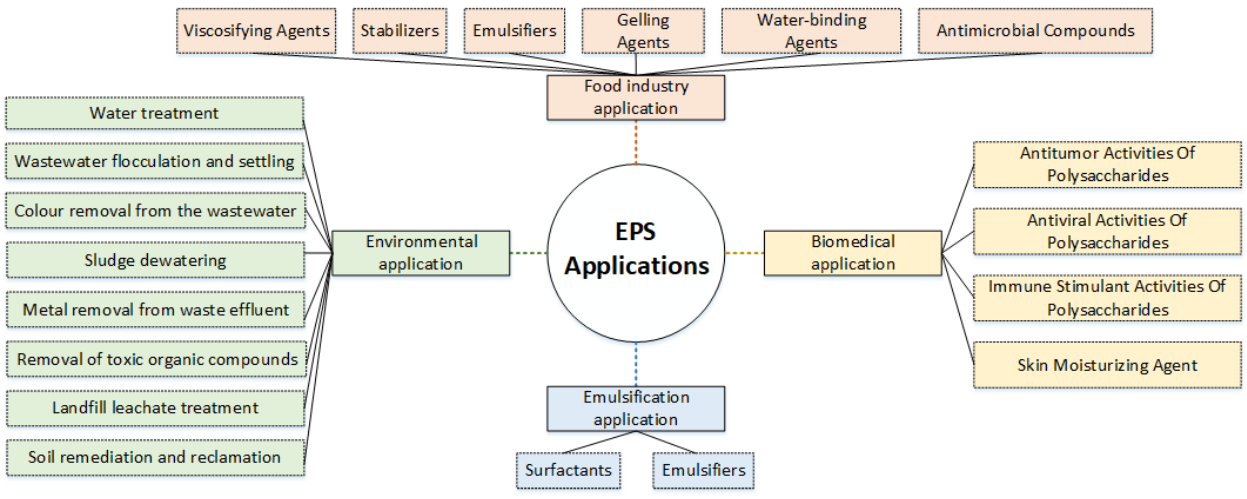

Figure 3-3 Potential applications of EPS

The employment of bacteria as a renewable source for biopolymers formation can introduce great value to industrial avenues and greener technologies. The environmental complications associated with climate change and greenhouse gas production have become critical global concerns, mainly confronting contaminated waste, pollution, depletion of natural resources, and environmental depreciation (Luzi et al., 2019). In parallel, polymer science and engineering studies are shifting towards promoting environmental-friendly polymers to minimize the detrimental effect of plastic leaks on ecosystems (Kumar et al., 2020). Ecological benign systems are the key answers to improve treatment systems; however eco-friendly polymeric methods are merely operated for a few exclusive products, mainly because of the restrictive features compared to conventional polymers, for example, high cost and inadequate mechanical and thermomechanical properties (Koncar, 2019). Bio-based polymers employment in highly challenging applications is poorly studied, explained by the following reasons; low durability of bio-substances in long-term applications, immediate need for fundamental adjustments of current processes, lower costs of oil-based polymers compared to bio-polymers, and less efficient performances of biological polymers weigh against oil-based mediums (Koncar, 2019) (Kumar et al., 2020).

Bio-polymers hold a very small segment of the whole inclusive plastic market with a share of less than 1% of the entire market. Advancements in biopolymers recovery from wastewater treatments sludge and the potential appliances can lead to an escalation in the ecological and economic sustainability of the processes (Lotti et al., 2019a). Slow-growing ANAMMOX bacteria self-assemble into dense granules/biofilms to enhance their bacterial activity and metabolism by expressing EPS. Considering the rapid proliferation of ANAMMOX biofilm-based technologies, ANAMMOX EPS signifies a new resource to upgrade the required modification from wastewater treatment to biorefineries (Wong et al., 2020).

It is a matter of concern to understand whether EPS recovery can aid in proceeding towards a circular economy or not. Improved resource recovery schemes and better biofilm management are two of the principal gains of expanded perception of EPS matrix. A major evolution of renewable resources led to EPS being an attractive path promoting the reduction of reliance on fossil fuels and increased sustainability and wastewater treatment economics. EPS-like polymers are merely originated from natural resources, including wastewater, and cannot be obtained from oil-based chemicals (Seviour et al., 2019). Understanding more about EPS can aid in targeting different engineering methods to promote more desirable properties. Yet, before shifting in the direction of enhanced control and engineering of biofilm-based systems in wastewater treatment, there is a call for identifying which molecules are the main contributors to each particular biofilm functions. These advancements all rely on improved EPS extraction, chemical characterization, biophysical analysis, and genetic assessments. In the recent future, we can look forward to a substantial growth of value-added products and technologies originated from bacterial EPS, principally established for a market niche.

3.10. Discussion and potential future work on EPS in ANAMMOX

The growing demand for a more sustainable advancement leads to a modification from pollutant removal in the direction of resource recovery by accepting wastewater as a resource not a waste stream (Kehrein et al., 2020). This review's goal was to investigate the ANAMMOX process from a fundamental standpoint to understand how far the process advancements are from enabling resource recovery. The main incentive behind this review was to build a fundamental perception of ANAMMOX microbiology and metabolism fundamentals and link it to identifying methods capable of extracting and recovering EPS products from ANAMMOX process that can ultimately be fed into the circular economy. This matter is not a substantial alteration comparing to the present

procedures however, rather than only focusing on the nitrogen removal aspect of the process, more emphasis will be on recovery. This paper then seeks to highlight the current gaps in ANAMMOX EPS extraction and characterization methods by providing a holistic overview of the most recent advancements and technologies. Successful implementation of EPS recovery from the ANAMMOX process requires a proactive administration of hypothetical bottlenecks coupled with obtaining an advanced perception of granular EPS matrix concept in the ANAMMOX process. Quantitative and qualitative EPS analysis is required to establish a correlation between EPS characteristics and process parameters.

EPS presence becomes critical for stable ANAMMOX reactor operation, as EPS has an immense drive to mediate dense biofilm and granule formation. Additionally, one of the reasons for unstable ANAMMOX processes can be related to inadequate EPS formation. The restrictive factor in EPS analysis is poor solubility and heterogeneity of the substances (Boleij et al., 2019). A number of established EPS extraction advances, target restriction of cell lysis, but there is limited structural polymer solubilizing associated with the methods, and the polymers in the biofilm and granules are not analyzed. Methods for protein and polysaccharides characterization in EPS primarily included colorimetric assays that have fairly low accuracy and might cause radical over or underestimating particular elements . These traditional colorimetric methods are only proficient in classifying separate classes of molecules, and there is a major gap in the provision of the macromolecular structure of the components (Boleij et al., 2018).

The conventional solubilization methods used for EPS extraction require high volumes of concentrated sludge, and the used sludge could not be recovered. ANAMMOX-based processes, carried out by extremely diverged *Planctomycetes*, struggle with low biomass yields and extended doubling times, introducing restrictions for efficient process applications (Kocamemi et al., 2018).

Considering the extended cultivation periods, repeated sampling and extraction are not cost-effectively reasonable for laboratory and pilot-scale systems . Moreover, due to ANAMMOX bacteria's unique structure, in which the cells contain no peptidoglycan, more moderate extraction methods of EPS are selected to prevent any potential high degree cell lysis. Given that the extraction protocols employed for ANAMMOX biofilms are originally designed for other biomass types with different mechanical properties, extreme inconsistencies are perceived. Consequently, bearing in mind that EPS composition is strongly based on the bacterial community that is producing it and depends on the biomass aggregation status, it is fundamentally compulsory to develop a specific extraction method for the ANAMMOX process (Lotti et al., 2019b).

One potential substitution for the existing photometric detection of EPS components could be *in-situ* visualization of sludge after selective staining. This specific approach delivers data on the spatial dissemination of various EPS constituents in the aggregated structures. This method demands minor volumes of cells, and as a result, it may perhaps be practical as a systematic analysis and an evaluation of process performance (Ding, 2016). Additionally, there is a window for sampling from reactor sections to allow for a promoted representativeness. For instance, SEC, together with fluorescence and UV, delivers information on the macromolecules' weight dissemination. It is of utter significance to extract and decontaminate the particular segment and lead to additional protein and/or polysaccharide structural examination (Ding, 2016).

A concluding statement on the perception of EPS analysis in ANAMMOX bacteria is the extracellular enzyme. Different researchers believe that protein has the major role in ANAMMOX EPS; consequently a large number of studies on extracellular protein emphasized the structural character in sustaining the EPS matrix (Kocamemi et al., 2018) (Lotti et al., 2019b) (Ding, 2016). Considering that extracellular enzymes were supposed to be capable of hydrolyzing particular

organics, it is valuable to determine its exact enzymatic activity principally intended for layered structural granules (P. Zhang et al., 2015). Without appropriate reference proteins, direct functional assignment is needed, which primarily demands non-destructive extraction and isolation of relevant functional EPS . On the other hand, at this point, no specific technique for isolating a functional EPS from ANAMMOX biofilms has been illustrated (Wong et al., 2020).

3.11. Conclusion

Anaerobic ammonia oxidation is a more sustainable method of nitrogen removal from wastewater compared to conventional processes. ANAMMOX bacteria have a strong propensity to develop in aggregate forms and the competence to self-assemble by EPS production in biofilms or granules. Biofilm generation and granulation process assists the syntrophic interactions with other bacteria, augments the sludge retention, and boosts the bacterial tolerance to environmental stresses, shear forces, and salinity. Understanding the formation of ANAMMOX aggregates requires significant elucidation of the EPS composition and their broader function in microbial communities. A number of studies focused on identifying ANAMMOX EPS, yet there is a poor perception of primary data on the composition, molecular structure, and functions of sludge EPS. Extracting EPS from ANAMMOX granular sludge is an impending product-recovery path, yielding a valuable end-product. Identifying key biopolymers within ANAMMOX EPS has always been a major challenge, and although there have been several efforts to extract and characterize ANAMMOX EPS, reported methods might either be destructive, achieving poor matrix solubilization or inefficient. Several valuable findings and breakthroughs concerning the ANAMMOX EPS extraction, distribution in microbial aggregates, analytical procedures, and characteristics are elaborated in this comprehensive review.

CHAPTER 4

Parin Izadi[a] , Parnian Izadi[a] , Ahmed Eldyasti*[a]

[a] Civil Engineering, Lassonde School of Engineering, York University, 4700 Keele Street, Toronto, ON, Canada , M3J 1P3

* Corresponding author

Authors' contributions All authors were directly involved in the process of concept design of the literature review. Material preparation, data collection and was performed by Parin Izadi and Parnian Izadi, mutually. The first draft of the manuscript was written by Parin Izadi and Parnian Izadi commented on previous versions of the manuscript. Dr. Ahmed Eldyasti drafted and critically revised the work. All authors read and approved the final manuscript.

Review: Towards Mainstream Deammonification: Comprehensive Review on Potential Mainstream Applications and Developed Sidestream Technologies [2]

Abstract

Deammonification (partial nitritation- ANAMMOX) is a favorable and innovative process for treating nitrogen-rich wastewater due to decreased oxygen and carbon requirements at very high nitrogen loadings. The bacterial groups responsible for this process are anaerobic ammonium oxidation (ANAMMOX) bacteria in symbiosis with ammonium oxidizing bacteria (AOB), which have an active role in the development of nitrogen removal biotechnology in wastewater. Development and operation of sidestream deammonification processes has augmented since the initial full-scale systems, yet several aspects mandate additional investigation and deliberation by the practitioners, to reach the operating perspective, set for the facility. Process technologies for the treatment of streams with high ammonia concentrations continue to emerge. Correspondingly further investigation towards the feasibility of applying the deammonification concept in the mainstream treatment process is required. Mainstream deammonification can potentially improve achieving more sustainable and energy-neutral municipal wastewater treatment; however feasible applications are not accessible yet. This critical review focuses on a comprehensive assessment of the worldwide lab-scale, pilot-scale, and full-scale sidestream applications and identifying the major issues obstructing the implementation of mainstream processes, in addition to the designs, operational factors, and technology advancements at both novel and/or conventional levels. This review aims to provide a novel and broad overview of the status and challenges of both sidestream and mainstream deammonification technologies and installations worldwide to assess the global perspectives on deammonification research in recent years. The different configurations, crucial

[2] A version of this chapter has been published in the Journal of Environmental Management, Volume 279, November 2020, https://doi.org/10.1016/j.jenvman.2020.111615

factors and overall trends in the development of deammonification research are discussed, and conclusively, the future needs for feasible applications are critically reviewed.

Keywords: ANAMMOX; Deammonification; Sidestream; Mainstream; Innovative technologies; Design and operation

4.1. Introduction

The release of nitrogenous compounds into municipal wastewater is the principal impel of eutrophication and oxygen diminution in receiving water bodies (J. Li et al., 2018). The autotrophic ANAMMOX (ANX) process, in which ammonium and nitrite are directly transformed into dinitrogen gas under anoxic conditions (Qiu et al., 2020), is gaining interest because of the strategic significance of energy conservation. ANAMMOX is typically operated in conjunction with partial nitrification known as deammonification process, where ammonium is oxidized to nitrite using ammonium oxidizing bacteria (AOB), supplying nitrite for ANAMMOX bacteria (Y. Miao et al., 2019).

To date, nineteen different ANAMMOX species have been detected, all belonging to the phylum Planctomycetes (Kuenen, 2020). Recent advancements succeeded to describe at least 25 ANAMMOX species from mixed consortia within six different ANAMMOX genera as *Candidatus* (well characterized but not studied in pure culture) with a range of 87-99% for 16s RNA species characteristics (Kallistova et al., 2016) (Ding et al., 2020). The doubling time associated with ANAMMOX bacteria is between 10 to 30 days resulting in them being defined as slow growers (Niftrik et al., 2004). The initial estimates of the ANAMMOX bacterial growth rate in the order of 10 days doubling time showed a specific growth rate of 0.0027 h^{-1} (Kuenen, 2020). The engineering application of ANAMMOX bacteria is interesting and is principally reliant on the capacity to shunt nitrification at nitrite efficiently. Thus, the path towards efficient

deammonification is the proper balance between the different microbial groups involved (Lackner et al., 2014).

High nitrogen level wastewaters with low C:N ratios are mainly produced by specific domestic and industrial processes. One of the most common examples of high-nitrogen wastewater is reject water, also known as sidestream, which is a product of anaerobic digestion of solid waste in the treatment plants, with elevated levels of nitrogen and low concentrations of biodegradable COD (a ratio of below 1) (Zekker et al., 2020). The process application for the mainline of municipal wastewater (mainstream) treatment with low nitrogen levels and low temperatures, is of great practical interest. In mainstream wastewater treatment, there are several challenges linked to ANAMMOX process applications: depressed temperature, organic content and, low TOC/TN ratio (Laureni et al., 2016b). Judge against sidestream, the critical complication affecting the effective implementation of ANAMMOX in mainstream is wastewater's low annual average temperature (12.5–19°C in northern climates) (Lotti et al., 2015).

Deammonification process, discovered in 1999, has been effectively applied for sidestream centrate treatment (Nifong et al., 2013). Nitrogen is removed through a two-step reaction in which AOB and ANX play the leading roles (Nifong et al., 2013) (Neethling, 2014). Approximately half of the loaded ammonia is converted to nitrite by AOB (Neethling, 2014), leaving the remaining ammonia for ANX bacteria (Pereira et al., 2019)(Rikmann et al., 2017). In the anaerobic part of the process, nitrogen gas is generated through the oxidation of NH_4^+ with NO_2^- as the electron acceptor (L. Miao et al., 2019) (Neethling, 2014). ANAMMOX includes the energy-producing reaction of NH_4-N oxidation by NO_2-N and the uptake of CO_2 plus nutrients via autotrophic ANAMMOX bacteria used for biomass growth (Jetten et al., 2009) (Van Hulle et al. 2010). Deammonification reduces the oxygen demand by nearly 60%, besides initiating a major decrease

of carbon requirement and biomass production by 100 and 80%, respectively, in comparison with the conventional nitrification-denitrification process (Yang et al., 2018) (Neethling, 2014) (Feng et al., 2017).

Advantages of the deammonification process, including the lessened amount of biomass generation, zero external carbon addition, along with a lowered aeration energy requirement as oxygen provision, against the conventional nitrogen removal processes are indicated in Table 4-1. Data presented in Table 4-1 are based on the reported stoichiometry, with acetate as the exogenous carbon source for denitritation and denitrification (Güven et al., 2005). As indicated in Table 4-1, the COD demand for deammonification process is approximately 30% and 45%, lower than nitritation/denitritation (with 89% efficiency in denitritation) process and conventional nitrification/denitrification (with 89% efficiency in denitrification) processes, respectively (He et al., 2015b). Deammonification has been proven to reduce ammonia up to 90-95% and allow for a total nitrogen decline of 80-85%. The initial full-scale facility was built in 2001 (Neethling, 2014). Ever since the number of installed systems promptly augmented with a growing number in the design and construction phase (Bowden and Stensel, 2016), some operating on sidestream dewatering reject water and some others mainly focusing on industrial applications (Winkler et al., 2012) (Kartal et al., 2007).

Due to the rising public concerns around the energy crisis and climate change, the operation of conventional nitrogen removal methods with intense energy use, elevated operational costs and, significant carbon footprint are not financially sustainable or environmentally balanced to any further extent (Ma et al., 2020). Energy neutrality/positivity of wastewater treatment plants has been the main trigger for the significant efforts made to research and develop mainstream deammonification (Cao et al., 2017). Mainstream deammonification implementation is commonly

consistent with the current wastewater infrastructure, resulting in minor adjustments (Maureen O'Shaughnessy, 2016). On the other hand, effective employment of full-plant deammonification can potentially save wastewater utilitiy operations expenses for aeration and additional carbon costs in the life cycle (Gilbert et al., 2015a). According to several recent studies, mainstream deammonification is an emerging energy-efficient technology, however, its application for municipal wastewater treatment has barely been reported (Gu et al., 2020). The utilization of this novel technology is principally restrained because of temperature instabilities and reduced nitrogen levels in influent water. Additionally, insignificant microorganism dynamics, including the dissolved oxygen, free ammonia, and nitrous acid concentrations, can potentially instigate destructive impacts on deammonification systems (Y. Miao et al., 2019).

Table 4-1 Comparison between conventional nitrogen removal and deammonification in terms of oxygen demand and biomass production

	Deammonifiation	Nitritation/ 89% denitritation	Nitrification/ 89% denitrification	References
Oxygen demand (gO_2/gNH_4-N removed)	1.84	2.65	3.3	(Neethling, 2014) (Capodaglio et al., 2016)
COD demand (g acetate COD/g NO_3-N or NO_2-N removed)	0	4.5	6.6	
Biomass production (g biomass VSS/g NH_4-N removed)	0.12	1.5	1.93	
Quantitative comparison based on conventional nitrification/denitrification (All numbers are ratios)				
	Deammonifiation	Nitritation/ denitritation	Nitrification/ denitrification	References
Reactor Volume	0.83	0.67	1	(O'Shaughnessy et al., 2012)
Methanol Requirement	0	0.75	1	
Oxygen required	0.3	0.6	1	

Estimated energy Demand	0.3	0.5	1
Solids produced	0.05	0.7	1
Ammonia removal efficiency	90%	90%	95%
Nitrogen removal efficiency	80-85%	80-85%	80-95%
Solids retention time (days)	≥ 25	≥ 2	≥ 3
Hydraulic retention time (days)	2	2	3

In this paper, a complete understanding of the sidestream and mainstream deammonification process is summarized to give the readers a background on the concept. A comprehensive study on the full-scale installations of the sidestream deammonification process has been included to specify the process development in recent years. This document collects a wide variety of nitrogen removal and recovery processes from municipal sidestreams and ammonia-rich industrial wastewaters. The advantages of the technologies are defined together with the design approaches and full-scale plant experiences. This review paper then aims to update the overview of the current state of technology and research development of the mainstream deammonification process, including the progress in knowledge and applications as well as process technology and the remaining bottlenecks for scale-up towards full-scale applications.

4.2. Sidestream deammonification

4.2.1. Process and operational characteristics

Deammonification is an appealing alternative for the treatment of high-strength ammonia streams, and it also offers a high resource-saving capacity (Wett, 2007). Generally, deammonification process can be categorized into sidestream for high-ammonia wastewater such as anaerobic digester liquor and mainstream for low-ammonia wastewater, including municipal wastewater

(Lackner et al., 2014). Sidestream deammonification has been broadly employed in large-scale applications; however, mainstream deammonification is still in the early stages of investigation (Xu et al., 2015b). Thus far, deammonification process has been effectively implemented in elevated ammonia nitrogen levels of higher than 100 mg/L and temperatures above 26 °C in wastewater treatment systems, while the long-term process in low-strength ammonia nitrogen wastewater results in unforeseen unsteadiness of the system (Xiang et al., 2020). The effectiveness of the deammonification process depends on a synchronized activity linking AOB and ANX bacterial communities, along with an efficient selective nitrite-oxidizing bacteria (NOB) elimination strategy (Wang and Gao, 2017). Extreme overgrowth of NOB initiates disproportionate oxidation of nitrite to nitrate, obstructing the ANAMMOX nitrogen removal system (Xiang et al., 2020). Some of many strategies for continuous enduring suppression/wash-out of NOB are: temperatures above 25 °C, restricted dissolved oxygen levels, increased concentrations of free ammonia and free nitrous acid, short SRT, intermittent aeration patterns, adequate anaerobic periods (Wang and Gao, 2017) and addition of ANX process intermediates, such as hydrazine and hydroxylamine (X. Zhang et al., 2016).

On top of NOB's over-growth dilemma, ANX biomass retention is also a major challenge for reaching a stable deammonification process (Wang and Gao, 2017). Because ANAMMOX bacterial community is among very slow-growing groups with extended doubling times of approximately 11 days, implementation of selective enrichment methods is critical. Many deammonification processes potentially employ either biofilm or granular-based schemes (Flemming and Wuertz, 2019) to selectively retain the ANAMMOX biomass within the system (Rezania et al., 2015). So far, ANAMMOX granular cultures achieved considerable removal rates higher than 70 kg/m^3 d in two-stage processes (Rezania et al., 2015). On the other hand, suspended

ANAMMOX sludge was reported to undergo severe biomass losses (Wang and Gao, 2017). One of the critical factors in developed ANAMMOX-based processes designed for satisfactory biomass retention is bacterial immobilization through aggregation or biofilm formation (Boleij et al., 2018). The biofilm generation and granulation process assists the syntrophic interactions with other bacteria, augments the sludge retention and boosts the bacterial tolerance to environmental stresses (Wong et al., 2020). Suspended ANAMMOX processes were reported to obscure the potential network between nitritation and ANAMMOX activity in the mixed liquor (Lackner et al., 2014) and decrease the process cost efficiency (Vlaeminck et al., 2012).

In order to reach a high-performance sidestream deammonification, there are a number of specific details to be considered (Feng et al., 2017). Comprehensive assessment of the influent sidestream characteristics is the initial factor to be determined (Chamchoi et al., 2008). The influent total ammonia nitrogen should be in a range between 500 to 5000 mgN/L (Van Hulle et al., 2010), while the biodegradable organic carbon concentration should remain in a minimum range (Q. Zhang et al., 2016) (Lackner et al., 2015). Biodegradable organic matters do not directly affect the ANAMMOX bacteria. However, they can stimulate the growth of heterotrophic bacteria, which, due to a higher growth rate, heterotrophs will over-compete the ANAMMOX bacteria population (Xu et al., 2015b) (Chamchoi et al., 2008). The required total ammonia nitrogen and biodegradable COD ratio for single-stage deammonification are below 1gN:0.5gCOD (Chamchoi et al., 2008) (Lackner et al., 2015). Based on the stoichiometry, converting every one mole of ammonia to nitrite requires two moles of bicarbonate (Chamchoi et al., 2008). When excessive metal salts concentrations cause no significant limitations, the carbonate alkalinity naturally present in the sidestream is commonly sufficient for the ANAMMOX process (Xu et al., 2015b). A 3 to 4 alkalinity ratio as $CaCO_3$ to 1 total ammonia nitrogen (TAN) will support a good anaerobic

nitrogen removal up to 70 – 80 % (Lackner et al., 2014). Different studies indicate an optimal pH range of 6.7 to 8.3 for ANAMMOX bacteria, while further experimentations show that this range may increase to 9 (Tomaszewski et al., 2017b). The anaerobic ammonia-oxidizing bacteria lose their activity in an environment with a pH lower than 6.5 (Hollowed et al., 2013) (M Strous et al., 1998).

Several aspects demand additional analysis by the specialist, to achieve the operating goal established for the system (Wett et al., 2007). High or varying influents solids due to low capture efficiency of the dewatering pretreatment can negatively impact the deammonification performance (Q. Zhang et al., 2016). High influent TSS concentrations may result in an increase in nitrate production and active biomass withdrawal from the reactor (Van Hulle et al., 2010). For instance, the volumetric loading rate for deammonification process using a Sequential Batch Reactor (SBR) installation is usually between 0.25 to 0.75 kgN/m^3. d, while biofilm reactors can tolerate higher rates up to 1.3 kgN/m^3.d. Regardless of the technology utilized for the deammonification process, considering the operational staff's skills, abilities, and interests is a significant factor in maintaining high and efficient performance for the system (Tsuchihashi and Ryujiro, 2015).

4.2.2. Design approaches and technologies

Improved biomass retention in coupled nitritation-ANAMMOX reactors is a significant bonus, allowing for an improved environment for the slow growth ANAMMOX bacterial group (Shi et al., 2016). Several technical solutions have been established to grow and sustain ANAMMOX bacteria, whilst they are different in the method of growth and retaining the ANAMMOX bacteria, total number of operational phases, the configuration of the process, and control strategies implemented (Bowden and Stensel, 2016). An increase in the number of full-scale

deammonification installations led to a shift from two-step processes to single-stage reactors (Nsenga Kumwimba et al., 2020). Single-stage systems configurations have come to be the primary selected approach because of the depleted costs of infrastructure and operation, comparing to the two-stage designs. Approximately 90% of the entire full-scale deammonification facilities are single-stage systems (Lackner et al., 2014). The main recent design approaches for sidestream deammonification development has been: sequential batch reactors (Van Hulle et al., 2010), attached growth biofilm reactors and, upflow granular sludge reactor (UGSR) (Bailey et al., 2018), plus a small number of full scale rotating biological contactors (RBC) and activated sludge reactors. All different reactor designs are based on three main factors: suppression of NOB, maintaining a partial aerobic/anaerobic environment to support all necessary microbial communities, and retain the slow-growing biomass inside the system (Vlaeminck et al., 2012). Sustaining the AnAOB biomass in the SBR and UGSR is based on gravimetric selection, while the attached growth biofilm reactors use plastic media to promote and retain slow-growing biomass in a continuous flow system (Van Hulle et al., 2010) (Lackner et al., 2014). Recent studies reported that SBR technology is the most common system design holding over 50% of the total deammonification installations, and subsequently, Moving Bed Biofilm Reactor (MBBR) systems are highly prevalent (Nsenga Kumwimba et al., 2020).

A number of different reactor designs and arrangements for deammonification have been determined and made available on the market (Wang and Gao, 2017). As stated, the main configuration used for the majority of the deammonification systems is SBR-based, which are operated in DEMON mode (with >80% of all SBR reactors), in which suspended/ granular biomass is selectively retained by hydro-cyclones (Lackner et al., 2014). This technology was initially presented in Austria, treating reject water in a nitritation/ denitritation SBR (Wett, 2006). MBBR

(Moving Bed Biofilm Reactor) and UASB (Upflow Anaerobic Sludge Blanket) employ biofilm and granular systems, respectively (Li et al., 2016), while IFAS (Integrated Fixed Film Activated Sludge) is dependent on using ANAMMOX biofilm and floc AOB sludge (L. Zhang et al., 2015). A considerable gain of these biofilm/granule-based configurations is low aeration in the process, which initiates a reduction of aeration requirement by 60%, in addition to eliminated demand for external carbon supplementation, achieving a very cost- and energy effective process (Veuillet et al., 2014). EGSB (Expanded granular sludge bed) has been extensively employed for granular ANX operation, which enhances the mass transfer amongst substrates and granules through promoted recirculation rates and liquid upflow velocity, which also retains the granular biomass in addition to washing out the floc biomass (Wang and Gao, 2017). The majority of these processes are autotrophic and have been declared to attain low costs (using decreased oxygen demand and organic carbon source) and minimal environmental impacts. However, there is a vital need for more technical developments in autotrophic nitrogen removal processes to improve the inadequate effluent quality without added energy expenditure (Nsenga Kumwimba et al., 2020).

Table 4-2 Summary of the most common sidestream deammonification processes configurations

Deammonification Technologies		**Configuration**
SBR	DEMON	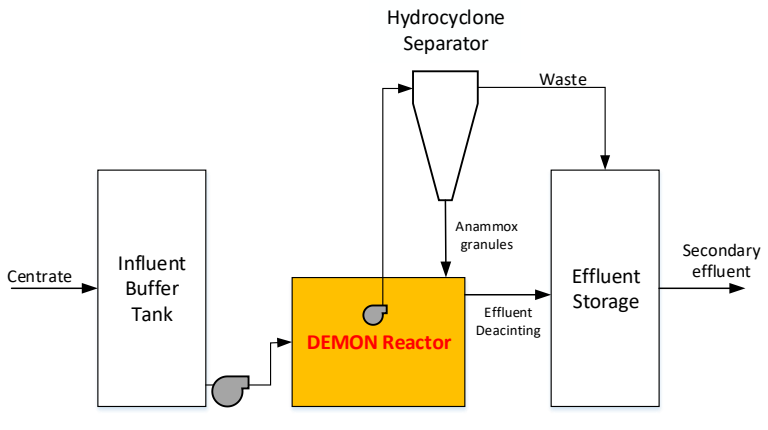

UASB	ELAN	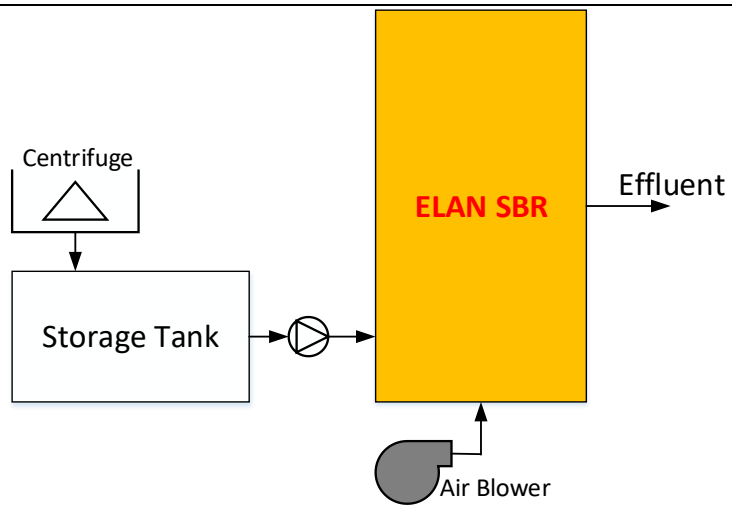
	Cleargreen	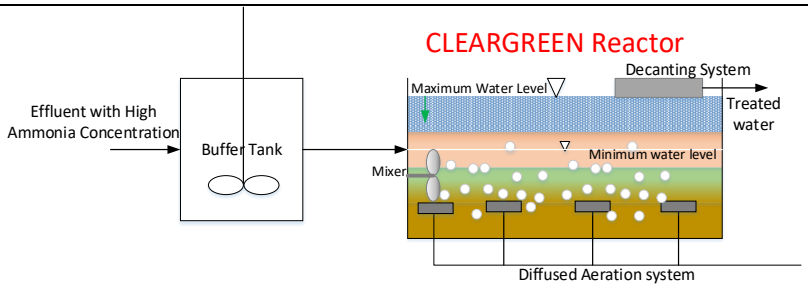
	SHARON-ANAMMOX	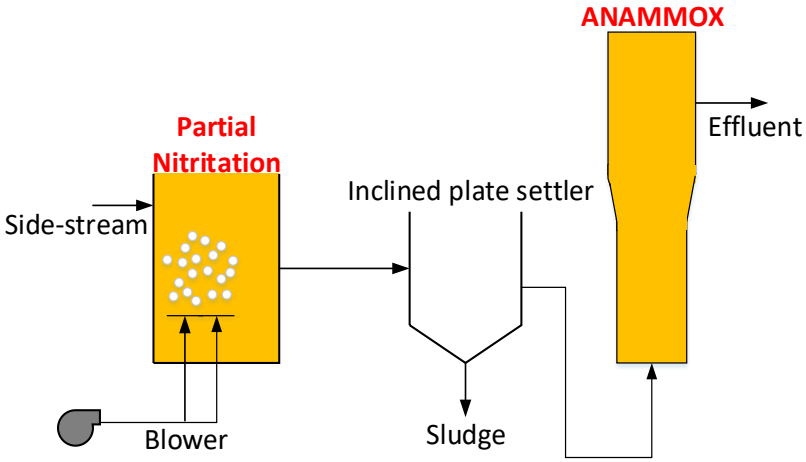
	ANAMMOX	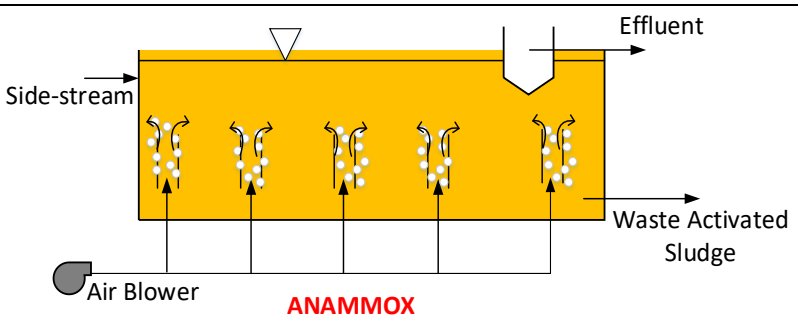

MBBR	DeAmmon	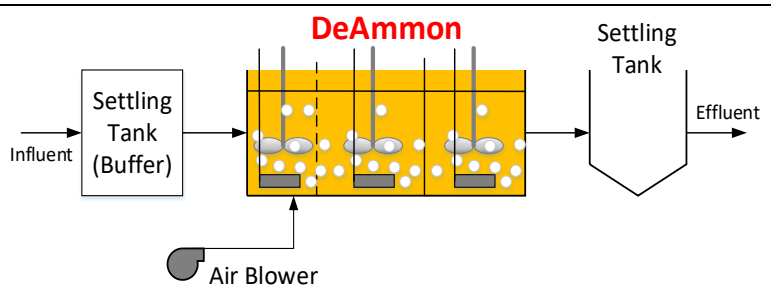
	ANITAMox	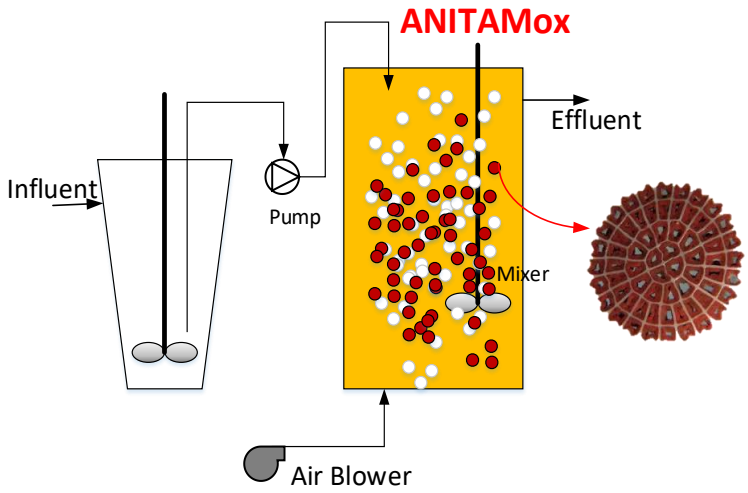
	TERRAMOX	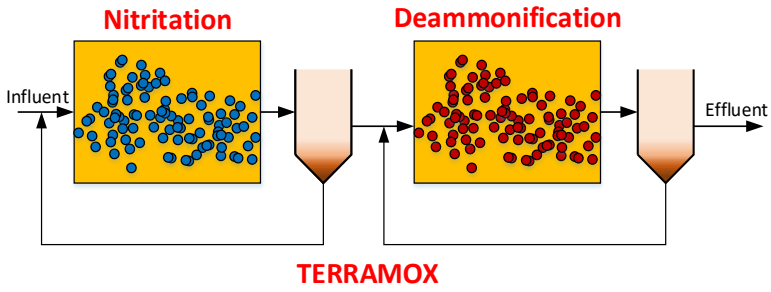

**References: (Tsuchihashi and Ryujiro, 2015) (Liu et al., 2017) (Plaza et al., 2011) (Krampe and Leak, 2012) (Wett et al., 2012)*

4.2.2.1. Sequential batch reactor (SBR)

Attributable to SBR's potential for slow-growing bacteria selection, the initial deammonification designs were achieved using this configuration (Wett, 2007) (Lackner et al., 2015). Some of the advantages of employing SBR technology include enhanced biomass retention of slow-growing ANX bacteria, boosted performance, excellent flexibility, and a reduced amount of impact on substrate toxicity (Choi et al., 2018). Deammonification SBR process, known as the DEMON process, is an innovative combination of aeration control with mini sequential cycles (Van Hulle

et al., 2010) (Kuai and Verstraete, 1998). One of the most critical features of DEMON is the selection and detainment of granular sludge using hydrocyclones (Hippen et al., 1997). Cleargreen SBR process is a sequential batch reactor that operates based on the processing load and flows (Monfet et al., 2018). In the Terra-N SBR configuration, bentonite is added to the reactor to help improve biomass retention (Val del Río et al., 2016). Bentonite has the potential to increase the solid settling rate and compact settled solids and prevent any significant potential loss of biomass. ELAN process is a SBR process that depends on bacterial stratification by electron acceptor's gradient (Val del Río et al., 2016). The outer layers are enriched with AerAOB, and AnAOB biomass is located in the granules' inner anoxic core (M. Strous et al., 1998)(Wett, 2007).

4.2.2.1.1. DEMON

DEMON process was initially developed through a collaboration between the University of Innsbruck and the Achental-Inntal-Zillertal Wastewater Treatment Association (Austria) (Weissenbacher and Wett, 2018), which included SBR reactor(s) (Table 4-2) with intermittent aeration having a maximum dissolved Oxygen (DO) concentration of 0.3 mg/L (Wett, 2006). The cycle control factor for this process configuration is either pH or time, where most full-scale plants rely on a time-based system. In the pH-based control strategy, the interval is as low as 0.01 to reduce the potential impact of nitrite inhibition, leading to an aerated and unaerated phase of 10-15 and 5-7 minutes, respectively (Val del Río et al., 2016) (Joss et al., 2009). DEMON reactors contain both anaerobic and aerobic ammonia-oxidizing bacteria in the form of granules, while other heterotrophs and inerts endure as flocculated sludge (Nifong et al., 2013). The use of hydrocyclones supports the retaining of the slow-growing biomass inside the system, in which, because of the higher specific gravity of ANAMMOX granules, they are separated from the waste sludge in the bottom part of the hydrocyclones and recycled back to the SBR (Wett et al., 2015). This configuration increases the SRT to ensure that AOB has sufficient growth time and NOB is

fully suppressed (Bowden et al., 2016). A typical design factor for a DEMON process is an ammonium loading rate of 0.7 Kg/m^3. d, with an optimum value of 1.2 Kg/m^3. d, which will potentially result in 90-95% ammonium and 80-85% total inorganic nitrogen removal efficiencies (Van Hulle et al., 2010). The initial startup time for the first DEMON SBR was 2-3 years to seed a full-scale plant, but this time period can be reduced to 1-3 months if the reactor is seeded with DEMON sludge from an existing full-scale reactor (Bowden et al., 2016). The operation of deammonification processes had improved extensively from when the first full-scale systems were custom-built in Germany and The Netherlands in 2001- 2002 (Wett, 2007). Several technical solutions have been developed to grow and support ANAMMOX bacteria. Error! Reference source not found. shows a list of full-scale DEMON installations worldwide from 2004 to 2015 (Wett, 2007)(Tsuchihashi and Ryujiro, 2015). On top of the significant application in Europe, full-scale sidestream deammonification technologies are greatly originated in China and North America, etc. (Nsenga Kumwimba et al., 2020). Error! Reference source not found. highlights the rising trend of full-scale process employment in different countries, in which for instance the total number of full-scale DEMON installations increased from 1 in 2009 to 10 in 2014, in the Netherlands individually.

4.2.2.1.2. Other SBR technologies

One of the most eminent SBR deammonification processes is Eawag SBR, which was developed by the Swiss Federal Institute of Aquatic Science and Technology's support. This technology includes a reactor with a suspended growth system, continuously aerated at a DO concentration of less than 0.1 mg/L, for a single-stage nitritation-ANAMMOX process (Val del Río et al., 2016). The main control factors for the process are the influent loading rate and the aeration level, controlled at a rate between 0.23 to 0.71 KgN/m^3.d and 0.2 mgO_2/L, respectively (Joss et al., 2011). There are already five full-scale Eawag SBR installations located in Switzerland (Val del Río et

al., 2016). ELAN (ELiminacion Autrofica de Nitrogeno) SBR deammonification process, as indicated in Table 4-2, was initially developed by FCC Aqualia in Madrid, Spain, in collaboration with the University of Santiago de Compostela. This process is based on the SBR process with biomass granulation and the establishment of aerobic and anoxic zones within the granule (Morales et al., 2015), used for nitrogen removal through partial nitritation and ANAMMOX processes in one stage. ELAN operates with a dissolved oxygen concentration of 0.8 to 4 mgO_2/L and cycles with a length between 3 to 6 hours (Morales et al., 2015). To improve the flocculent biomass washout from the system, which is one of the main operational parameters of ELAN technology, short settling times are imposed. This supports the process to enhance the NOB microbial community's washout and growth suppression. The stability control factor in this process is consumed alkalinity: conductivity ratio (Vázquez-Padín et al., 2010) (Vázquez-Padín et al., 2014). Two full-scale industrial plants were implemented in 2015 to treat the supernatant from an anaerobic digestion system (Val del Río et al., 2016).

Cyclic low-energy ammonia removal developed by the the Suez environment is applicable for plants that struggle with high influent nitrogen load (Val del Río et al., 2016). Cleargreen (Table 4-2) is a suspended growth deammonification SBR process method that improves the nutrients removal rate up to the point where it meets the stringent effluent nutrients limit, through continuous monitoring of all nitrogenous compounds, DO, and dynamic regulation of the aeration flow. This technology reduces the treatment line size and operates in cycles of around 8 hours (Val del Río et al., 2016). The sub-cycles result in ammonia selection at each period, fewer ammonia shocks, and reduced pH variations. There are two cleargreen technologies designed and constructed in Spain. One installation is located in Burgos with a N-load of 4200 lb N/d, finished in 2015, while

the other process is located in Ourense with a load of 1300 lb N/d (Tsuchihashi and Ryujiro, 2015) (Bowden et al., 2016).

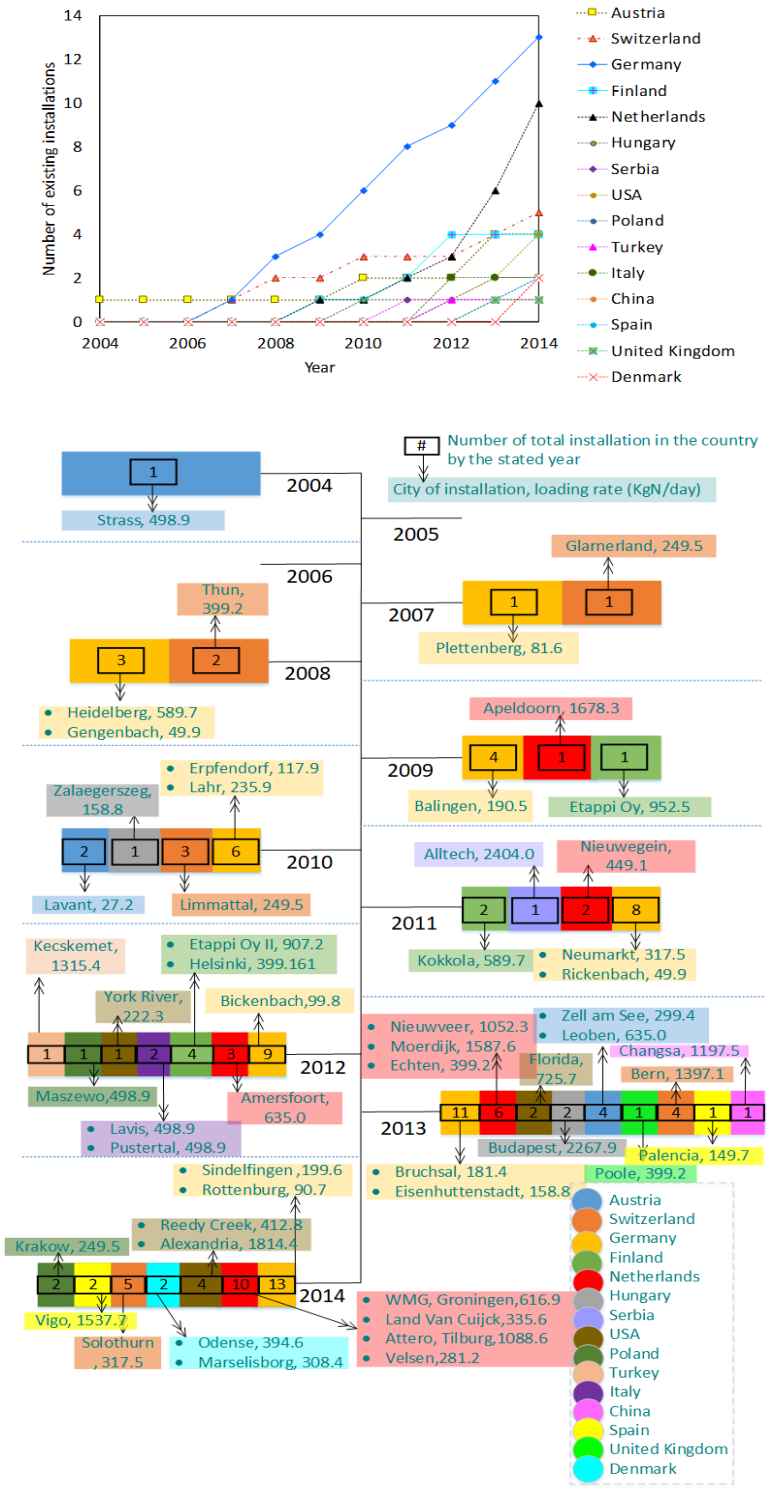

Figure 4-1 Comprehensive study of increasing trend of full-scale DEMON installations worldwide, in one decade (Cumulative data)

4.2.2.2. Upflow granular sludge reactors

Based on a collaboration between the Delft University of Technology and Paques BV, an upflow granular reactor performing as second stage ANAMMOX after partial nitritation was developed (Val del Río et al., 2016). The ANAMMOX biomass enriched by Paques tended to develop robust granules with excellent capability to be separated by gravity; thus internal circulators with three-phase separators were applied to the reactor designs (Val del Río et al., 2016). In contrast to other bacteria, ANAMMOX bacteria's growth rate is relatively slow, with an exponential phase between 10 to 22 days or within 10 to12 days when cultivated at 35 ◦C. The initial estimates by Kuenen. (2020) indicated that ANAMMOX doubling time is in order of 10 days corresponding to a specific growth rate of 0.0027 h^{-1}, and the microorganism's yield was 0.066 C-mol/mol of NH_4^+, with a maximum ammonium consumption rate of 45 nmol/mg protein/min (Kuenen, 2020) (Third et al., 2005). The maximum anaerobic ammonium oxidation activity achieved by the anaerobic culture has been reported to be 0.58 kg total N $m^{-3}day^{-1}$ (Third et al., 2005). Therefore, granule formation is an essential factor in the enrichment and maintenance of slow-growing bacterial communities. Since ANAMMOX enrichment culture's growth rates are tremendously low, the process requires reactors with effective biomass retention. The extreme shear forces in upflow reactors result in physical breakdown of filamentous outgrowth of granules, increasing the mass transfer across little granules. As a slow-growing organism, ANAMMOX bacteria form durable and compact microcolonies, which leads to an ideal equilibrium amongst the microbial environment and thus a stable nutrient removal from wastewater (Izadi et al., 2020a).

The first ANAMMOX system required a startup time of two to three years due to bacterial growth rate limitation and lack of a concentrated seeding regime for the reactor (Abma et al., 2007). The preliminary full-scale designs included a partial nitritation stage accomplished by a SHARON

reactor and an upflow column reactor for anaerobic ammonia oxidation. With knowledge advancements and further proficiency, upflow granular reactors migrated into single-stage designs. ANAMMOX process is one of the upflow granular deammonification reactor designs with specific tilted plate settlers to retain particles with higher specific gravity, allowing the low gravity particles to be washed out of the reactor (Tsuchihashi and Ryujiro, 2015).

4.2.2.2.1. SHARON-ANAMMOX process

SHARON reactor is a low SRT reactor in which, due to lack of alkalinity, about half of the ammonium concentration present in the sidestream is converted to nitrite. Alkalinity control is required to prevent excessive ammonia conversion to nitrite, which may potentially cause an unbalanced molar ratio . ANAMMOX reactor is an upflow granular reactor that provides hydrodynamic conditions to develop thick granulated biomass under superficial velocity. The flocculated low-density sludge are washed out of the reactor. A nitrogen gas lift mechanism is imposed to provide necessary mixing and liquid upflow velocity (Table 4-2). Design loadings for the second-stage ANAMMOX reactors change from 3-7 kgN/ m^3.d (van der Star et al., 2007a), nevertheless loading rates as extreme as 10 kgN/m^3.d have slight influence on the nitrogen removal efficiency, which is generally between 90 to 95% (L. G. J. M. van Dongen, M. S. M. Jetten, 2001). The initial installation of this two-stage process was in 2002 in Dokhaven, which achieved ammonia conversion rates of approximately 80%, with ammonia loadings of 1.2 kgN/m^3.d (Van Dongen et al., 2001). Although this development has a major advantage of better control of each process, the large total volume of the system and high investment costs results in significant setbacks (Val del Río et al., 2016).

4.2.2.2.2. ANAMMOX process

Single stage ANAMMOX reactor was developed to achieve high rate anaerobic ammonia removal through synergistic growth of bacterial communities on granules (Table 4-2). Alkalinity control is

required to prevent excessive ammonia conversion to nitrite, which may potentially cause an unbalanced molar ratio (Bowden et al., 2016). Two important operational factors are maintaining a high SRT for sufficient enrichment of ANX consortium and preventing any potential multiplication of bacterial communities that may compete with ANX bacteria for substrates (more specifically NOB) (Val del Río et al., 2016). A combination of internal separation devices with controlled pH, DO, and redox potential can fulfill the process requirements; however, studies showed that aeration intensity control alone could provide a stable system (Abma et al., 2010). The initial ANAMMOX reactor design lacked any additional seeding and contained an airlift aeration tube system, which, as a result of the hydrodynamic conditions, thick and well-granulated fluidized biomass was developed. Still, after the first system's startup and seed production, the riser tubes were eliminated from the design. The main advantage of this process configuration lies within a reduced footprint due to the compactness of large biomass concentrations within a single reactor. However, the main challenge is maintaining a balance between partial nitrification and ANX processes (Abma et al., 2010) (Lackner et al., 2014). There are many single-stage ANAMMOX configurations (Table 4-2) because of the design flexibility and constraints for reduced space and a simple operational system. The design loading can reach up to 2 KgN/m^3. d with a removal efficiency and accumulated sludge concentration from 90 to 95% and 10 to 15 g/L, respectively. This specific deammonification configuration requires a pretreatment step for sulfide oxidation. However, in other processes, due to lower specific loading rates and higher hydraulic retention times, there is sufficient time for sulfide oxidation to reach a non-inhibitory level (Tsuchihashi and Ryujiro, 2015). A comprehensive Study of all full-scale ANAMMOX installations worldwide is shown in Figure 4-2. As indicated in Figure 4-2, there is an increasing trend in ANAMMOX installation in the Netherlands, wherein the number increased from one

system in 2001 to nine in 2015. China had the highest rate of increase with 83.3% rise in a number of full-scale ANAMMOX installations between years 2009 to 2013.

4.2.2.3. Moving bed biofilm reactor

Similar to other upflow granular sludge and sequential batch configurations, attached growth biofilm reactors have also significantly impacted the high-strength ammonium-rich deammonification process development (M. Han et al., 2016). The deammonification process is strongly governed by the activity of the AOB for partial nitritation, in addition to the substrate diffusion rate and DO transmission into the internal layers of the biofilm because ANAMMOX bacterial group activity is obstructed by oxygen introduction (Strous et al., 1997a). The beneficial correlation on the media demands different sludge retention times by the nitrifiers and ANAMMOX bacteria (SM Jetten et al., 2001). The slow-growing ANAMMOX bacteria located on the inner section of the biofilm, with protection, experience a moderated extent of sloughing action from shear stress and erosion from other particles and solids. The AOB grows on the granule surface where they are exposed to air, while ANAMMOX bacteria grow in an anoxic zone inside the granule (Wilson, 2017). Moving bed biofilm reactors (MBBR) were initially proposed after ANAMMOX bacteria's presence was discovered to be the main cause of nitrogen losses in rotating biological contactors treating landfill leachate (Seyfried et al., 2002)(M. Han et al., 2016). This configuration is generally greatly stable and uncomplicated for operation. Additionally, since a high SRT is a key factor for retaining ANAMMOX bacteria in the reactor, and ANAMMOX biomass are identified as bacteria which tend to attach to surfaces or grow in clusters (Kuenen, 2008b), the MBBR is incredibly appropriate for deammonification process (Kanders, 2019).

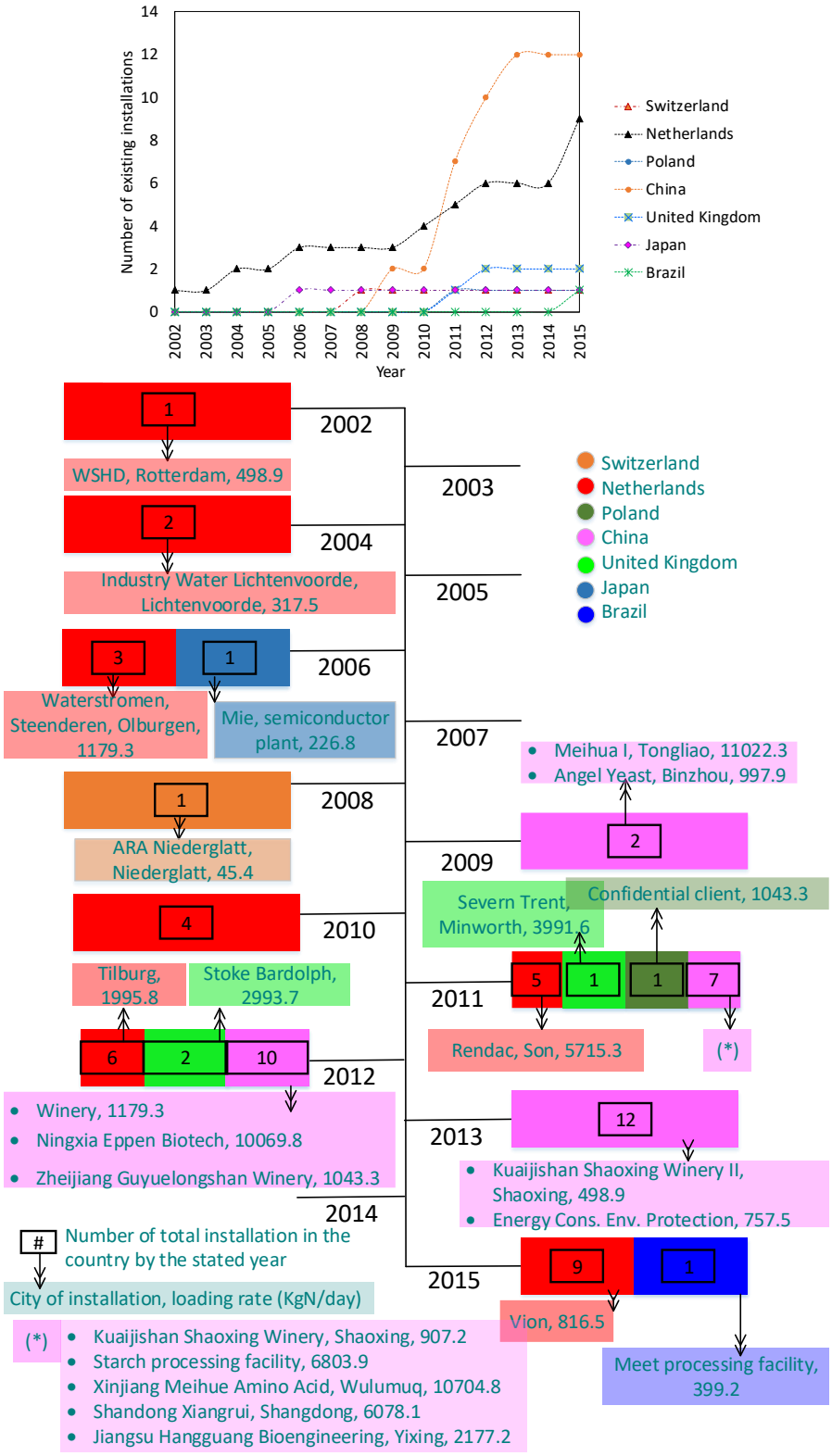

Figure 4-2 Comprehensive study of increasing trend of full-scale ANAMMOX installations worldwide, in thirteen years (Cumulative data)

4.2.2.3.1. DeAmmon

Purac/Lackeby AB (Sweden) in Germany was the first to install a moving bed deammonification system in collaboration with the university of Hannover and the Ruhr river Association (Figure 4-3). The process consists of a single- or dual-train reactor system with three stages per reactor (Table 4-2). Purac's one-step installation for DeAmmon was appropriate for lower nitrogen concentrations, approximately 1000 mgNH_4-N/L, which is standard for small to medium-sized wastewater treatment plants. The process includes both one or two-train reactor having three stages. Moreover, the series of stages is commonly mediated with AnoxKaldnes K1 up to a 40-50% filling volume. Screens between stages are the main strategy to retain biomass media in the system (Bowden et al., 2016) (Kanders, 2011). As indicated in Table 4-2, this process configuration is very stable for variations in flow and nitrogen levels, and it can convert almost 90% of the ammonium to nitrogen gas (Kanders, 2011).

Aeration and anoxic periods are regulated to control nitrite accumulation in the bulk liquid and confining the growth of aerobic nitrite-oxidizing bacteria . Intermittent aeration in each zone supports the partial nitritation and ANAMMOX processes, where an aeration period of 20-50 minutes with a maximum DO concentration of 3 mg/L and an anoxic phase of 10-20 minutes can be suitable for design and operation (Plaza et al., 2011). Some of the important DeAmmon operational and design factors are mentioned in Table 4-3. the initial appearance of ANAMMOX bacteria on the media is enhanced when a bed of heterotrophic bacteria exists on the surface. As a result, adding a carbon source, such as primary effluent, can be valuable in the introductory phases. A solid removal phase for extensive inert screening and separation is required to reduce the potential accumulation in the MBBR (Plaza et al., 2011) (Klaus et al. 2017) (Christensson et al., 2013).

4.2.2.3.2. ANITAMox

ANITAMox is a single-stage continuously aerated (0.5-1.5 mg/L) moving bed deammonification reactor (Table 4-2) designed and developed by AnoxKaldned/ Veolia. There are no mechanical mixing requirements as sufficient mixing energy is provided by the continuous aeration (Christensson et al., 2011). The dissolved oxygen level is based on the ammonium and nitrate concentration and NOB suppression (Tsuchihashi and Ryujiro, 2015). The higher specific surface area of the media had the potential to increase the volumetric removal rates. BiofilmChipM, an Anoxkaldnes media with a surface area of 1200 m^2/m^3 and filling of 40% can result in an Ammonium-N removal rate of 1.2 KgN/m^3. d in a temperature range of 27-30 °C (Christensson et al., 2011). Moreover, K_5 media (surface area of 800 m^2/m^3) with a filling volume of 50%, appears to be a more appropriate media for full scale processes, owing to less mixing energy requirement, resulting in an ammonium removal efficiency of 90%. The initial startup period of this process can be reduced by 4-6 months by providing an external seeding with media containing a firm ANAMMOX biofilm up to a filling volume of 2-3% (Christensson et al., 2013). The total number of full-scale ANITAMox installations from 2010 to 2015 is indicated in Figure 4-3, in which it is shown that the highest number of installations were in Sweden, the USA, and Denmark.

Table 4-3 Design and operational parameters of DeAmmon process

Design Parameters			**Operational data**		
Parameters	**Unit**	**Value**	**Parameter**	**Unit**	**Value**
Fill volume	-	40-50%	Reactor type	-	
Aeration time	Minutes	20-50	Volumetric N removal rate	KgN/m^3 d	0.3-0.4
Anoxic time	Minutes	10-20	Volumetric N loading rate	KgN/m^3 d	0.42-0.5
DO concentration	mg/L	3	Efficiency for total N	(%)	70

pH		Not controlled	Electrical energy consumption	KWh/Kg N	5.6
Optimized energy consumption rate	KWh/KgN	2.3	Personnel requirements	Man/year	0.25
Maximum deammonification rate	g-N/m^2.d	2 (28°C) 1.5 (27°C)	Maximum size	KgN/d	2455
Temperature	°C	25-30	Minimum size	KgN/d	130
K1 filter media active area	m^2/m^3	500	First installation	year	2001
Kaldnes K1 media design load	KgN/m^3 d	0.6	pH	-	7.3-7.7
			DO concentration	mg/L	3
			Inorganic nitrogen removal efficiency	%	70-85

**References: (Plaza et al., 2011) (Capodaglio et al., 2016) (Jardin et al., 2006) (Bozkurt et al., 2016) (Rosenwinkel and Cornelius, 2005)(Gustavsson, 2010)*

4.2.2.3.3. TERRA-MOX

This specific deammonification configuration was first developed by E&P Anlagenbau GmbH through a collaboration with Clariant/SÜD-Chemie AG (Germany). This process is a two-staged CSTR (Table 4-2), mediated with bentonite as the support media. TERRANA 510, a fine powder produced from thermal activation of calcium bentonite with a mean surface area of 60 m^2/g, is added to nitritation stage at a concentration of 10-12 g/L, and a concentration of 5-7 g/L in the second stage ANAMMOX process (Tsuchihashi and Ryujiro, 2015). This media results in high and compact settled solids. Due to the high settling rate of bentonite (SVI of 20 mL/g), there is insignificant media loss in the clarifier. However, there is always a need for a fresh product since a portion of it will be lost through the solid-waste stream (Tsuchihashi and Ryujiro, 2015). TERRAMOX design can also include two SBRs in which intermittent aeration is used to create the required aerobic/anoxic pattern. With SBR design, loading rates as high as 1.5 KgN/m^3d and inorganic nitrogen removal efficiencies of 80-90% are feasible (Clariant/SUD Chemie, 2012)

(Bowden et al., 2016). A broad review of all installations of moving bed bioreactors performing deammonification in sidestream, is indicated in Figure 4-3. As shown, TERRA-MOX has been mainly employed in Germany with five installations from 2008 to 2012.

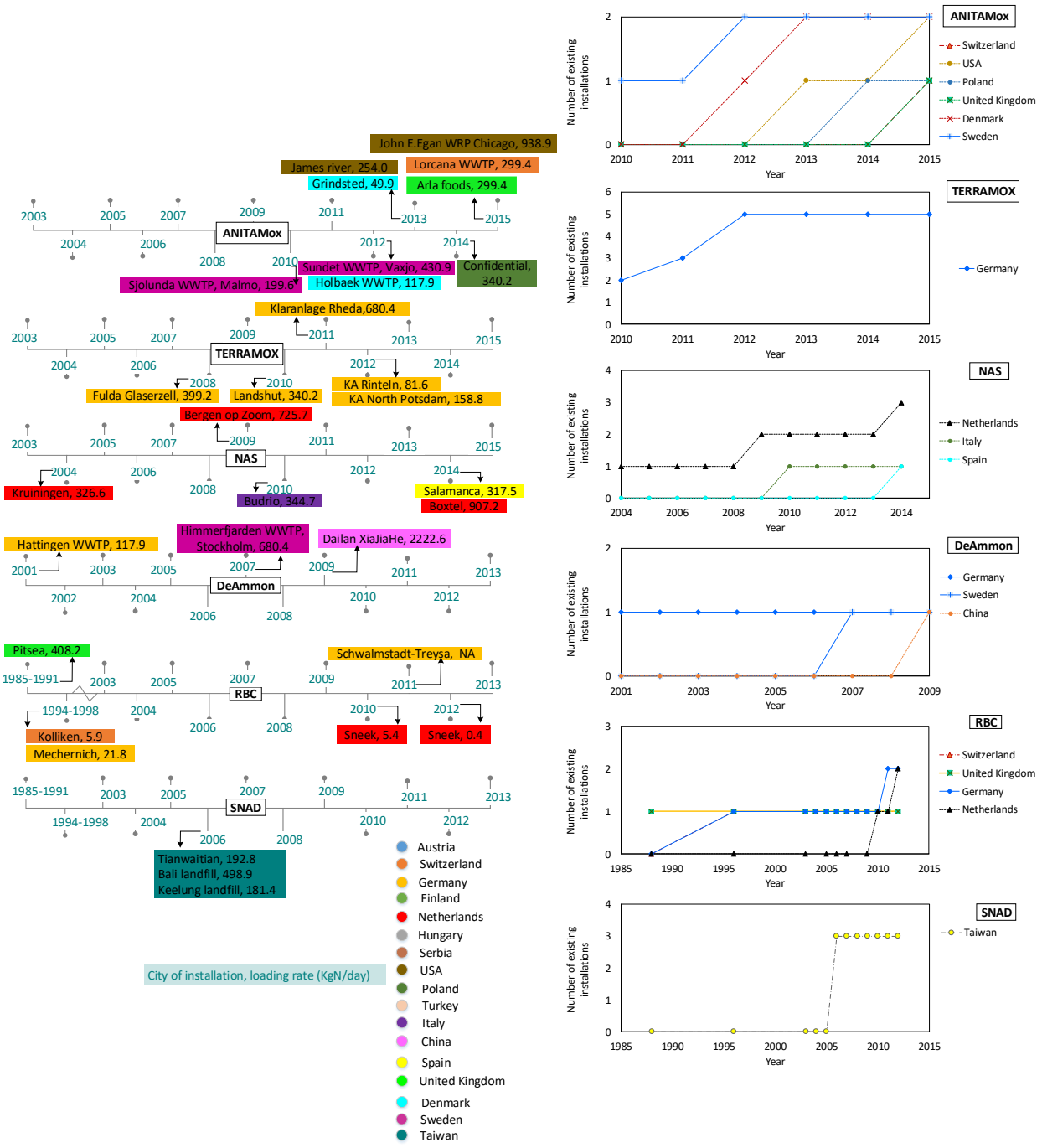

Figure 4-3 Comprehensive study of full-scale moving bed bioreactor's configuration installations worldwide (Cumulative data)

4.2.2.4. RBC, NAS and SNAD

Rotating biological contactors have various configurations and media applied for leachate treatment in Europe (Seyfried et al., 2002). The average deammonification rate was reported to be in a range of between 70-90% with an average 2.5 gN/m^3.d and 4.8 gN/m^3.d, of surface-specific

deammonification rate and peak rates, respectively, which are consistent with the rates observed in the DeAmmon® and ANITA™Mox MBBR processes (Tsuchihashi and Ryujiro, 2015). NAS (new activated sludge) process was initially developed in the Netherlands, with three and four staged series of suspended growth processes in which the primary stage operated in DO concentration of 0.3 to 0.9 mg/L to accumulate nitrite. Total ammonia, inorganic nitrogen and COD removals are achieved in third and fourth stages (Table 4-4) (Bowden et al., 2016). The system incorporates internal mixed liquor recycles and relies on the tank's quantity installed in series and their potential functions. ANAMMOX cultivation in the second stage initiates a hybrid nitritation-denitritation and deammonification process, in which the deammonification pathway is considered to be accountable for 70% of the nitrogen removed in the overall process (Tsuchihashi and Ryujiro, 2015). Simultaneous partial nitrification ANAMMOX and denitrification (SNAD) was established in Taiwan in 2008 by collaborating with National ChiaoTung University (Taiwan) and Leaderman and Associates. This process consists of two plug flow aerated tanks operated in parallel plus a gravity clarifier (Siegrist et al., 1998) (Seyfried et al., 2002) (Lackner et al., 2014). With the aim of modifying the process configuration, spherical plastic media were inserted to the reactors to verify if a hybrid biofilm plus suspended growth system may perhaps offer an enhanced performance, however the results are not fully reported.

Table 4-4 Comparison between the design factors of RBC, NAS and SNAD

RBC		**NAS**		**SNAD**	
Typical DO Concentration	1 mg/L	Specific loading rate	0.17-0.23 kg-N/m^3 d	Average ammonia-N loading rate	0.5 kg-N/m^3 d
pH	7.3-8.8	DO concentration	0.3-0.9 mg/L	DO concentration	0.2 to 0.5 mg/L
Rotation speed	1-4 rpm	Overall energy gain	40-50 %	SRT	18 days

Total nitrogen removal	70-90%	Contribution by AnAOB	~ 71 %	Ammonia removal efficiency	80%
Average surface specific deammonification rate	2.5 gN/m^2 d	Influent ammonium level	≤ 5 gN/L	Temperature	~ 30 °C
Operating temperatures	≤ 20°C	Ratio of biochemical oxygen demand to nitrogen	≤ 2.5	COD removal rates	67.7 %
Influent ammonia-N concentration	≥ 1000 mg/L			Contribution by AnAOB and AOB	96-97 %
				Maximum ammonia removal rate	99 %

**References: (Seyfried et al., 2002)(Tsuchihashi and Ryujiro, 2015) (Colsen et al., 2010) (Wang et al., 2020)*

Cost reduction and lower total nitrogen, total Ammonia-N and Nitrate-N in the effluent, increased the interest of plant operators towards sidestream nitrogen removal. However, deammonification's capital costs and footprint is higher than physiochemical processes, but a no-chemical process is one of the lowest cost process options for separate sidestream nitrogen removal. There area a number of research needs that are required to be addressed for process improvements, such as nitrite control strategies to prevent NOB activity, free ammonia and free nitrous acid's concentration effects, nitrogen loadings, bioaugmentation biomass, aeration and transient anoxia phase and, etc. (Tsuchihashi and Ryujiro, 2015).

4.3. Mainstream Deammonification

4.3.1. Influential factors and operational challenges

Thus far, there have been over 100 full-scale facilities treating high ammonia wastewater streams using shortcut nitrogen removal processes. Due to this success, applications of shortcut nitrogen removal in mainstream process is gaining more attention; however, the stream's dilution and low temperatures cause issues with NOB suppression and therefore no full-scale installations have

been reported (Pedrouso et al., 2019) (Xu et al., 2015b) (Blackburne et al., 2008). Generally, municipal wastewater has high COD and low ammonia levels with a ratio of 10-14 and 7-10 for raw and settled wastewaters (Xu et al., 2015b), which causes a major issue for mainstream deammonification, considering that high COD concentrations trigger the growth of denitrifying microorganisms that compete with ANAMMOX bacteria for nitrite (Figure 4-4) (Kumar and Lin, 2010). A number of factors can affect the competition between the ammonia and nitrite oxidizers, such as the dissolved oxygen concentration, residual ammonia, solid retention time and the organic carbon limitation (Mao et al., 2017) (Yongzhen et al., 2007). A comprehensive review of all potential factors affecting the NOB suppression process which may potentially influence the mainstream deammonification is presented in Figure 4-4. As indicated in the figure, a variety of elements including DO concentrations, alkalinity levels, aeration patterns, residual ammonia concentrations, COD and TSS levels of the sludge and bioaugmentation strategies, are capable of manipulating the NOB suppression procedure significantly.

The most important factor affecting the NOB repression in low-strength waste streams is the dissolved oxygen concentration (Zhou et al., 2020)(Blackburne et al., 2008). Several studies indicate NOB repression in low DO concentrations, possibly due to the higher oxygen affinity of AOB in comparison to NOB (Laanbroek and Gerards, 1993) (Yongzhen et al., 2007). The stated hypothesis is well accepted, but there are several studies that highlight a completely different outcome. DO concentration strongly relies on the floc size because of the variations in oxygen mass transfer and oxygen affinity coefficient ($K_{\circ}$), which is a result of mass transfer limitations and does not represent an intrinsic biological characteristic of the bacteria (Xie et al., 2019) (Cao et al., 2018). Despite all the contradictions towards oxygen affinity and its effects on NOB repression for shortcut nitrogen removal process, as indicated in Figure 4-4, DO is still one of the

most important factors for NOB elimination and control in mainstream processes (Sliekers et al., 2002) (Yongzhen et al., 2007) (Manser et al., 2005). DO levels under 0.5 mg/L are advantageous for selective repression of NOB growth because of the lower oxygen affinity of NOB compared to AOB. However, recent studies show beneficial effects associated with DO concentrations of around 1.5 mg/L in mainstream nitritation (Ge et al., 2014). Based on a study done by Cao et al. (2015), there was 75 % nitrite accumulation in the oxic units being operated at DO concentrations of 1.4–1.8 mg/L. On the other hand, intermittent aeration patterns are proven to be effective for NOB repression due to the delay period imposed on NOB to act in response to the switch from anoxic to aerobic condition (Xu et al., 2012).

ANAMMOX bacterial population are the only organisms capable of oxidizing ammonium in anoxic environments and are crucial for the ultimate polishing technologies (Le et al., 2016). The presence of oxygen in the mainstream application inhibits ANAMMOX bacteria as obligatory anaerobes and promotes the growth and activity of NOBs over AOBs . Due to the higher growth rate of NOBs in lower temperatures (~ 20 °C) and their higher affinities to oxygen comparing to AOBs, O_2 presence leads to complete nitrification and depletion of nitrite. Nitrite consumption by NOBs can significantly impact the metabolism of ANAMMOX bacteria since the main substrates of the bacteria are abolished from the system (Sobotka et al., 2017).

The online aeration and SRT controls are critical parameters affecting the NOB suppression and washout in mainstream conditions (Regmi et al., 2014). Given that ANAMMOX bacteria have meager growth rates with long doubling times of around 11 to 25 days, extended SRT is vital for deammonification process (Figure 4-4) (Hendrickx et al., 2012). It has been suggested to run the mainstream process in SRTs close to AOB's critical retention, in which NOB will be washed out, but AerAOB would not be distressed (Regmi et al., 2014). Hydrocyclone has been an effective

method for partitioning ANAMMOX aggregates from waste sludge, in which the SRT of ANAMMOX bacteria is considerably extended in the deammonification system (Wett et al., 2013). Another proposed effective method to maintain adequate retention of ANAMMOX biomass in the deammonification system was granular and biofilm-based systems (Fernández et al., 2008), in which various classes of bioreactors including UASB, SBR, MBBR, dynamic membrane bioreactor (DMBR), RBC were presented (Xu et al., 2015b).

Aerobic AOB's growth rate can be affected by the residual NH_4^+ concentrations in the stream (Figure 4-4), in which alternating aerobic and anoxic conditions as well as maintaining a high residual ammonium concentration has shown promising results for NOB suppression in mainstream conditions (Wett et al., 2015). Different studies indicate that bulk ammonium concentrations above a specific level limit the nitrite oxidation reaction in single-stage nitritation/ANAMMOX reactors operating as continuous mainstream deammonification systems (Wett et al., 2015) (Pérez et al., 2014). As also shown in Figure 4-4, sustaining a residual ammonium concentration is critical to overpower NOB and can be linked with additional control strategies to reach efficient NOB suppression. Although free ammonia and free nitrous acid concentrations are known to be important control parameters in sidestream deammonification due to low ammonia concentrations (15-50 mg/L) in the mainstream, such strategies are no longer practical (Negulescu, 2011). Lack of a sufficient amount of inorganic carbon leads to lower ammonia removal efficiencies due to a drop in the growth rate of aerobic ammonia oxidizers and biomass washout due to insufficient SRT provided for the process (Khunjar et al., 2011) (Xu et al., 2015b). Ammonia oxidation was observed to be more sensitive to inorganic carbon limitation, where the AerAOB were limited in organic carbon concentrations below 3 mmol/L in comparison

to NOB, which was not affected by the limitation down to concentrations below 0.1 mmol/L (Khunjar et al., 2011) (Wett and Rauch, 2003).

4.3.2. Design approaches and technologies

4.3.2.1. Mainstream deammonification challenges and potential resolutions

Half of the ammonium present in wastewater is oxidized to nitrite through the integration of ANAMMOX process with partial nitritation (Chen et al., 2016), in which suppression of NOB and transformation of nitrite to nitrate is of great importance (Jeanningros et al., 2010). Considering that AnAOB belongs to a slow-growing bacterial group with a relatively long doubling time, which is considerably longer than 0.3–1.5 days of AOB and 0.5–1.8 days of NOB (In 't Zandt et al., 2018), a process with a long SRT, as indicated in Figure 4-4, retaining the essential biomass in the system is vital (Ibrahim et al., 2016)(Chi et al., 2018). However, a higher retention time improves the selective retention of ANAMMOX bacteria, increasing the plant's capital costs (Szabó et al., 2017). There are two main methods for AnAOB retention in the system: suspended growth and attached growth configurations, wherein biofilms and granules are better than the suspended biomass (Qiu et al., 2020). Sludge characteristics of both granules and flocs are the main factors affecting selective retention. These characteristics include density, size and, compressibility (Zhang et al., 2008). Suspended growth biomass retention is dependent on the sludge settling characteristics.

Moreover, a minimum SRT of between 30 to 45 days is required for proper biomass retention. Sequencing batch reactors create the required environment for granules formation and settling sludge (Mao et al., 2017). The competition of nitrite and anaerobic ammonia-oxidizing bacterial groups is an important factor in NOB repression (Mao et al., 2017). In the case of granular sludge processes, due to NOB's high aerobic fraction, it is more favorable for nitrite-oxidizers to grow in

tiny granules. Granules with larger diameters have a limited aerobic fraction, and as a result, NOB can be easily inhibited. Larger granule systems facilitate the system's control and monitoring, aid with process robustness and, increase the settling velocities. To have systems with large granular sludge, nitrite and ammonium should be fed in the startup period (M Strous et al., 1998). In real-world applications, equipment such as hydroyclones - a selective retention system- working based on different densities of particles and retention sieves dependent on particle size distribution, can be used for effective collection and recycling of ANAMMOX biomass (Wett et al., 2012) (Mao et al., 2017) (Wett et al., 2013). Settling velocity is one other selective retention factor that can be applied through internal or external settling devices. Attached growth deammonification systems operated with moving carrier media with large surface area for biomass attachment are considered a more practical alternative than granule-based deammonification systems due to stable ANAMMOX activity and retention elevated performance (Wett et al., 2012) (M. O'Shaughnessy, 2016). There is increasing evidence confirming the better efficiency of a hybrid system that integrates both suspended and biofilm biomass rather than a pure biofilm-based system (Trojanowicz et al., 2019).

To stabilize the process and suppress the nitrite-oxidizers, AnAOB bioaugmentation is used to suppress the NOB, maintain a sufficient nitrite uptake rate in the anoxic phase, accelerate startup, and recover collapsing deammonification systems (Figure 4-4) (X. Li et al., 2018). The AnAOB can be obtained from cyclones underflow or directly from sidestream reactor (Sliekers et al., 2002) (Yongzhen et al., 2007) (Manser et al., 2005) (M Strous et al., 1998). In terms of attached growth systems, continuous bioaugmentation of AnAOB-rich biofilm carrier media results in partial regeneration of ANAMMOX biofilm in the sidestream reactor with more favorable conditions for the microbial community (Blackburne et al., 2008). Another effective bioaugmentation method for

ANAMMOX bacterial growth enhancement in mainstream process is redirecting the high-strength ammonium wastewater as a periodic feeding source to the system (Wett et al., 2015).

A critical parameter in mainstream deammonification is NOB suppression (Figure 4-4), mainly because NOB competes with ANAMMOX bacteria and AOB for nitrite and oxygen, respectively (Cao et al., 2017). Even though vast amounts of efforts have been devoted to different challenges comprising of intermittent aeration, real-time control of aeration, inorganic carbon, and bioaugmentation with AOB to maintain sustainable mainstream nitritation, it is of yet-resolved challenge. Successful NOB repression is vital for reaching operational mainstream wastewater treatment using deammonification process (Klaus et al. 2017). Thus far, most frequently performed engineering methods in connection with nitritation are based on the alternating dissolved oxygen (DO) control and short SRT, which involves the setting up online sensors, solenoid valves, and aeration control protocols (Xu et al., 2015b). Oxygen-based control strategies can be categorized into flexible-DO control and intermittent aeration (Qiu et al., 2020). Higher DO affinity of AOB compared to NOB is the fundamental basis of the fixed-DO control method, and as a result, limited oxygen concentrations can promote AOB and lead to potential washout of NOB from the system (Arnaldos et al., 2015). The flexible-DO control is mainly established based on variations in ammonium and nitrite concentrations and pH profiles (Klaus et al. 2017). This specific control approach depends on the strength and dependability of the control system and general online sensors (Qiu et al., 2020). The different starvation recovery dynamics and energy requirements of AOB and NOB is the central core of intermittent aeration suppression strategy (Li et al., 2011). Recent studies have shown that sole DO-based control strategy cannot guarantee a stable mainstream deammonificaion system, and the effectiveness alters case by case (Val Del Rio et al., 2019). For instance, the fixed-DO strategy has been illustrated to be efficient when combined with

FA inhibition for sidestream systems, but it was not successful for mainstream conditions (T. R. V. Akaboci et al., 2018).

4.3.2.2. Potential mainstream technologies

There is a number of parameters to be considered when applying a shortcut nitrogen removal for mainstream deammonification, where some of the most important ones are the operational costs, effluent regulations, and solid treatment technology (Maureen O'Shaughnessy, 2016). Mainstream deammonification processes are established based on principal technologies for sidestream processes. However, developments are made to reduce the unfavorable impacts of mainstream conditions (M Han et al., 2016). Mainstream deammonification technologies can be studied in pilot and full scale in three main categories: suspended flocculants, suspended granular, and attached growth systems. Several technologies can be considered for shortcut nitrogen including MBBR, RBC, biological aerated filters (BAF), integrated fixed-film activated sludge (IFAS), or granular activated sludge (Maureen O'Shaughnessy, 2016). Poor biomass retention was observed in suspended growth processes, and as a result, improvement strategies are investigated to improve nitrogen removal. In addition to bioaugmentation, biomass selection without hydrocyclones employment is being tested to overcome the negative effect of cyclones on granule size, considering that the shear forces enforced by hydrocyclones limit the size of the aggregates (M Han et al., 2016). Screen treatment provided an efficient biomass selection and enhanced suppression of NOB, and it was employed as a replacement for hydrocyclones at the full-scale mainstream deammonification process at Strass WWTP in Austria (Jardin and Hennerkes, 2012). In the case of attached growth systems, ANAMMOX retention is effective; however, AOB's activity can cause challenges and struggles for process maintenance. As a result, IFAS configurations, adopted for most MBBR processes such as the ANITA Mox process by

AnoxKaldnes, improved AOB's activity. One additional advancement for attached growth processes is the circulation of carriers between sidestream and mainstream deammonification processes. Ultimately it is crucial to recognize that mainstream deammonification pathway can be achieved and there is a potential for wastewater treatment plants to retrofit with minor adjustments (Gilbert et al., 2014a). Several different considerations govern technology selection. Based on different concept studies, the principal concern is the potential to install the treatment process within the existing process sequences and technology to take a full advantage of the existing infrastructure and lessen the capital costs (Maureen O'Shaughnessy, 2016).

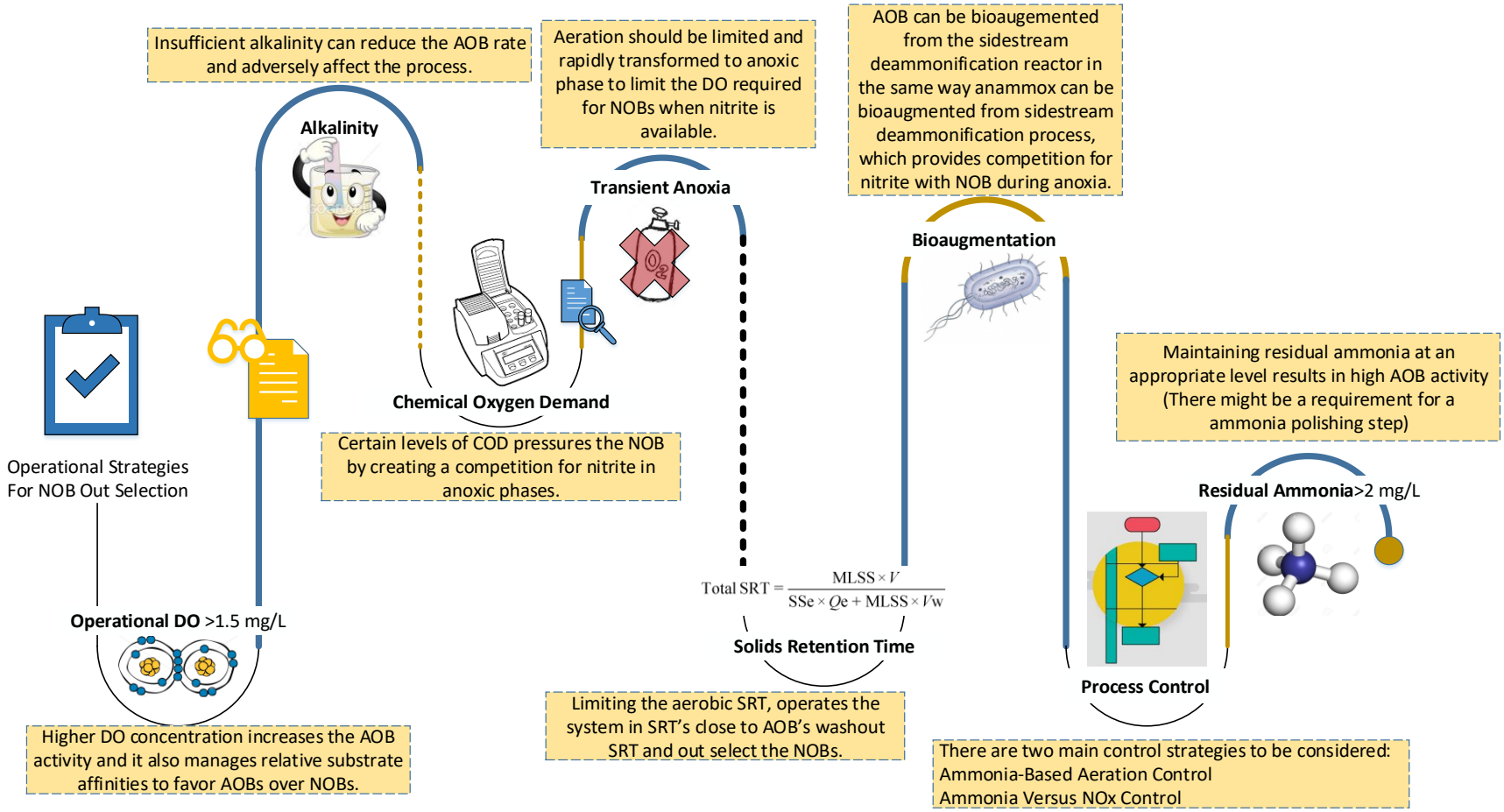

Figure 4-4 Operational strategies for NOB repression in mainstream deammonification

4.3.2.3. Mainstream deammonification case studies

In a bench-scale sequential batch reactor in Washington D.C. (DC Water), operating for one year from 2011 to 2012, a dual aeration mode, including both intermittent and continuous aerations, was applied. Three key process components: SRT decoupling, NOB repression, and ANAMMOX bioaugmentation, were investigated in the bench-scale experiments (Maureen O'Shaughnessy, 2016). The system was continuously fed with AnAOB seed from a sidestream process (Strass WWTP, Austria), performing as mainstream deammonification in two temperatures of 15 and 25 °C, with a wide range of DO concentrations reaching as low as 0.05 mg/L. Numerous testings show a great NOB repression through intermittent aeration with either low or high DO levels in contrast to continuous aeration system (Lotti et al., 2015)(T. Lotti et al., 2014). The ANAMMOX biomass bioaugmentation aided in sustaining an adequate ANAMMOX activity by partly outcompeting the NOB in the SBR system. However, the bioaugmentation effectiveness was discovered to be dependent on the reactor operating temperature (Maureen O'Shaughnessy, 2016). Based on the performance profiles of the operating test reactors, low DO operation was an ineffective NOB suppression strategy (Maureen O'Shaughnessy, 2016). The results from K_o analysis demonstrated that the NOB had greater oxygen affinity than AOB, which is conflicting with the proposed literature (Sin et al., 2008).

Full-scale deammonification was installed in Strass WWTP (Austria), in which an A/B process and a sidestream DEMON process were the main contributors to the positive net energy plant. The successfully operated sidestream deammonification supplies the required volume of seed for mainstream B-stage bioaugmentation (Maureen O'Shaughnessy, 2016). The facility's performance is principally based on two fundamental parameters which directly affect the AnAOB enrichment and growth. The first one is a seed-line to provide adequate biomass from sidestream

to mainstream, and the second one would be hydrocyclones employment to retain the slow-growing biomass in the system and waste the extra sludge from mainstream (Hu et al., 2013) (Morales, 2014). Bioaugmentation was applied in two different methods, one being a semi-continuous seeding from sidestream cyclone overflow, and the other aperiodic sidestream mixed liquor transfer (Lotti et al., 2015) (T. Lotti et al., 2014) (Isaka et al., 2007). The B-stage with a lower loading rate was operated in a Modified Ludzack-Ettinger (MLE)-mode in which intermittent aeration was utilized for the second tank in series and it was mainly monitored by an on-line ammonia signal installed at the effluent section of the tank (Maureen O'Shaughnessy, 2016). The total SRT in the B-stage ranged between 5 and 20 days during one year of operation, and the COD removal efficiency in A-stage reached 50-60%, to lower the potential heterotrophic competition in the mainstream deammonification process (Maureen O'Shaughnessy, 2016).

Chesapeake Elizabeth nutrient removal pilot study was established by the U.S. Environmental Protection Agency (U.S. EPA) in 2010 to restore clean water in Chesapeake Bay and the region's streams, creeks, and rivers. For evaluation of prospective developing process configurations for the plant, several nitrogen removal process alternatives that include a novel deammonification process are included in the potential pilot-plant scheme (Maureen O'Shaughnessy, 2016). The novel deammonification configuration consisted of a CSTR activated sludge process with a MBBR ANAMMOX and a clarifier. NOB suppression was induced by an aeration controlling strategy based on in-situ DO, ammonia, nitrite, and nitrate sensors. The AOB's activity was higher than NOB's activity in the course of the study; furthermore, the total bacterial population indicated that NOB population dropped through the phase of low NOB activity, which confirms the NOB suppression process (Wett et al., 2015). The total inorganic nitrogen removal rate of approximately 0.15 kg/m^3/d was detected in this study (influent at COD/N ~6.7 at 25°C), which was similar to

the rates measured in shortcut nitrogen removal in the full-scale plants such as Strass wastewater treatment plant (WWTP). However, ANAMMOX bacterial group was not considered the major contributor to N-turnover in the system (Maureen O'Shaughnessy, 2016) (Wett et al., 2015).

With the aim of the fish canning industry's effluent treatment, the University of Santiago de Compostela and FCC Aqualia in Spain developed an ELAN process in a water resource recovery facility (WRRF) with a successful upper running sidestream treatment. The initial laboratory scale ELAN indicated a 90% reduction of volume and waste sludge as well as 80% less aeration energy requirements. The pilot scale mainstream ELAN process was operated at 15°C and 50 mgN-NH_4^+/L, with granular biomass seeding from sidestream (Pedrouso et al., 2018). Regarding attached growth mainstream system installation case studies, two sidestream ANITAMox MBBRs were transformed into mainstream IFAS ANITAMox in Sjolunda wastewater treatment plant in Malmo, Sweden, wherein one of the initial reactors was used as a settling tank in the second configuration (Lotti et al., 2015) (T. Lotti et al., 2014). The DO concentration in the reactor was maintained at a level ranging between 0.2 to 0.8 mg/L. The influent for the mainstream system was the full-scale high rate activated sludge effluent which had an average ammonia concentration of 26 mgN/L, SCOD of 65 mg/L and, total suspended solid concentration of 1770 mg/L. To maintain a sufficient ammonia content (50 mgN/L) in the influent, a portion of the reject water was constantly mixed with the HRAS effluent (Hu et al., 2013) (Morales, 2014) (Isaka et al., 2007). In a different case, a two-staged system performing as a mainstream deammonification, comprising a C-stage for COD removal in a MBBR reactor followed by a N-stage for nitrogen removal in a IFAS reactor, was employed in France. The mainstream influent was domestic wastewater with average ammonia concentration of 45±15 mgN/L, while the waste stream's total and soluble COD content was 390±80 and 148±50 mg/L, respectively (Lemaire et al., 2016).

Although there are no full-scale mainstream deammonification systems yet, recent research focusing on removing nitrogen from mainstream wastewater using partial nitrification followed by ANAMMOX process has gained extensive attention (Qiu et al., 2020). A summary of research advancement as well as improvement of mainstream deammonification process and the effectiveness is presented in Table 4-5. As indicated in Table 4-5, mainstream process applications conducted at lower temperatures suffered from poor efficiency, instability and reduced effluent qualities. In a study executed by (Pedrouso et al., 2019), a 200 liter IFAS reactor which was previously used for low-strength nitrogen stream treatment, was operated as a continuous system filled with K1 carriers (500 m^2/m^3, 40% filling degree) at 21-25 °C for 20 days. The system achieved approximately 66% nitrogen removal efficiency with a total nitrogen concentration of 15 mg/L in the effluent, yet further optimization was required for the system (Pedrouso et al., 2019).

Table 4-5 Implementation of mainstream deammonification process in lab-scale and pilot-scale studies

Reactor Configuration	Reactor volume (Liters)/scale	Influent ammonium concentration (mg/L)	Temperature (°C)	Removal efficiency (%)
MBBR	8/lab-scale	50	30	~80
	200/ pilot-scale	45	17	25
	12/lab-scale	21	15	~73
	1/lab-scale	50	10-20	8-40
	2300/pilot-scale	28	15	<60
	340, 450/pilot-scale	33.4	25	75
IFAS	60/pilot-scale	50	28	63
	200/pilot-scale	35-50	25	70
	8/lab-scale	50	25	47
	200/pilot-scale	38-48	21-25	66
	200/pilot-scale	38-48	18	74
	2000/pilot-scale	30-60	17-20	22-70
	50000/pilot-scale	40-60	15-18	50-82
	200/pilot-scale	47	17	44
	2000/pilot-scale	35	17-23	70
	2000/pilot-scale	20-25	12-18	40
SBR	10/lab-scale	~100	34	81
	10/lab-scale	65-80	15	10-40

12/lab-scale	~21	15	~63
10/lab-scale	74.5	15	4-60
10/lab-scale	70	15	10-45
10/lab-scale	60-80	15	5-60
5/lab-scale	70	12	70
2.9/lab-scale	190	18	85
270/pilot-scale	60-160	20	89-95
270/pilot-scale	60-160	15	73-89
270/pilot-scale	60-160	10	47
4.2/lab-scale	61	10	81
12/lab-scale	19	29	-

**References: (Laureni et al., 2015) (Hendrickx et al., 2014) (T Lotti et al., 2014) (Winkler et al., 2012) (Hu et al., 2013) (T. R. V Akaboci et al., 2018) (Laureni et al., 2016c) (Dai et al., 2015) (Dai et al., 2015) (Gustavsson et al., 2014) (Trojanowicz et al., 2016) (Lemaire et al., 2016) (Pedrouso et al., 2019) (C. Wang et al., 2018) (Malovanyy et al., 2015) (R. Chen et al., 2019a) (Regmi et al., 2014) (Gilbert et al., 2014b) (Lv et al., 2019)*

As indicated in Table 4-5, a lab-scale SBR granular system was implemented to achieve mainstream deammonification at 15°C within 150 days of operation. The system was fed with an influent ammonium concertation of 65-80 mg/L and supplied with an intermittent aeration system. The system's nitrogen removal efficiency lessened from 40% to 10% after 30 days of operation and subsequently reduced from 30% to 10% for a second time after recovery (T. R. V Akaboci et al., 2018). The same system was operated at an influent ammonium level of around 74.5 mg/L, with continuous aeration at 15 °C, and the process fully collapsed after 63 days of operation (T. R. V Akaboci et al., 2018). In a study done by Trojanowicz et al. (2016), a 200-liter MBBR reactor was operated for three years at a low temperature range of about 10 °C for initial biofilm enrichment on K1 carriers. The system was equipped with online DO control and intermittent aeration system and was ran at 17 °C for mainstream deammonification (Table 4-5). During the 130 days of operation, NOB's activity and nitrite concentration increased each time the influent ammonium concertation decreased to approximately 20 mgN/L. The study showed that intermittent aeration alone is not a sufficient method to suppress NOB, and, as a result, an extra polishing step was required (Trojanowicz et al., 2016).

4.4. Discussion and potential future framework

The study of deammonification in the mainstream and sidestream is a fast emerging topic (Maureen O'Shaughnessy, 2016). The fundamental reason behind deammonification process gaining attention is the linkage with the novel energy-neutral municipal wastewater treatment plants concept, which has major advantages compared to the conventional biological nitrogen removal processes (Qiu et al., 2020). Effective deammonification can result in 63% reduction in oxygen demand, an almost 100% drop in organic carbon requirements, and a decline in sludge yield by 80% (Lackner et al., 2014). Partial nitrification followed by ANAMMOX process has been effectively applied for ammonium removal in dewatering liquor from anaerobic digesters in the sidestream municipal wastewater treatment and industrial wastewater treatment plants (Cao et al., 2017), wherein as of 2014 there were over 200 full-scale sidestream deammonification installation worldwide (Lackner et al., 2014). There are several major challenges linked to mainstream deammonification process when compared to the sidestream deammonification process, which results in mainstream deammonification being studied in its early development stages (Wett et al., 2013). Some of the major challenges are high COD to nitrogen ratios leading to heterotrophic denitrifiers over-competing the ANAMMOX bacteria, critical issues with biomass retention and sufficient initial enrichment and accumulation of ANAMMOX sludge plus number of complications associated with selective retention of AOB and suppression of NOB in the system (Xu et al., 2015b).

The technological and financial feasibility of high-strength dewatering return flows deammonification has been proven. As a result there are numerous technology opportunities that have been verified and commercialized to deliver the suitable environment and control headed for providing a stable operation. Numerous practical methods and strategies have been determined to

grow and support ANAMMOX bacteria, and, as a result, over 100 full-scale deammonification are installed. Sidestream deammonification has shown ammonia reduction of 90- 95% and total nitrogen reduction of 80-85% (Tsuchihashi and Ryujiro, 2015). Although there are number of full-scale sidestream deammonification installations, several of these processes are proprietary, and there is a potential to identify certain routes for additional optimization to enhance the loadings or to lessen the projected operating costs (Tsuchihashi and Ryujiro, 2015). Some of many general research gaps which require additional experimentation include identifying the most efficient organisms for sidestream nitrification to optimize the bioaugmentation process, restricting the nitrite concentration and controlling the NOB's activity by potential substitution of archaea instead of bacteria, understanding the fundamentals behind FA inhibition and the link between levels and degree of suppression, improved understanding of ANAMMOX process kinetics and the possible effects of transient anoxic conditions on NOB population (Bowden et al., 2016). Regardless of the operational mode (suspended growth, biofilm on support media, granular sludge), the vital constraint for effective deammonification is nitrite's presence for ANAMMOX bacteria. Despite the success of the sidestream technologies, none are issueless, and, as a result, site-specific trouble-shooting strategies are vital. The potential future framework should optimize the operational conditions, resolve the remaining obstacles associated with the solids regime, and develop a more comprehensive process automation (Lackner et al., 2014). There is a lack of understanding on the effects of different influent constituents on the overall process, which requires several inhibitory or stimulation testing (Fernández et al., 2012).

Mainstream deammonification has been proven to be a feasible technology to achieve energy-neutral municipal wastewater treatment, although there are a few reports of the large-scale installations of these processes (M. Zhang et al., 2019). The critical bottleneck in achieving an

efficient mainstream deammonification rests on attaining a stable nitritation, mainly associated with selective retention of AOB over NOB (D. Wang et al., 2016). There are a number of parameters that directly affect the NOB suppression process, including pH, temperature, DO levels, SRT, FA and FNA concentrations and, etc., wherein a combination of optimized factors can result in a stable nitritation process in sidestream. However, mainstream stabilization remains a major challenge (Law et al., 2015). Research into single-stage applications of mainstream deammonification, in which nitritation and ANAMMOX take place in a single reactor, have demonstrated that single-stage systems do not have the potential to reach low effluent total nitrogen levels (Maureen O'Shaughnessy, 2016). On the other hand, two-stage applications (individual reactors for nitritation and ANAMMOX) show more promising results in process stability and potential of attaining low effluent total nitrogen concentration (Polli, 2019). To reach a revolution in use of mainstream deammonification process, an efficient up-front carbon diminution process is required to reduce the COD/N ratio to a level essential for the succeeding mainstream process (Qiu et al., 2020).

4.5. Conclusion

The deammonification process linking partial nitritation and anaerobic ammonium oxidation has been reflected as a practical opportunity for energy-effective wastewater treatment. Successful nitrogen removal from wastewater with elevated ammonium concentrations and limited organic substrate has been fully established in sidestream full-scale applications. On the contrary, its application in treating mainstream wastewater continues to be a major challenge. The paper presents some of the most recent advances in deammonification process. The design criteria of sidestream and mainstream processes along with technological innovations have been reflected. Important progressions have been accomplished through pilot and full-scale tests to reduce the

effects of the major complications under mainstream circumstances, for instance, suppression of nitrite-oxidizing bacterial community, restraining the overgrowth of denitrifying, in addition to practical selection and retention of ammonia-oxidizing bacteria and ANAMMOX bacteria. The represented full-scale case studies have the potential to illustrate the significance of an effective control approach to assimilate side-stream and mainstream deammonification systems into a daily-based procedure, in which the greatest priority should be given to effective biomass control, particularly ANAMMOX biomass retention.

CHAPTER 5

Parin Izadi[a] , Parnian Izadi[a] , Ahmed Eldyasti*[a]

[a] Civil Engineering, Lassonde School of Engineering, York University, 4700 Keele Street, Toronto, ON, Canada , M3J 1P3

* Corresponding author

Authors' contributions Parin Izadi and Dr Eldyasti contributed to the study concept and design. Experimental system setup, material preparation, data collection and experimental analysis were performed by Parin Izadi and Parnian Izadi. The first draft of the manuscript was written by Parin Izadi and all authors commented on previous versions of the manuscript. Dr. Ahmed Eldyasti prepared the final submitted draft and critically revised the work. All authors read and approved the final manuscript.

Influence of Microbial Population Dynamics on Accelerated Development of ANAMMOX Micro-Granular Consortium [3]

Abstract

Micro-granules structure integrates different functional groups, leading to an effective, operational, and compact alternative system for nutrient removal processes. ANAMMOX process long startup period continues to be a major issue because of low bacterial growth rates and cellular yields, causing a shortage in providing sufficient amounts of ANAMMOX seed and operational limitations worldwide. In this study, a fast startup using micro-granular development of anaerobic ammonium oxidation (ANAMMOX) reactor was investigated to evaluate ANAMMOX activity, population dynamics, and core community members in an upflow anaerobic sludge blanket (UASB) reactor seeded with municipal returned activated sludge (RAS). The micro-granular UASB reactor has been operated under steady-state conditions with an average nitrogen loading rate of 0.22 KgN /m^3/day and the average SRT of the reactor ranged from 36 to 72 days. The long-term operational performance showed nitrogen removal efficiencies of up to 95 ± 2.7%. The physicochemical analysis indicated that around 75% of the granules were in a size range of 253.2–465.7 μm, and the sludge volume index improved by 53 ± 0.2 %. The ANAMMOX sludge activity was recovered within approximately 15 days after 63 days of critical inhibition conditions. At steady-state reactor operation, the microbial analysis showed the dominance of two major genera, "*Candidatus* Brocadia" and "*Ca.* Kuenenia" and an escalation in the abundance of filamentous bacteria, *Chloroflexi,* as a distinct indication of granulation process occurrence in microbial analysis level.

[3] A version of this chapter has been published in the Journal of Water Process Engineering, Volume 36, May 2020, https://doi.org/10.1016/j.jwpe.2020.101384

Keywords: Microbial community structure, Micro-Granular sludge, ANAMMOX Startup time, Granule size, Nitrogen removal

5.1. Introduction

One of the major challenges of wastewater treatment plants is the growing demand for capacity enlargement, while simultaneously, the available surface area is limited (Szabó et al., 2017). There is an increasing identification of the prospective significance of granular-based process configurations that can enhance the interactions between bacterial communities to effectively manage the fundamental bacterial resources and robust reactor performances (Jianhua Guo et al., 2016). Mixed-culture biological nutrient removal (BNR) processes rely on the metabolic activities of specific engineered microbial communities that mainly function in advanced granular forms to facilitate the process efficiency and optimize interactions and system dynamics (Aqeel et al., 2019). ANAMMOX process is an innovative alternative BNR process (Kallistova et al., 2016), carried out by an entirely autotrophic method for shortcut N-removal in the nitrogen cycle. In addition, this technological advancement resulted in less aeration demand, decline in organic matter addition, and nitrite reduction (Henze et al., 2008).

ANAMMOX-based processes, carried out by highly diverged *Planctomycetes*, struggle with low biomass yields and extended doubling times, introducing restrictions for efficient full-scale applications (Kocamemi et al., 2018) . Strong shock load capacities and excellent settling properties of ANAMMOX granular biomass increase the retention and survival rate of these sensitive bacterial communities in the startup course (Aqeel et al., 2019). Biomass granulation significantly affects the metabolism and activity by enhancing the interactions and synergy in the bacterial consortium. The use of shear force for granulation in BNR processes, associated with the up-flow velocity of wastewater and produced gases, in addition to the downward settling of the

biomass, was accomplished in UASB reactors (Aqeel et al., 2019). The high shear forces in UASB reactors physically break filamentous outgrowth of granules, improving the mass transfer through smaller-sized granules. Slow-growing organisms, including ANAMMOX bacteria, form strong and dense microcolonies, resulting in an optimal balance in the microbial ecology and consequently a durable nutrient removal from wastewater (Weissbrodt et al., 2014).

In most granular reactor configurations, the size of the aggregates is considered to be a key factor altering the system performance, controlled by the balance between granule growth, erosion, and deterioration process, which is an outcome of the reactor's structural design, hydraulic shear force, and substrate loading rate (Ma et al., 2013). High shear force in reactors with a completely mixed regime potentially results in smaller-sized granules; however, to attain a good nitrogen removal, no distinctive, optimum aggregate size distribution is required. Even though the activity and community structure of micro-sized aggregates are not yet well understood, but there is a number of studies associated with very small size ANAMMOX granules (Zhu et al., 2018) to overcome the undesirable impacts of large granules on reactor performance linked to an increased possibility of biomass washouts (R. Chen et al., 2019b). However, there is always inconsistency in the optimal granule size, ranging from micro to millimeter; the ideal ANAMMOX granules diameter in treating ammonium sewage is still little known. Despite this, in extremely slow-growing bacterial communities, retaining the sludge within the system is of great importance, highlighting the valuable role of micro-sized granules (Ma et al., 2013).

To date, struggles to reduce startup period, mostly headed for large-sized granular reactor configurations, diverse categories of media and carriers using a mature ANAMMOX seed (van der Star et al., 2007a), yet, minimal studies have been directed towards prompt micro-granule ANAMMOX startup from the conventional activated sludge (C.-J. Tang et al., 2011). This study

then aims to improve the operational factors for syntrophic micro-granular ANAMMOX consortium cultivation in a laboratory-scale UASB reactor from solely activated sludge without any bioaugmentation from a previously enriched ANAMMOX biomass, to overcome the issues related to seed availability as well as sludge retention and growth in newly started ANAMMOX reactors. This configuration is a progressive anaerobic system for wastewater treatment to retain granular sludge and create a stable system to culture ANAMMOX. To achieve study's goal, the ANAMMOX micro-sized granules, acclimatized to sustain high loading rates and reactor shear forces, were primarily enriched, and subsequently, immobilization factors were evaluated. The development of microbial populations in micro-granules and the morphology and structural physiognomies of the micro-granules were examined. Dynamics for reaching a stable operation and efficient nitrogen removal performance were assessed. Microbial communities were investigated using qPCR, and the physicochemical properties of the micro-granules formed were detected through particle sizes distribution. The results provide an alternative and efficient configuration for ANAMMOX cultivation and demonstrate the effectiveness and high-performance efficiency of micro-sized granules in the ANAMMOX process.

5.2. Materials and methods

5.2.1. Experimental setup

A single-stage continuous flow lab-scale UASB reactor was performed to evaluate ANAMMOX micro-granular biomass enrichment from municipal returned activated sludge as the only seed source. As indicated in Table 5-1, the reactor had a working volume of 4.8 L, being continuously fed with synthetic wastewater and operated at around 35 ± 0.5 °C, to mimic sidestream ANAMMOX process environment. ANAMMOX is a type of bacteria which is sensitive to specific ecological situations, including pH, oxygen, and temperature. The optimal range of temperature and pH for the growth of the ANAMMOX bacteria is 30 to 40 °C and 6.7 to 8.3. The system

operated with an average HRT of 24 hours and continuous mixing through water recirculation from top part to bottom of the reactor. The average SRT of the reactor was controlled at approximately 35-70 days from the top to the bottom section, and the system had a stable performance for three turnovers of the system's SRT.

A glass funnel was placed on top to function as a three-phase separator to collect the generated gas and prevent any biomass wastage from the system. The mixing inside the reactors was achieved using peristaltic pumps, resulting in an average upflow velocity of 0.5-0.6 m/h and a sludge bed height of 85-90 % of height to gas collector. The system was mainly operated in the absence of light to prevent any potential inhibition. Main substrates were provided by (NH4)2SO4, NaNO2, the synthetic feeding medium, and the operational and design factors as indicated in Table 5-1. The amount of ammonia and nitrite is based on experimental design to achieve influent ammonia and nitrite concentrations of 52.02 and 62.42 mgN/L, respectively. The pH of the influent was 7.9 on average.

Table 5-1 Design and control parameters, synthetic feed composition for the UASB reactor

Design and control parameters			**Synthetic feed composition (g/L)**		
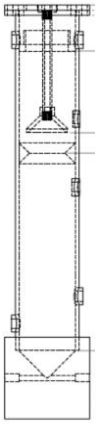	Total volume	5 Liters		$NaHCO_3$	0.420
SRT~ 36 days	Work volume	4.8 Liters	Inorganic Solution	$CaCl_2.2H_2O$	0.18
	Ammonia Load	0.75 $KgNH_4$-$N/m^3.day$		$MgSO_4$	0.059
SRT~ 49 days	Temperature (controlled)	35°C		KH_2PO_4	0.027
	HRT (controlled)	24 Hours	Trace Elements Solution	EDTA	5
SRT~ 72 days	SRT (controlled)	34.5-74.5 Days		$FeSO_4$	5
	Dissolved oxygen (monitored)	0.08-0.1 mg/L		$CuSO_4•5H_2O$	0.25
	pH (monitored)	7.8± 0.3		$ZnSO_4•7H_2O$	0.43
	Feed nitrite/ammonia	0.84-1.32		$NaMoO_4•2H_2O$	0.22

	$MnCl_2•4H_2O$	0.99
	$NiCl_2•6H_2O$	0.19
	$CoCl_2•6H_2O$	0.24
	$NaSeO_4•10H_2O$	0.21
	H_3BO_4	0.014

5.2.2. Seeding sludge

The seeding source for the UASB reactor was returned activated sludge collected from the Humber treatment plant (Toronto, ON, CA). Total and volatile suspended solids concentrations were 21840 and 16650 mg/L with pH and alkalinity of 6.9 and 1460 mg$CaCO_3$/L, respectively. The initial biomass had soluble chemical oxygen demand (SCOD) of 1700 mg/L and total chemical oxygen demand (TCOD) of 24280 mg/L. RAS was allowed to settle; then the reactor was seeded with two-thirds of its working volume (3.2 L of the settled RAS).

5.2.3. Analytical methods

The influent and effluent samples were collected daily and were analyzed instantaneously (all samples were collected in triplicates). Water samples were analyzed based on the standard methods of water and wastewater examination. Simultaneous determination of anions and cations were implemented through ion chromatography (IC) by the Thermo Scientific™ Dionex™ Integrion™ HPIC™ system. In advance of all IC measurements, samples were diluted correctlywith deionized water and passed through a membrane filter (0.45 µm). Further analytical determinations (e.g., pH, TSS, VSS, Alkalinity, etc.) were conducted according to Standard Methods (APHA, 2005). The biomass concentration was indicated as suspended solids (SS) and volatile suspended solids (VSS). To monitor the anaerobic environment required for ANAMMOX bacterial community, dissolved oxygen (DO) was measured using an IntelliCAL LDO Lab Probe (HACH Company, Loveland, Colorado, USA). In order to confirm ANAMMOX enrichment in the reactor, samples were withdrawn and analyzed using PCR (RNA was extracted, amplified using PCR, then the products

were subjected to gel electrophoresis to confirm the existence of ANAMMOX bacteria). The intensity of each band can be related to the genomic density of the target gene in the original sample. Specific primer sets targeting the 16S rRNA for both the subjected bacteria type were used, and detailed descriptions for the sequence of the primers, the target genus, and the procedures followed during the molecular biology analysis are described in the Appendix (A4) data file. The successful amplification of the desired bacterial RNA confirms the presence of the investigated bacterial family.

DNA extraction and the amplification of the V4 region of the 16S SSU rRNA were accomplished using the formerly illustrated technique (Stearns et al., 2015)(Thevaranjan et al., 2016). DNA was extracted utilizing MoBio PowerMag Soil DNA Isolation Kit as per the manufacturer protocol. The V4 hypervariable region primers 515F (5′-GTGCCAGCMGCCGCGGTAA-3′) and 806R (5′-GGACTACHVGGGT- WTCTAAT-3′) were used to amplify 16S rDNA genes (Laureni et al., 2016a) and the barcodes integrated into the forward primer allowed for the use of diverse reverse primer structures to achieve extended amplicons and elimination of biases.

In brief, each 25 µl PCR mixture to amplify V4 of the 16S rRNA gene by PCR contained the following: 13 µl of PCR-grade water (Sigma), 10 µl of Platinum Hot Start PCR Master Mix (2x) (ThermoFisher), 1 µl of Template DNA, 0.5 ml of 515FB primer (10 µM), 0.5 ml of 806RB primer (10 µM). The reaction was later operated for 35 cycles (94 °C for 2 min, 94 °C for 30 s, 50 °C for 30 °C, 72 °C for 30 s), with an ultimate polymerization step at 72 °C for 10 min. The results were divided by electrophoresis in a 2% agarose gel and visualized under a UV trans illuminator light, and the outcomes linking with the amplified V4 (300–350 bp) were excised and purified using standard gel extraction kits (Qiagen). Products were then quantified with Quant-iT PicoGreen dsDNA Assay Kit (ThermoFisher). The identical volume of products from each sample (240 ng)

were mixed into a distinct, sterile tube then cleaned using MoBio UltraClean PCR Clean-Up Kit. The highest concentration was measured using a Nano-drop spectrophotometer, and the qualityof the products was verified by confirming that the absorbance ratio at 260/280 nm ranges from 1.8 to 2. Samples were sent to Farncombe Metagenomics Facility at McMaster University DNA Sequencing Facility and sequenced using an Illumina MiSeq per the manufacturer's instructions. The completed run was demultiplexed with Illumina's Casava software. Cutadapt used the resulting sequenced data to trim the forward and reverse paired-end reads at the opposing primers for input into DADA2 for processing. Chimeras were removed, and sequences were organized into operational taxonomic units (OTUs) with a clustering threshold of 97% using Abundant OTU+. Output from this tool was then formatted where taxonomy was assigned using the Silva database.

To assess the nitrogen gas production, gas samples were collected from the headspace by gas tight syringe (all samples were collected in duplicates). The gas samples were then analyzed using SRI 8610C gas chromatography (SRI instrumentation, Torrance, USA) equipped with a thermal conductivity detector (TCD). In the temperature program, the injector was 60 °C; oven was 80 °C; TCD was 80 °C, and helium gas was the carrier gas with a flowrate of 15 mL min^{-1}. External calibration curves were constructed. An inverted microscope (BioImager, ON, Canada) with a 2.5× objective and 10× objective was utilized. The microscope was setup with a camera (SN 14120187, Point Gray Research Inc. Canada), and a computer wherein the logged images and videos were saved for additional assessment. Scanning electron microscopy was used for further understanding of the development and structure of micro-granules. The samples for SEM were prepared by fixing with 5% glutaraldehyde in 0.1 M phosphate buffer at pH 7.2 at 4°C. After the samples were washed in a buffer three times and subsequent post-fixation in 1% Osmium tetroxide, they were rinsed twice in distilled water. The samples were dehydrated with 35%, 50%, 75%, and 95% ethanol and

then immersed in tetramethylsaline for 10 minutes. The samples were then dried at room temperature for 24 hours. Dried samples were coated with platinum to make them electrically conducting and avoid space change influence during SEM. Then, the SEM micrographs were taken with a scanning electron microscope (Thermo Fisher Quanta 3D electron microscope, York University, Ontario, Canada). The particle size distribution was measured using a laser light diffraction particle size analyzer (LS 230, Coulter-Beckman, Germany). Particle size measurement ranges from 0.017 μm to 2000 μm, using the Polarization Intensity Differential Scattering (PIDS) technology.

5.2.4. Ex-situ autotropic ammonia removal bacteria activity evaluation

BOD Trak II implemented batch tests on ANAMMOX activated sludge, a manometric device consisting of six vessels (492 mL) placed in a warm chamber at 35 °C and mixed by a magnetic stirrer (All batch tests were conducted and analyzed in triplicates). The batch test bottles were sealed to prevent external atmospheric pressure changes in the test. Additionally, in gas-tight batch reaction vessels, pressure increases due to dinitrogen gas release, which is censored over time to quantify the reaction kinetics. Two alternatives were considered to track the evolution of the ANAMMOX process: Chemical tracking, which is done by assessing the ammonium, nitrite and nitrate concentration in the specific period, and manometric tracking by assessing the overpressure caused by dinitrogen release in a gas-tight reactor. Before and after each test, the pH was measured and a liquid sample was collected for analysis. The pH was kept within the range 7.6–8.0, and adjusted after each test. Bicarbonate salt ($KHCO_3$) was added, if necessary, to guarantee a sufficient inorganic carbon amount required for the anabolic pathway of the ANAMMOX reaction.

5.2.5. Theory and calculations

Nitrogen loading rate (NLR), nitrogen removal rate (NRR) and nitrogen removal efficiency (NRE) were calculated based on the nitrogen balance and stoichiometry according to Equations 3 to 5 in Table 5-2. It was presumed that the ANAMMOX reaction primarily removes nitrogen, however since alkalinity was available in the system and based on nitrate/ammonia ratio coupled with the microbial community analysis, autotrophic denitrification could have a potential contribution (Equations 12 and 13) (Wang et al., 2017).

Table 5-2 Theoretical equations

1	Total nitrogen in the effluent (mg/L)	TN_{eff}= ($[NH_4^+$-N] + $[NO_2^-$-N] + $[NO_3^-$-N])
2	Difference in nitrogen in the influent and effluent (mg/L)	ΔN= ($[NH_4^+$-N] + $[NO_2^-$-N])$_{in}$ - TN_{eff}
3	Nitrogen loading rate (KgN/m^3/day)	$NLR = TN_{in}/HRT$
4	Nitrogen removal rate (KgN/m^3/day)	$NRR = \Delta N/HRT$
5	Nitrogen removal efficiency (KgN/m^3/day)	$NRE = \Delta N/[NH_4^+\text{-}N]_{in}$
6	Maximum specific ANAMMOX rate (mgN_2-N. gVSS^{-1} h^{-1})	$qAMX,N2 = \frac{rAMX,NH4 + rAMX,NO2 - rAMX,NH4\_NO3}{XVSS}$
7	Ammonia to nitrite ratio	$YNH4_{NO2},AMX = \frac{rAMX,NO2}{rAMX,NH4}$
8	Ammonia to nitrate ratio	$YNH4_{NO3},AMX = \frac{rAMX,NH4\_NO3}{rAMX,NH4}$
9	Free ammonia (mg/L)	$FA = \frac{17 \times TAN \times 10^{pH}}{14 \times [\exp\left(\frac{63334}{273 + ℃}\right) + 10^{pH}]}$
10	Free nitrous acid (mg/L)	$FNA = \frac{47 \times TNN}{14 \times \left[\exp\left(\frac{-2300}{273 + ℃}\right) + 10^{pH}\right] + 1}$
11	ANAMMOX reaction stoichiometry	$NH_4^+ + 1.32NO_2^- + 0.066HCO_3^- + 0.13H^+ + \rightarrow 1.02N_2 + 0.26NO_3^- + 2.03H_2O + 0.066CH_2O_{0.5}N_{0.15}$

12	Elemental sulfur-utilizing autotrophic denitrification reaction stoichiometry	$1.06NO_3^- + 1.11S + 0.3CO_2 + 0.785H_2O \rightarrow 0.5N_2 + 1.11SO_4^{2-} + 1.16H^+ + 0.06C_5H_7O_2N$
13	Hydrosulfide utilizing autotrophic denitrification reaction stoichiometry	$HS^- + 1.23\ NO_3^- + 0.573H^+ + 0.438\ HCO_3^- + 0.027\ CO_2 + 0.093\ NH_4^+ \rightarrow 0.093\ C_5H_7O_2N + 0.866\ H_2O + 0.614\ N_2 + SO_4^{2-}$

Linear regressions of substrates concentrations over time were conducted to monitor the total nitrogen conversion rates. The linear correlation coefficients (R_2) were higher than 0.9 in all cases. The maximum specific ANAMMOX rate as mgN_2-N. $gVSS^{-1}$ h^{-1} was calculated through Equation 6. Similarly, specific biomass ammonium oxidation rate based on nitrogen gas production from ammonia loading ($q_{AMX,\ NH4\_N2}$) mgN. $gVSS^{-1}$ h^{-1} and specific biomass nitrite reduction calculated based on nitrite and nitrogen gas ratios ($q_{AMX,\ NO2\_N2}$) and nitrate production ($q_{AMX,\ NH4\_NO3}$) rates based on ammonia and nitrate ratios, were calculated. In the activity test experimentation, the $Y_{NH4\_NO2,AMX}$ and $Y_{NH4\_NO3,AMX}$ ratios were calculated using Equation 7 and 8, respectively (Van Loosdrecht et al., 2016). Pearson's correlation analysis was applied to examine the correlation between operating parameters and nitrogen removal performance. One-way analysis of variance (ANOVA) was used to examine the significance of the differences under different experimental conditions and nitrogen removal performance.

The detrimental influence of free ammonia (FA) on ammonia and nitrite oxidizing bacteria is well studied, where ANAMMOX bacteria are commonly inhibited by presence of 10 to 150 mg/L of FA in the environment. Similarly, free nitrous acid (FNA) might result in process instability and inhibition. To monitor and control the inhibition factors induced on ANAMMOX bacteria, the concentrations of FA and FNA were continuously calculated using Equations 9 and 10 (J Y Jung et al., 2007).

5.3. Results and discussion

5.3.1. Performance of UASB reactor and batch experiments

The experimental analysis was studied in three main phases that coincides with different feeding medium and subsequent inhibition effects, in which phase I (~55 days) is the startup and initial ANAMMOX activity observation stage, phase II (~63 days) points out the effect of high influent ammonia concentration on the process and phase III (~200 days) specifies a stable ANAMMOX process with high ammonia and nitrite removal rates. For the initial five days of reactor performance, the conventional nitrogen removal, specifically denitrifying activity, was the governing process, and there was no detectable ANAMMOX activity. Observed ammonia's concentration fluctuation can be related to its production during the adaptation, due to cell deterioration and malnourishment and dead bacteria discharge organic matter, which heterotrophic denitrifiers use as organic carbon source and electron donor to sustain denitrification activity (Q. Wang et al., 2018). In phase I, the influent NH_4^+-N was maintained at approximately 50.4 mgN/L, and the average NLR was 0.2 KgN/m^3/d (Figure 5-2 A). At the beginning of the adaptation period, within four days of operation, the average NRE reached 70.6%, indicating initiation of ANAMMOX activity in the inoculation sludge. Ammonia removal in phase I started from 13.96 mgN/L, and it reached 45.85 mgN/L after 14 days of operation (Figure 5-1 A). In addition, nitrite removal increased from 54.7 to 90.7% in 2 weeks of the startup period. The observed nitrite removal was potentially a result of denitrifier's activity, which was initiated by the endogenous substrate in the inoculum (Kocamemi et al., 2018).

Phase I started with a high pH, ranging between 9-9.5, which had the potential to inhibit the bacterial community involved in the nitrogen removal process in the reactor; however, after only five days of operation, pH was decreased to 7.99 and was stabilized in an acceptable range (Wett and Rauch, 2003). Similar to pH, alkalinity concentration was adjusted after six days of operation

to enhance the targeted bacterial consortium enrichment and growth (Figure 5-1B). Through 55 days of startup stabilization, the fraction of unionized ammonia lessened from 0.53 to 0.16 as the ammonia removal rate improved. As shown in Figure 5-1C, the unionized ammonia's fraction declined as the system reached a stable condition in which the pH was stabilized in a range between 7.5 up to 8.2 (Jin et al., 2012). At the end of this phase, the NRE reached above 85% while the NRR increased from an initial 0.11 $KgN/m^3/d$ to 0.16 $KgN/m^3/d$ (Figure 5-2 A).

In the second phase of operation, effects of a sudden increase in the influent's ammonia concentration were studied (ANOVA, $P \leq 0.05$) to evaluate the system's response behavior to a shock load and ultimately adjust the synthetic behavior feed composition. The influent ammonia concentration was increased by approximately 20 mgN/L, while the nitrite concentration was reduced to reach ammonia:nitrite ratio of approximately 0.85. The influent's pH and alkalinity concentrations were decreased due to feed alterations, in which the pH ranged between 6.9 to 7.8, and the alkalinity was reduced by almost 500 $mgCaCO_3/L$. As indicated in Figure 5-1 A, both ammonia and nitrite started to accumulate in the reactor. Although the ammonia removal rate reached 90% in phase I in less than 50 days, it declined by 41±5% in phase II due to inhibition caused by excessive substrate concentration. Several studies indicated ANAMMOX inhibition resulting from high ammonium concentrations, which may also cause ANAMMOX bacteria cell destruction (Jin et al., 2012). It has been suggested that the actual inhibitor of the process is free ammonia (FA) afore ammonium, which has been broadly studied for anaerobic digestion and nitrification process (Jin et al., 2012). During phase II (day 55 to 124), the NLR increased to 0.28 $KgN/m^3/d$ by changing the influent ammonium concentration (Figure 5-2 A), and as a result, the NRE decreased from 85.4% on day 54, to 66.4% by the end of the second operational phase.

FA concentration increased drastically by 77 ± 0.6% when the influent ammonia concentration was raised in the second phase. As shown in Figure 5-2 B, the average FA concentration increased from an average of 0.005 KgN/m^3/day in phase I to 0.007 KgN/m^3/day, in the inhibition stage of the second phase of the reactor operation. Studies on the effects of ammonium concentration on the ANAMMOX process showed a 50% decrease in specific ANAMMOX activity in a high concentration of free ammonia-nitrogen (FA-N), resulting in extensive instability and efficiency reduction (Fernández et al., 2012) (WAKI et al., 2007). Comparably, in this study, after an increase in FA concentration ammonia and nitrite removal rates decreased by, 35 ± 3% and 12 ± 5%, respectively. It was found that the reactor performance was under the stable operation period when the NO_3^--N to NH_4^+-N ratio was maintained within the relatively narrow range of 0.04-0.08 (Figure 5-2 B). The unstable condition was observed under high ammonia load in phase II and the recovery stage in phase III in which nitrate to ammonia ratio reached a high level of approximately 0.5. The NO_3^--N to NH_4^+-N ratios, at both adaptation and stabilizing periods in phase I and phase III, were lower than the theoretical value of 0.256.

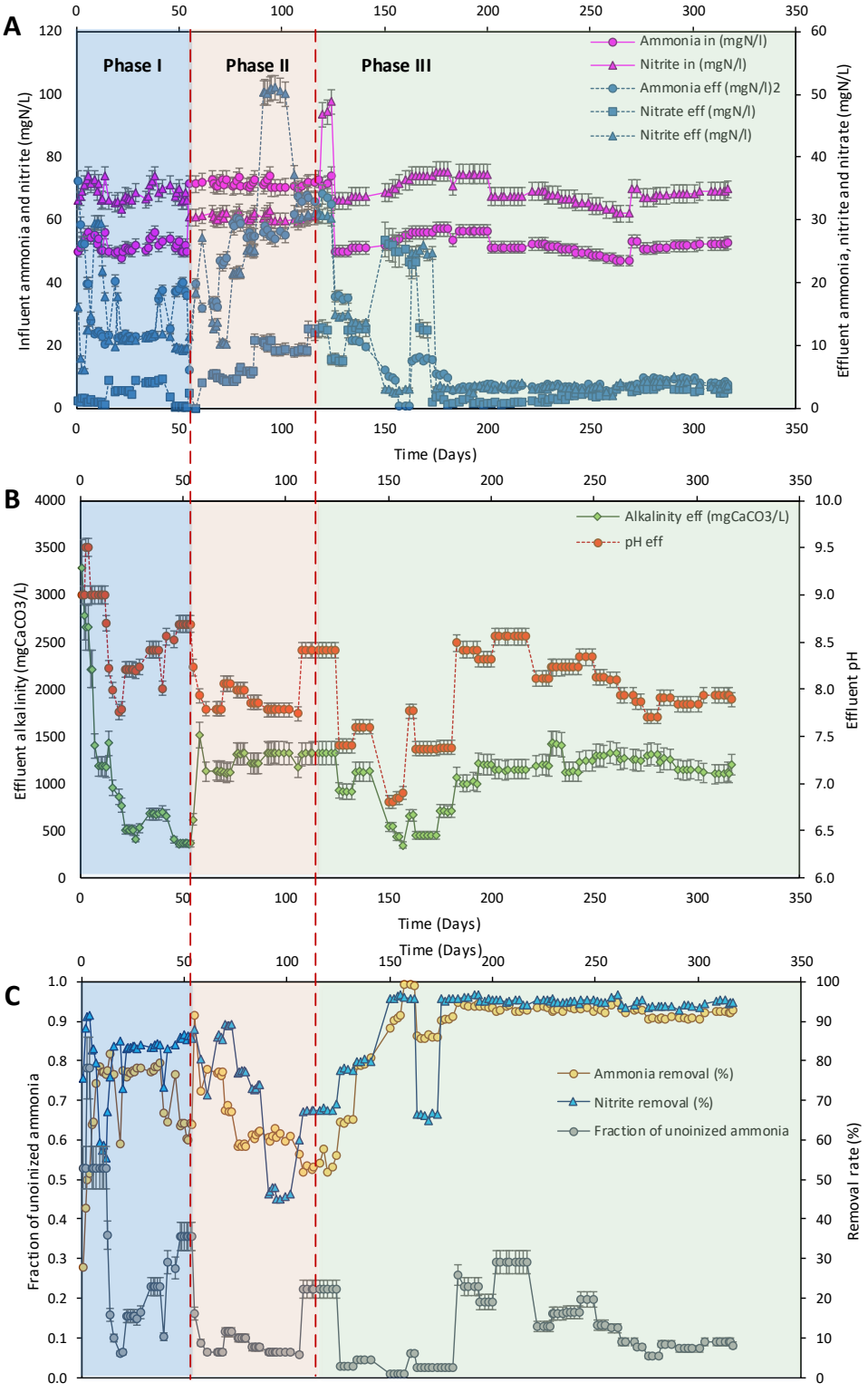

Figure 5-1 UASB reactor performance: A) Nitrogen compounds profile B) pH and alkalinity alterations in the effluent C) fraction of unionized ammonia in effluent and removal rates

Pearson's correlation coefficients (ρ) were applied to measure significant correlations between the influent ammonia concentration and the reactor's relative total nitrogen removal rates. Correlation analysis showed that these two variables had a significant negative correlation at the 0.05 level (Pearson correlation: -0.801). Based on the results, studying the increased residual ammonia concentration after this specific feeding phase, with a rise in the ammonia concentration of the feed injections, the effect of feeding strategies was shown strongly associated with the enhancement/inhibition of nitrogen removal performance in the UASB reactor. Thus, improved operational strategies were employed in phase III to better the relationship between effluent TN concentration and feed ammonia concentration. One-way ANOVA performed on the results, at a significance level of 0.05, indicating that ammonia and nitrite removal rates, as well as the TN removal efficiency, were significantly affected by the synthetic media composition.

In the final phase, the NLR returned to 0.2 $KgN/m^3/d$ (Figure 5-2 A) by reducing influent ammonium concentration. The influent's composition and nitrogen compound's concentrations were re-adjusted to have a molar nitrite: ammonia ratio ranging between 1.14-1.3. The third phase (Figure 5-2 A) indicated a stable ANAMMOX reaction after a fast recovery from strict inhibitory conditions and constant improvement of ANAMMOX activity. Along with ammonia removal of 90.3-94.8%, a concurrent depletion of nitrite was observed, in which the nitrite removal rate reached 96.06% over the period. At this influent ammonium level, a mean NRE of 91.6% was reached, highest in all phases (Table 5-3). The average NLR and NRR were 0.20 $KgN/m^3/d$ and 0.18 $KgN/m^3/d$, respectively. Analysis of variance (ANOVA) test shown that ammonia removal was significantly different ($p < 0.05$) from the previous phase under the new synthetic wastewater composition. Simultaneously, NO_3^- started to accumulate in the effluent of the reactor; however, the ratio is lower, which indicates the presence of autotrophic denitrifiers in the system. As

indicated in Figure 5-2 B, the observed NO_3^--N/NH_4^+-N ratios were also much lower than the proposed ratio of 0.256 after the recovery period, possibly caused by the activities of autotrophic denitrifiers. The co-existence of ANAMMOX bacteria and denitrifiers can positively affect the concurrent removal of nitrogen and organic carbon in a single system, decreasing the need for a sequential treatment process (Kumar and Lin, 2010). *Paracoccus denitrificans* species are mainly present in activated sludge samples and are able to utilize $S_2O_3^{2-}$, HS^- as their electron donor and NO_3^- as the electron acceptor to produce dinitrogen gas (Di Capua et al., 2019).

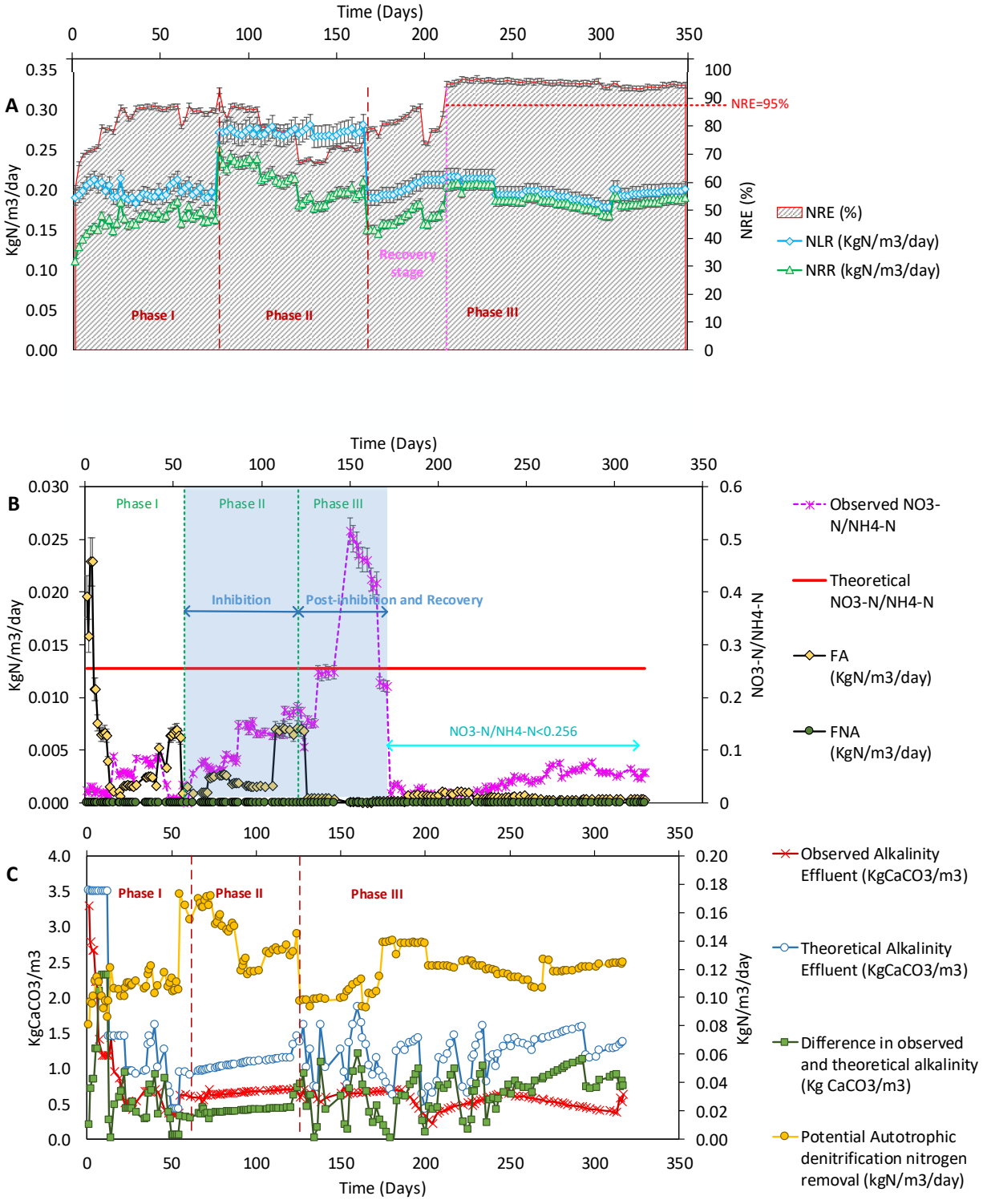

Figure 5-2 The performance of the reactor with continuous operation. (A) Nitrogen load rate (NLR), nitrogen removal rate (NRR), and nitrogen removal efficiency (NRE), (B) Nitrate to ammonia ratios, FA and FNA (C) Potential autotrophic denitrification analysis based on alkalinity concentration alterations

To confirm the ANAMMOX activities, a number of activity tests were done in parallel to monitor the nitrogen gas production capacity from the cultivated biomass. Through initial reliability and calibration tests, ammonium consumption and nitrogen gas production were detected, which confirmed ANAMMOX activity in the batch trial tests. Nitrogen gas production rate (NPR) was monitored to specify the biomass activity and stabilization during batch assays. NPR was monitored from day 53 to day 237, to specify the biomass enrichment and stabilization during the study (Van Loosdrecht et al., 2016). The NPR increased from 0.54 to 0.98 mgN/gBiomass.hr (Table 5-3)**,** from the startup to the final phase, indicating an increase in biomass activity rate and confirmation of ANAMMOX activity. Monitoring the alkalinity in the batch assays, the concentration of mg$CaCO_3$/L in the effluent followed the stoichiometry based on ammonium removal efficiency with a maximum of 3.45 ± 0.87 % error (Figure 5-1 B).

Table 5-3 Summary of variations in ANAMMOX process efficiency, granulation, microbial community and nitrogen gas production rate in different phases of operation

Operational phases	Mean NLR ($KgN/m^3/day$)	Mean NRE (%)	Mean particle size diameter (µm)	SVI (cm^3 g VSS^{-1})	$VSS_{Reactor}$ (g/L)	NPR (mgN/gbiomass.hr)	*Planctomycetes* Relative abundance (%)	*Chloroflexi* Relative abundance (%)
Start-up	-	-	145.8	81.29	8.49	-	0.70	0.66
Phase I	0.198	81.6	173.1	50.12	8.58	0.54	2.17	2.86
Phase II	0.272	76.3	180.6	48.61	8.74	0.61	5.34	4.94
Phase III	0.198	91.6	234.7	38.33	8.96	0.98	9.64	6.33

The maximum specific ANAMMOX rate of 357.85 as mgN_2-N. $gVSS^{-1}$ h^{-1} was calculated in phase III of reactor operation, by Equation 6 in Table 5-2. Similarly, specific biomass ammonium oxidation rate ($q_{AMX,\ NH4\_N2}$) of 7.41 mgN. $gVSS^{-1}$ h^{-1} and specific biomass nitrite reduction ($q_{AMX,\ NO2\_N2}$) and nitrate production ($q_{AMX,\ NH4\_NO3}$) rates were calculated for final phase, resulting in the maximum specific rates of 9.72 and 0.95 mgN. $gVSS^{-1}$ h^{-1}, respectively. The calculated

$Y_{NH4\_NO2,AMX}$ and $Y_{NH4\_NO3,AMX}$ ratios (Equation 7 and 8) were 1.135 and 0.152 gN. g N^{-1}, respectively, in which the reported values are different from the referenced stoichiometry because of the potential simultaneous occurrence of autotrophic denitrification indicated by nitrite and nitrate ratio in the process effluent (Van Loosdrecht et al., 2016).

5.3.2. Development and characteristics of micro-granules

Compared to the initial seed source, the RAS, the ANAMMOX consortium had significantly improved settling properties due to the micro-granulation process. Sludge volumetric index (SVI) of the sludge was improved substantially (SVI changed from 81.29 for the initial RAS sludge to 38.33 cm^3. $gVSS^{-1}$) where the average concentration of VSS measured in the effluent was 5–10 mgVSS/ L (SRT = 110±20 days) (Table 5-3). All the analysis done for comprehension of sludge settlibility and granulation process was completed on triplicate samples to minimize the error and increase the accuracy of the measurements. All samples for this analysis series were collected from the bottom portion of the reactor where the mature ANAMMOX biomass was cultivated. To ensure that all measurements represent the entire reactor, the sampling was done by taking the sample when the solids were in motion, and the entire cross section of the entire stream was sampled three times. When the liquid sample was stored in the plastic container, it was continuously mixed by rolling and tumbling (the container was only half to two-thirds full). The continuous mixing was performed before grabbing a sub-sample with a pipet. Studying the volume statistics from RAS and ANAMMOX samples, the standard deviation decreases from 324.4 to 112.9 µm, respectively. Based on particle size distribution analysis in start-up sludge, as indicated in Figure 5-3 A, the sample's mean, median and mode of particle diameter were 142.8, 113.8 and 140.1 µm with a standard deviation of 111.4 µm and a variance of 12404 $µm^2$.

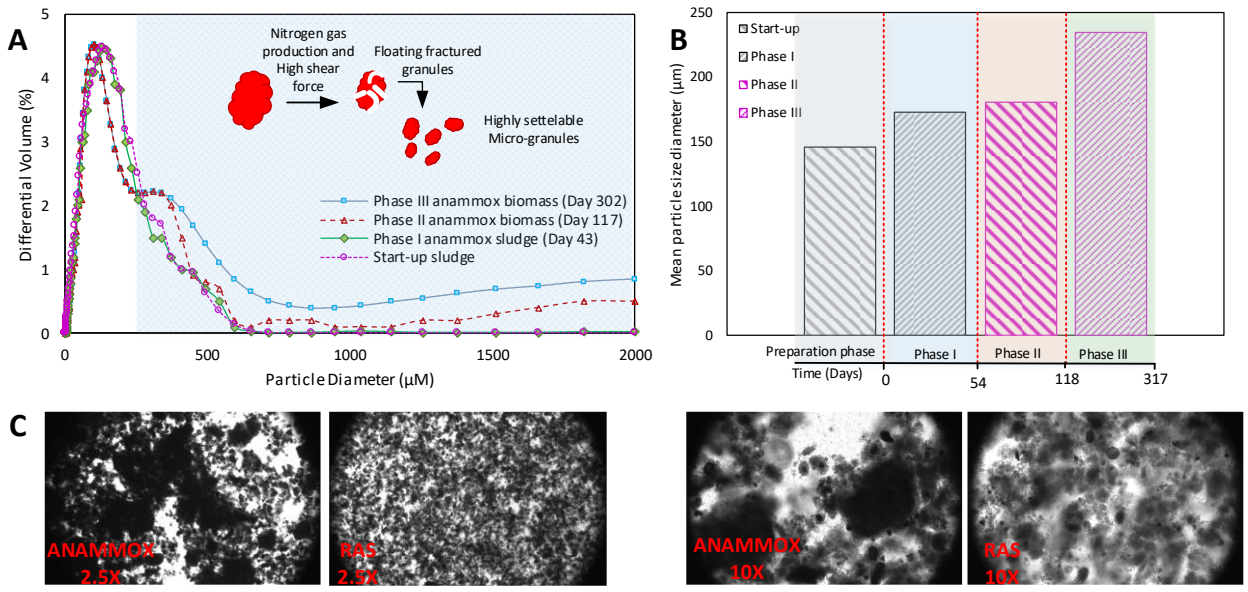

Figure 5-3 A and B) Variation of granule size distribution in sludge during three phases of operation and the startup period C) Microscopic images of micro-granules in mature ANAMMOX sludge in comparison to suspended RAS

The results indicated that below 10%, 50% and 90% of the sample had a particle diameter size of 30.17 µm, 113.8 and 301.0 µm. As shown in Figure 5-3 B, ANAMMOX biomass cultivated from RAS, had a relatively higher mean particle diameter, by approximately 39.15±2.4 %. The mean, median, and mode for the mature ANAMMOX sludge were 234.7, 121.8, and 105.9 µm. The size distribution in the anaerobic ammonia oxidation consortium shows a particle diameter of between 253.2– 465.7 µm for above 75% of the total sample volume. Granules adopt a variety of diameters and structures owing to the different operational states and influents conditions (Szabó et al., 2017); however, looking into the samples collected from the later phases of operation, the floc size distribution was getting more uniform. Then, based on the extensive data set available from a continuous triplicate sampling of the reactor in different operational phases, it was shown that despite local heterogeneities probably associated with the morphological elements of the sludge bed, the particle size distribution of the biomass is uniform at the scale of the final operational phase. The reported suspended-grown micro-sized granules are considerably smaller in diameter

than those from a number of fixed-growth granule systems, with an average diameter of 1mm or larger. To maintain a stable ANAMMOX process in a biological wastewater treatment system, it is important to consider improving the microbial stability, diversity, and activity (Zhu et al., 2018). One of the most important factors in stability and efficiency for processes dealing with slow-growing bacteria is reaching a proper settlebility to retain the enriched consortium within the reactor by ANAMMOX granulation and to achieve fast startup of the ANAMMOX process with high efficiency (Ye et al., 2018). The size distribution of the granules in different operation phases (Figure 5-3 B), shows an increasing trend in the particle size and improvement in the micro-granulation process as the system reaches a stable ANAMMOX condition in phase III with high ammonia and nitrite removal rate. A noticeable shift in process efficiency occurred in the final phase of reactor performance when the sludge began to develop more robust micro-sized granules.

Volumetric size distribution of the UASB reactor's sludge in the startup period and after the granulation process in phase III, was carried out through inverted microscopy and as indicated in Figure 5-3 C, mature granules were formed. Figure 5-3 C demonstrates that a high number of granules have a round shape with a distinct outline; nevertheless, smaller aggregates with curved-in forms were also present, proposing the potential breakdown process of the larger granules as a result of high shear forces in the UASB reactor (Figure 5-3 A). The scanning electron microscopy (SEM) photos also indicated micro-granular sludge development in the UASB reactor. SEM was used to investigate the structures of micro-sized granules in a mature ANAMMOX sludge sample from the reactor. The SEM shows the presence of spherical granules with diameters of approximately 240 μm. As indicated in Figure 5-4, the scanning electron microscopy results indicated a common cocci-shaped cell structure as the main microorganisms on the granule surface surrounded by extracellular polysaccharide (EPS) matrix; however, diverse bacterial morphologies

were observed in the sludge due to synchronization of ANAMMOX consortium with other organisms. EPS is a major factor in the granulation process since it creates a gel-like network that keeps the microorganisms together in all types of biofilm formations (Oshiki et al., 2011). EPS presence becomes critical for stable ANAMMOX reactor operation, as EPS has an immense drive to mediate dense biofilm and granule formation. (Strous et al., 1999).

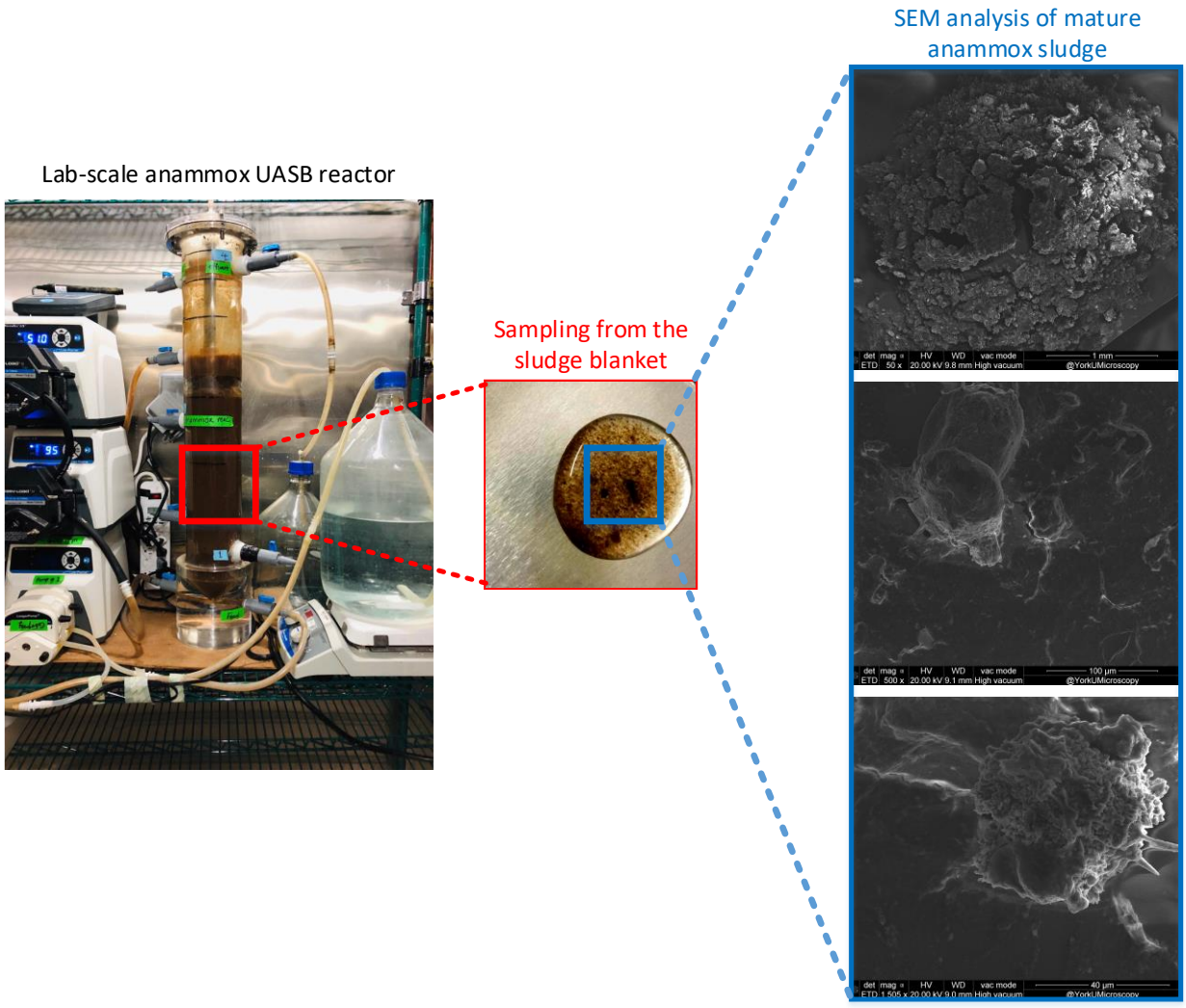

Figure 5-4 Analysis of morphological properties of the granules by SEM

Microscopic analysis in the present study indicates an observable transformation in sludge floc size (Table 5-3). Based on the microscopic results, ANAMMOX sludge has approximately 20 times larger flocs than the initial seeded RAS. At early stages in the startup period, in the UASB

reactor, granule-shaped aggregates start to accumulate, and sludge settleability improves. High shear stress induced by UASB reactor produced granules with smaller diameters than observed by other studies (Zhu et al., 2018). As indicated in Table 5-3, the results from this study indicate that the process efficiency (NRE) improved when the ANAMMOX biomass from the initial phases shifted to mature ANAMMOX micro-granular sludge.

5.3.3. Microbial population dynamics in three phases of operation and during granulation

There is a lack of focused studies on variations of microbial communities at different time slots of the process to better assess the dynamics, standard connections, and exchanges between ANAMMOX bacteria and other microorganisms in the early startup periods. Results of the analysis indicated, bacteria belonging to more than 30 phyla were detected in both samples of activated sludge and enriched ANAMMOX consortium. The bacterial community of the activated sludge from the full-scale treatment plant, which was used as the inoculum for the start-up of the experimental setup, differed significantly from that of the ANAMMOX sludge of the UASB reactor. As indicated in Figure 5-6, the analysis from RAS sludge samples shows dominancy of members in three main genera: *Nitrosomonas*, *Thermomonas*, *Domibacillus*, with relative abundances of 30.23, 8.76, and 9.65 %, respectively. The results show a major decline in all specified genera after three phases of reactor operation, wherein samples from the final phase, *Nitrosomonas*, *Thermomonas*, *Domibacillus*, relative abundances reached 0.35, 4.59, and 0.00 %, correspondingly. Changes in the relative abundances between phases I to III were confirmed by one-factor analysis of variance. There were significant changes in relative abundances of the ANAMMOX bacteria, AOB, *Nitrobacter*, and *Nitrospira* during the reactor operation from the startup phase to the final phase of operation, as measured by qPCR (ANOVA, $P > 0.05$).

The bulk of the bacteria were members of *Proteobacteria*, with two in alpha-subdivision, four in the beta-subdivision, and eight in the gamma-subdivision for the majority of samples from both RAS and ANAMMOX sludge. The results of this study indicate that the overall percentage of *Planctomycetes*, which are the main phylum responsible for anaerobic ammonia removal, had increased from 0.69 % to 9.63% (Figure 5-5 A). There were four major phyla *Proteobacteria*, *Chloroflexi*, *Planctomycetes*, *Bacteroidetes* in collected samples from all three phases of reactor operation. Relative abundance of *Chloroflexi* increased gradually from 0.66 to 6.3 % (Figure 5-5 B). Abundance of *Proteobacteria* decreased from 61.5% to 51.7% and stayed in that range, during which, abundance of *Bacteroidetes* stayed in the range between 21.6- 23.1%.

As shown in Figure 5-6, the possible effective bacteria in both ANAMMOX granular sludge and RAS samples were evaluated by genus level heat-map analysis. The relative abundances of two groups of autotrophic denitrifiers, *Thiobacillus,* and *Denitratisoma,* changed substantially from 0.00 to 7.81% and 0.00 to 4.33%, respectively, in the course of startup to the final stage of operation. *Thiobacillus* is a sulfur-based denitrifican and is mainly involved in sulfur oxidization and production of sulfates under both aerobic and anaerobic conditions (Morrison et al., 2018). Since ammonium sulfate was introduced to the reactor as the process substrate continuously, a sufficient dosage of sulfur was available for nitrate reduction to nitrogen gas through autotrophic denitrification pathway by *Thiobacillus* genera. *Thiobacillus denitrificans* belong to class β of *Proteobacteria* and utilize S^0, HS^- or $S_2O_3^{2-}$ as electron-donor to oxidize NO_3^- or NO_2^- to produce N_2, NO_2^- or N_2O (Di Capua et al., 2019). Results indicated in Figure 5-6 also show a major increase in abundance of *Paracoccus* genera from 0.56% to 4.63%. *Paracoccus denitrificans*, are nitrate-reducing bacterium belonging to *α- Proteobacteria*, involved in reducing NO_3^- to either N_2 or N_2O, by using HS^- or $S_2O_3^{2-}$ as the electron-acceptor for the reaction (Di Capua et al., 2019).

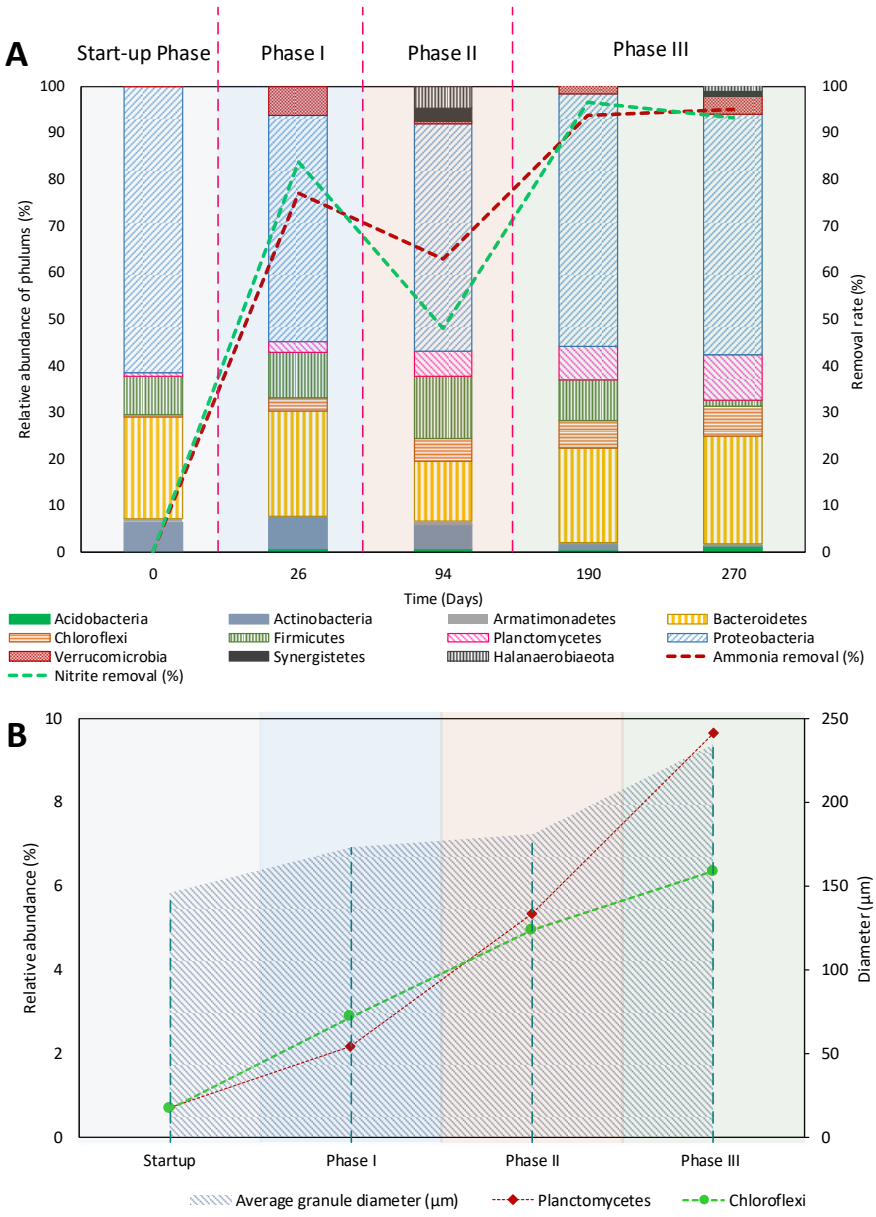

Figure 5-5 Evolution of the bacterial community compositions; A) Phylum variations B) Variation of granule size distribution and microbial composition alterations in sludge, during 3-phase operation

Approximately entire bacteria belonging to *Planctomycetes* detected on day 270 were ANAMMOX bacteria. Microbial analysis results indicated, ANAMMOX bacteria closely related to "*Ca.* Brocadia sp.", including "*Ca.* Brocadia caroliniensis" (KF810110, 99% similarity in the 16S rRNA gene sequences) were predominant in the inoculum. As shown in Figure 5-6 the second

major genera in mature ANAMMOX sample was "*Ca.* Kuenenia", which confirmed the results from previous studies suggesting that the ANAMMOX process in a laboratory or pilot-scale reactors is principally performed by bacteria of the genera "*Candidatus* Kuenenia*"* or "*Candidatus* Brocadia*"* (Reino et al., 2018) (Jianhua Guo et al., 2016). Pearson correlation evaluations were applied to recognize any potential quantitative relationship between microbial abundance and the operational phase (a *p*-value of lower than 0.05 was considered as significant). Pearson correlation examination revealed that the relative abundance of the ANAMMOX bacterial population positively correlates with the reactor operational phases and correspondingly the operation duration and synthetic feed composition (Pearson = 0.501, $p = 0.014$), whereas the AOB bacteria abundance negatively correlated with the reactor phases (Pearson = −0.719, $p < 0.001$).

The increase in the abundance of filamentous bacteria belonging to the phylum *Chloroflexi* from 0.6 to 6.3%, were potentially due to their presence on the surface of the ANAMMOX micro-granules and around the ANAMMOX bacterial aggregates (Kocamemi et al., 2018). Considerable detection of *Roseiflexus* and *Herpetosiphon* with relative abundances of 4.24 and 5.23% in phase III, suggests that this group may perhaps be a prominent factor for micro-granulation (Figure 5-5 B) by forming the preliminary structure of the granules and by engaging in the role of a core or carrier that accepts other microorganisms to attach and grow (Pereira et al., 2017). The simultaneity of bacterial groups similar to *Chloroflexi* with ANAMMOX bacteria in granules has already been stated in previous studies, and as observed in this study, a good granulation was maintained in the UASB reactor (Cho et al., 2010).

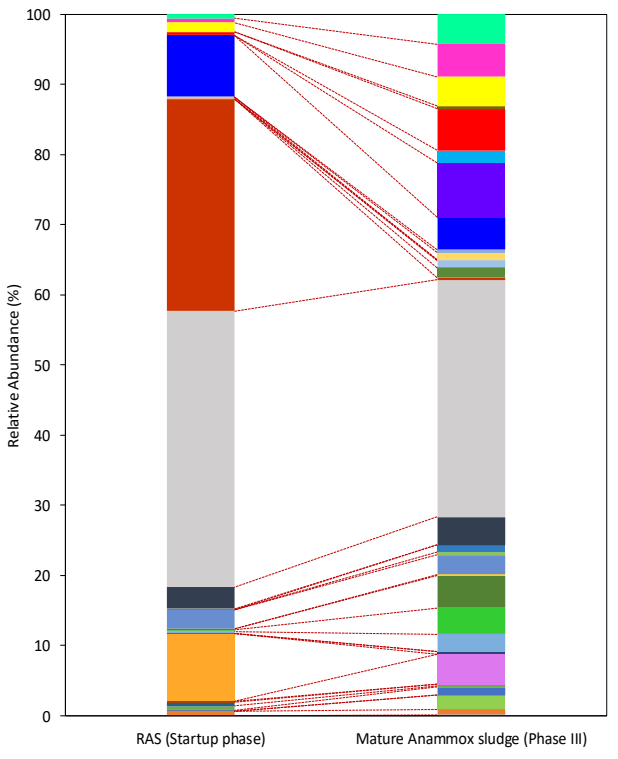

Genus Level Analysis	RAS (Startup phase)	Mature Anammox sludge (Phase III)
Alkaliphilus	0.02	0.12
Amaricoccus	0.63	0.78
Aminivibrio	0.00	2.01
Anaeromyxobacter	0.01	0.00
Arenimonas	0.13	1.17
Bryobacter	0.60	0.17
Comamonas	0.48	0.24
Dechloromonas	0.18	0.00
Denitratisoma	0.00	4.33
Domibacillus	9.65	0.00
Geobacter	0.00	0.29
Geothrix	0.03	0.00
Hyphomicrobium	0.26	2.52
Ca. Kuenenia	0.24	3.75
Lautropia	0.20	4.55
Lentimicrobium	0.00	0.20
Limnobacter	2.70	2.79
Longilinea	0.00	0.48
Lutispora	0.00	0.92
Lysinibacillus	0.09	0.00
Mycobacterium	3.12	4.01
NA	39.38	33.83
Nitrosomonas	30.23	0.35
Proteiniborus	0.00	1.38
Proteiniclasticum	0.03	1.04
Pseudomonas	0.03	0.14
Rhodobacter	0.28	0.00
Soehngenia	0.00	0.96
Tabrizicola	0.00	0.44
Thermomonas	8.76	4.59
Thiobacillus	0.00	7.81
Tissierella	0.00	1.77
Candidatus Brocadia	0.46	5.93
Youngiibacter	0.00	0.35

Figure 5-6 Relative abundance of the functional species at the genus level and the heat-map showing the microbial community structure of the ANAMMOX sludge collected from the reactor in comparison with the initial seed (RAS), Green color are for higher abundance values (above 30%), red for lower abundance values (below 0.05%), orange in different shades for values between 0.05 up to 0.3 and yellow in different shades for values from 0.3 to 30.

Nitrifying bacteria including ammonia-oxidizing bacteria (AOB) were detected in high levels (30.23%) in the RAS samples in the present study (Figure 5-6). Giving the phylogenetic analysis, after 270 days of operation, over 25% of the identified bacteria in the suspended biomass can contribute to nitrogen removal. The results of the microbial analysis illustrated in the heat map in Figure 5-6, indicated the presence of different anaerobic denitrifying bacteria, *Pseudomonas*, *Methylobacterium*, *Bacillus*, *Paracoccus*, and an aerobic denitrifying bacterium, *Hyphomicrobium*, which were potentially responsible for nitrate to dinitrogen gas transformation. Coexistence of a significant number of denitrifying bacteria specified a prospective for conventional denitrification occurrence in the system which had an important role in nitrogen removal. Based on the continuous effluent analysis in Figure 5-2 C, the measured

alkalinity was constantly lower than the theoretical amount calculated from the stoichiometry. According to the stoichiometry of S-based autotrophic denitrification (Table 5-2), the reduction of 1 mgN-NO_3 consumes 3.36 mg/L of alkalinity as $CaCO_3$ (Di Capua et al., 2019), which is the potential trigger of alkalinity reduction in the UASB reactor. In the Autotrophic denitrification pathway, sulphur is the electron donor for the microorganisms, along with calcium carbonate being a neutralizing agent for protons released in microbial respiration (Lewandowski et al., 1987). The cohabitation of ANAMMOX with other bacteria such as denitrifiers and nitrifiers has been found of importance in wastewater treatment plants for nitrogen removal, and it is well studied. However, the coexistence of denitrifying and ANAMMOX bacteria has been validated and reviewed recently (Huang et al., 2018). Anoxic conditions and maintaining an influent carbon to nitrogen ratio of below 2, are essential factors, to attain a stable denitrifying and ANAMMOX bacteria coexistence (Huang et al., 2018) (Pereira et al., 2017). This coexistence can play a major role in nitrogen and COD-containing wastewater treatment (T. Wang et al., 2009).

5.4. Conclusion

The study focused on the influence of microbial population dynamics on stable and efficient nitrogen removal performance to generate micro-sized granules and to overcome dominant-negative effects of large size granules on process performance, including particle floatation and run-off. Enrichment was achieved from RAS in a UASB reactor without bioaugmentation. The reactor, running for approximately one year, reached 95% nitrogen removal, after less than two months in the stabilization phase, with a loading rate of 0.22 KgN /m^3/day. Settling properties of biomass improved while the SRT of the reactor was 36-72 days. ANAMMOX bacteria abundance increased in process of granule formation and the microbial species present in the sludge changed throughout the three phases. Species identified at the end of process in phase three were more

member of ANAMMOX or filamentous bacterial groups, than the species of the seeding sludge. This study successfully achieved ideal micro-sized ANAMMOX granular sludge to obtain high nitrogen removal efficiency and minimum biomass washouts and prompt ANAMMOX enrichment from activated sludge within less than 50 days of operation.

CHAPTER 6

Parin Izadi[a] , Parnian Izadi[a] , Ahmed Eldyasti*[a]

[a] Civil Engineering, Lassonde School of Engineering, York University, 4700 Keele Street, Toronto, ON, Canada , M3J 1P3

* Corresponding author

Authors' contributions Parin Izadi and Dr Eldyasti contributed to the study concept and design. Experimental system setup, material preparation, data collection and experimental analysis were performed by Parin Izadi and Parnian Izadi. The first draft of the manuscript was written by Parin Izadi and Parnian Izadi commented on previous versions of the manuscript. Dr. Ahmed Eldyasti prepared the final submitted draft and critically revised the work. All authors read and approved the final manuscript.

From Sidestream Restoration to Warm-Mainstream Mitigation: Evaluation of Nitrogen Loading Rate Impact on ANAMMOX Activity and Potential Contribution of Intermediates in Inhibition-Recovery Dynamics[4]

Abstract

ANAMMOX is a developing process for nitrogen removal; however, mainstream line conditions could upset the slow-growing ANAMMOX microbial activity and dynamics. To assess the mainstream ANAMMOX process applicability, it is essential to study the obstructing or stimulating impacts of a range of common additives. This study mainly focused on a set of manometric batch experiments to evaluate ANAMMOX performance efficiency in different conditions, emphasizing high-temperature mainstream conditions. Increasing the ammonia and nitrite concentrations to above 1000 mgN/L, disrupted the process performance, leading to complete ANAMMOX activity inhibition. Decreasing the load down to 0.1-0.36 $KgN/m^3/day$, mimicking mainstream ANAMMOX process, resulted in a slight decrease of nitrogen removal efficiency. With the addition of 10 and 30 mgN/L of hydroxylamine to mainstream-based tests, the removal efficiency was restored, showing the recovery potential of intermediates in damaged ANAMMOX systems plus being a boosting agent for high-temperature mainstream ANAMMOX process implementation.

Keywords

ANAMMOX, Mainstream, Granular sludge, Batch test, Inhibition and stimulation, Specific ANAMMOX activity (SAA)

[4] This Chapter is under review in the International Journal of Environmental Science and Technology, JEST-D-21-01821R1

6.1. Introduction

The ANAMMOX process is highly sensitive to a number of potential inhibiting factors, including substrate concentrations, dissolved oxygen levels, free ammonia, and nitrous acid concentrations (Zekker et al., 2012). Even though nitrite is a necessary substrate for ANAMMOX process, but disproportionate concentrations of this constituent can result in process destruction (Jin et al., 2012). There have been several confirmations on the severe inhibition effect of nitrite on the ANAMMOX consortium, even at low concentrations (Bettazzi et al., 2010). A number of studies identified the considerable impact of nitrite concentration on ANAMMOX process; however the stated threshold considerably fluctuated from 5 to 280 mgN/l with different operational and environmental conditions (Jin et al., 2012). Strous et al. observed inhibition effects on a sequential batch reactor (SBR) ANAMMOX process when 23.3 mgN /L was introduced to the system, and a complete loss of activity was reported when the reactor was subjected to 42.5 mgN /L (Strous et al., 1999). A 50% decrease in ANAMMOX activity was identified when nitrite concentrations reached high levels of 80.5 mgN /L (Bettazzi et al., 2010). Fernandez et al, suggested that free nitrous acid (FNA), the undissociated compound, is mainly accountable for the inhibitory impacts detected from the introduction of elevated concentrations of NO_2^- to ANAMMOX bacteria (Fernández et al. 2012), yet other studies suggest that the suppression is just conditional on the total NO_2^- concentrations (Carvajal-Arroyo et al., 2014). Enzymatic inhibition has been reported as a result of NO_2^- exposure in various microorganisms (Hurst and Lymar, 1997). In a few cases, nitrite radicals or reactive derivatives become the main toxic agents and react with biomolecules, including the major development of nitrotyrosine resulting from reaction with tyrosine moieties (Carvajal-Arroyo et al., 2014). NO_2^- is in equilibrium with FNA, while free nitrous acid enters bacterial membranes thru passive diffusion and becomes a potential protonophore which acts as a troublesome element for transmembrane proton gradients (Zekker et al., 2017). Based on a

hypothesis by Caravajal-Arroyo et al, the inhibition resulting from nitrite introduction to ANAMMOX bacteria occurs in riboplasm and ANAMMOXOSOME, which inactivates the oxidizing enzymes and results in interruption of NO_2^- detoxification by active pumps that are mainly energized by transmembrane proton motive forces (Carvajal-Arroyo et al., 2013).

Ammonium has been detected as a potential cause of low-grade inhibition for ANAMMOX microorganisms (Waki et al., 2007). Strous et al, reported that ANAMMOX process is not inhibited by NH_4^+ introduction up to a concentration level around 1gN/L (Strous et al., 1999). Several studies reported the ANAMMOX activity destruction by the presence of high ammonium concentrations (Van Hulle et al., 2010). A 50% loss of ANAMMOX activity was observed when the ammonia concentration reached 770 mgN/L (IC50=770 mg/L), and free ammonia was detected as the main contributor to the inhibition process rather than ammonium itself (Dapena-Mora et al., 2007b). In presence of 38 mgN/L of free ammonia-nitrogen (FA-N) in a short-term batch test, a 50% decrease in specific ANAMMOX activity was observed. FA-N concentrations over 20-25 mgN/L in sequencing batch reactors as a long-term effect study resulted in performance instability (Jin et al., 2012) (Fernández et al., 2012). Increasing the concentrations over 20-25 mgN/L in the long-term process resulted in instability and efficiency reduction, down to zero. The optimal FA-N concentration to maintain a stable ANAMMOX performance is reported to be below 20-25 mgN/L (WAKI et al., 2007). Based on the results of different studies, it can be concluded that the ANAMMOX bacteria has the capability to endure free ammonia (FA) through adaptation (Jin et al., 2012). ANAMMOX bacteria can tolerate high ammonium concentrations; however FA concentration levels beyond a specific limit constrains the process. The dissimilarities between the results of various studies can be explained through operational and environmental variants distressing the anaerobic process (Jin et al., 2012) (Anthonisen et al., 1976).

In mainstream conditions with low nitrogen concentration levels, ANAMMOX bacteria are easily over competed by other nitrogen-based bacterial groups such as ammonia-oxidizing bacteria (AOB) and nitrite-oxidizing bacteria (NOB) because of their low growth rates and depressed bacterial yields (T. R. V Akaboci et al., 2018). Despite numerous studies, reaching a possible mainstream ANAMMOX application continues to be a significant burden, and no full-scale installations have been reported (Qiu et al., 2020). Some studies achieved removal efficiencies of 51-81% with nitrogen removal rates in a range of 190-434 mgN/L.d (R. Chen et al., 2019a), with mainstream nitrogen levels in warm conditions (Dai et al., 2015). The results were comparable to conventional nitrogen removal systems in full-scale treatment plants; however the quality of the effluent in terms of nitrate levels was not stable and guaranteed (Cao et al., 2017). Despite the major challenges in implementation, mainstream ANAMMOX is becoming a critical technology for energy-neutral treatment systems (C. Wang et al., 2018). Various approaches are necessary to be studied to accelerate bacterial metabolism, especially in mainstream conditions, restore the ANAMMOX activity, and stimulate the nitrogen removal rate in the system (Liu et al., 2013). There are no specific explications of the activity decline mechanism in mainstream conditions; however Z. Hu et al. (2013), linked the low yield and high maintenance energy of the ANAMMOX bacteria to low-temperature levels, resulting in a disruption in nitrate formation and ammonium removal in the process (Cao et al., 2017). ANAMMOX activity level drops sharply at lower temperatures leading to process instability (Straka et al., 2019).

Based on van de Graaf et al. (1997), ANAMMOX pathway model, hydroxylamine and hydrazine are the main intermediate metabolites of anaerobic ammonium oxidation. A recent proposed biochemical pathway consists of nitrite reduction to nitric oxide by cytochrome cd1-type or copper-containing nitrite reductase (Hira et al., 2012), followed by the production of

hydroxylamine coupled with ammonia to generate hydrazine by hydrazine synthase (Dietl et al., 2015), and eventually oxidation of hydrazine to nitrogen gas via hydrazine dehydrogenase (Oshiki et al., 2016). Hydroxylamine has been proven to benefit anaerobic oxidation of ammonia in low concentrations (Hu et al., 2010). Optimum concentrations of hydroxylamine can potentially improve the total nitrogen removal rate and accelerate the recovery from previous inhibitions within a reasonable period (Zekker et al., 2012). After adding hydroxylamine, an increase in hydrazine level was detected, which led to the production of dinitrogen gas and ammonia (Wouter R L van der Star et al., 2008). M Strous, Kuenen, and Jetten 1999, reported on different promotional effects of hydroxylamine and hydrazine. On the other hand, Bettazzi et al. 2010, reported on the elevated positive effects of both hydrazine and hydroxylamine when added in combination, rather than separate injections. A set of experiments performed with ANAMMOX granules indicate an improved nitrite utilization rate when the hydroxylamine to nitrite ratios were increased from 1:1 to 2:1 (Hu et al., 2010).

The main purpose of the present work is to uncover a link between ANAMMOX activity, granule structure, total nitrogen removal efficiency, and substrate loading rate to ultimately facilitate the path towards mainstream ANAMMOX application. This study aimed to investigate the dynamic response of the micro-granular ANAMMOX consortium when either inhibition or stimulation factors, including the main process substrates and intermediates, are introduced. There has been a lack of focus on the prospective impacts of inhibition factors on ANAMMOX granular structure; furthermore the potential contribution of intermediates in recuperating the impaired structure has been neglected. This research focuses on identifying the intermediate-based recovery opportunities in harsh loading rates at the sidestream level and links hydroxylamine's potential stimulatory effects to mainstream application. To the best of our knowledge, there are few reports which

focused on the effects of intermediates in low substrates loading rates (high-temperature mainstream conditions) on the ANAMMOX microorganisms enriched in the form of micro-granules. In this study, a thorough analysis of the granular size distribution and the settlibility characteristics leads to an improved understanding of the projected mass transfer and correlation between different bacterial groups, possibly enhancing the bacterial activity and process metabolism. The driving hypothesis that understanding the effect of hydroxylamine on microbial activity and aggregated structure in warm-mainstream conditions can promote the process applicability, offering a sound basis for considering intermediates as ANAMMOX-accelerators.

6.2. Materials and methods

6.2.1. ANAMMOX enrichment system

The biomass was collected from a single-stage continuous flow lab-scale upflow anaerobic sludge blanket (UASB) reactor containing reddish-brown micro-granular sludge. The reactor with a working volume of 4.8 L, being continuously fed with synthetic wastewater and operated at around 35 ± 0.5 °C, was used to simulate sidestream ANAMMOX process. The amount of ammonia and nitrite was based on experimental design to achieve influent ammonia and nitrite concentrations of 52.02 and 62.42 mgN/L, respectively. The pH of the influent was 7.9 on average. The micro-granular UASB reactor has been operated under steady-state conditions with an average nitrogen loading rate of 0.22 KgN /m^3/day and the average SRT of the reactor ranged from 36 to 72 days. HRT of the system was controlled at an average rate of 24 hours, and the mean nitrite, and ammonium removal efficiencies were 95.32% ± 1.2 and 93.61% ± 1.8, respectively. The system operated for over 320 days led to a 4.5 ± 0.67% increase in the overall percentage of *Planctomycetes*, which are the main phylum responsible for anaerobic ammonia removal (Izadi et al., 2020a).

A comprehensive elucidation of all operational elements and data is included in a previous study done by Izadi et al., (2020). A summary of the principal operational factors of the ANAMMOX-UASB reactor is mentioned in Table 6-1.

Table 6-1 Overview of the fundamental operational factors and outcomes of UASB reactor

Operational phases	**Start-up**	**Phase I (~55 days)**	**Phase II (~63 days)**	**Phase III (~200 days)**
Mean NLR ($KgN/m^3/day$)	-	0.198	0.272	0.198
Influent Nitrite/Ammonia ratio	-	1.1-1.3	0.85	1.1-1.3
Temperature (°C)	35	35	35	35
HRT (Days)	1	1	1	1
pH	9.5-9	9.5-7.99	6.9-7.8	8.0-8.5
Alkalinity ($mgCaCO_3/L$)	~3000	~2500-3000	~1500-2000	~1000-1800
$VSS_{Reactor}$ (g/L)	8.49	8.58	8.74	8.96
Mean NRE (%)	-	81.6	76.3	91.6
Mean particle size diameter (μm)	145.8	173.1	180.6	234.7
SVI ($cm^3\ gVSS^{-1}$)	81.29	50.12	48.61	38.33
NPR (mgN/ gbiomass.hr)	-	0.54	0.61	0.98

6.2.2. Batch test experimental setup

The collected biomass from the UASB reactor was fully washed with nitrogen-free media, three times before adding to the batch experiment bottles. The batch tests (Table 6-2) on ANAMMOX micro-granular sludge were implemented by BOD Trak II, a manometric device consisting of six vessels (492 mL) placed in a warm chamber at 35 °C and mixed by a magnetic stirrer. The studies mainstream ANAMMOX processes deteriorated in low temperatures and generally could not sustain a stable nitrogen removal (Qiu et al., 2020). The temperature was kept at an optimum level to avoid any poor efficiency and process instability, to focus on the effect of loading rate and intermediates addition as the driving dynamics. The batch test bottles were sealed to prevent external atmospheric pressure changes. Additionally, in gas-tight batch reaction vessels, pressure

increased due to dinitrogen gas release, which is censored over time to quantify the reaction kinetics. During every test period, stir bars mix the sample completely and help simulate natural conditions. Two alternatives were considered to track the evolution of the ANAMMOX process: Chemical tracking, which is done by assessing the ammonium, nitrite, and nitrate concentration in the specific period, and manometric tracking by assessing the overpressure caused by dinitrogen release in a gas-tight reactor. The batch system consisted of different elements such as; a container for NaOH pellets located in the bottle headspace and serving as a CO_2 trap, a manometric measuring device with a data logger and fixed on the top of a glass bottle, constant temperature control to limit temperature fluctuations to ± 0.2 °C and a magnetic stirrer that can operate at around 100-200 rpm. Before and at the end of each test, pH was measured and a liquid sample was collected for analysis. The pH was kept within the range of 7.6–8.0 and adjusted after each test. Bicarbonate salt ($KHCO_3$) was added, if necessary, to guarantee a sufficient inorganic carbon amount required for the anabolic pathway of the ANAMMOX reaction.

Table 6-2 Overview of the test configuration for added substrates and intermediate to ANAMMOX batch experiments

	Influent NO_2-N^-: NH_4-N^+ /Temperature (°C)	**Test name**	**Ammonia levels (mgN/L)**	**Nitrite levels (mgN/L)**	**Hydroxylamine levels (mgN/L)**
1	1.32	High Ammonia (**HA**)	1000 1500 2000	Set based on influent ratio	-
2	1.32	High Nitrite (**HN**)	Set based on influent ratio	1000 1500 2000	-
3	1.32	Low Ammonia (**LA**)	50 100 150	Set based on influent ratio	-
4	1.32	Low Nitrite (**LN**)	Set based on influent ratio	50 100 150	-

5	1.32	High Hydroxylamine (**HH**)	Based on the influent concentrations	10 (**HH1**) 15 (**HH2**) 22.5 (**HH3**) 30 (**HH4**)
6	1.32	Low Hydroxylamine (**LH**)		1.5 (**LH1**) 3 (**LH2**) 3.5 (**LH3**) 4.5 (**LH4**)
7	1.32	Ammonia Recovery with Hydroxylamine (**ARH**)	1000, 50 1500, 100 2000, 150	Set based on influent ratio	10, 30 10, 30 10, 30
8	1.32	Nitrite Recovery with Hydroxylamine (**NRH**)	Set based on influent ratio	1000, 50 1500, 100 2000, 150	10, 30 10, 30 10, 30

6.2.3. Feeding configuration

Stock solutions containing specific concentrations of ammonium and nitrite were dosed to the wastewater at the beginning of each test to provide the desired amount of substrate. Stock solutions were prepared using ammonium sulfate and sodium nitrite salts. Main substrates were provided by $(NH_4)_2SO_4$, $NaNO_2$, and $NaHCO_3$ (0.420 g L^{-1}). The inorganic solution consisted of $CaCl_2.2H_2O$ (0.18 g L^{-1}), $MgSO_4$ (0.059 g L^{-1}), and KH_2PO_4 (0.027 g L^{-1}). The trace elements solutions contained (g/L): EDTA 5 and $FeSO_4$ 5, EDTA-$2Na_{15}$, $CuSO_4 \cdot 5H_2O$ 0.25, $ZnSO_4 \cdot 7H_2O$ 0.43, $NaMoO_4 \cdot 2H_2O$ 0.22, $MnCl_2 \cdot 4H_2O$ 0.99, $NiCl_2 \cdot 6H_2O$ 0.19, $CoCl_2 \cdot 6H_2O$ 0.24, $NaSeO_4 \cdot 10H_2O$ 0.21 and H_3BO_4 0.014. The amount of ammonia and nitrite is based on experimental design. The pH of the influent was 7.9 on average.

6.2.4. Experimental configuration

The first set of tests were carried out as trials to monitor the reliability of the batch experiments by evaluating the accuracy of the method for N_2 gas production detection and analyzing the total nitrogen mass balance in the liquid phase through 120 hour periods. Duplicate batch tests were

performed using mature ANAMMOX biomass collected from the lab-scale UASB, with the volatile suspended solids (VSS) concentration of 3.79 ± 0.2 g/L. The batch assays were conducted to study the effect of various concentrations of ammonium and nitrite (NH_4-N^+ and NO_2-N^-) as process substrates and hydroxylamine ($NH_2OH \times HCl$) as main process intermediate (Table 6-2) on the ANAMMOX activity, total nitrogen removal and nitrogen gas production rate. To evaluate the short-term effects (inhibitory or enhancing) of different substrate levels on ANAMMOX activity and process performance, different nitrite and ammonium concentrations were added simultaneously to 12 different vessels (Table 6-2**,** Test 1-4). The HA and HN tests were mimicking sidestream ANAMMOX process with an influent COD/N ratio of 1.5 to 2. The COD concertation in Tests 1 and 2 ranged between 1750-3000 mgCOD/L. The COD concentration in Tests 3 and 4, mimicking mainstream ANAMMOX process, was set to a range between 500-2100 mgCOD/L to have a COD/N ratio between 6-8. The next set of tests (Tests 5 and 6) focused on the effect of hydroxylamine in two series of low and high concentrations, in which the ammonium and nitrite concentrations were adjusted to remain at the initial influent levels. The final assessments (Table 6-2, Test 7 and 8) evaluated the effect of two particular concentrations of hydroxylamine on the post-inhibition recovery process for both ammonium and nitrite high concentrations and mainstream conditions.

6.2.5. Analytical methods

Linear regressions of substrates level fluctuations throughout the tests, were performed to examine the total nitrogen conversion rates. The linear correlation coefficients (R_2) were above 0.9 in every single one of the instances. The maximum specific ANAMMOX rate (mgN_2-N. $gVSS^{-1}$ h^{-1}) was analyzed through Equation 4 in Table 6-3. Correspondingly, specific biomass ammonium oxidation rate based on nitrogen gas production from ammonia loading ($q_{AMX,\ NH4\_N2}$) mgN. $gVSS^-$

^{1} h^{-1} and specific biomass nitrite reduction calculated based on nitrite and nitrogen gas ratios ($q_{AMX, NO2\_N2}$) and nitrate production ($q_{AMX, NH4\_NO3}$) rates established on ammonia and nitrate ratios, were assessed. In the activity test assessment, the $Y_{NH4\_NO2,AMX}$ and $Y_{NH4\_NO3,AMX}$ ratios were evaluated via Equation 5 and 6 specified in Table 6-3, correspondingly (Van Loosdrecht et al., 2016). The MS Excel 2016 Analysis ToolPak were used to complete data and statistical examinations. In the activity testing procedure, the determined $Y_{NH4\_NO2, AMX}$ and $Y_{NH4\_NO3, AMX}$ ratios (Equation 5 and 6) were 1.135 and 0.152 gN. gN^{-1}, respectively. The stated amounts are contrasting to the suggested stoichiometry due to the potential of concurrent occurrence of autotrophic denitrification (Izadi et al., 2020a).

Table 6-3 Theoretical equations

1	Nitrogen loading rate ($KgN/m^3/day$)	$NLR = TN_{in}/HRT$
2	Nitrogen removal rate ($KgN/m^3/day$)	$NRR = \Delta N/HRT$
3	Nitrogen removal efficiency ($KgN/m^3/day$)	$NRE = \Delta N/NLR$
4	Maximum specific ANAMMOX rate (mgN_2-N. $gVSS^{-1}$ h^{-1})	$qAMX,N2 = \frac{rAMX,NH4 + rAMX,NO2 - rAMX,NH4\_NO3}{XVSS}$
5	Ammonia to nitrite ratio	$YNH4_{NO2},AMX = \frac{rAMX,NO2}{rAMX,NH4}$
6	Ammonia to nitrate ratio	$YNH4_{NO3},AMX = \frac{rAMX,NH4\_NO3}{rAMX,NH4}$

The influent and effluent samples were collected before and after the 120-hour batch time period and analyzed without delay (All samples were collected in triplicates). Water samples were evaluated based on the standard methods of water and wastewater examination. Concurrent examination of anions and cations was applied via ion chromatography by Thermo Scientific™

Dionex™ Integrion™ HPIC™ system. Ahead of all IC measurements, samples were accurately diluted with deionized water and passed over a membrane filter (0.45 µm). Additional analytic assessments (e.g., pH, TSS, VSS, Alkalinity, etc.) were operated according to Standard Methods (APHA, 2005). The biomass concentration was specified as suspended solids (SS) and volatile suspended solids (VSS). In an attempt to examine the anaerobic environment compulsory for ANAMMOX bacterial, dissolved oxygen (DO) was measured using an IntelliCAL LDO Lab Probe (HACH Company, Loveland, Colorado, USA). To validate ANAMMOX development in the reactor, samples were obtained and examined by PCR (RNA was extracted, amplified using PCR, then the products were subjected to gel electrophoresis to confirm the existence of ANAMMOX bacteria). The intensity of each band can be linked to the genomic density of the target gene in the primary sample. Specific primer sets aiming for 16S rRNA for both the exposed bacteria type were used, and inclusive description for the sequence of the primers, the object genus, and the techniques pursued thru the molecular biology analysis are portrayed in the Appendix (A4) data file. The effective amplification of the wanted bacterial RNA proves the manifestation of the examined bacterial family. The particle size distribution was determined using laser light diffraction particle size analyzer (LS 230, Coulter-Beckman, Germany). Particle size quantities range from 0.017 µm to 2000 µm, with the Polarization Intensity Differential Scattering (PIDS) technology. An inverted microscope (BioImager, ON, Canada) with a 2.5× objective and 10× objective was employed. The microscope was arranged with a camera (SN 14120187, Point Gray Research Inc. Canada), in addition to a computer in which the recorded images and videos were saved for further evaluation.

Nitrogen loading rate (NLR), nitrogen removal rate (NRR) and nitrogen removal efficiency (NRE) were considered through the nitrogen balance and stoichiometry per Equations 1-3 in Table 6-3. It was assumed that the ANAMMOX reaction principally eliminates nitrogen, yet because alkalinity

was available in the system, and based on nitrate/ammonia ratio together with the microbial community analysis, autotrophic denitrification may perhaps have a possible influence (Wang et al., 2017). The unfavorable effect of free ammonia (FA) on ammonia and nitrite-oxidizing bacteria is thoroughly studied, where ANAMMOX bacteria are frequently hampered by 10 to 150 mgN/L of FA in the environment. Likewise, FNA may cause process variability and inhibition. To observe and manage the inhibition factors induced on ANAMMOX bacteria, the concentrations of FA and FNA were constantly evaluated using Equations 7 and 8 (J Y Jung et al., 2007).

$$FA = \frac{17 \times TAN \times 10^{pH}}{14 \times [\exp\left(\frac{63334}{273 + ℃}\right) + 10^{pH}]}$$

Equation 6-1

$$FNA = \frac{47 \times TNN}{14 \times \left[\exp\left(\frac{-2300}{273 + ℃}\right) + 10^{pH}\right] + 1}$$

Equation 6-2

6.3. Results and discussion

6.3.1. Lab-scale UASB reactor performance

The continuous UASB reactor system was evaluated in three main phases. Phase III, going on for more than 200 days, designates a stable ANAMMOX process with high ammonia and nitrite removal rates. During phase I, the influent NH_4^+-N concentration was maintained at about 50.4 mgN/L, in addition to the mean NLR being 0.2 KgN/m^3/d (Figure 6-1 A). In the first four days of process, which was essentially the acclimatization interval for bacterial populations engaged, the average NRE reached 70.6%, validating the launch of ANAMMOX activity in the sludge. Near the end of this phase, the NRE was more than 85%; at the same time, the NRR improved from an early 0.11 KgN/m^3/d level to 0.16 KgN/m^3/d (Izadi et al., 2020a). Exploring the impact of substrate concentration on the continuous ANAMMOX process in the UASB reactor, ammonia

concentration was increased gradually in the ongoing experiment from phase I to phase II. In the period of phase II, NLR increased to 0.28 KgN/m^3/d (Figure 6-1 A); thus, as an outcome, the NRE declined from 85.4% on day 54, to 66.4% by the end of the second phase. Free ammonia (FA) concentration drastically increased by 77 ± 0.6% as soon as the ammonium load in the influent raised. Though FA and FNA are both capable of critically obstructing the ANAMMOX process, the inhibition threshold for FNA is lower than that of FA (Ma et al., 2017). The average FA level ascended from 0.005 KgN/m^3/day in phase I to 0.007 KgN/m^3/day, in the inhibition stage of phase II. The high free ammonia concentration is inhibitory to ANAMMOX bacteria because of the capacity of ammonia to readily diffuse within the cell membrane and dissolve in the lipid structure. Uncharged and lipid-soluble ammonia molecules trigger proton disproportion leading to a particular enzyme suppression (Aktan et al., 2012). In phase III, the NLR was reinstated and reached a level of 0.2 KgN/m^3/d (Figure 6-1 A), due to lessening the concentration of influent ammonium (Izadi et al., 2020a). The mean NRE reached 91.6%, which was more than two initial phases, while the NRR was roughly 0.18 KgN/m^3/d (Izadi et al., 2020a).

6.3.2. UASB reactor micro-granules development and microbial analysis

Regarding the physicochemical analysis, roughly 75% of the granules were in a size range of 253.2–465.7 μm. Assessment of the granules size dissemination in different phases of operation specifies a growth in the particle size and a boost in the micro-granulation process. The system shifts to a more stable ANAMMOX condition in phase III with higher ammonia and nitrite removal rates. (Izadi et al., 2020a). The total percentage of *Planctomycetes*, the primary phylum responsible for anaerobic ammonia removal had raised from 0.69 % to 9.63% (Figure 6-1 B) (Izadi et al., 2020a). Nearly the entire bacteria in the *Planctomycetes* group, classified on day 270, were ANAMMOX bacteria. Microbial analysis, as shown in Figure 6-1 B proposed that detected

ANAMMOX bacteria were solidly associated with "*Ca.* Brocadia sp.", including "*Ca.* Brocadia caroliniensis" were abundant in the reactor sludge. The second crucial genera in mature ANAMMOX sample was "*Ca.* Kuenenia", which confirmed the results from previous studies (Reino et al., 2018) (Jianhua Guo et al., 2016) (Izadi et al., 2020a). As indicated in Figure 6-1 B, there is a major drop in the abundance of Nitrosomonas spp, from RAS to the mature ANAMMOX biomass. Nitrosomonas is a genus of gram-negative bacteria, fitting into the Betaproteobacteria class. Nitrosomonas is one of the most important of the five genera of ammonia-oxidizing bacterial populations. This genus use ammonia as their electron donor source and carbon dioxide as a carbon source in the presence of oxygen. It is of importance to mention that, Nitrosomonas are abundant in the returned activated sludge from municipal wastewater treatment plants, however, as shown in the figure, as a result of the reactor conditions (no oxygen), the nitrogen removal bacterial community shifts towards anaerobic ammonia oxidizers in phase III of reactor operation rather than AOBs.

6.3.3. Effect of substrates in ANAMMOX batch test experimentations

6.3.3.1. HA and HN batch tests

During preliminary reliability and calibration tests, there was an indication of ammonium depletion and nitrogen gas generation, which approved ANAMMOX activity in the batch trial tests. Nitrogen gas production rate (NPR) was examined, to identify the biomass activity and stabilization thru batch assays. The NPR improved from 0.54 to 0.98 mgN/gBiomass.hr from the startup to the final phase, representing an increase in biomass activity rate and proof of ANAMMOX activity. Examining the alkalinity in the batch tests indicated that the concentration of $mgCaCO_3/L$ in the effluent followed the stoichiometry based on ammonium removal efficiency with a maximum error of 3.45 ± 0.87 %. Batch assays were completed to analyze nitrogen conversion rates by the ANAMMOX process with the diverse amounts and mixtures of ANAMMOX main substrates,

ammonium and nitrite (NH_4-N^+ and NO_2-N^-), and primary intermediate (NH_2OH). Based on the substrates and intermediate used in batch assays as well as the specific injection concentration, the experiments performed could be categorized into categories shown in Table 6-2.

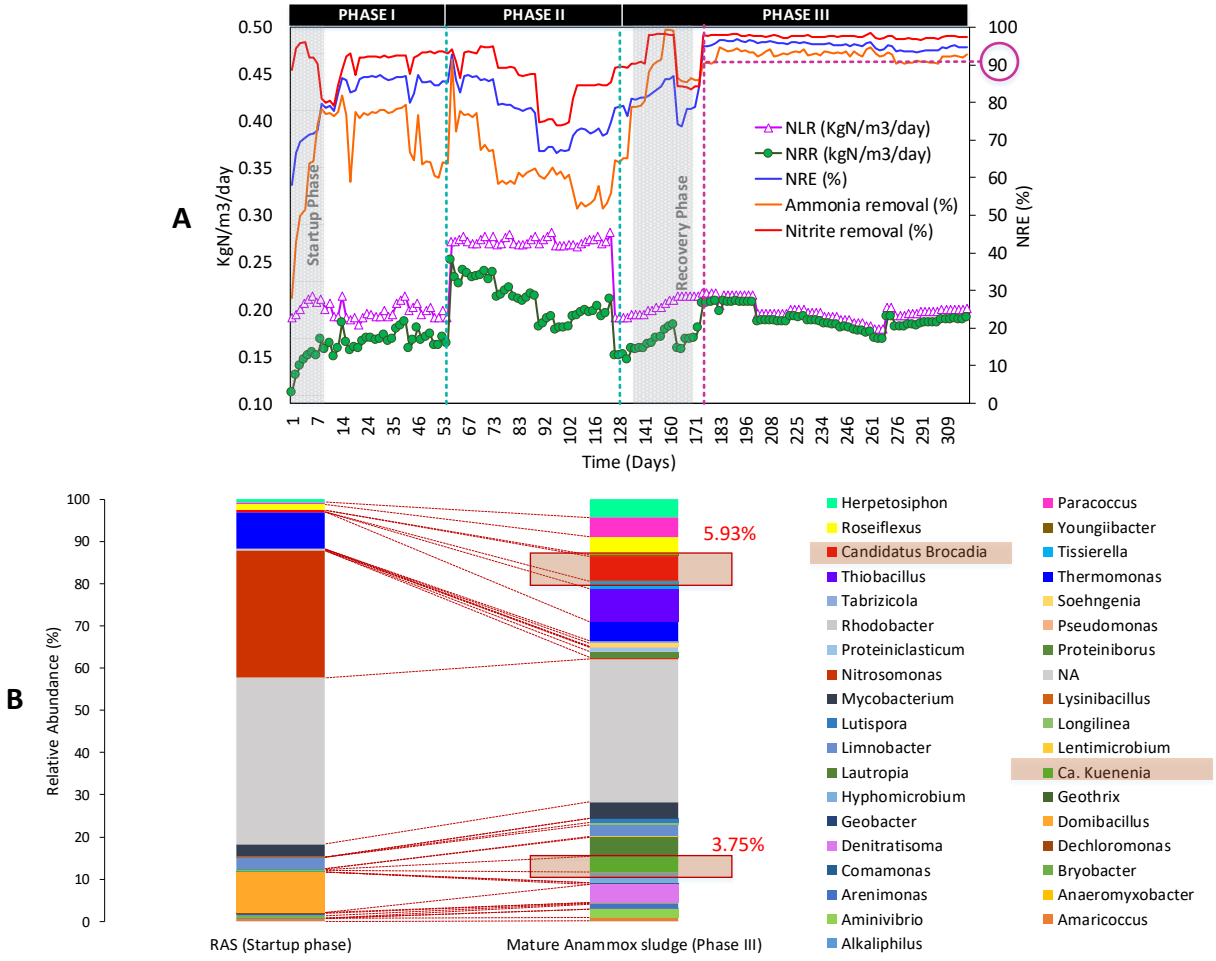

Figure 6-1 A) Nitrogen load rate (NLR), nitrogen removal rate (NRR), and nitrogen removal efficiency (NRE), B) Relative abundance of the functional species at the genus level showing the microbial community structure of the ANAMMOX sludge collected from the reactor in comparison with the initial seed (RAS) (Izadi et al., 2020a)

In each of the batch assays, two blank tests, one seeded with returned activated sludge (RAS) and the other one seeded with mature ANAMMOX sludge (ANX), were applied to obtain an analysis base-line for each test round and to generate a calibration curve without the effect of synthetic feed and additives involved. The reason behind employing RAS as a seed source for the blank tests is that it was the initial seed source for the continuous UASB ANAMMOX enrichment process. All

the tests were completed in duplicates to minimize the potential errors. The duplicate control tests have the same conditions as other ANX batch assays, but without the additives, to have a basis for final analysis and data validation. Ammonium is the standard electron donor in the ANAMMOX process and was combined with nitrite as the nitrogenous substrates and added during the batch cultivation, which would provide a reference for the following transformations of different nitrogenous substrates. The HA and HN tests (Figure 6-2 A), demonstrate a critical inhibition in the assays experiencing high ammonium and nitrite levels of approximately 1000, 1500, and 2000 mgN/L during a 120-hour period of batch experimentation mimicking concentrated wastewater streams produced in food and agro-industry. Raw anaerobic digester filtrate has an expected high-strength ammonium level with 1000 to 1400 mgNH_4-N/L due to cell destruction and the breakdown of amino acids (Huang et al., 2011). Although there has been an increase in sidestream ANAMMOX development, there are numerous elements that call for further analysis and consideration by the specialists to accomplish the operational standpoint established for the facility. High or fluctuating influents nitrogen loads, higher than 2000 mgN/L, can destructively affect the sidestream ANAMMOX performance (Q. Zhang et al., 2016) (Van Hulle et al., 2010), demanding an efficient and practical recovery route.

In the ANX control tests, the ammonium and nitrite concentrations in the effluent reached a level of 43.87 and 55.15 mgN/L, respectively, showing a total ammonium and nitrite removal rate of 92.98 and 92.75%. However, in all the tests with additional ammonium and nitrite concentrations with NLR ranging between 2.08 to 4.81 KgN/m^3/day (Table 6-4), both substrates started to accumulate in the effluent, resulting in almost no removal (nitrogen removal efficiency (NRE) ~ 0 KgN/m^3/day) of the nitrogen compounds in the batch system (Figure 6-2 A). Addition of 1000 and 1500 mgN/L of ammonia resulted in a major drop in ammonia and nitrite removal efficiencies

from approximately 92.9% in the ANX control test down to zero in ANX-Ammonia 1000 and 1500 (Figure 6-2 A). The operation of ANAMMOX-based bioreactor systems is not stable when substrate inhibition resulting from high nitrogen loading rates is applied, resulting in a considerable drop of specific oxidation rates in the system (Figure 6-2 C). As indicated in Table 6-4, excessive nitrogen loading increased resulted in major deterioration of both specific biomass ammonium and nitrite oxidation rates (q AMX, NH_4-N_2 and q AMX, NO_2-N_2). A preliminary investigation into the batch experimentation results indicated the potential accumulation of both nitrite and ammonia in the systems, which will persist without any subsequent conversion to dinitrogen gas and residual nitrate concentrations. It is postulated that the inhibition is linked to the FA and FNA concentrations (Table 6-4). Both free ammonia and free nitrous acid can manipulate the anabolic and catabolic processes of enriched ANAMMOX bacterial consortiums, yet they become inhibitors under high substrate concentrations. ANAMMOX activity measured in ANAMMOX granules by regular examination of normalized manometric batch tests broadened the understanding by considering the lag times, highest conversion rates during the tests, and substrates/product transformation ratios (Figure 6-2).

Several studies indicated that the ANAMMOX process could tolerate ammonium concentration up to 1000 mgN/L (Strous et al., 1999). However, other studies reported that high levels of ammonium suppress ANAMMOX activity and process performance (Jin et al., 2012). High nitrite concentration can severely inhibit a wide range of microorganisms, including ANAMMOX. Nitrite's inhibition threshold is lower than ammonium, making ANAMMOX more vulnerable to high nitrite levels (Isaka et al., 2007). Different studies' results deviated in analyzing the nitrite inhibition limit, reporting a wide range from 5 to 280 mgN/L, depending on the process configuration employed (Jaroszynski et al., 2011). This highlights the significance of identifying

the substrates inhibition threshold and uncovering a potential revival method for already hindered sidestream ANAMMOX processes.

Table 6-4 Overview of the overall batch experiment performance in HA, HN, LA, LN, ARH and NRH tests

	$mgN_2/L.hr$	**NLR ($KgN/m^3/day$)**	**q AMX,NO_2-N_2 (mgN/gVSS.d)**	**q AMX,NH_4-N_2 (mgN/gVSS.d)**	**FA (mgN/L)**	**FNA (mgN/L)**
ANX Blank	0.56	0.01	10.24	4.67	0.024	0.003
RAS Blank	0.00	0.02	5.69	0.00	0.094	0.006
ANX Control	3.73	1.40	1679.79	1296.31	0.86	0.02
ANX-Ammonia 1000	0.00	2.67	0.00	0.00	20.69	0.57
ANX-Ammonia 1500	0.00	4.53	0.00	40.23	38.00	0.84
ANX-Ammonia 2000	0.00	4.81	0.00	0.00	47.70	1.14
ANX-Nitrite 1000	0.00	2.08	0.00	0.00	17.76	0.45
ANX-Nitrite 1500	0.00	2.66	0.00	0.00	23.24	0.56
ANX-Nitrite 2000	0.00	2.71	0.00	0.00	28.01	0.53
ANX-Ammonia 50	2.98	0.10	106.99	73.37	0.0022	0.0006
ANX-Ammonia 100	3.28	0.20	223.47	161.85	0.0046	0.0002
ANX-Ammonia 150	3.47	0.29	325.86	235.83	0.0049	0.0004
ANX-Nitrite 50	3.10	0.13	129.47	101.08	0.0019	0.0001
ANX-Nitrite 100	3.32	0.26	278.63	211.51	0.0039	0.0004
ANX-Nitrite 150	3.36	0.36	381.62	274.74	0.0122	0.0014
ARH 1000-10	2.85	2.71	508.52	320.72	19.47	0.013
ARH 1000-30	2.18	2.75	821.16	571.27	14.23	0.0072
ARH 1500-10	1.93	4.51	991.93	498.91	37.13	0.012
ARH 1500-30	1.92	4.35	1186.42	800.12	39.7	0.0025
ARH 2000-10	0.39	5.29	1567.74	773.33	47.1	0.0128
ARH 2000-30	0.96	5.36	1257.29	816.65	47.0	0.0036
NRH 1000-10	1.70	1.87	323.58	153.03	18.4	0.0243

NRH 1000-30	1.75	2.04	573.18	168.89	17.9	0.0057
NRH 1500-10	1.44	2.63	474.32	96.57	28.1	0.0307
NRH 1500-30	1.46	2.62	811.82	185.74	27.6	0.0061
NRH 2000-10	0.32	2.75	437.06	50.37	23.9	0.027
NRH 2000-30	0.30	2.86	638.52	113.95	23.7	0.0054

As indicated in Table 6-4, increasing the ammonium loading rate from 2.67 to 4.81 KgN/m^3/day, resulted in an impulsive escalation in FA and FNA levels from 20.69 to 47.40 and 0.57 to 1.14 mgN/L respectively. Results attained from the short-term batch tests included in Table 6-4, analyzed to assess the impacts of ammonium and nitrite, are reported based on the FA and FNA concentrations since unionized ammonia and nitrite are reflected as the actual hindering compounds. In addition, because of the considerable inhibition imposed on ANAMMOX bacterial community, the nitrate production rate started to decrease, reaching zero in the highest ammonium loading rate. As indicated in Table 6-4, an increase in NLR in almost all batch experiments resulted in a major increase in FA concentration in the system (95-99%), leading to significant suppressions on the bacterial community. Dapena-Mora et al. 2007, observed that FA is the ANAMMOX reaction's true inhibitor rather than ammonium. Fernández et al. 2012, showed that short-term batch experiments experienced a 50% decrease in specific ANAMMOX activity when the FA-N concentration reached a level of 38 mgN/L.

Similarly, Waki et al. 2007, reported FA as an inhibition parameter for the ANAMMOX process, and concentrations between 13 to 90 mgn/L could be toxic for bacterial performance (Jin et al., 2012). The main reason for different FA resistance and inhibition levels is the different physiological characteristics of dissimilar ANAMMOX species and various bacterial community structures (Oshiki et al., 2011). In this study, the inhibition led to a substantial decrease in ANAMMOX activity (Figure 6-2 C), resulting in a major drop in both specific biomass ammonium

and nitrite oxidation rates from 1296.31 and 1679.79 mgN/gVSS.d, respectively, down to 0 (Table 6-4). In a study executed by (Egli et al., 2001), complete deactivation of ANAMMOX bacteria was reported when nitrite concentration reached above 185 mgN/L. Comparably, Dapena-Mora et al. (2007), indicated a 50% reduction in ANAMMOX activity when 350 mgN/L of nitrite was added to the batch experimentations. The inconsistency in the conclusions of these researchers with each other and our study was most probably instigated by alterations in the operational conditions. However, the ANAMMOX process analysis has been going on for over two decades; there are many challenges and issues concerning understanding the bacterial community's behavior and process performance even in sidestream conditions, resulting in process limitation. Considering that ANAMMOX is a group of slow-growing bacteria, accumulation of adequate volume of biomass might require weeks. Consequently, substrate-inhibition-based failures risk the effluent quality and are cost and time-consuming to resuscitate (Janiak and Miodonski, 2017).

6.3.3.2. LA and LN batch tests

In the low-level batch tests, the substrate concentration was reduced to 50, 100, and 150 mgN/L, while the other test conditions were similar to HA and HN tests, resulting in high COD and low ammonia concentrations at the ratio of 10 to 14, mimicking mainstream ANAMMOX process conditions. The results show a major shift in nitrogen removal rates and nitrate accumulation scheme in the batch tests. As shown in Figure 6-2 B, there is only around 7-19 % decrease in NRE, when the ANAMMOX substrates levels were set to be at low concentrations (close to mainstream ANAMMOX conditions) and simultaneously the nitrogen removal rate (NRR) declined by an average rate of 1.02 KgN/m^3/day in the LA and LN batches (Table 6-4) comparing to the control test in which the NLR was 1.04 KgN/m^3/day. The amount of ammonia and nitrite is in the ANX control test was based on experimental design to achieve influent ammonia and nitrite

concentrations of 529.02 and 621.42 mg N/L, respectively. The pH of the ANX control test was 7.9 on average. Decreasing the nitrogen loading rate resulted in a drop in both specific biomass ammonium and nitrite oxidation rates (q AMX, NH_4-N_2, and q AMX, NO_2-N_2); however the drop was less than expected due to temperature levels in the batch study. Lessening the NLR from 1.4 down to 0.29 KgN/m^3/day led to a reduction of ANAMMOX activity from 129.8 to 120.7 mgN/d.gVSS as shown in Figure 6-2 C, while further NLR decrease to 0.1 KgN/m^3/day resulted in an ANAMMOX activity of 103.7 which was approximately 20% lower than the control test. The observed poor performance was directly linked with the increase of COD/N ratio, in which no adverse effect was detected on ANAMMOX activity and growth rate when the ratio was < 2-3.

Furthermore, based on the Monod equation, the reduced ammonium and nitrite concentrations demote the growth rate and activity of the ANAMMOX bacterial population. Limiting the bulk ammonium concentration has a key role in stipulating the ammonium oxidation rate. The level of residual ammonium alters the ammonium saturation term (or Monod term) and consequently constrains the growth rate of ANAMMOX bacteria (Qiu et al., 2020). On the other hand, the shortened HRT in the batch experiments makes the granular bacterial structure preservation more complicated, resulting in a deteriorated nitrogen removal performance. Figure 6-2 B indicates a slight inhibition in ANAMMOX performance when the loading rates were lower than 1.4 KgN/m^3/day. However, as seen in Table 6-4 the FA and FNA levels in LA and LN tests were less than the control assay. Bearing the probable impacts of the NLR on the performance of the ANAMMOX process in the course of sewage treatment in mind, there is a major scarcity of knowledge on the topic. A number of studies investigated the effect of low NLR on ANAMMOX process total nitrogen removal efficiency, and the results indicate 99.7% in NLR between 2-35.14 KgN/m^3/day (Li et al., 2013), 88% in 0.75-2 KgN/m^3/day (Dapena-Mora et al., 2004), 86% in

1.43-1.62 KgN/m^3/day (Yu et al., 2013). This study also agrees with previous results, in which with a nitrogen loading rate from 0.1 to 1.4 KgN/m^3/day the total nitrogen removal efficiency ranged between 64.5 up to 83.7%, respectively.

One of the key hitches of mainstream ANAMMOX operation is coping with a reduced net biomass production rate, directly linked to the low nitrogen levels in the influent, being orders of magnitude smaller than the sidestream (Reino et al., 2018). Simultaneously, restraining the heterotrophic bacterial growth in mainstream process conditions with a high COD/N ratio is critical in process characteristics. Over-competition of heterotrophic microorganisms in the reactor is unavoidable even when there is a lack of exogenous carbon due to endogenous soluble microbial decay products discharge (Cao et al., 2017). For an effective sidestream ANAMMOX-based process, the influent COD/N ratio should range between 2-3 to maintain the suspended/granular sludge system, yet in this study, the mainstream batch tests were operated under a COD/N ratio level of 6-8, and as a result, a slight decrease in the process NRE was observed (Figure 6-2 B). In this study, the drop in NRE was significantly lower than in studies with low temperatures since the temperature was maintained at the original 35 °C. This scenario where the inoculation of the ANAMMOX consortium was completed in a UASB reactor operated with different levels of NLR, would point out an extra challenge. The suggested application may initiate quality loss of the inoculum because its NLR scope is noticeably different from the NLR employed in the batch reactor test system, probably leading to partial destruction of the ANAMMOX process.

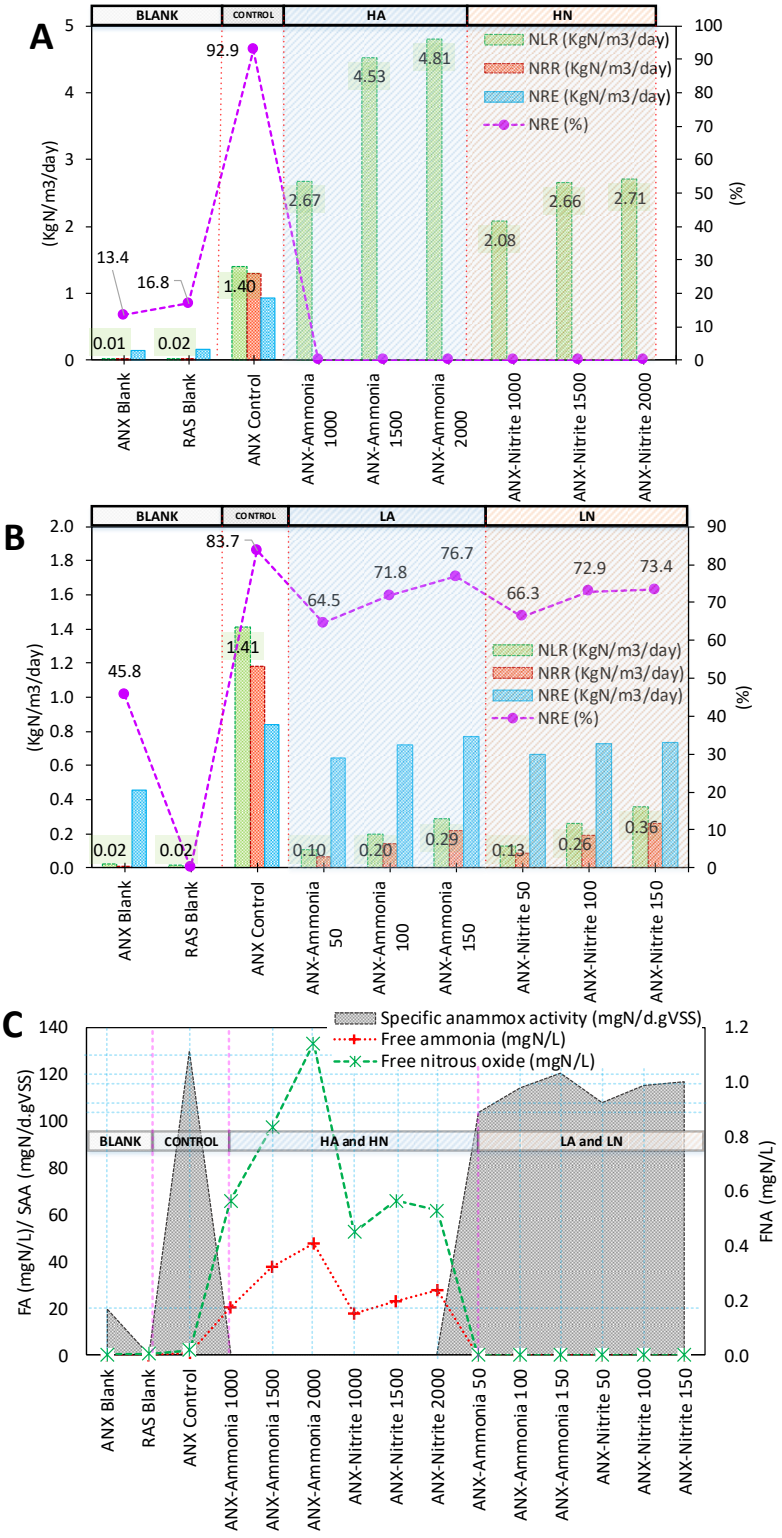

Figure 6-2 The performance of the batch reactors. (A) Nitrogen load rate (NLR), nitrogen removal rate (NRR), and nitrogen removal efficiency (NRE) in HA and HN tests (B) NLR, NRR and NRE in LA and LN tests (C) variation of the FA and FNA concentration over the batch tests along with specific ANAMMOX activity in different nitrogen loadings

6.3.4. Potential accelerating and recovery effects of hydroxylamine

Hydroxylamine oxidoreductase enzyme has been detected in ANAMMOX enrichment biomass, and production of hydroxylamine has been verified (Hu et al., 2010). Several studies showed the positive effect of hydroxylamine on ANAMMOX process in low concentrations (Hu et al., 2010). As a result, two sets of batch assays, one with low-concentration hydroxylamine injection and the other with high concentration dose (Table 6-2, Tests 5 and 6). Subsequently, two sets of tests were conducted to understand the potential recovery effect of hydroxylamine addition to inhibited ANAMMOX biomass, which was repressed due to high ammonium and nitrite presence in the process influent (Table 6-2, Tests 7 and 8). Prompt and efficient in-situ approaches are obligatory to recover the damaged biomass, including adding external chemicals, yet these tactics have been restricted because of the lengthy restoration phases (Z. Wang et al., 2018). As far as we can tell, there are limited details on employing a hydroxylamine treatment scheme to augment nitrogen removal of warm-mainstream micro-granular ANAMMOX process.

As indicated in Figure 6-3 A, there was no significant alteration in the system's performance in terms of total nitrogen removal efficiency when 1.5, 3, 3.5, and 4.5 mgN/L (LH1, LH2, LH3, and LH4) of hydroxylamine was supplemented to the batch assays. The ANOVA test shown that the th total nitrogen removal efficiency of the tests, was not significantly different ($p = 0.080$) from the control test, at 0.05 level, under different low-level hydroxylamine content. On the other hand, increasing the hydroxylamine concentration to levels above 10 mgN/L, led to a shift in ANAMMOX activity and an increase in NRE (Figure 6-3 A). The addition of 10 and 15 mgN/L (Table 6-2, tests HH1 and HH2) of the specific intermediate increased the NRR by 0.09 and 0.11 $KgN/m^3/day$, which corresponds to an approximately 6% increase in overall nitrogen removal efficiency of the system (illustrated in Figure 6-3 A). The ANOVA test showed that NRE was

significantly different ($p < 0.05$) in HH1 and HH2 comparing to the control test, under high-concentration hydroxylamine content.

Hydroxylamine oxidoreductase (HAO) enzyme in ANAMMOX bacteria, operates via inter-transformation of nitric oxide and hydroxylamine, augmenting the activity of hydrazine oxidizing enzymes and can be exercised to modify the ANAMMOX reactions in the batch experiments when optimum concentrations of the intermediate is available. Hydroxylamine additions at a total concentration of 30 mgN/L boosted the ANAMMOX process. Increasing the hydroxylamine level to 22.5 and 30 mgN/L resulted in higher nitrogen removal rate of up to 1.34 and 1.36 KgN/m^3/day, respectively, thus in HH3 and HH4 batch tests, NRE reached the highest rate of around 96.3 and 97.8 % correspondingly. A greater NRR with particular ammonium to nitrate conversion ratio in the HH ANAMMOX systems indicates a higher capacity ANAMMOX population in the batch systems supplemented with optimum levels of hydroxylamine. Based on results from ^{15}N-labelling studies, hydroxylamine was proposed to be one of ANAMMOX process intermediates, which is eventually converted to dinitrogen gas (Bettazzi et al., 2010). A similar study, indicated an increase in maximum nitrite removal rate when hydroxylamine was supplemented to a batch scale experiment (Bettazzi et al., 2010). ANAMMOX bacteria appear to have a flexible metabolism, but several studies confirmed that increase of hydroxylamine concentration can potentially trigger an enhancement in substrate conversion (Hu et al., 2010). Based on a study done by van der Star et al. 2008, the combination of ammonium with hydroxylamine for hydrazine production is shown to be the rate-limiting step in the ANAMMOX process. Ammonium conversion decreases substantially when hydroxylamine levels start to fall, and hydrazine starts to accumulate in the system.

To fully examine the potential contribution of hydroxylamine in the high-temperature mainstream ANAMMOX process, 10 and 30 mgN/L of the intermediate were added to mainstream batch tests. As also indicated in Figure 6-3 C, due to the unique eco-physiological features of ANAMMOX bacteria, there is a potential for adaptation to low-substrate conditions (Ma et al., 2016). As reported in Figure 6-2 B, the introduction of low-strength wastewater resulted in a 10-20% decrease in the total NRE, yet the addition of hydroxylamine slightly recovered the total efficiency of the process (Figure 6-3 C). The presence of optimal concentrations of intermediate metabolites of the ANAMMOX process (Hydroxylamine (NH_2OH)) promoted the TN removal (Figure 6-3 A). Intermediate-based ANAMMOX stimulation strategy offers a prospective method for the successful application of the mainstream processes.

Nevertheless, additional investigation is necessary to expand this technology. The nitrogen removal rate was fairly stimulated with 30 mgN/L of hydroxylamine added, perhaps because of the ANAMMOX enzymatic reactions increase (Figure 6-3 A). In similar studies, the addition of ANAMMOX metabolites at higher concentrations in optimal temperatures of 30 °C, shown a rapid conversion of the intermediates to dinitrogen gas (Zekker et al., 2012). This matter opens a new window for ANAMMOX process metabolism acceleration and promoting the practical full-scale mainstream ANAMMOX applications. The high ANAMMOX activity in intermediate-based methods assists in maintaining a reasonable ANAMMOX activity at low temperature by highlighting the neglected optimization potential of the reaction components (Zekker et al., 2012). Mainstream ANAMMOX has drawn extensive attention owing to its energy-saving advantages; however feasible applications are not accessible yet. The technological and financial feasibility of high-strength ANAMMOX has been proven, and as a result, there are numerous technology opportunities that have been verified and commercialized to deliver the suitable environment and

control, to provide a stable operation (Tsuchihashi and Ryujiro, 2015). However, there is a limited number of reports of the large-scale installations of mainstream processes (M. Zhang et al., 2019), signifying the importance of metabolic enhancement studies. Based on the results of the current study, adding high-level concentrations of hydroxylamine can aid in achieving a faster startup period, and a stable, high efficiency, and operative mainstream ANAMMOX process .

Augmentation of post-inhibition recovery of the ANAMMOX process is of great value. Nitrite has been confirmed to be an important element since it possibly will initiate severe inhibition at high concentrations, yet hindering NO_2^- inhibition varies based on biomass maturation along with periods of nitrite exposure (Zekker et al., 2012). The addition of optimal concentrations of intermediate metabolites of the ANAMMOX, hydroxylamine, could promote TN removal and recover the bacterial activity after inhibition. As observed in Figure 6-3 B, the addition of 10 and 30 mgN/L of hydroxylamine could restore the overall nitrogen removal efficiency of the obstructed ANAMMOX batch assays by 22 to 47%. The impacts of increasing the relative hydroxylamine concentration on the conversion of substrates are as shown in Figure 6-3 B and D. Addition of ANAMMOX metabolites (hydroxylamine) at concentrations higher than optimal (total of around 10-30 mgN/L) improved the nitrogen removal rate in batch assays (Figure 6-3 A). Increasing the influent ammonium concentration to 1000 mgN/L resulted in a major drop of NRR to almost 0 (Figure 6-2 A). However the addition of 10 and 30 mgN/L of hydroxylamine increased the NRR to 0.74 and 1.36 $KgN/m^3/day$, which corresponds to 22.4 and 68.8% NRE, respectively (Figure 6-3 B).

As presented previously, the ANAMMOX process is sensitive to several inhibiting factors, including high substrate loading rate levels, yet as shown in Figure 6-3 D, the process performance can be partially recuperated when hydroxylamine is added. The obtained results indicate that

hydroxylamine has a positive effect on batch assays inhibited by 1000 and 1500 mgN/L of nitrite (NRH 1000 and NRH 1500), considering that the NRE reached up to a range between 26.13 - 42.29 % for intermediate concentrations of 10 and 30 mgN/L (Figure 6-2 A). In a study completed by Ivar Zekker et al. 2012, the addition of 1.31 mgN/L hydroxylamine potentially recovered an inhibited moving bed biofilm reactor system from shock load in a short time. In a similar study a system fully inhibited by high nitrite loading rate could overcome the inhibition by trace concentrations of 0.7 mg of nitrogen per liter of hydroxylamine (Strous et al., 1999). Based on Hu et al. 2010, findings, ANAMMOX enrichment converted hydroxylamine to hydrazine, with the average conversion rates of 0.207 mmol g/VSS.h, which were enhanced by 26.7% via increasing the hydroxylamine to nitrite ratio in the influent. The results from this study agree with Hu et al. 2010, wherein increasing the hydroxylamine concentration from 10 to 30 mgN/L, increased the substrate conversion rates in all inhibited batch assays. Bettazzi et al. 2010, reported a 20% recovery of ANAMMOX activity with 2 mgN/L intermediate addition after partial nitrite inhibition. This study reveals an intermediate-based ANAMMOX sludge treatment effective in restoring the deteriorated sidestream process performance after high nitrogen shock loads and a potential pathway towards successful execution of mainstream.

All short-term recovery-based batch experiments (ARH and NRH) indicated in Figure 6-3 C, showed better removal efficiencies when using hydroxylamine as an additive as compared with the tests indicated in Figure 6-3 B. With intermediate addition, more than 20 % higher TN removal rates were registered. The control test indicated in Figure 6-3 B and C have higher NRE and NRR comparing to all ARH and NRH tests. The control tests had identical conditions to the cultivation and stabilization phase of the bacterial consortium in the UASB setup, with low COD/N ratio of between 2-3 and nitrite/ammonia molar ratio of 1.1-1.3. The control tests had the highest rate of

NRR and highest NRE among all tests assessed in the study. Although all ARH and NRH tests supplemented with 10-30 mgN/L of hydroxylamine showed performance recovery (Figure 6-3 B and C), none of the test conditions reached the ANX control optimum environment ANAMMOX performance.

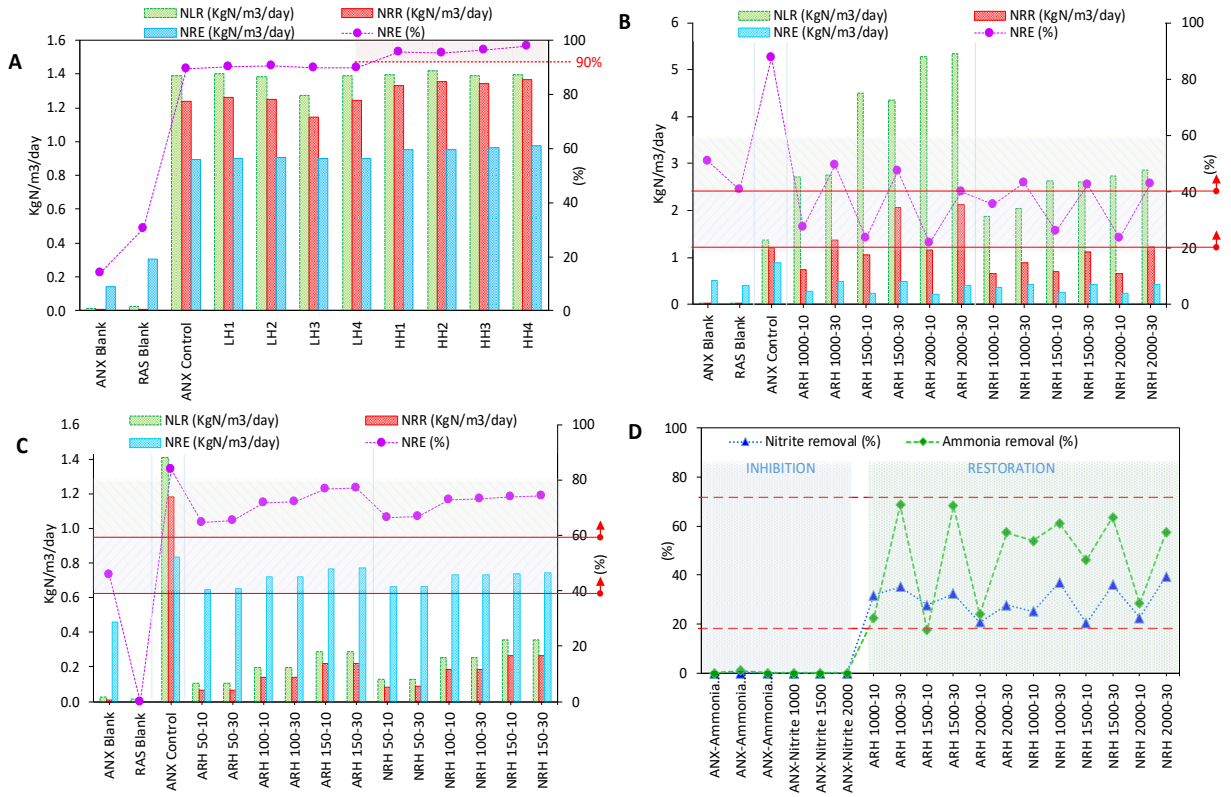

Figure 6-3The performance of the batch reactors; (A) Nitrogen load rate (NLR), nitrogen removal rate (NRR), and nitrogen removal efficiency (NRE) in LH and HH tests (B and C) NLR, NRR and NRE in hydroxylamine recovery batch assays (D) comparison of ammonia and nitrite removal rates in high-substrate inhibition tests with intermediate recovered tests

6.3.5. Micro-granular structure shifts and sludge settlibility factor

Tha size of the aggregates is reflected as a strategic element in controlling the system performance, regulated by the equilibrium linking granule growth, erosion, and deterioration process, which is a result of the reactor's structural design, hydraulic shear force, and substrate loading rate (Ma et al., 2013). Granules with high density and elevated settling properties strengthen the mass transfer

and cooperation among bacterial communities and enhance the bacterial activity and process metabolism (R. Chen et al., 2019a). Microbial granular auto-immobilization results in an intricate assortment of synergetic bacteria forming a unique microbial ecosystem (Luo et al., 2017). The procedures manipulating the restraining effects of substrates on ANAMMOX bacteria as well as the circumstances under which the ANAMMOX process performance is distressed are yet to be understood (Carvajal-Arroyo et al., 2014). Specific approaches must be in place to prevent such upsetting measures; however in the case of incident there is a critical need for practices reducing the period of the disruption.

The ANAMMOX biomass collected from the UASB reactor signified as ANX control (Figure 6-4), had an average sludge volumetric index (SVI) of 38.88 cm^3/gVSS with an average effluent VSS concentration of between 5-10 mgVSS/L and SRT of 110+20 days. The average granule diameter size in the control test was around 234.8 µm, however, increasing the NLR from 1.4 to 2.6 KgN/m^3/day resulted in approximately 35% decline in average particle size diameter in the system (Figure 6-4). ANAMMOX micro-granules tend to adopt a range of diameters and arrangements based on the diverse operational statuses and influents conditions (Szabó et al., 2017). Different granular size ranges significantly impact substrate transport/transfer along with the functional microorganism's profusion and activity (Luo et al., 2017). The size distribution of the granules in Figure 6-4 indicates a major drop in granular size and particle settleability in HA and HN tests, while low nitrogen loadings in LA and LN tests had a minor impact on diameter size (5-8% decrease) and SVI (1-8% increase).

Both FA and FNA, which become more concerning with the increase in nitrogen loading rate in influent, impose additional inhibition to the ANAMMOX granules (Y.-P. Wang et al., 2016). FA has been reported to extremely deter the development of anaerobic granules due to the potential

inhibition to metabolic energy pathway of microorganisms (Yang et al., 2004). Meanwhile, FNA in known to be more destructive, having a lower inhibition threshold for ANAMMOX bacteria. Consequently, elevated loading rates may enforce harsher suppressions on the granules, triggering greater stress to ANAMMOX granules and bring about prompt malfunction of the system (Anthonisen et al., 1976). The physical structure breakdown and reduction of catabolic activity in anaerobic granules is not thoroughly acknowledged in the literature, most notably in short-term operations. Protracting the granules integrity is a significant issue obstructing the practical exploitations of anaerobic granular processes (Mota et al., 2014). Activation of filamentous bacterial communities and the clogging of granule outlets and pores by extracellular polymeric substances (EPS) are two potential factors that might influence the deterioration of granules after the short-term operation (Liu and Liu, 2006). However, EPS over-production as a result of stress conditions imposed on the bacteria can be a potential explanation for the fast deterioration of granules reported in this current study (Lemaire et al., 2008), yet, the hypothesis that the granular integrity, internal granule structure, mass transfer gradients, and spatial arrangements as well as the interactions among microbial communities which play an important role in granule activity were once suddenly disrupted, resulting in a detrimental effect on reaction rates and process performance, is more logical. Decrease in reaction rates observed after bacterial suppression due to high substrate loading leads to inactivation or extermination of microorganisms resulting in granular structure rupture.

One of the most significant factors affecting the yield of systems coping with slow-growing bacteria, such as ANAMMOX process is achieving a suitable settleability to preserve the bacteria within the reactor by ANAMMOX granulation and improve the mass transfer dynamics (Ye et al., 2018). Consequently, as shown in Figure 6-4, batch assays with improved NRE have a higher

range of granule diameter size and a better sludge settleability. The addition of 10 and 30 mgN/L of hydroxylamine increased the average particle size diameter by 12 and 21%, respectively, corresponding to 20 to 50 % improvement of NRE in the batch tests. Maintaining an adequate substrate load per unit of biomass in ANAMMOX tests may potentially stabilize the granular size and enhance the nitrogen removal performance in terms of NRR and NRE (R. Chen et al., 2019a). The presence of toxic or inhibitory compounds for ANAMMOX bacteria in the influent wastewater could explain the decrease of NRR in batch tests, which directly corresponds to sludge settleability and granulation quality. Figure 6-4 also demonstrates that a high percentage of micro-granules in the control test has a spherical form with a discrete structure. Examining the inverted microscopy results for the high-substrate inhibited tests, signifies smaller aggregates, suggesting a prospective collapse of the granules due to granular sludge deterioration. The perceptible shift in process efficiency after inhibition (Figure 6-2 A), can also be linked to damaged mass transfer and degraded interactions between bacterial communities due to granular matrix breakdown, promoting the production of more low-density flocs (Figure 6-4).

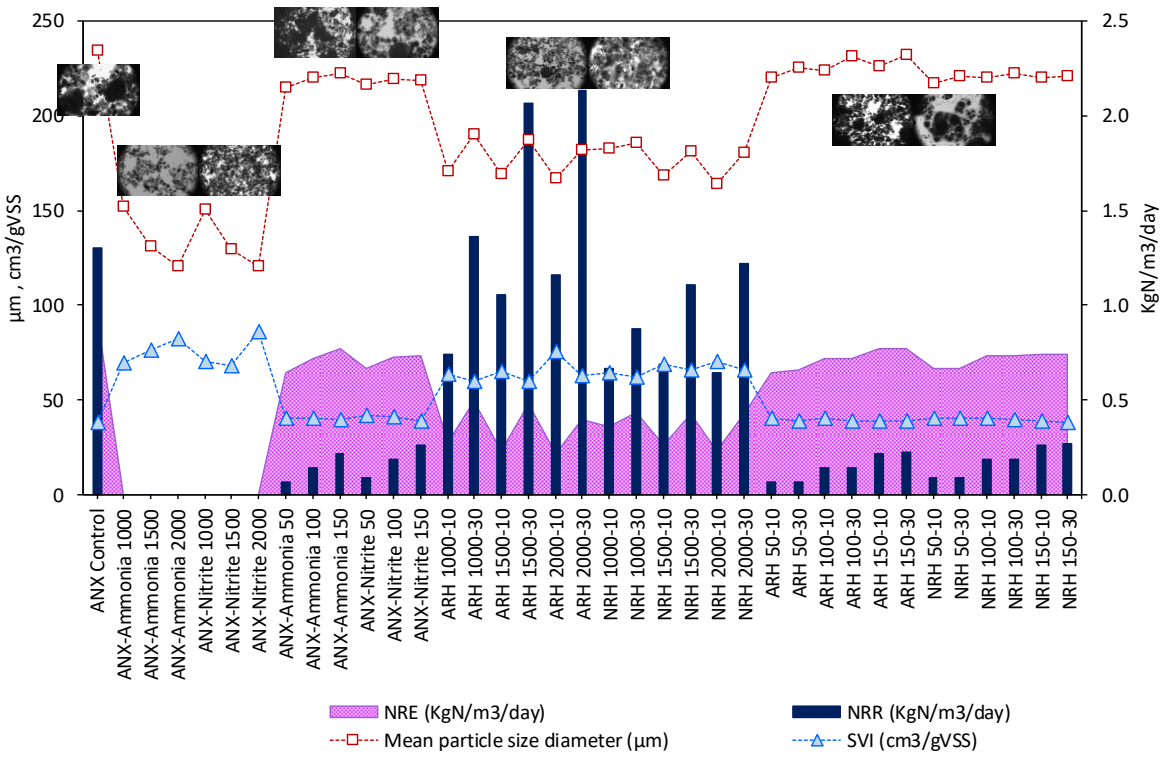

Figure 6-4 Variation of granule size distribution with alteration of NRE and NRR in HA, HN, LA, KN, ARH, and NRH batch assay experiments

The observed trend in sludge SVI indicates a substantial decline in biomass settlebility, from 38.33 cm^3/gVSS in the control test to approximately 82.5 and 85.7 cm^3/gVSS in assays with 2000 mgN/L of ammonia and nitrite, respectively. As seen in Figure 6-4, the presence of hydroxylamine reduced the detrimental effect of high substrate loads on sludge settlebility by about 8.9-22.3%. Granular floatation and the following washout is a prospective damaging factor for full-scale ANAMMOX-based processes. Looking into ANAMMOX process, the principal origin of granule flotation is poorly understood, plus the necessary granule floatation controlling scheme has been neglected (Chen et al., 2010). One potential reason behind granular floatation can be the generation of voided aggregates as result of substrate diffusion impediment (Alphenaar et al., 1993).

Several approaches have been explored to promote retention of the slow-growing ANAMMOX bacteria within mainstream systems, including selective enrichment in aggregated biomass (Xu et

al., 2015a). One possible solution towards sustainable and stable mainstream ANAMMOX is the promotion of bacterial retention to prevent any potential loss of highly valued biomass from the system. One of the mainstream ANAMMOX process's major challenges is decreasing net biomass production rates due to low nitrogen loadings, which leads to biomass washout and loss. Therefore, procuring an approach to guarantee the high solid retention time to enhance the growth of the slow-growing bacterial population is of great importance (Reino et al., 2018). As shown in the results of the hydroxylamine addition on granule structure preservation, the introduction of intermediates to ANAMMOX process can enhance the metabolic activity in combination with sustaining a stable granular constitution (Figure 6-4). As indicated, the addition of 10 and 30 mgN/L of hydroxylamine to ARH 50, resulted in a slight increase (> 10 µ) of average granule size. A similar trend is observed in all tests injected with doses of hydroxylamine. Although the size change is not significant (1-10 µm), it proves the potential constructive effect of hydroxylamine in improving the mainstream ANAMMOX-based process by reducing the impairment of bacterial aggregates and the settling properties. The microscopy images illustrated in Figure 6-4, can also corroborate the fact that the aggregate sizes and structures were less ravaged when hydroxylamine was present in the test bottles. Thus, sustaining the granular sludge stability with addition of specific doses of hydroxylamine in ANAMMOX-based processes can pave the path towards guaranteeing a stable biomass and developing efficient wastewater treatment.

6.4. Conclusion

To assess the stability of ANAMMOX-based nitrogen removal systems and applicability of mainstream implementation, it is necessary to study the effect of nitrogen loading rate and potential recovery or stimulation impact of intermediates on the process. This study investigated the effects of high loading rates, with elevated concentration of both ammonium and nitrite (HA and HN) .

The HA and HN tests, reveal severe repression in the batch assays undergoing extreme ammonium and nitrite concentrations of approximately 1000, 1500, and 2000 mgN/L, during a 120-hour period of batch testing. Decreasing the loading rate in LN and LA tests to simulate high-temperature mainstream conditions indicate a considerable alteration in nitrogen removal rates and nitrate accumulation, in which only about 7-19 % drop in NRE was observed. ANAMMOX intermediate compound hydroxylamine, accelerated the process in batch tests. Based on the results of this study ANAMMOX activity can be partially recovered by the addition of hydroxylamine during post-inhibition period. The addition of 10 and 30 mgN/L of hydroxylamine increased the NRE from zero to 26.13 and 42.29% in nitrite-inhibited tests. Ammonium and nitrite inhibition directly affected the granules structure and sludge settleablity, wherein increasing the substrate loading rate resulted in further destruction of the ANAMMOX micro-granules. In tests with NLR of 2.7 and 4.8 $KgN/m^3/day$, the granule size was reduced by approximately 35 and 46 % compared to the control sludge. As a result, the SVI was increased by 45 and 54 %, respectively, which indicated a significant decline in sludge settleability.

CHAPTER 7

Parin Izadi[a] , Parnian Izadi[a] , Ahmed Eldyasti*[a]

[a] Civil Engineering, Lassonde School of Engineering, York University, 4700 Keele Street, Toronto, ON, Canada , M3J 1P3

* Corresponding author

Authors' contributions Parin Izadi and Dr Eldyasti contributed to the study concept and design. Experimental system setup, material preparation, data collection and experimental analysis were performed by Parin Izadi and Parnian Izadi. The mathematical modeling setup was prepared by Parin Izadi. Modeling performance analysis and statistical analysis was done by Parin Izadi and Parnian Izadi. The first draft of the manuscript was written by Parin Izadi and Parnian Izadi commented on previous versions of the manuscript. Dr. Ahmed Eldyasti prepared the final submitted draft and critically revised the work. All authors read and approved the final manuscript.

Development of Long-Term Dynamic BioWin® Model Simulation for ANAMMOX UASB Micro-Granular Process [5]

Abstract

Three different innovative mathematical models were established to assess the volumetric nitrogen conversion rates of a sidestream lab-scale ANAMMOX upflow anaerobic sludge blanket reactor. Despite the vast technological and economic advantages of ANAMMOX, major challenges in process implementation call for mathematic simulations of the process, optimization of operating conditions, and kinetic/statistical analysis of the entire process. In this study, all developed mathematical models implemented via BioWin® were calibrated and validated, with adequate representations of a bench-scale micro-granular ANAMMOX process, to understand the potential setbacks of the ANAMMOX process startup and stabilization. Fundamental calculations of the kinetic and stoichiometric constants were integrated into the BioWin® software, and the adjusted parameters based on experimental analysis were applied for the assessments. Based on the results from the statistical approach, one of the models (Model III) exhibited a precise prognosis of the effluent data for the entire operational phases with a mean relative error (MRE) of approximately 1.96, 4.36, and 2.54 % for nitrogen removal efficiency, removal rate and loading rate, respectively. Evaluating alkalinity and pH during the operation led to identifying an acceptable fit between the experiment and Model III results, with a MRE of -7.19 and -0.35 %, correspondingly. This study confirms the reliability of ANAMMOX-based process modeling and high predictive ability with BioWin®. The presented simulation constants and modeling outline can be further employed in full-scale applications design and development.

[5] A version of this chapter has been published in the Chemosphere Journal, Volume 286, August 2021 https://doi.org/10.1016/j.chemosphere.2021.131859

Keywords

ANAMMOX, BioWin®, Modeling, Simulation, Dynamic analysis, Statistical analysis

7.1. Introduction

As a result of the energy-intensiveness of conventional designs, there has been a significant shift from nitrification-denitrification system configurations to a new and innovative generation of nitrogen removal processes (R. Chen et al., 2019a). One of the most promising substitutes for initiating an energy-producing treatment system is ANAMMOX-based processes (Reino et al., 2018). Biological nitrogen removal through anaerobic ammonium oxidation (ANAMMOX), leads to significant savings in aeration cost and organic carbon addition requisites, along with less sludge production (Wang et al., 2017). The bacterial community responsible for anaerobic ammonia oxidation is exemplified as an extremely slow-growing population, having an approximated doubling time of 10-30 days, leading to low biomass yields (M. Strous et al., 1998). The main obstacle for applying the ANAMMOX process is the slow growth rates associated with the bacterial community (Ali and Okabe, 2015), instigating prolonged startup times and important full-scale application limitations (Kocamemi et al., 2018). Even though ANAMMOX-based methods are characterized as one of the most favourable treatment strategies for direct ammonia oxidation to dinitrogen gas, considerable complications delay the practical applications of the process (Ye et al., 2020).

ANAMMOX bacterial activity directly affects the volumetric removal rates of the process, during which high-rate system configurations are of great value (Tang et al., 2013). The total nitrogen removal rate (NRR) of conventional biotechnologies were generally less than 0.5 $KgN/m^3/day$; however, ANAMMOX-based schemes reached a NRR of more than 5 $KgN/m^3/day$ in specific granule-promoting reactors, such as upflow anaerobic sludge blanket (UASB) reactor and gas-lift

systems (C.-J. Tang et al., 2011). For the mentioned granule-based reactors the removal efficiency and robustness of the system are principally dependent on the quality of granulation and quantity of the granule-shaped aggregates in the sludge (Lettinga, 1995). Compared to conventional system configurations, UASB offers various practical aspects for ANAMMOX cultivation and process operation, including an enhanced rate of startup and sludge immobilization (Lettinga, 1995). Sludge granulation drastically influences the bacterial population's metabolism and activity by increasing the connections and interactions in the consortium. The employment of shear force for granulation in UASB system design, coupled with the up-flow velocity of wastewater and emitted gases, plus the downward settling of the biomass, improves the mass transfer through the generated granules, leading to a balanced microbial ecology required for biological nutrient removal from wastewater (Izadi et al., 2020a).

ANAMMOX evaluation through experiments is a tremendously time-consuming process, mainly because of the slow growth rates associated with the bacterial community (Mattei et al., 2015). Consequently, mathematical modeling is an up-and-coming method to assess a wide range of environmental and operational parameters (Hao et al., 2002). Mathematical models signify valuable means to investigate microbial collaboration and synchronicity in multi-species aggregates (Mattei et al., 2015). Physical and mathematical modeling of the ANAMMOX granular process can aid in identifying the prospective implications of the treatment method and assess its potentials for biotechnological aspects (Dorofeev et al., 2017). Tang et al. (2013), created an innovative mathematical model for a high-rate ANAMMOX UASB system to assess the volumetric nitrogen conversion rates, in line with the packing arrangements of the granular sludge. The study results indicated that the model was able to simulate the performance of the reactor accurately. In another study, mathematical modeling was employed to evaluate the reactor

performance in an ANAMMOX MABR (Liu et al., 2016). Simulation of the microbial structure and MABR reactor performance was done via a multi-species one-dimensional biofilm model (software AQUASIM 2.1d), and the results showed a promising alternative to previous systems. Based on a study by Ni et al. (2009), a mathematical model was established to illustrate ANAMMOX process in a UASB reactor. The results show an accurate simulation for the one-year reactor performance.

One powerful method to accelerate the scale-up of these ANAMMOX-based processes is establishing a process model at dynamic conditions to generate a baseline for data evaluation (Soliman and Eldyasti, 2017). Numerous software's, including BioWin® (EnviroSim Associates Ltd., Canada), focus on modeling the microbiological processes implicated with wastewater treatment, which allow for mathematical simulation of ANAMMOX bacterial activity (Dorofeev et al., 2017). One of the main advantages of mathematical process modeling is the potential to analyze various operational factors to optimize the effective approaches (Elawwad, 2018). Yet, there is a limited number of studies focusing on biological nutrient removal optimization through activated sludge models such as BioWin® (Elawwad et al., 2017). Mathematical modeling of biological systems, including ANAMMOX, by BioWin®, allows for examining microbial competition and coexistence of various species (Mattei et al., 2015).

Most of the previous ANAMMOX-based studies focused on process startup from a mature ANAMMOX biomass to expedite the initiation period (Q. Wang et al., 2018). Conversely, supplying a sufficient amount of ANAMMOX biomass for engineering purposes is one of the key process drawbacks, owing to the low cellular yields and extended generation times related to the bacterial consortium (M. Strous et al., 1998). Hence, an appropriate seeding scheme and optimized reactor design and configuration may pick up the startup pace of the ANAMMOX process (Q.

Wang et al., 2018). Moreover, there is a limited number of studies that focused on mathematical modeling of the ANAMMOX process via BioWin® software due to insufficient knowledge on the physiology of ANAMMOX bacteria (Ni et al., 2014) (Hubaux et al., 2014) and to the best of our knowledge, there are no studies on UASB-ANAMMOX modeling. Dorofeev et al., 2017, proposed a mathematical model to estimate the potential of using the BioWin® software, intended for providing a predictive method for nitritation/ANAMMOX technology through assessment of the data collected from both mathematical modeling and experimental setup. The algorithms and simulations showed a high rate of predictive potential for BioWin®, simulating the ANAMMOX process (Dorofeev et al., 2017).

Effective simulation procedures can facilitate the interpretation of complex biological and chemical processes involved in the ANAMMOX process. Furthermore, the advancement of adapted methods can be restructured by employing a simulation technique, with no extra expenses of time and resources in constructing experimental test fundamentals. The research studies on BioWin® mainly focus on using this software to simulate and optimize the wastewater treatment processes. Additionaly, in this study in addition to simulation and optimization, the developed models were used to analyze and improve the experimental UASB system setup. On the other hand, the literature review revealed very few publications adopting BioWin® for anaerobic wastewater treatment processes, including ANAMMOX. The aim of this study was to assess the response and overall performance of a lab-scale UASB micro-granular ANAMMOX process in a long-term operation period, using both mathematical modeling data and experimental data, to represent a comparison between the two methods. This study illustrates the potential of BioWin® software to estimate and predict ANAMMOX process and to describe the long-term dynamic behavior of a UASB system setup. Evaluating the possibility of using BioWin® for process

prediction intended for potential future scaleups is of great importance. Results of this study will be valuable in enhancing the efficiency of UASB-ANAMMOX's practical operation on an industrial scale.

7.2. Materials and methods

7.2.1. UASB lab-scale system

A single-stage UASB system with a working volume of 4.8 L was utilized as the experimental setup for the study. A schematic diagram and other specifications are illustrated in Figure 7-1 A. The reactor was initially seeded with returned activated sludge (RAS) collected from the Humber treatment plant (Toronto, ON, CA), with total chemical oxygen demand (TCOD) and volatile suspended solids (VSS) of 24,280 mg/L and 16,650 mg/L, respectively. System was operated with an average hydraulic retention time (HRT) of 24 hours, along with a controlled SRT between 35 to 72 days, varying from top to the bottom of the reactor. UASB reactor was operated in sidestream conditions, being fed with synthetic wastewater, and placed in a warm chamber with a temperature of approximately 35 ± 5 °C. Correspondingly, the amount of ammonia and nitrite is based on experimental design to attain influent ammonia and nitrite levels of 52.02 and 62.42 mgN/L. Day-to-day measurements of ammonium, nitrite, and nitrate provided the foundation for all calculations. The pH was not regulated but assessed off-line, and pH of the influent was 7.9 on average throughout the entire operation (Izadi et al., 2020a). As indicated in Table 7-1 A, the experimental assessment was analyzed in three principal phases that correspond to various feeding mediums and following inhibition results, wherein phase I (~55 days) is the startup and early ANAMMOX activity detection step, phase II (~63 days) draws attention to the impact of elevated influent ammonia levels on the process. Phase III (~200 days) affirms a steady ANAMMOX process with high ammonia and nitrite removal rates. Accordingly, by the end of the operation of

this study, the sludge bed in the UASB reactor was highly enriched with ANAMMOX bacteria, directly associated with "*Ca*. Brocadia sp." and "*Ca*. Kuenenia".

7.2.2. BioWin® general model development

BioWin is a wastewater treatment process simulator that links biological, chemical, and physical process models. BioWin is used globally to design, upgrade, and optimize wastewater treatment plants of all varieties. BioWin models assist engineers and operators in making choices that lessen the principal and operational expenses and guarantee treatment goals are met. Nitrogen removal biotechnology has been developed by software suite (EnviroSim Associates Ltd., Canada), which is established on the broadly applied activated sludge model (ASM) founded by a global scientific organization, the International Water Association (IWA) (Dorofeev et al., 2017). Based on the design configuration and the assessed data from the UASB-ANAMMOX system and its valid operational results, three different theoretical models were composed using BioWin® 4.1 software. As illustrated in Figure 7-1 B, C and D (Model I, Model II and Model III, respectively), the UASB reactor conformation is mainly characterized by an anaerobic digester element linked to a point settler component simulate the flow state of the fluid. In Model II and III, the top and bottom of the UASB are separated accounting for the deviations based on the reactor's different height scopes and reaction zones. The UASB reactor's hydrodynamic behavior creates a concentration gradient, wherein the sludge blanket height is considered an important key parameter. As a result, height affects biomass concentration at different zones of UASB, which sequentially will influence the granular particles motion, biological activity, and fluid transfer into the structure of the granules (Zinatizadeh et al., 2020). The fixed values related to the biomass of ammonia-oxidizing bacteria (AOB), nitrite-oxidizing bacteria (NOB), ANAMMOX bacteria cultivating in the system, and the determined levels of the principal compositions of dissolved

nitrogen, total phosphorous element, and biologically degradable organic (BOD) substance in treated water were estimated via BioWin® software. The principal approximations of the kinetic and stoichiometric factors of the microbial and chemical processes involved in the BioWin® software suite were instigated for the calculations.

The primary flowsheet of the process includes the wastewater source (synthetic wastewater coupled with the nitrite addition stream), bioreactor which is combination of anaerobic digesters/anoxic tank and the point settler, splitter, output of treated wastewater, and output of excess sludge (Figure 7-1 B, C and D). One of the key characteristics of high strength nutrient removal processes is increased biomass retention and decoupling of HRT and SRT in the system, leading to considerable declines in treatment times (Chong et al., 2012). In UASB system configurations, extended biomass retentions are achieved through granulation, resulting in aggregates with high settling properties (Chan et al., 2009). As elucidated in Figure 7-1 B, C, and D**,** the underflow rate of the point settler is adjusted to allocate a relatively high recirculation ratio in the UASB. Moreover, to draw in the granulation process in the simulation outline, the solids removal in the point settler is adjusted to sustain total suspended solids (TSS) accumulation in the digester, which is standard for UASB-based processes. As shown in Table 7-1 B, a number of the kinetic parameters were adjusted for anaerobic ammonia-oxidizing bacteria (AAO), according to the experimental data attained. Furthermore, a number of the influent fractions was adjusted to resemble the synthetic feed's properties. A few of the readjusted values were as following; ammonia fraction (Fna) to 1.0 g NH_3-N/gTKN, particulate organic nitrogen fraction (Fnox) to 0 gN/g organic N, along with soluble unbiodegradable TKN fraction (Fnus) to 0 gN/gTKN, considering that the feed was synthetic solution consisting of ammonia (Table 7-1 B). Comparably, the phosphate fraction (Fpo_4) was customized to be 1.0 g PO_4-P/gTP.

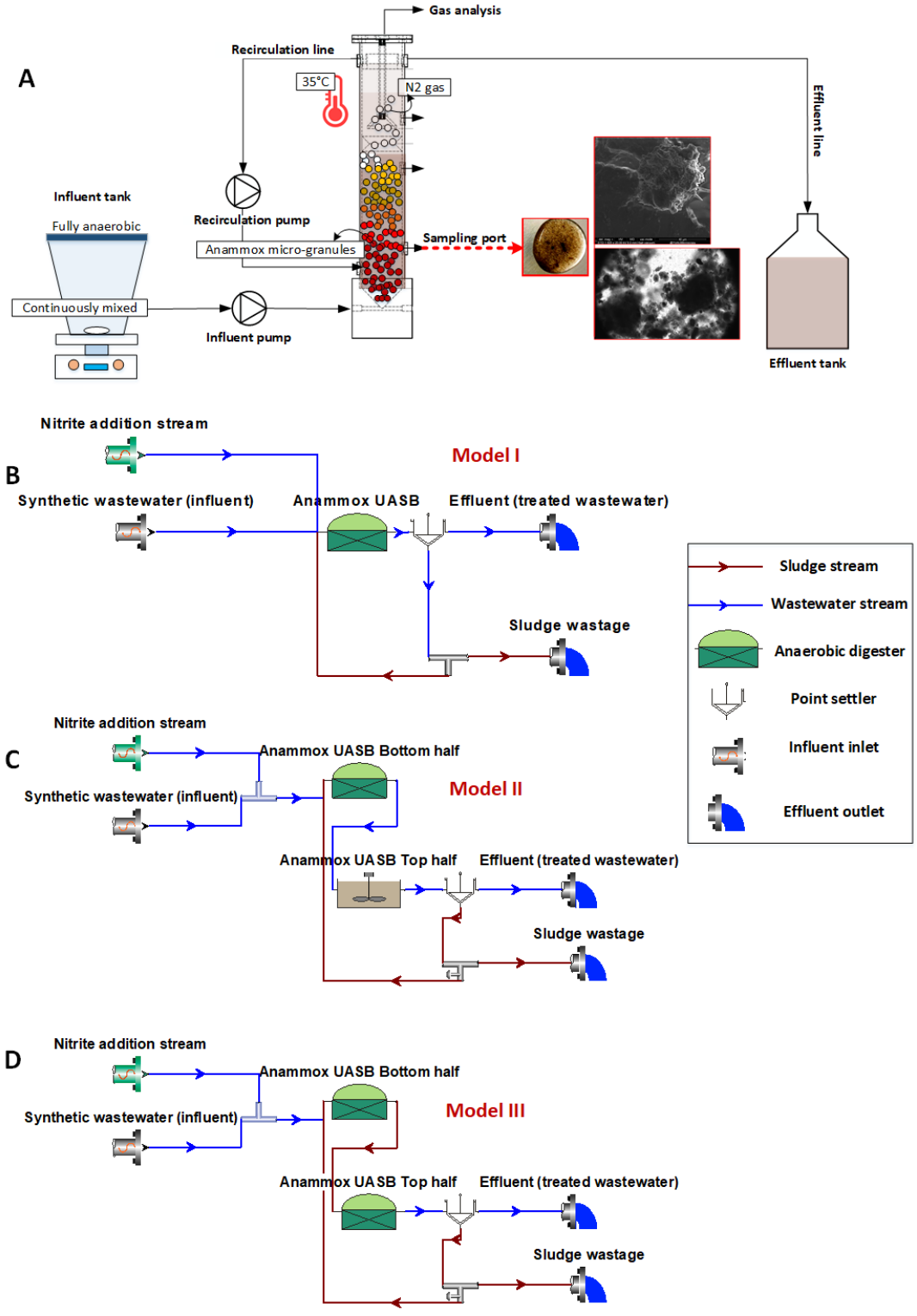

Figure 7-1 A) Conceptual schematic diagram of the laboratory continuous UASB setup, B, C and D) Three different Model configuration of the process used for the simulation (Model I, II and III, respectively)

7.2.3. Model calibration and sensitivity analysis

All models were calibrated based on the BIOMATH calibration protocol (Corominas et al., 2011), in which the characterization of main objectives is a vital factor in the process simulation procedure (Vanrolleghem et al., 2003). Extensive studies have been performed to build an efficient model calibration methodology. As a result of the studies, experience-based approaches were proposed, including BIOMATH, introducing programmatic flow based on professionals' comprehension and experience. The data for model calibration and validation can be from diverse feeding and operation settings, and a few of the parameters are predetermined to achieve a precise approximation of the affecting ones (Zhu et al., 2015). This specific methodology consists of four main stages and can be implemented for a variety of activated sludge-based models, including ANAMMOX; in addition, it can be adjusted according to the simulation goals and the accessible data (Makinia, 2010).

7.2.3.1. Outlining the simulation targets

The primary goals of this study were to simulate the experimental data of a single-stage UASB-ANAMMOX process, to develop a model that would reasonably match the collected experimental data, and potentially have the capacity to elucidate the long-term dynamic performance of ANAMMOX- UASB system configurations. There is a lack of accurate studies on ANAMMOX bacterial behavior modeling due to the poorly studied physiology of ANAMMOX bacteria and process complexity (Dorofeev et al., 2017). This algorithm and simulation can aid in estimating the BioWin® suitability for predicting and calculating of ANAMMOX-based technologies for biological nitrogen removal from wastewater.

Table 7-1 A) Detailed operational conditions during different phases of the UASB process, B) Adjusted kinetic and stoichiometric parameters for UASB-ANAMMOX system, C) Theoretical equations for experimental and simulation assessments

A)

Phase	HRT (hours)	DO (mg/L)	Mean NLR ($KgN/m^3/day$)	$VSS_{reactor}$ (g/L)	Mean influent ammonia (mgN/L)	Mean influent nitrite (mgN/L)
I	24	0.08-0.1	0.198	8.58	52.0 ± 2.13	68.7 ± 2.81
II	24	0.08-0.1	0.272	8.74	71.6 ± 1.07	60.9 ± 0.91
III	24	0.08-0.1	0.198	8.96	53.0 ± 4.45	69.97 ± 5.88

B)

Component	Default	Value
Fbs - Readily biodegradable (including Acetate) [gCOD/g of total COD]	0.16	0.22
Fus - Unbiodegradable soluble [gCOD/g of total COD]	0.05	0.12
Fup - Unbiodegradable particulate [gCOD/g of total COD]	0.13	0.65
Fna - Ammonia [gNH_3-N/gTKN]	0.66	0.9
Fnox - Particulate organic nitrogen [gN/g Organic N]	0.5	0
Fnus - Soluble unbiodegradable TKN [gN/gTKN]	0.02	0
FZbh - OHO COD fraction [gCOD/g of total COD]	0.02	1.00E-04
AAO substrate (NH_4) half saturation [mgN/L]	2	0.1
AAO substrate (NO_2) half saturation [mgN/L]	1	0.1
Nitrite sensitivity constant [L / (d mgN)]	0.016	0

C)

	Equation	Parameters definition
1	$TN_{eff} = ([NH_4^+\text{-}N] + [NO_2^-\text{-}N] + [NO_3^-\text{-}N])$	TN_{eff}: Total nitrogen in the effluent (mg/L)
2	$NLR = TN_{in}/HRT$	NLR: Nitrogen loading rate ($KgN/m^3/day$)
3	$NRR = \Delta N/HRT$	NRR: Nitrogen removal rate ($KgN/m^3/day$)
4	$NRE = \Delta N/[NH_4^+\text{-}N]_{in}$	NRE: Nitrogen removal efficiency ($KgN/m^3/day$)
5	$qAMX,N2 = \frac{rAMX,NH4 + rAMX,NO2 - rAMX,NH4\_NO3}{XVSS}$	qAMX, N2: Maximum specific ANAMMOX rate ($mgN_2\text{-}N.\ gVSS^{-1}\ h^{-1}$)
6	$S_{i,j} = (\lvert\Delta Y_i/Y_i\rvert)/(\lvert\Delta X_i/X_i\rvert)$	$S_{i,j}$: Normalized sensitivity coefficient X_i: Input values
7	$\delta j^{msqr} = (1/n(\sum_{i=1}^{n} S^2_{i,j}))\text{^}1/2$	δj^{msqr}: Mean square sensitivity measure

8	$MRE= (1/n(\sum_{i=1}^{n}((m_i-p_i)/m_i))\times 100$	MRE: Mean relative error n: Number of observations m_i: Measured value p_i: Predicted value

7.2.3.2. Data analysis and process characterization

This model calibration stage points towards a combination of design, operational and measured data to specify the system configuration. Samples were collected daily from both the influent and effluents lines and were immediately analyzed according to the standard methods of water and wastewater examination. The entire water samples were examined via ion chromatography (IC) by the Thermo Scientific™ Dionex™ Integrion™ HPIC™ system. Further analytical determinations (e.g., pH, TSS, VSS, Alkalinity, etc.) were conducted according to Standard Methods (APHA, 2005). The anaerobic conditions in the UASB reactor were monitored by measuring the dissolved oxygen levels (DO) using IntelliCAL LDO Lab Probe (HACH Company, Loveland, Colorado, USA). Confirmation of ANAMMOX enrichment was done through PCR (RNA was extracted, amplified using PCR, then the products were subjected to gel electrophoresis to confirm the existence of ANAMMOX bacteria). Nitrogen gas production was assessed using SRI 8610C gas chromatography (SRI instrumentation, Torrance, USA) equipped with a thermal conductivity detector (TCD). Several microscopic analyses were conducted (Figure 7-1 A) to confirm the granulation process in the UASB system configuration, including an inverted microscope (BioImager, ON, Canada) and scanning electron microscope (Thermo Fisher Quanta 3D electron microscope, York University, Ontario, Canada). Nitrogen loading rate (NLR), nitrogen removal rate (NRR) and nitrogen removal efficiency (NRE) were analyzed based on the nitrogen balance and stoichiometry according to Equations (2-4) in Table 7-1 C, and it was assumed that the ANAMMOX reaction mainly eliminates the nitrogen. The maximum specific

ANAMMOX rate as mgN_2-N. $gVSS^{-1}$ h^{-1} was determined via Equation 5. In this specific study as indicated in Table 7-1 C -Equation 8, MRE was selected to assess the accuracy of the validation process and the model estimates. Additionally, MRE can provide an indication of decency-of-correspondence for the BioWin® models (Elawwad, 2018).

7.2.3.3. Steady-state calibration

In this specific step of process model calibration, the model is calibrated to correspond to average effluent concentration and sludge waste data, presuming that this average characterizes a steady-state (Makinia, 2010). The entire collected data were assessed, and a total mass balance was executed to determine any impending inaccuracies and miscalculations and to develop the view on the ANAMMOX-based UASB system configuration. All data calculations involved mean and standard deviation analysis for comparison purposes. Each data analysis step was taken to assess the reactor performance and validate that all gathered data are consistent and dependable. The main objective behind this stage of process calibration is to approximate the suitable biomass structure in the UASB reactor. The biomass composition acquired from the steady-state calibration would be the basis of the dynamic model calibration as the primary seed constitution.

7.2.3.4. Dynamic calibration and end results assessment

In the final stage of the calibration protocol, the dynamic calibration of the sludge model is implemented to potentially fit the model to the experimental data. Both the kinetics and stoichiometric parameters were adjusted to meet the experimental UASB design criteria. The available data for 317 days in this study allowed for a better understanding of the system behavior and led to a more precise estimation of parameters. A comprehensive sensitivity analysis was performed to understand which of the influential parameters are more valuable. Then, all models' calibration was done by adjusting the parameters based on matching the model to dynamic data

attained from the measurements. Choosing the appropriate, sensitive parameters is a key stage in model calibration and validation. The sensitivity analysis was carried out by identifying six of the most influential kinetic and stoichiometric parameters for AAOs, and three main outputs of the process including, effluent ammonia, effluent nitrite and nitrate concentrations (Table 7-2) (Soliman and Eldyasti, 2017). Conventional sensitivity analysis approach, Si, j, shown in Table 7-1 C signifies a specific parameter's effect on a particular water quality index (Ji et al., 2019). The sensitivity analysis followed several general standards, including the fact that the system output (Yi) was adequately sensitive to the parameter (Θj) adjustment. The sensitivity measure δj^{msqr} is intended to evaluate particular parameter significance in a least-squares parameter assessment framework (Table 7-1 C, Equation 6 and 7), in which it determines the average sensitivity of the model output in response to an alteration in the parameter Θj (Brun et al., 2002). The theory behind sensitivity assessment was that the greater the value, the more the influence of the parameter on the simulation outcome (Ji et al., 2019).

Principal data analysis for investigating the differences in performance between all three models was performed by Matlab R2015a (MathWorks, USA), which from the literature does not look as if it has been employed formerly for statistical analysis in UASBs. The statistical software package Matlab 2015a was used to design curve fitting analysis and hypothesis testing of the experimental and modeled data. For the statistical analysis, the t-test (for two groups of samples), *F*-test for equal variances (for two groups of samples), and Kolmogorov-Smirnov test (for two groups of samples) were applied with Matlab® Statistics and Machine Learning Toolbox™ to evaluate the significance of differences in efficiency, performance and fit between models. The significance level of probability (p-value) was 0.05 in this study.

7.3. Results and Discussions

7.3.1. Model calibration and data validation

The critical gain of employing a computer model for a certain wastewater treatment process is the capacity to examine various operational constraints to achieve an optimal operating scheme (Elawwad, 2018). Two essential stages included in process simulation are calibration and validation, where the calibration course is a fundamental phase in process modeling and is commonly accomplished by applying steady-state simulation mode (Hulsbeek et al., 2002). Calibration is the frequentative process of linking the model with the real system and adjusting the model parameter values to fit the experimental data set (Gaganis, 2009). Calibration of the ANAMMOX-UASB models were accomplished by modifying the main parameters spotted during the sensitivity analysis as indicated in Table 7-2. However, the irrelevant parameter or the ones with insignificant influence (less than 5%) remained as BioWin® default values for the subsequent analysis. A process of direct assessment of the predicted simulation data concerning the experimental outcomes was carried out to validate the simulation. The model's reliability was approximated by evaluating the simulation results with regards to the experimental data attained from UASB reactor performing the continuous ANAMMOX process. Undoubtedly, there are certain inconsistencies between the models outcomes and the determined experimental values. In this study, running the simulations with default parameters initiated a substantial discrepancy amongst models and experimental outcome numbers, mainly the ammonia, nitrite, and nitrate concentrations. When the default parameters were used, the main substrates of the process started to accumulate in the reactor(s), and there was limited production of nitrate, resulting in a major inhibition of the bacterial community. Thus a calibration of both kinetic and stoichiometric parameters (Table 7-2) were completed to readjust the structure to meet the experimental system requirements.

The dynamic simulation, with calibrated values in Model I and III resulted in successful ammonia and nitrite removal and nitrate residual accumulation in the reactor, in which as indicated in Figure 7-2-1 and Figure 7-4-1, the average NRE reached 80.2 ± 4.47 % and 77.15 ± 7.16 % in the third phase of operation, implying an effective alteration of the bacterial community towards ANAMMOX consortium. The experimental analysis was investigated in three main phases. In phase I, the influent NH_4^+-N was maintained at approximately 50.4 mg N/L, and the average NLR was 0.2 KgN/m^3/d. In the second phase of operation, the effects of a sudden boost in the influent's ammonia concentration were considered with influent ammonia concentration increase of approximately 20 mg N/L, while the nitrite concentration was reduced to reach a nitrite: ammonium ratio of approximately 0.85. In the final phase, the NLR returned to 0.2 KgN/m^3/d. At this influent ammonium concentration, a mean NRE of 91.6% was achieved, which was highest in all phases (Figure 7-2). As illustrated in Figure 7-2, the average experimental NLR and NRR were 0.20 KgN/m^3/d and 0.18 KgN/m^3/d, respectively. The experimental results calculated based on the continuous sampling analysis from the UASB reactor system setup showed a mean NRE of approximately 78.31 ± 6.51 % for the final operational phase. The maximum specific ANAMMOX rate of 357.85 as mgN_2-N. $gVSS^{-1}h^{-1}$ was calculated in phase III of reactor operation. In a similar study with higher NLR, C. J. Tang et al. (2011), investigated the performance of two high-loaded ANAMMOX UASB reactors. The study results indicated a high-rate performance with NRR of 74.3-76.7 KgN/m^3/d and specific ANAMMOX activity of 5.6 KgN. $KgVSS^{-1}day^{-1}$.

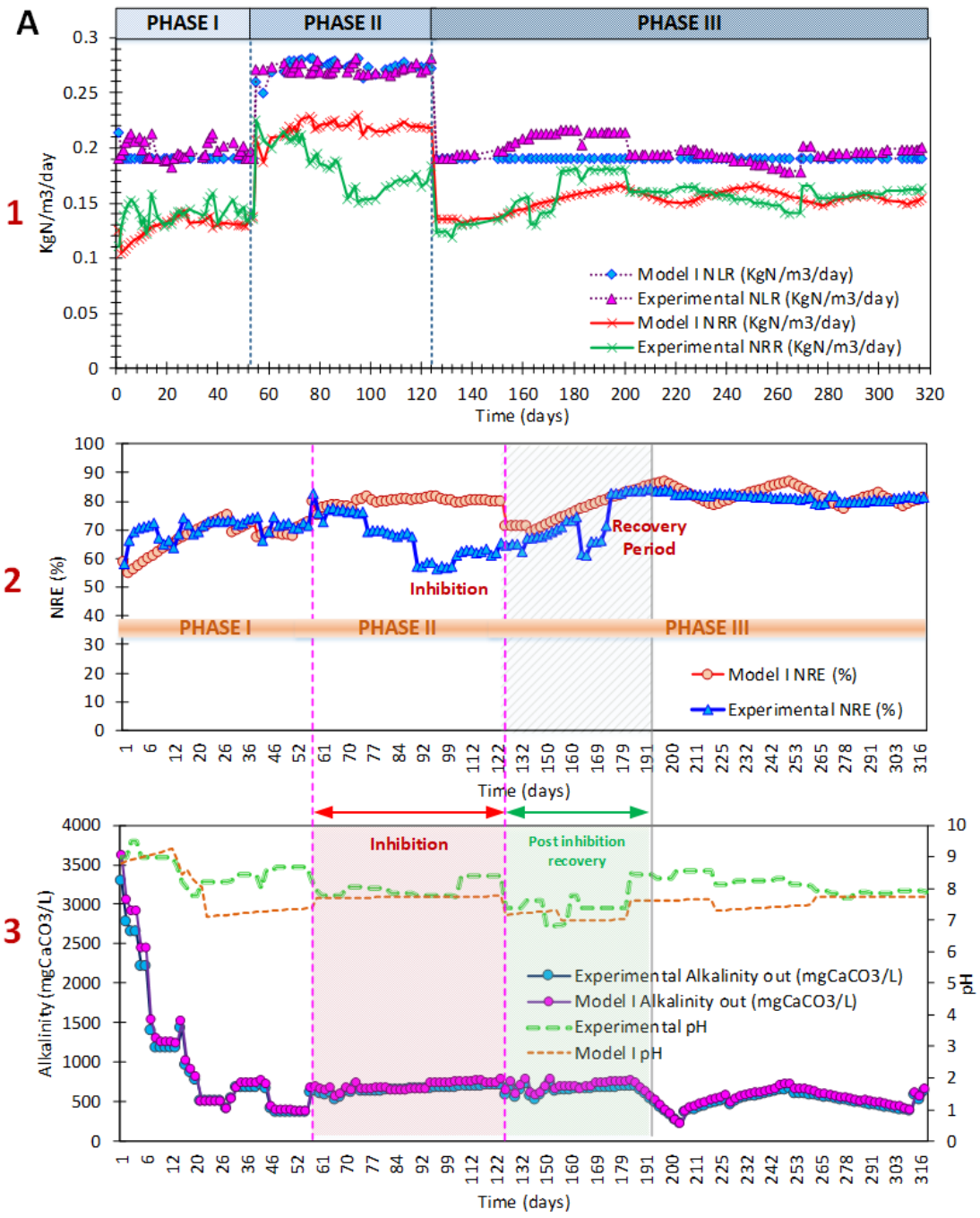

Figure 7-2 Comparison between daily experimental effluent measurements and the dynamic models data for 317 days of operation: (A-1) NLR and NRR levels for Model I (A-2) NRE (%)for Model I (A-3) Alkalinity and pH for Model I

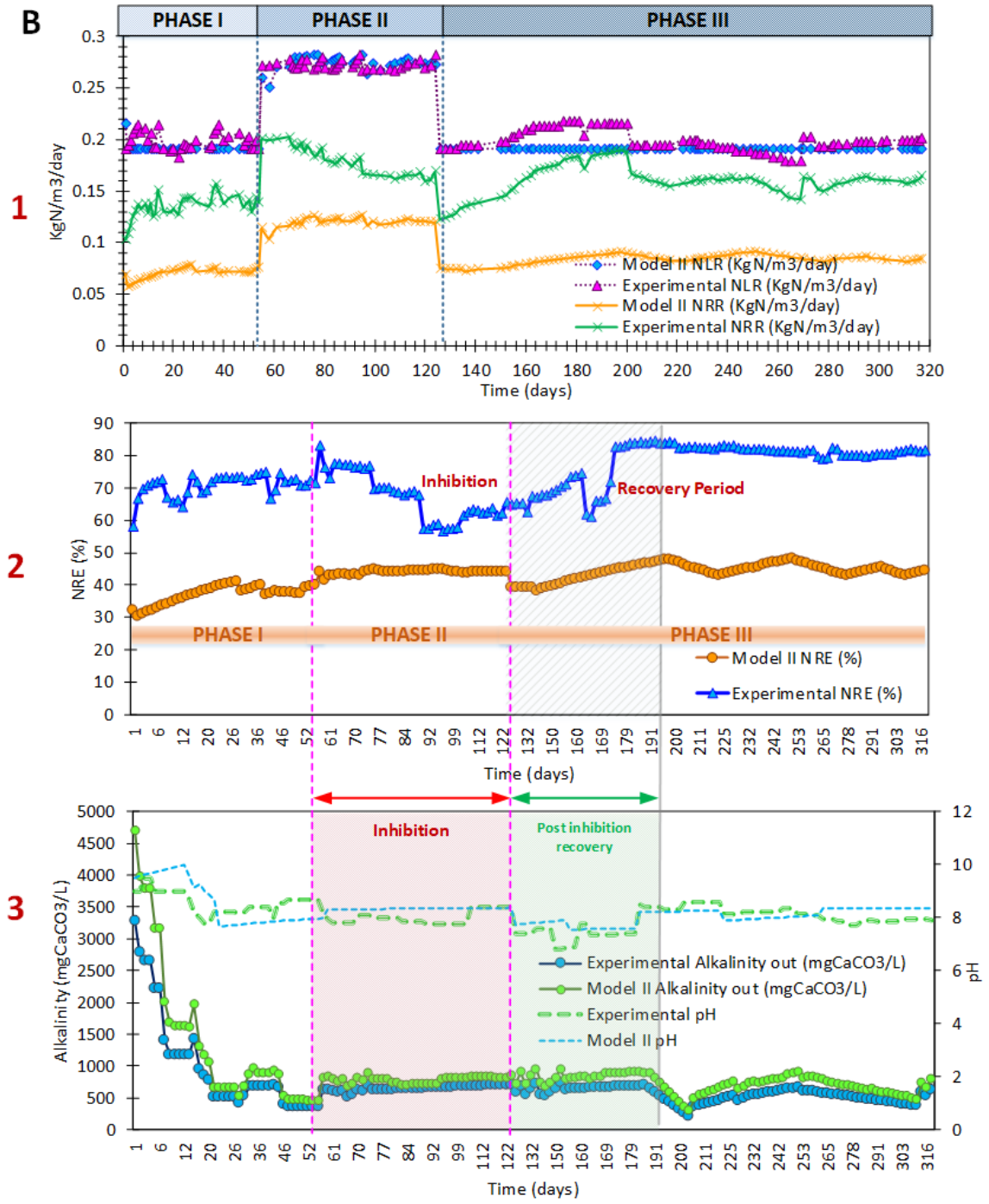

Figure 7-3 Comparison between daily experimental effluent measurements and the dynamic models data for 317 days of operation: (B-1) NLR and NRR levels for Model II (B-2) NRE (%)for Model II (B-3) Alkalinity and pH for Model II

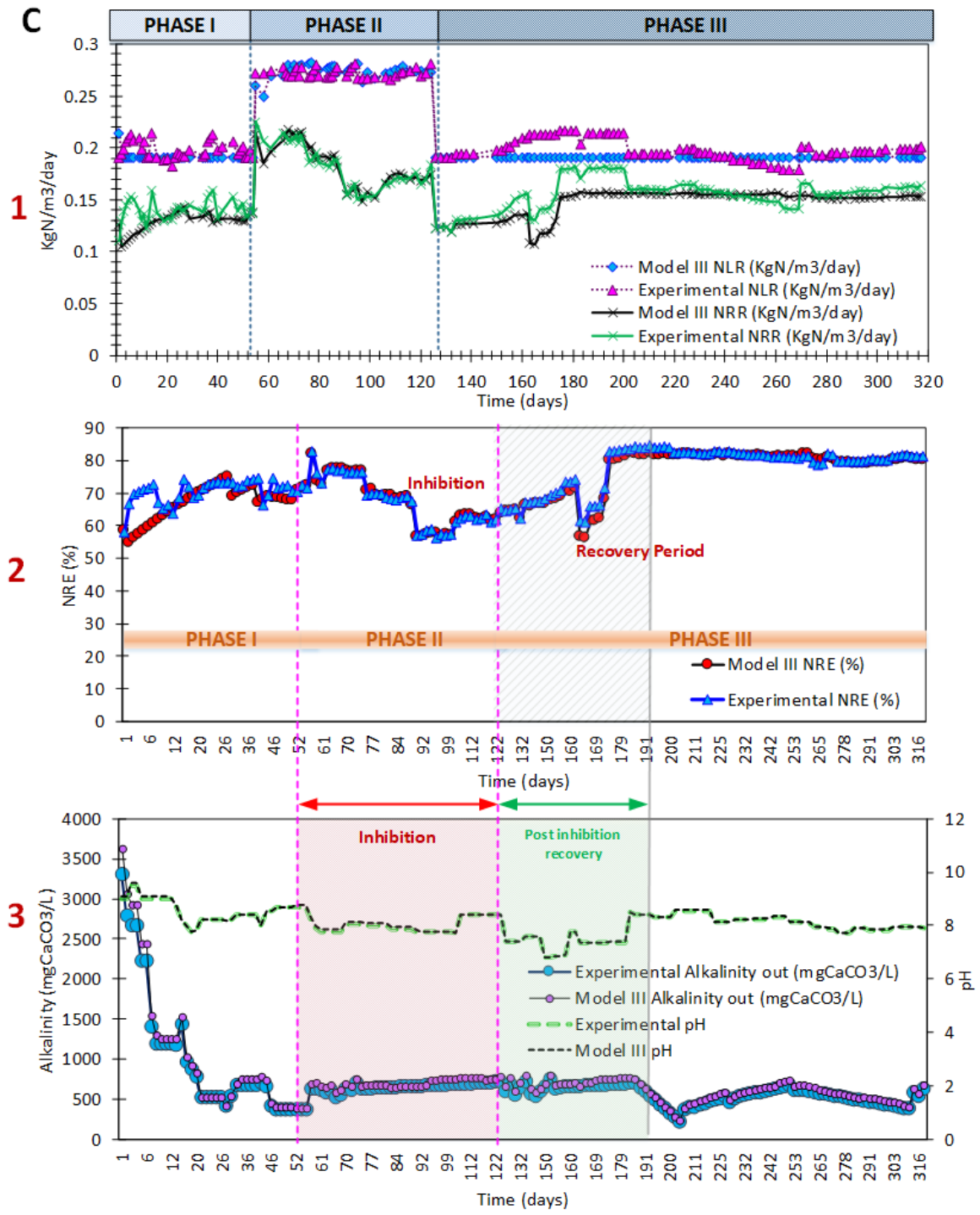

Figure 7-4 Comparison between daily experimental effluent measurements and the dynamic models data for 317 days of operation: (C-1) NLR and NRR levels for Model III (C-2) NRE (%)for Model III (C-3) Alkalinity and pH for Model III

The high activity was a significant element initiating the enhanced NRR of the UASB reactor. In a similar study, high values of 5.6 ± 0.9 KgN. $kgVSS^{-1}$ day^{-1} were detected for the ANAMMOX granules when the NRR was greater than 70 KgN/m^3/day (C.-J. Tang et al., 2010b). The results presented in Figure 7-4, show that Model III perfectly projected the effluent data for all three phases with a MRE (Table 7-1-Equation 8) of around 1.96, 4.36 and 2.54 % for NRE, NRR and, NLR, respectively. In Model III the average AAO concentration in the UASB system setup reached an average of 27.7 mgCOD/L. Figure 7-4-1 shows that Model III could predict the daily nitrogen loading and removal rates during the final stabilized operational conditions. Comparably, a matching trend was observed in the other two phases between the experimental and predicted NRE, NLR, and NRR values specifying the success of the calibrated model to mimic the ANAMMOX UASB process initiated from returned activated sludge. Previous studies have been able to prove the competence of activated sludge-based modeling. This has been confirmed by various mathematical simulations of nitrogen removal processes based on the activity of heterotrophic, nitrifying, and denitrifying microorganisms (Van Loosdrecht et al., 2015). Dorofeev et al. (2017), assessed the potential use of the BioWin® for analytical computation of nitritation/ANAMMOX biotechnology. The result of the study showed a great prognostic capacity for the ANAMMOX process mathematical modeling, where the modeled and measured ammonium, nitrite, and nitrate concentrations in the effluent of the process were comparable, plus they were 10.7 and 11.7% of the influent, respectively.

Moreover, reviewing the alkalinity and pH results (Figure 7-4-3), an extremely close match between the experiment and model outcomes was observed, with an average MRE of -0.35 and -7.19 %, respectively. Phase I began with a high pH range above 9, which had a prospective inhibition effect on the bacterial community present in the reactor. Nevertheless, after five days of

operation, pH was declined to a range around 7.99 and was stabilized in an acceptable range (Wett and Rauch, 2003), because according to the literature the optimum pH range for ANAMMOX organisms ranges between 7-8.5 (Strous et al., 1997b). Similar to pH, alkalinity concentration was modified after six days of operation to boost the objective bacterial group development and growth. Accordingly there is a drop in both pH and alkalinity levels in the effluent of the process in the first phase of operation. After the pH and alkalinity adjustments, there was a sharp increase in the process NRR due to a decrease in nitrite accumulation in the reactor (Jaroszynski et al., 2011).

A suitable equivalence was found while comparing the main nitrogen characterization of the effluent wastewater from the experimental setup with the typical nitrogen characterization of Model III effluent wastewater values. The discrepancy amongst the measured ammonia and nitrite in comparison with the predicted values of the same output variables by BioWin® did not surpass 20%, suggesting that the calibration process of the BioWin® model was completed adequately (Liwarska-Bizukojc et al., 2013). The MRE for ammonia and nitrite concentrations in the effluent of the Model III process were, 1.13 and 2.54 %, respectively.

Model I was able to accurately predict the daily effluent data during all different operational conditions, except for phase II, in which an inhibition factor was imposed on the system. As illustrated in Figure 7-2-1 and Figure 7-2-2, a major discrepancy between the modeled and experimental NRR and NRE is observed in phase II, indicating a MRE of -21.16 ± 15.35 % and -20.13 ± 14.33 %. In Model I, the average AAO concentration in the UASB system setup reached an average of 26.2 mgCOD/L. It can be concluded that a single anaerobic digester was unable to sufficiently simulate the UASB system setup and, Model I was unsuccessful in predicting the ANAMMOX system's behavior in the occurrence of abrupt shock loads. Based on the simulation results, the AAO concentration in Model I (average of 26.22 mgCOD/L) starts to rise when the

loading rate increases in the second phase, yet in Model III there is a sharp drop in AAO concentration when the nitrogen loading rate reaches a higher level in phase II. Concurrently, the dissolved nitrogen gas dropped significantly in the second phase of Model III configuration, indicating a major inhibition, yet in Model I, no noticeable changes were detected. Reviewing the nitrous acid levels in the reactors of both Model I and III configurations, specify a sudden increase in phase II. However, in Model I the HNO_2 concentration reaches approximately 0.2 mmol/L, but in Model III the HNO_2 level in the inhibition period is around 5.77 mmol/L. A few of the most important characteristics affecting the performance of anaerobic digestion reactors setups include mixed suspended solids, complicated microorganism populations, extended hydraulic and solids retention periods, and mesophilic temperatures. For a digestion system, the reaction and microbial activity are directly proportional to the SRT. The average SRT of the ANAMMOX-UASB reactor was controlled at approximately 35-70 days from top to bottom section, and the system had a stable performance for three turnovers of the system's SRT. Since in Model III the SRT of the top, and bottom of the reactor were modeled separately based on the experimental data, the system exhibits a better representation of the UASB-ANAMMOX lab-based process. The value of SRT influences the capacity of the system for biomass retention. Triumph of high-rate ANAMMOX-based treatment method is, comparatively, attributable to sustaining a long SRT at short a HRT due to sludge immobilization in the sludge blanket. Nevertheless, in Model I, having an identical SRT for the entire UASB system setup and an inadequate sludge immobilization in the bottom part of the UASB (blanket) resulted in discrepancies in phase II reactor performance.

There are several studies on the effect of free nitrous acid (FNA) on the ANAMMOX process, suggesting that FNA has a destructive effect on the process and can obstruct and slow down the start of the reaction. Inhibition initiated by HNO_2 is reversible, and the restoration period is usually

about one month (Fernández et al., 2012). On the other hand, Model II failed to simulate the experimental ANAMMOX-UASB system. As shown in Figure 7-3, there is a considerable discrepancy in the results, stemming from the inefficiency of an anoxic tank to model the top portion of the UASB reactor (Figure 7-4). In Model II the average AAO concentration in the UASB system setup reached an average of 0.05 mgCOD/L. This system configuration was incompetent to accumulate sufficient AAO concentrations to perform a stable and high efficiency ANAMMOX process. As presented in Figure 7-3-1 and Figure 7-3-2, the NRR and NRE trends in Model II are extremely distinct from the experimental outcomes, with a MRE of 43.97 ± 7.77 % and 42.31 ± 6.93 %, respectively. Moreover, Model II exhibited poor performance in projecting the pH and Alkalinity with MRE levels of 5.87 ± 1.99 % and -30.81 ± 7.97 %, respectively.

7.3.2. Sensitivity analysis

A sensitivity analysis can spot the parameters most sensitive to uncertainties (Lauwers et al., 2013). These parameters are the ones that will be reflected in the calibration of all three models. Measured data from the influent are commonly employed as inputs for sensitivity assessment (Ji et al., 2019). It is important to point out that the number of modified parameters, as indicated in Table 7-1, were limited to the minimum possible level, as a result of a full sensitivity analysis being completed on the most influential factors regarding measured outputs, including NH_4-N, NO_2-N, and NO_3-N. To recognize the most influential parameters leading to a shift in ANAMMOX process performance, six kinetic and stoichiometric parameters of AAOs, underwent ±50% alteration from their default and literature-based model values in BioWin®. As shown in Table 7-1 C, Equation 6, the normalized sensitivity coefficient was assessed in line with three of the main process effluent characteristics. During the sensitivity analysis, it was perceived that the sensitivity coefficient had an elevated range of values for ammonia levels, in connection with the variations in the input

parameters (Table 7-2), which can be directed to the high dependency of ANAMMOX process to a number of potential factors, including substrate concentrations, mainly ammonia (Zekker et al., 2012). The consequence of introducing a critical range of parameters and changing the biomass structure is highly complex for ANAMMOX, which can potentially result in substrate build-ups in the process effluent. Comprehension of the parameters affecting the activity of ANAMMOX bacteria is necessary for improving process applicability (Carvajal-Arroyo et al., 2013).

Table 7-2 Normalized sensitivity coefficient and mean square sensitivity measure of three main effluent characteristics of kinetic and stoichiometric parameters

Rank of influence	**Parameter name**	**Symbol**		**Default value**	**Unit**	**Normalized sensitivity coefficient (Si, j)**			***δj^msqr***
						Ammonia	Nitrate	Nitrite	
1	Maximum specific growth rate	$\mu_{max, AAO}$	Kinetic	0.1	1/d	3.50	2.77	0.23	17.11
2	Anoxic/ anaerobic decay rate	$b_{anaerobic, AAO}$		0.0095	1/d	8.72	1.00	0.86	1.66
3	Yield	Y_{AAO}	Stoichiometric	0.114	mgCOD/mgN	0.25	1.17	0.23	0.51
4	Substrate (NH_4) half saturation	K_{NH4}	Kinetic	2.0	mgN/L	1.01	0.01	0.01	0.35
5	Substrate (NO_2) half saturation	K_{NO2}		1.0	mgN/L	0.03	0.0001	1.91 E-05	0.002
6	Nitrite sensitivity constant			0.016	L/ (d mgN)	0.018	8.99 E-05	1.27 E-05	0.0005

Additionally, δj^{msqr} calculation was taken into account for all the parameters indicated in Table 7-2, in which they are ranked based on their influence potency. Outcomes of the mean square

sensitivity analysis were then employed as parameters in BioWin®, which were ranked in terms of the order of δj^{msqr} value and the greatest factors. As seen in Table 7-2, the most influential parameter was ANAMMOX bacteria maximum specific growth rate, in which decreased values led to an immense impact on ammonia accumulation and restriction of nitrate production in the system, resulting in process suppression. Moreover, reducing the Y_{AAO}, by 50% led to 14.81% accumulation of ammonia and an increase of 43.26 mgN/L in nitrite concentration in the process effluent. Conversely, adjusting the substrate (NH_4) half-saturation constant from 2 mgN/L as the default value to 0.05 mgN/L as the models value resulted in a substantial decrease of effluent ammonia concentration of approximately 98.3%. Both substrate (NO2) half-saturation constant and nitrite sensitivity constant did not significantly affect the ANAMMOX UASB performance.

7.3.3. Statistical analysis

7.3.3.1. Curve fitting analysis

A curve fitting was employed to specify the model that best fits the specific curves in the experimental dataset. Fitted curves can be used to aid data visualization and summarize the relationships among the experimental and modeled NRE. Post-fitting diagnostics were completed to evaluate the validity of the performed models. The goodness-of-fit statistics presented helped with determining how well the resulting curve fits the data. The square root of the mean squared residuals (RMSE) and the adjusted R-square statistics calculations facilitated verifying the best fit. The goal of linking the available data to models via data fitting for NRE (Figure 7-5) was to determine the most rational demonstration of the process which has produced the presented experimental data (Jaqaman and Danuser, 2006). For data fitting analysis, NRE was selected as the main factor. The total nitrogen removal efficiency calculations incorporate all nitrogenous parameters available in the system, including the concentrations of ammonia, nitrite, and nitrate in the influent and effluent of the system. Since the developed models are approximations of the

experimental UASB system, more than one model may seem to fit the data to an acceptable degree (both Model I and Model III), however considering the R-squared and adjusted R-squared for Models #I and III (0.1848, 0.1797 and 0.898, 0.8974, respectively), the models were not as similar as they appeared. Correspondingly, the decent R-squared value for Model III signifies that this configuration can potentially explain a good proportion of the variability in the dependent variable. Figure 7-5 B shows a discrepancy in nitrogen removal efficiency results between the experiment and Model II in all operational phases. The data fitting analysis, indicates a high divergence among the measured and simulated numbers in the second model similar to the other simulations. The fitting analysis for Model II accounts for 18.25% of the variance, while Model III accounts for 89.80%. A positive correlation was found between the Model III and experimental NRE ($P < 0.01$). The low R-squared detected for Models #I and II are considered problematic for delivering fair predictions of the UASB-ANAMMOX system performance. To better assess the strength of the fit and understand how close the estimates are, the square root of the mean squared residuals (RMSE) was estimated for all three models. The fit standard error (RMSE) evaluated for Models #I, II and III (3.44, 6.2 and 1.69, respectively), indicated a close fit of Model III to the experimental data and the capacity to predict the system's responses. It is always expected to detect some unusual observations, which do not conform to the suggested curve fitting equation appropriately (Nurunnabi et al., 2016). The residuals analysis of all three models points out that the independent variables do not capture the entire deterministic component and that the residuals are consistent with random error. The residuals are not systematically high or low, and as observed, most of the residuals are arranged around the vicinity of zero all through the span of fitted values (Law and Jackson, 2016).

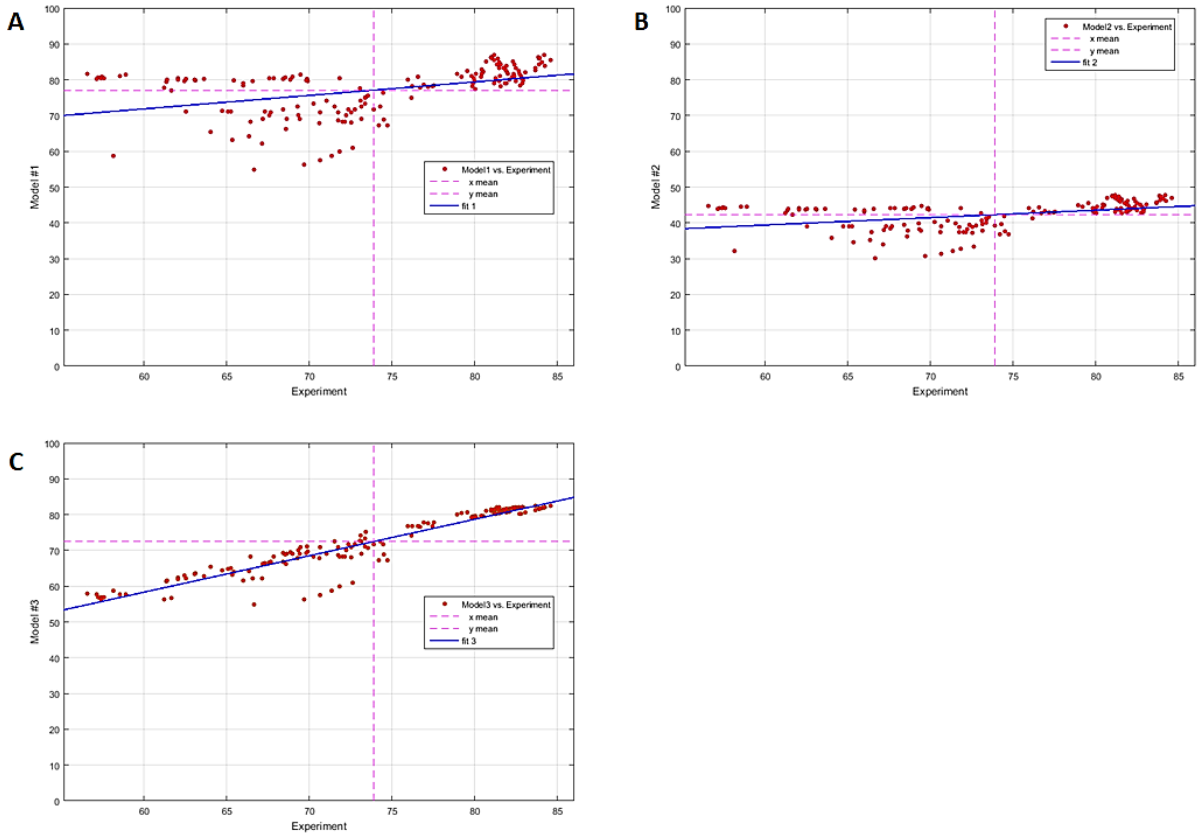

Figure 7-5 Curve fitting analysis: (A) Fitted line plot for experimental and Model I NRE, (B) Fitted line plot for experimental and Model II NRE, (C) Fitted line plot for experimental and Model III NRE

7.3.3.2. Significance testing

7.3.3.2.1. Two-sample t-test

A two-sample *t*-test (*t*-test 2) method was used to test whether the modeled and experimental data means are equal or not and identify if the difference between the two data sets is in fact, significant or if it is caused by random possibility. The performed *t*-test 2 returns a test assessment for a null hypothesis that the data in the two separate groups are from independent random samples and normal distributions with equal means and equal but unknown variances (Limentani et al., 2005). Additionally, the alternative hypothesis is that the data are from populations with unequal means. As shown in Table 7-3, the p-value is greater than the significance level for Model III (0.1145), the outcome is failing to reject the null hypothesis (h=0), indicating that the difference between

the population means is not statistically significant, and there is a good match between the data from the model and the experiment. As a result of the p-value being less than the significance level for Models #I and II in *t*-test 2 (Table 7-3), the decision is to reject the null hypothesis (h=1), leading to the conclusion that the difference between the population means in Models #I, II and the experimental data set is statistically significant. Moreover, the presented specific confidence intervals represent of the margin of error or the amount of uncertainty in the significance test. As seen in Table 7-3, considering that the ci range is bigger for Model I and II, the inherent uncertainties of using these sample data are also higher.

Table 7-3 Comprehensive results of three different hypothesis tests

***t*-test 2**					
	h (Hypothesis test result)	p (p-value)	ci (Confidence interval)	tstat (Value of test statistic)	sd (Standard deviation)
Model I vs. Experiment	1	1.0743e-04	-4.8107 -1.5965	-3.9218	7.3518
Model II vs. Experiment	1	2.7753e-144	30.2614 32.9496	46.2609	6.1488
Model III vs. Experiment	0	0.1145	-0.3473 3.2036	1.5825	8.1221
***ks*-test 2**					
	h (Hypothesis test result)	p (Asymptotic p-value)		ks2stat (Test statistic, nonnegative scalar value)	
Model I vs. Experiment	1	7.6691e-05		0.2469	
Model II vs. Experiment	1	7.2928e-73		1	
Model III vs. Experiment	0	0.0693		0.1420	
***var*-test 2**					
	h (Hypothesis test result)	p (p-value)	ci (Confidence interval)	fstat (Value of test statistic)	df (Degrees of freedom of the test)

Model I vs. Experiment	0	0.0909	0.9582 1.7813	1.3065	161
Model II vs. Experiment	1	1.1881e-18	3.1217 5.8034	4.2563	161
Model III vs. Experiment	0	0.3623	0.6351 1.1807	0.8660	161

7.3.2.2.2. Two-sample Kolmogorov-Smirnov test (Two sample ks-test)

The two-sample *ks*-test is one of the most valuable and universal nonparametric approaches for comparing two samples (Massey, 1951), returning a test decision for the null hypothesis that the data in two populations are from the same continuous distribution. Similar to *t*-test 2, the results for the *ks*-test 2 are illustrated in Table 7-3. Asymptotic p-value of the tests as indicated in Table 7-3, specifies the possibility of detecting a test statistic as severe as, or more intense than, the perceived rate in the null hypothesis (Marsaglia et al., 2003). The small p-value seen for Models #I and II leads to the conclusion that the models have different distributions compared to the experimental data set. In case of Model III results, p-value 0.0693 > 0.05, the null hypothesis is accepted (h=0). According to the test results, the difference between two samples (Model III and Experiment) is not significant enough to say that they have different distributions, so the model matches the measured data from the UASB-ANAMMOX system.

7.3.2.2.3. Two-sample F-test for equal variances (Two sample var-test)

A *F*-test is employed to test if the variances of two populations are equal or not. *var*-test 2 responds with an assessment for the null hypothesis that the data in two samples come from normal distributions with the same variance, yet the alternative hypothesis is that they come from normal distributions with different variances. Examining the result in Table 7-3 from *var*-test 2, shows a slightly different pattern than the other hypothesis tests defined before. As seen in the results, both Models #I and III fail to reject the null hypothesis (h=0), so both configurations are a decent match

to the experimental data. However, on the other hand, Model II results show a rejection of the null hypothesis (h=1) (Table 7-3), indicating a significant difference between the two data sets. Looking into the p-values for Model I and III, a considerable difference is evident. As small values of p may cast doubt on the validity of the null hypothesis, the match between Model III and the experiment is more reliable. On the other hand, the Model II differences are highly significant ($p = 1.1881e\text{-}18 < 0.01$), indicating the poor predictability of the model configuration. Considering all three statistical analysis results, it was proven that Model III was the best configuration simulating the experimental UASB-ANAMMOX system.

7.4. Conclusions

Three different mathematic models simulating the performance of micro-granule-based ANAMMOX UASB reactor were developed following the BioWin® principals. One of the long-term dynamic calibrated models (Model III) could project the day-by-day effluent data precisely for the duration of all operational conditions. The model estimated the effluent data for all three phases with a MRE of approximately 1.96, 4.36, and 2.54 % for NRE, NRR, and NLR, respectively. All BioWin® models were calibrated and validated to have a good representation of the UASB-ANAMMOX system that receives high-strength ammonium wastewater. To acknowledge the most influential parameters, a sensitivity analysis using six kinetic and stoichiometric parameters of AAOs went through ±50% shift from their default and literature-based model values in BioWin®. Fundamental values of the kinetic and stoichiometric coefficients were integrated in the BioWin® software, and the adjusted ones according to the outcomes of the experimental studies, were employed for the calculations. The results collected from simulation runs of Model III were comparable to those acquired from the experiments, which confirmed the feasibility of achieving ANAMMOX process in a UASB system setup.

Additionally, several hypotheses and significance testing were performed to confirm the efficiency of the different model configurations. The test of significance showed that the difference between the Model III mean/ variance and the Experimental mean/variance was not statistically significant, indicating the model's success in predicting the experimental data. The Model III stated in this study is appropriate for the conditions mentioned, nonetheless, the methodologies can be beneficial for user-specific conditions and distinct data collections. Upcoming advances should focus on the biological viewpoint of modeling wherein the process performance is mathematically linked to microbial diversity and activity.

CHAPTER 8

Parin Izadi[a] , Parnian Izadi[a] , Ahmed Eldyasti*[a]

[a] Civil Engineering, Lassonde School of Engineering, York University, 4700 Keele Street, Toronto, ON, Canada , M3J 1P3* Corresponding author

Authors' contributions Parin Izadi and Dr Eldyasti contributed to the study concept and design. Experimental and methmatical system setup, material preparation, data collection and experimental and statistical data analysis were performed by Parin Izadi and Parnian Izadi. The first draft of the manuscript was written by Parin Izadi and Parnian Izadi commented on previous versions of the manuscript. Dr. Ahmed Eldyasti prepared the final submitted draft and critically revised the work. All authors read and approved the final manuscript.

Experimental and Modelling Perspectives of Gradual Development and Sustainment of a Single-Stage Mainstream ANAMMOX

Abstract

Application of ANAMMOX-based processes for mainstream municipal wastewater treatment is an ongoing challenge because of the elevated COD/N ratios, stringent temperature constraints, low bacterial growth rates, and competition from heterotrophic denitrifiers. Thstudy aimed to investigate the potential operation of an Upflow Anaerobic Sludge Blanket (UASB) reactor treating a low-strength synthetic influent for more than 500 days, at temperatures as low as 15 °C, from both experimental and mathematical modeling standpoints. The long-term effects of gradual N-load and temperature decrease on ANAMMOX activity were assessed, in which the operation of a lab-scale UASB reactor was divided into two main periods. Moreover, a nitrogen loading rate as low as 0.18 KgN/m^3/day with 0.43, 0.31, and 0.14 KgN/m^3/day of nitrogen removal was achieved at 35, 25, and 15 °C treating the low-strength synthetic influent. Furthermore, to stimulate the autotrophic denitrification at 15 °C, the effects of injecting 15 and 30 mg/L of a Sulphur salt as a source of electron donor were evaluated, and an evident 26-46% increase in nitrogen removal was detected. Coupling between ANAMMOX and sulfide-dependent denitrification may play a substantial role in improving the startup, implementation, and performance of the mainstream ANAMMOX process.

Keywords

Autotrophic nitrogen removal; ANAMMOX; Mainstream; Gradual development; BioWin®

8.1. Introduction

ANAMMOX, microbial anaerobic ammonium oxidation, discovered in the 1980s (Cao et al., 2017), has been projected to be a prospective sustainable alternative technology for nitrogen removal from municipal wastewater (Du et al., 2020). As a result of outstanding energy-saving

potentials, autotrophic ANAMMOX-based processes have been the center of attention for the recent decade (Y. Miao et al., 2019). The three main advantages of ANAMMOX-based nitrogen removal pathways include 60% decrease in oxygen demand, about 100% cutback of carbon requirement, and 80% less excess sludge production (Daigger, 2014). Up to now, studies generally reported ANAMMOX-related processes being applied in high-strength wastewater streams with temperatures above 25°C and elevated influent nitrogen levels of greater than 0.1 gN/L (Lotti et al., 2015), such as sludge digester's effluent, industrial wastewater and landfill leachates (Pijuan et al., 2020). There are over hundred full-scale sidestream ANAMMOX-based installations worldwide, treating anaerobic digestion reject water (Erdim et al., 2019). The triumph of ANAMMOX-based nitrogen removal in the sidestream sector urges further investigation of the potential applications in mainstream municipal wastewater (X. Li et al., 2018). However, despite the numerous attempts on implementing ANAMMOX in mainstream processes to accomplish maximum efficiency and reach an energy-positive wastewater treatment plant (Reino et al., 2018), the application continues to be a fundamental challenge, prompting an attractive and growing research topic (X. Li et al., 2018). Therefore, reaching a stable, high efficiency, and long-term mainstream ANAMMOX process is of great interest.

Countless efforts have targeted mainstream ANAMMOX-based technologies in recent decades to deduct the prospective energy costs and move towards energy positive plants (Laureni et al., 2016d). Despite all attempts and activities, there are still a number of challenges linked to mainstream ANAMMOX application including, low nitrogen removal rates, reduced nitrogen concentrations and inconsistent loads, lowered temperatures, presence of chemical oxygen demand (COD), competition with other bacterial communities, strict effluent qualities and long-term process stability (Pijuan et al., 2020). One important factor affecting the successful operation of

mainstream ANAMMOX process is biomass availability (X. Li et al., 2018). Despite the success of suspended sludge in full-scale sidestream implementations (Joss et al., 2011), decreased net biomass production and critical biomass washouts were spotted in mainstream conditions, potentially due to the absence of efficient separation strategy for slow-growing bacterial groups present in the system (Laureni et al., 2015). The path taken to overcome this challenge is adopting granule/biofilm-based structures in a system with high solids retention time and increased biomass concentration (X. Li et al., 2018). A comprehensive overview of the microbial communities and the structure of the aggregates can troubleshoot and improve the system operation (Laureni et al., 2016d). The microbial community and biomass granulation are primarily affected by the reactor configuration, operational modes, and influent characteristics (Izadi et al., 2020a). Occurrence of ANAMMOX granules/biofilm biomass have been identified in different bioreactor configurations comprising of upflow anaerobic sludge blanket reactor (UASB), sequential batch reactor (SBR), moving bed biofilm reactor (MBBR), dynamic membrane bioreactor (DMBR), and rotating biological contactor (RBC) (Xu et al., 2015a). In the UASB reactor, efficient biomass accumulation is accomplished because of the successful sludge granulation procedure (Jin et al., 2007). Granulation has been perceived as a critical element in the ANAMMOX process (Bagchi et al., 2010). UASB reactor design elements demonstrate certain qualities such as the capacity to cope with extreme influent substrate loadings, the ability to perform under decreased hydraulic retention times (HRT), and contain significant volumes of granular biomass. When comparing UASB reactor configuration with flocculent sludge-based systems, good settling ability and resistance to fluctuating operating conditions are two of the most highlighted elements (Xing et al., 2014). As a result of high shear forces in UASB systems, the granules are physically broken into smaller-sized aggregates with enhanced mass transfer. ANAMMOX bacteria form robust

micro-colonies, similar to other slow-growing communities, balancing the microbial ecology and nutrient removal from wastewater (Izadi et al., 2020a).

Most bacterial populations acclimatize a range of fluctuating situations and stresses in the environment to endure and reproduce (Berry and Foegeding, 1997). However, a key unanswered inquiry is how bacterial communities within complex populations react to gradual or sudden environmental alterations, such as substrate reduction (Scheuerl et al., 2020). The constrained availability of substrates combined with low temperatures results in a slower growth rate of most bacterial groups. Different bacterial communities use distinctive approaches to conquer this state of hunger, yet there is still a lack of attention to this constant struggle for feed source (Egli, 2010). Substrate concentration is recognized as an essential factor manipulating the startup process and granulation procedure via the selection and development of various bacterial groups (Tay and Yan, 1996). For better comprehension of bacterial growth and performance under distinct environmental conditions, research can potentially reflect on this topic from two routes: one would be designing specific laboratory experiments and examining the growth kinetics and physiology under outlined circumstances. Other would be working on mathematical simulation of complex environmental compartments with defined bacterial populations and substrates levels. One important factor to keep in mind is that bacterial communities are much more resistant in their stationary/slow growth phase rather than the exponential/fast growth period (Berney et al., 2006). As a result, the sludge collected for mainstream ANAMMOX startup is more suitable to be from a long-term, stabilized, and high-efficiency sidestream process.

Due to the extreme challenges and the slow growth rates of the ANAMMOX bacterial population in mainstream conditions, experimental approaches for process optimization can be extremely time-consuming (Li et al., 2019). A practical method for process evaluation in varying conditions

is mathematical modeling. Mathematical simulation methods and extended advancements functioning based on the actual operational data are an excellent approach to enhance the technical design and optimization during which the additional expenses and risks are being prevented (Ji et al., 2019). There is a broad understanding that the advancement of mathematical models leads to a more comprehensive interpretation of ANAMMOX process dynamics, offering optimization prospects and potential system performance improvements (Lauwers et al., 2013). Recent studies focused on using mathematical models to simplify the perception of the biological nutrient removal process (Elawwad, 2018). Subsequently, researchers established several different computer software packages to replicate a distinctive range of wastewater treatment processes. Numerous simulator packages are represented for wastewater treatment, yet BioWin® is known as one of the most acknowledged simulators in North America, established by EnviroSim Associates Ltd (Yang et al., 2019). Among all available packages, BioWin® has been the most extensively exercised software in wastewater treatment plants (Ji et al., 2019). BioWin® activated sludge models (ASM) contain numerous practical aspects, including pH modelling, which facilitates complex wastewater treatment systems (Elawwad, 2018). There are a number of research focused on BNR optimization in municipal wastewater treatment plants (Al-Omari et al., 2015; Brdjanovic et al., 2007; Elawwad et al., 2017; Moussa et al., 2004). Yet, there is a lack of studies which have used ASM models to optimize complex BNR processes (Elawwad, 2018), such as ANAMMOX to assess the competency of activated sludge modeling to improve the performance of ANAMMOX-based systems. The literature review indicated very limited publications implementing BioWin® for anaerobic wastewater treatment processes, such as ANAMMOX.

The main goal of this study was to exhibit an innovative and economical solution for the gradual adjustment of a sidestream single-staged ANAMMOX UASB process towards mainstream

conditions. With the aim of mainstream ANAMMOX process efficient and stable implementation, this study focused on both experimental and mathematical evaluation of gradual transition from sidestream nitrogen levels to low-strength nitrogen concentrations, with decelerated biomass acclimation and temperature decrease. Based on these results, the dynamic response of ANAMMOX bacterial community to diminished ammonium and nitrite concentrations was analyzed. Cold temperature can intensely distress the microbial activity in ANAMMOX systems and alter nitrogen species equilibrium. A proper equilibrium leads to successful nitrogen removal in ANAMMOX-based systems, and the temperature reduction may cause loss of balance. Results of a study by (Straka et al., 2019) propose that reaching a cold (< 15 °C) mainstream wastewater from warm sidestream ANAMMOX obliges significant volumes of biomass and/or extended retention times to indicate any activity. The ANAMMOX seed culture assessed in this research was collected from a sidestream ANAMMOX UASB-reactor system sustained at a temperature ranging from 25 to 30 °C for over 500 days, in which the optimal growth temperature would potentially be in this span. Considerable cold adjustment of ANAMMOX biomass was further investigated in both the experimental system and BioWin® model. Not much research has been carried out to the best of our knowledge, focusing on mathematical models development, calibration, and performance in ANAMMOX-based processes. The results indicated a suitable match between the model and experimental data in higher temperatures, and a more evident discrepancy was observed in lower temperature levels. Further extrapolation was completed to elucidate the biomass and time constraints for ANAMMOX process at mainstream level temperatures.

8.2. Materials and Methods

8.2.1. Experimental setup

The schematic of the experimental setup is presented in Figure 8-1 A. The 4.8 L single-stage continuous-flow lab-scale UASB reactor was continually injected with synthetic wastewater and controlled at a temperature around 35 ± 0.5 °C, to represent sidestream ANAMMOX process environment. The system had an average HRT of 24 hours, and the mean SRT of the reactor was contained at about 35-70 days from top to bottom section. Mixing within the reactor was accomplished by peristaltic pumps, leading to an average upflow velocity of 0.5-0.6 m/h and a sludge bed height of 85-90 % of the height to the gas collector (Izadi et al., 2020a). The ammonia and nitrite levels in the reactor were based on the experimental design with influent ammonia and nitrite concentrations of 125.6 mgNH_4-N/L and 266.5 mgNO_2-N/L. The pH of the influent was maintained at an average amount of 7.9. The initial biomass for seeding the ANAMMOX UASB reactor was obtained from the Humber treatment plant (Toronto, ON, CA). As indicated in Table 8-1, total and volatile suspended solids levels were 21840 and 16650 mg/L along with pH and alkalinity of 6.9 and 1460 mg$CaCO_3$/L, respectively. Ammonium and nitrite were included in the synthetic media as $(NH_4)_2SO_4$ and $NaNO_2$, correspondingly, with varied concentrations during the experiment. A full description of the mineral medium composition is indicated in Table 8-1.

The sidestream UASB-ANAMMOX reactor had high efficiency and stable performance for over 200 days. For the stable sidestream phase of reactor operation, the influent's components and nitrogen-based constituent's levels were adapted to attain a molar nitrite: ammonia ratio of 1.14 to 1.3. The average NRE achieved 91.6%, while the NRR was approximately 0.18 KgN/m^3/d. In parallel, NO_3^- started to accumulate in the effluent of the reactor, yet the ratio was lower than the process stoichiometry, which implies the development of autotrophic denitrifiers in the system (Izadi et al., 2020a). Both ammonia and nitrite removal efficiencies in the course of all sidestream

phases of process reached above 90%. Evaluation of the granules size distribution in sidestream process operation, suggested growth in the particle size and an increase in the micro-granulation progression. The system operated for over 320 days overall led to a 4.5 ± 0.67% increase in the percentage of *Planctomycetes,* which are the main phylum responsible for anaerobic ammonia removal (Izadi et al., 2020a). The initial sludge for mainstream ANAMMOX process initiation was a mature micro-granular sidestream ANAMMOX sludge cultivated in a UASB system. The final 600 days of operation of the reactor in which mainstream conditions are gradually implemented are discussed in the results and discussion section of the manuscript, and the full experimental period detailed data are represented in the Supporting data file. Initially, the reactor's nitrogen load was declined on a step-wise basis, dropping from an initial load of 1.2 KgN/m3/day to an average final load of 0.18 KgN/m3/day. After system stabilization in low-strength nitrogen levels, the temperature was gradually decreased from 35 °C to 15 °C.

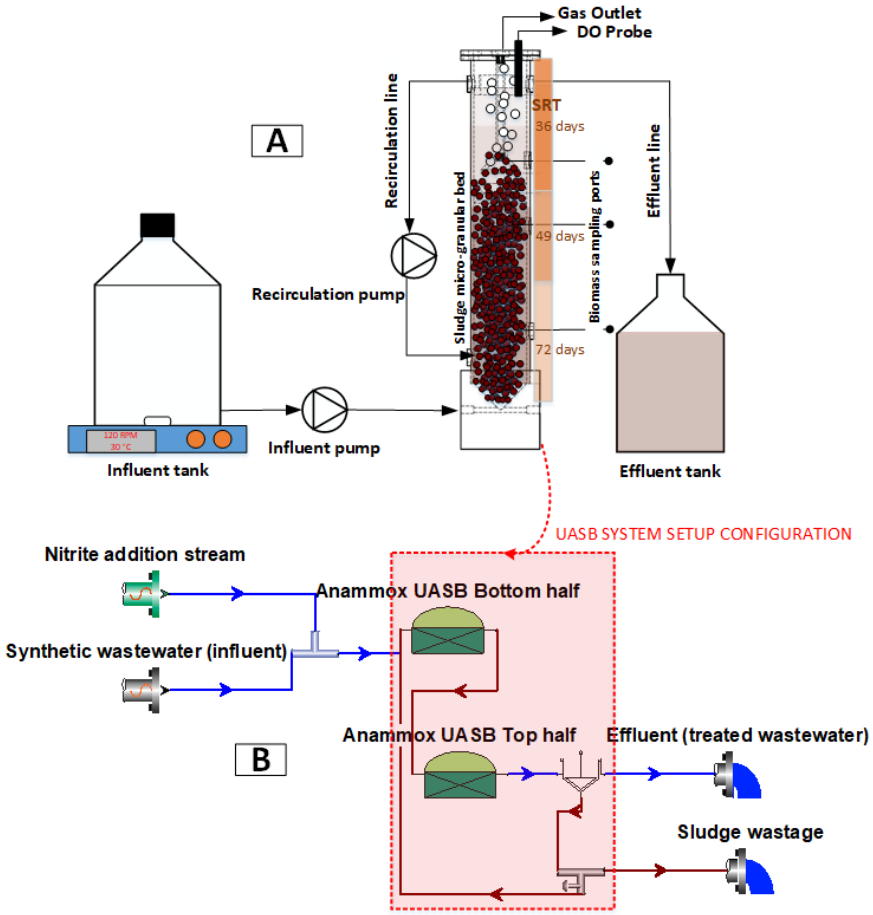

Figure 8-1 A) Schematic layout of the continuous UASB-ANAMMOX reactor experimental setup, B) BioWin model configuration used to simulate UASB-ANAMMOX sidestream and mainstream conditions

8.2.2. Model setup

As shown in Figure 8-1 B a dynamic model for the biological process was developed using BioWin® 4.1 software, a semi-open platform software that permits the operator to insert the model equations and parameters. As demonstrated in Figure 8-1 B, the UASB reactor design is principally considered by an anaerobic digester component connected to a point settler to mimic the flow state of the fluid. The underflow rate of the point settler was adjusted to allocate a relatively high recirculation ratio in the UASB. Several kinetic parameters were modified for anaerobic ammonia-oxidizing bacteria (AAO), consistent with the experimental data. Additionally, few influent fractions were adapted to represent the synthetic feed's characteristics (Chapter 7).

8.2.2.1. Model calibration and sensitivity analysis

The calibration process was completed via BIOMATH calibration protocol (Corominas et al., 2011), where the classification of main goals is a fundamental element in process modeling practice (Vanrolleghem et al., 2003). This particular procedure consists of four steps applied for a range of activated sludge-based models (Chapter 7) (Makinia, 2010). The primary stage is outlining the main objectives of the modeling practice. The fundamental aim of this analysis was to replicate the experimental data of the single-stage UASB-ANAMMOX process, generate a simulation logically fitting the gathered experimental data, and theoretically have the capability to explain the long-term dynamic behavior ANAMMOX-UASB system in mainstream conditions . The second stage of the calibration is delegating a structure for the design, operational and measured data to stipulate the system configuration. All samples were collected daily and were instantly analyzed according to the standard methods of water and wastewater examinations. For the third part of the procedure, the model is calibrated to characterize the mean effluent concentrations and sludge waste data, supposing that this average exemplifies a steady-state condition for the process (Makinia, 2010). For this step, an inclusive mass balance was conducted to eliminate potential errors and imprecisions and to develop a holistic overview of the ANAMMOX-UASB system arrangement. For the final phase of the calibration protocol, the operational calibration of the sludge model is employed to match the developed model to the available experimental data (Chapter 7).

In a thorough sensitivity analysis, a fundamental perception of the most influential parameters with higher values was developed. Subsequently, the calibration of the model was achieved thru modifying the parameters and fitting the model to the available dynamic data collected from analytical measurements. Selecting the correct sensitive parameters is a fundamental step in model

calibration and validation. In this study, the sensitivity analysis was fulfilled by pinpointing six of the most dominant kinetic and stoichiometric parameters for the ANAMMOX bacterial population and three key outputs of the process: effluent ammonia, effluent, effluent nitrite, and nitrate concentrations (Soliman and Eldyasti, 2017). Based on the standard sensitivity analysis method as shown in Equation *8-1*, Si, j, denotes the impact of a particular factor on a distinct water quality value (Ji et al., 2019). The sensitivity analysis procedure respected several collective specifications, such as the point that the system output (Yi) was sufficiently receptive to the parameter (Θj) alteration. The sensitivity measure δj^{msqr} (Equation *8-2*) aims to assess particular parameter significance in a least- squares parameter estimation context, where it ascertains the mean sensitivity of the model output according to any variation in the parameter Θj (Brun et al., 2002). The concept behind sensitivity evaluation is that the larger the value, the more the impact of the parameter on the model result (Ji et al., 2019).

$$S_{i,j} = (|\Delta Y_i/Y_i|)/(|\Delta X_i/X_i|)$$

(Si, j: Normalized sensitivity coefficient, Xi: Input values)

Equation 8-1

$$\delta j^{msqr} = (1/n\ (\sum_{i=1}^{n} S^2_{i,j}))\ ^{\wedge}1/2$$

(δj^{msqr}: Mean square sensitivity measure)

Equation 8-2

Table 8-1 Operational data for the experimental UASB-ANAMMOX system setup

Synthetic feed composition (g/L)		
	$NaHCO_3$	0.420
Inorganic Solution	$CaCl_2.2H_2O$	0.18
	$MgSO_4$	0.059
	KH_2PO_4	0.027
	EDTA	5

Trace Elements Solution	$FeSO_4$	5
	$CuSO_4•5H_2O$	0.25
	$ZnSO_4•7H_2O$	0.43
	$NaMoO_4•2H_2O$	0.22
	$MnCl_2•4H_2O$	0.99
	$NiCl_2•6H_2O$	0.19
	$CoCl_2•6H_2O$	0.24
	$NaSeO_4•10H_2O$	0.21
	H_3BO_4	0.014
Seeding sludge		
Total suspended solids (TSS) (mg/L)		21840
Volatile suspended solids (VSS) (mg/L)		16650
pH		6.9
Alkalinity ($mgCaCO_3/L$)		1460
Total chemical oxygen demand (TCOD) (mg/L)		24280
soluble chemical oxygen demand (SCOD) (mg/L)		1700
Process operation parameters		
Controlled		**Monitored**
Ammonia load	0.25-0.75 $KgNH_4$-N/m^3.day	Dissolved oxygen 0.08-0.1 mg/L
Temperature	25-35°C	pH 7.8± 0.3
HRT	24 Hours	
SRT	36-72 Days	
Feed nitrite/ammonia	0.84-1.32 (~1.2)	

8.2.3. Analytical methods

The influent and effluent samples were collected daily and were analyzed instantaneously (All samples were collected in triplicates). Water samples were analyzed based on the standard methods of water and wastewater examination. Simultaneous determination of anions and cations were implemented through ion chromatography (IC) by the Thermo Scientific™ Dionex™ Integrion™ HPIC™ system. In advance of all IC measurements, samples were diluted adequately with deionized water and passed through a membrane filter (0.45 µm). Further analytical determinations (e.g., pH, TSS, VSS, Alkalinity, etc.) were conducted according to Standard Methods (APHA, 2005). The biomass concentration was indicated as suspended solids (SS) and volatile suspended solids (VSS). To monitor the anaerobic environment required for ANAMMOX bacterial

community, dissolved oxygen (DO) was measured using an IntelliCAL LDO Lab Probe (HACH Company, Loveland, Colorado, USA) (Izadi et al., 2020a).

Nitrogen loading rate (NLR), nitrogen removal rate (NRR) and nitrogen removal efficiency (NRE) were calculated based on the nitrogen balance and stoichiometry according to Equation *8-3*, Equation *8-4*, Equation *8-5*. It was presumed that nitrogen is primarily removed by the ANAMMOX reaction, however since alkalinity was available in the system and based on nitrate/ammonia ratio coupled with the microbial community analysis, autotrophic denitrification could have a potential contribution (Wang et al., 2017).

$$NLR = TN_{in}/HRT$$

Equation 8-3

$$NRR = \Delta N/HRT$$

Equation 8-4

$$NRE = \Delta N/[NH_4^+\text{-}N]_{in}$$

Equation 8-5

For ANAMMOX culture cultivation verification, samples (triplicates) were collected and examined by PCR (RNA was extracted, amplified using PCR, then the outcomes were exposed to gel electrophoresis to verify the presence of ANAMMOX bacteria). The intensity of the bands can be linked with the genomic density of the objective gene in the initial sample. Particular primer sets aiming for the 16S rRNA for both the subjected bacteria type were exercised, and comprehensive explanation for the sequence of the primers, the target genus and the methods pursued throughout the molecular biology analysis are presented in the Appendix (A4) data file. The adequate amplification of the targeted bacterial RNA proves the existence of the studied

bacterial family. An inverted microscope (BioImager, ON, Canada) with a 2.5× objective and 10× objective was employed. The microscope was arranged with a camera (SN 14120187, Point Gray Research Inc. Canada), and a computer in which the recorded images and videos were saved for further evaluation. Scanning electron microscopy was employed for more interpretation of the growth and arrangement of micro-granules. The samples for SEM were set by fixing with 5% glutaraldehyde in 0.1 M phosphate buffer at pH 7.2 at 4°C. Subsequently, the samples were rinsed in a buffer three times followed by post-fixation in 1% Osmium tetroxide; they were then washed twice in distilled water. The samples were dehydrated with 35%, 50%, 75%, and 95% ethanol and then submerged in tetramethylsaline for 10 minutes. The samples were then dried at room temperature for 24 hours. Dried samples were coated with platinum to make them electrically conducting and avoid space change influence during SEM. Then, the SEM micrographs were taken with a scanning electron microscope (Thermo Fisher Quanta 3D electron microscope, York University, Ontario, Canada). The particle size distribution was quantified using a laser light diffraction particle size analyzer (LS 230, Coulter-Beckman, Germany). Particle size dimensions fluctuate from 0.017 μm to 2000 μm, using the Polarization Intensity Differential Scattering (PIDS) technology.

Primary data analysis for examining the disparities in performance among the modeled and experimental data was achieved by Matlab R2015a (MathWorks, USA), which has not been previously used for statistical analysis based on the literature ANAMMOX-based systems . The statistical software package Matlab 2015a was utilized to design fitting analysis and hypothesis testing of the experimental and modeled data. For the statistical analysis, the t-test (for two groups of samples) was employed with Matlab® Statistics and Machine Learning Toolbox™ to assess the

significance of differences in efficiency, performance, and fit between models. The significance level of probability (p-value) was 0.05 in this study.

8.2.4. Ex-situ autotropic ammonia removal bacteria activity evaluation

BOD Trak II was used to run the batch tests on ANAMMOX activated sludge. All batch tests were conducted and analyzed in triplicates. The batch test bottles were sealed to prevent external atmospheric pressure changes in the test. Additionally, in gas-tight batch reaction vessels, pressure increases due to dinitrogen gas release, which is censored over time to quantify the reaction kinetics. Two alternatives were considered to track the evolution of the ANAMMOX process: Chemical tracking, which is done by assessing the ammonium, nitrite and nitrate concentration in the specific time, and manometric tracking by assessing the overpressure caused by dinitrogen release in a gas-tight reactor. Before after the tests, the pH was measured and a liquid sample was collected for analysis. The pH was kept within the range of 7.6-8.0 and adjusted after each test. Bicarbonate salt ($KHCO_3$) was added, if necessary, to guarantee a sufficient inorganic carbon amount required for the anabolic pathway of the ANAMMOX reaction.

8.3. Results and discussion

8.3.1. Gradual decrease of nitrogen load in the experimental setup

As previously stated by Izadi et al. (2020), the lab-scale sidestream UASB system was formerly operated at high temperatures (~35 °C), treating a high-strength synthetic influent for 317 days. A stable operation with high nitrogen removal rates was achieved for more than 200 operating days. Afterward the nitrogen load to the reactor was gradually lowered in 550 days to reach an influent ammonia and nitrite concentrations of 21.8 mgNH_4-N/L and 16.3 mgNO_2-N/L. Each influent load drop was controlled to minimize the diverse effects of low substrate availability on the bacterial consortium and sufficient time was provided for the biomass to acclimatize to the new environment before shifting to a new N-loading rate. The reactor's performance in different N-loads was studied

in four main phases; Phase I (NLR~1.2 KgN/m^3/day), Phase II (NLR~1.0 KgN/m^3/day), Phase III (major NLR drop from ~1.0 to 0.3 KgN/m^3/day), Phase IV (NLR~ 0.2 KgN/m^3/day). The final phase of operation was maintained for more than 400 days, with a reasonably steady performance in terms of NRE (Figure 8-2 A), up until the stage where the influent ammonia concentration was dropped below 21.8 mgNH_4-N/L. Decreasing the N-load to points lower than 0.2 KgN/m^3/day after day 96 (Figure 8-2 A), resulted in a reduction of NRE (from an average of 78% to 51%). N-load reduction had significant impacts on ammonium, nitrite, and total nitrogen removals, reaching a level of approximately 72.6 ± 1.5%, 76.9 ± 3.1% and 50.7 ± 4.8%, respectively, based on the outlet ammonium, nitrite, and nitrate concentrations. At mainstream line conditions applied to the system, the low-strength nitrogen concentrations and the significant variations affected the microbial activity and dynamics. Unanticipated inconsistency in long-term operations under low-strength ammonia nitrogen wastewater treatment (seen in Figure 8-2), in mainstream ANAMMOX-based processes, depict a massive setback to process performance, efficiency and operation. Although NRR was declined during the transient NLR shock period in Phase III of UASB operation, the NRE in addition to ammonia and nitrogen removals (Figure 8-2 A and C) showed a robust resisting shock load capability in the reactor. On the other hand, in the final period of Phase IV, high effluent NO_3^--N concentration limited TN removal performance of the reactor, resulting in a major drop in NRE (Figure 8-2 A).

The nitrogen removal rates in the UASB were less stable in Phase III and IV, while the step-wise decrease in nitrogen load significantly lowered the efficiency of the system. Figure 8-2 shows the performance of the laboratory-scale UASB in different N-loads. As indicated in Figure 8-2 A, N-load decrease from 1.2 to 0.2 KgN/m^3/day resulted in a marked drop of the overall nitrogen removal rate in the UASB from 0.9 to 0.1 KgN/m^3/day in approximately 500 days. However, the

observed impacts on the performance in terms of ammonium and nitrite nitrogen removals as indicated in **Figure 2-C**, were less significant reaching a minimum level of about 72% in the final portion of Phase IV. Results from analyzing nitrate, nitrite, and biomass concentration variations in the bioreactor imply that nitrate production in the initial phases of operations is directly connected to the level of residual nitrite in the bioreactor. The yield of NO_3^- production over nitrogen consumed increased from Phase I to IV, reaching a level of 30 ± 5%. Primarily, in the sidestream ANAMMOX period, the calculated ammonia to nitrite and nitrate ratios were 1.135 and 0.152 g N. g N^{-1}, respectively, where the stated values were not the same as the referenced stoichiometry (Van Loosdrecht et al., 2016).

Given that ammonium sulfate was injected into the system as the process substrate, an adequate dose of sulfur was present for nitrate reduction to nitrogen gas via autotrophic denitrification pathway by *Thiobacillus* genera. Potential simultaneous occurrence of autotrophic denitrification is also indicated by nitrite and nitrate ratio in the process effluent. As stated by the stoichiometry of S-based autotrophic denitrification, reduction of 1 mgN-NO_3 utilizes 3.36 mg/L of alkalinity as $CaCO_3$, the prospective stimulus of alkalinity drop in the UASB reactor (Izadi et al., 2020a). The nitrate production rate normalized by the ammonia level in the reactor demonstrates an increasing trend, suggesting that the autotrophic denitrification in the reactor is partially inhibited due to lower ammonia levels and decreased nitrite availability in the reactor. In parallel, **Figure 2-B** shows a somewhat steady alkalinity level in Phases I, II and III, however, there is a gradual increase in both alkalinity and pH in the system in the final portion of Phase IV. The increase in alkalinity in Phase IV also proves the suppression of autotrophic denitrifiers in the system, since, in the autotrophic denitrification pathway, Sulphur is the electron donor for the microorganisms, and calcium

carbonate acts as a neutralizing agent for protons released in microbial respiration (Lewandowski et al., 1987) (Izadi et al., 2020a).

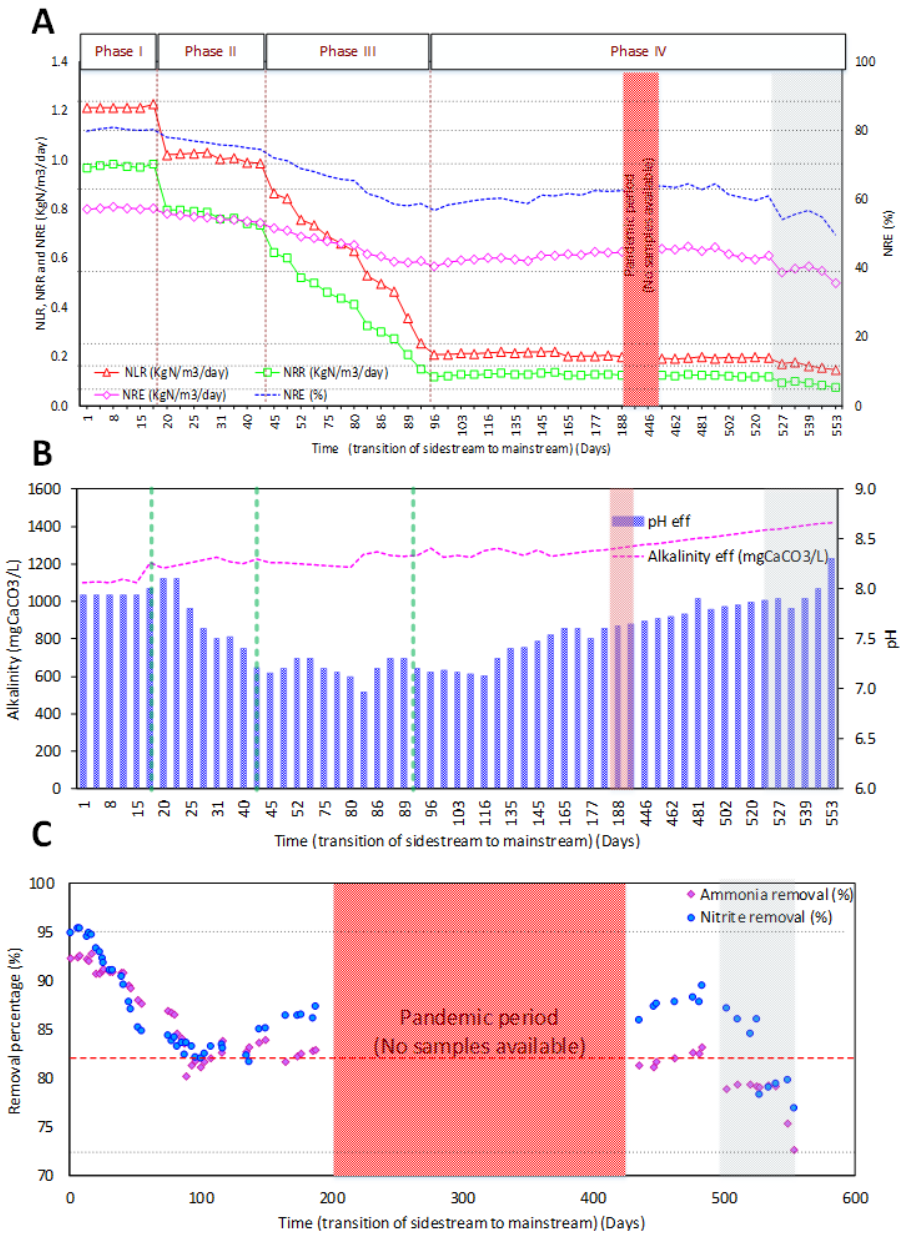

Figure 8-2 UASB performance in different N-load: A) NLR, NRR and NRE in four phases of system operation, B) pH and alkalinity variations, C) Ammonia and nitrite removal rates (the days in this figure signify the days of operation after the sidestream transition to mainstream)*

8.3.2. Gradual decrease of nitrogen load in the BioWin setup

Mathematical models, including BioWin models, propose a valuable means to study the microbial population and coexistence in multispecies consortiums, including ANAMMOX metabolism (Mattei et al., 2015). To assess the calibration of the Biowin model and validate the data, the simulated values are compared to the measured data from the effluent. If the simulation is effectual, there will be no significant statistical divergence between simulated and measured values of the examined variable (Liwarska-Bizukojc and Biernacki, 2010). The simulated and measured data of the fundamental output variables illustrating the effluent quality are reported in Figure 8-3. A complete description of the model development, validation, calibration and sensitivity analysis is included in a previous chapter (Chapter 7). Figure 8-3 A indicates both experimental and modeled NRE and NRR trends, with an equal NLR. The modeled and experimental NRE's were comparable in Phases I and II of reactor operation (mean NRE of 89-90%.), where the NLR was between 1.0-1.2 KgN/m^3/day. The gap between the measured NRE and the simulated NRE initiated when the NLR was pushed down to below 0.8 KgN/m^3/day in Phases III and IV, reaching a mean absolute percentage error (MAPE) of ~18%. As shown in Figure 8-3 A, the major divergence between the model NRE and the experimental NRE occurred in a NLR ranging between 0.21-0.15 KgN/m^3/day. MAPE is an example of regression quality measure, which statistically assesses the predicting accuracy of a modeling system.

Balance of different existing microbial populations and their activities is decisive for a durable and practical process (Jia et al., 2019). The nitrate concentration in the effluent of the process was considerably different in the experimental setup compared to the simulation results (Figure 8-3 C). A two-sample *t*-test (*t*-test 2) method was employed to assess if the means of the simulated and experimental data are the same or not and detect whether the divergence among the two data

collections is substantial or it is originated from unsystematic probability. The performed t-test 2 generates a test evaluation for a null hypothesis that the data in the two distinct sets are from independent random tests, normal distributions with equal means, and equal but unknown variances (Limentani et al., 2005).

Furthermore, the alternate hypothesis is that the data are from classes with disparate means. With a p-value smaller than the significance level for the *t*-test 2 (1.6821e-101), the conclusion is to reject the null hypothesis (h=1), resulting in the supposition that the divergence amongst the data sets means in the model, and the experiment is statistically significant. The model failed to predict the autotrophic denitrification co-occurrence with anaerobic ammonia oxidation in the UASB reactor, resulting in contradictory NREs in Phases III and IV of reactor operation. Sulphur-oxidizing autotrophic denitrification is carried out via several categories of inorganic Reduced-Sulphur compounds being the electron donors and energy sources of the process to ultimately reduce the oxidized inorganic nitrogen constituents (mainly nitrate and nitrite) and fix carbon dioxide for bacterial growth (Cui et al., 2019). The highest autotrophic denitrification activity was stated to occur at a pH range of 7.0–8.0 (Figure 8-3 B), while the ideal temperature for the majority of Sulphur-oxidizing autotrophic denitrifiers is about 25~35 °C (Table 8-1) in mesophilic environmental circumstances (Fajardo et al., 2014). The influent Sulphur/Nitrogen ratio has a strong impact on the denitrification reaction and bio-products, wherein Phases III and IV (Figure 8-3 A) with reduced N-load, the imbalanced S/N ratio resulted in a less effective autotrophic denitrification occurrence in mainstream-UASB setup. As Figure 8-3 C illustrates, there is a fair match between ammonia and nitrite removal efficiencies in the experimental setup and the modeling data, however, after day 89, in which the NLR drops down to below 0.2 $KgN/m^3/day$, the gap between the experimental values and modeling data start to increase. The MAPE between

the experimental and modeled ammonia and nitrite removal efficiencies reached a maximum level of 54.84% and 46.65%, respectively. Anaerobic ammonia oxidizers and autotrophic denitrifying bacteria are mainly cultivated in small granules and flocs structures. Any sort of alteration in the bacterial balance in the system can potentially interact with other operating parameters and determine the reactor performance. As seen in Figure 8-3 C, a significant change in the N/C ratio in the reactor after the major NLR decrease (day 89) resulted in a drop in the experimental system's ammonia and nitrite removal efficiencies leading to a lowered overall N-removal efficiency in the reactor.

Furthermore, evaluating the alkalinity and pH data (Figure 8-3 B) indicated a noticeable inconsistency between the experiment and model results, with an average MAPE of -6.45 and 2.90%, respectively. After day 137 (Figure 8-3 B), both pH and alkalinity levels started to increase due to autotrophic denitrification's failure, which resulted in a drop in NRR of the process. For this reason, the concentration of nitrate-nitrogen in the effluent of the reactor was gradually increased, causing a decrease in the experimental NRE to levels below 0.6 KgN/m^3/day after day 539 (Figure 8-3 A). The continuous effluent assessment showed that the measured alkalinity was lower than the theoretical amount estimated from the stoichiometry and modeled data (Figure 8-3 B). In line with the stoichiometry of S-based autotrophic denitrification, reduction of 1 mgN-NO_3 expends 3.36 mg/L of alkalinity as $CaCO_3$ (Di Capua et al., 2019), igniting the alkalinity diminution in the UASB reactor. Coexistence of ANAMMOX bacteria and autotrophic denitrifiers can theoretically influence the simultaneous removal of nitrogen and organic carbon in a single system. *Paracoccus denitrificans* species are principally extant in activated sludge samples and can consume $S_2O_3^{2-}$ and HS^- as electron donor and NO_3^- as the electron acceptor to generate dinitrogen gas. The results of the microbial analysis on the reactor reported previously by Izadi et

al. (2020), specified the existence of numerous anaerobic denitrifying bacteria, *Pseudomonas, Methylobacterium, Bacillus, Paracoccus* in the UASB bacterial consortium.

8.3.3. Gradual decrease of temperature effect in the experimental and model setup

Temperature is a vital operational element affecting the ANAMMOX process kinetics. All temperature shifts in the typical range lead to rapid and transitory cell components adaptations; nonetheless, fluctuations are more evident in temperatures higher or lower than the standard range, emphasizing the essential conversions required for growth (Berry and Foegeding, 1997). Several studies have reported that the alterations in the microorganism's fatty acid structures in the membrane phospholipids are in response to fluctuations in the growth temperature (de Mendoza and Cronan, 1983). To describe the effect of temperature on ANAMMOX biomasses, the activities were normalized at 35 °C, subsequently, the microbial activity and process performance were evaluated in lower temperatures, including; 25 and 15 °C. Expanding the process operation to lower temperatures with depressed nitrogen levels can theoretically lead to broadening the application potential of ANAMMOX-based processes for municipal wastewater treatment, introducing innovative and promising scenarios in introducing energy-generating treatment plants. Even though ANAMMOX activity has been detected in the arctic ice at extremely low temperatures, sustaining a stable and long-standing process in reduced temperatures is not practicable in engineered procedures. The existence of ANAMMOX bacteria in a broad temperature scope shows their exploitation in different classes of wastewater treatment systems (Sobotka et al., 2021). Several studies have reported that the ANAMMOX activities significantly drop at temperatures lower than 20 °C (Sobotka et al., 2016). In this study, a novel approach was applied to describe the low-temperature effect on the micro-granular ANAMMOX process after low nitrogen load stabilization, using a combination of both experimental and BioWin-based

approaches. The attained results are evaluated and further compared with literature data; moreover, the practical implications of modeling and practice of ANAMMOX for mainstream treatment are deliberated. The process has been refined to work at low temperatures (15 and 25 °C) and low nitrogen concentrations for this demonstration.

Figure 8-3 Comparison between daily experimental effluent measurements and the dynamic models data for 538 days of mainstream operation: (A) NLR, NRR and NRE levels (B) Alkalinity and pH (C) Nitrate levels and ammonia and nitrite removal efficiencies (the days in this figure signify the days of operation after the sidestream transition to mainstream)*

Table 8-2 signifies the actual removal rates for the single-stage ANAMMOX after the sudden decrease in temperature from 35℃ to 25℃, then to 15℃. The lab-scale UASB reactor was initially operated at high temperatures (~ 35 °C) from phase I to V, treating a low-strength synthetic influent for over 450 days. Subsequently, the temperature was promptly reduced to 25 °C (phase VI as shown in Table 8-2). The reactor operation decreased temperature to assess its impact on ANAMMOX in a long-term process operation. Primarily, the reactor was operated at 25 °C for 49 days, and then, the temperature was impulsively decreased to 15 °C in phase VII and further maintained for 83 days. Based on the results of this analysis, the long-term operation at temperatures around 15 °C triggered the destabilization of the ANAMMOX process. A similar evaluation arrangement was executed for the modeling analysis of the system, with temperature drops to 25 and 15 °C. The reported rates were calculated through mass balances from daily data. Generally, bacteria should reach lower specific activity at lower temperatures when other operational parameters have remained constant. Because ANAMMOX required additional biomass to preserve its activity in minor temperatures, and due to lower substrate uptake rates and decreased anoxic volume at 25 and 15℃, bacterial activity considerably declined at 15℃. A shift of substrate concentration from phase I to phase V operated at 35°C, prolonged ANAMMOX mainstream reactor startup, yet combined temperature and concentration changes in phases V and VI greatly disturbed the ANAMMOX activity. As indicated in Table 8-2, when the temperature dropped from 35 to 15 ◦C from phase I to VII, the specific ANAMMOX activity (SAA) in the experimental setup declined by approximately 70%, yet, it is still promising that ANAMMOX activity was detected at 15°C. Temperature dependency of the SAA, as articulated in Table 8-2, escalated at reduced temperature levels (15–25 °C) weighed against elevated temperatures (35 °C) for samples from the UASB reactor.

Based on the experimental analysis, decreasing the temperature from 35 to 15 °C (phase V to VII) adversely affected the overall NRE, ammonia, and nitrite removal rates by 67%, 64%, and 76%, respectively. As indicated in Table 8-2, the most significant shift in the experimental NRE was identified when the temperature was reduced to 15 °C from phase VI to VII. Compatibly, the major nitrogen removal efficiency reduction was parallel with significant drops in ammonia removal, nitrite removal, and SAA from approximately 60% to 27%, 58% to 18%, and 4.5 to 1.8 gN_2-N/m^2. Day, respectively. Diverse system designs and dissimilar temperature decline patterns result in major discrepancies in the system reaction to the temperature decrease. Several studies confirmed a stable ANAMMOX activity at 10 °C and less instability in highly enriched ANAMMOX systems; however, nitrite accretion leading to diminished ANAMMOX activity was detected in a granular-based system at 15 °C (Gilbert et al., 2015b). Distinct ammonia and nitrite accumulation were spotted in the reactor system in all operation phases with temperatures below 25 °C. This substrate buildup was initiated at 25 °C and reached its maximum level when the system's temperature was pushed to 15 °C in phase VII. The evident nitrite accumulation observed in the reactor was potentially triggered by the impact of ANAMMOX activity suppression together with reduced volumes of anaerobic ammonia oxidizers, in addition to a decrease in autotrophic denitrification rates. Examining the results, the BioWin model was incompetent to simulate temperature decrease on ANAMMOX performance and activity. As illustrated in Table 8-2, temperature reduction from 35 ℃ to 25 ℃ and further to 15 ℃, did not affect the SAA and the NRE in the modelling setup. The MAPE between the experimental and modeled ammonia and nitrite removal efficiencies in phases VI and VII reached a maximum level of 69.14% and 78.44%, respectively. The overall profiles of ammonia and nitrite were better predicted by the model when the system was operated under 35 ℃. The model's and experimental NRE outcomes are

significantly different (p= 4.2871e-112 < 0.01), indicating the poor predictability of the model configuration. Considering the statistical analysis results, it was proven that the model configuration was only successful in simulating the experiment when the system was operated in conditions comparable to sidesream ANAMMOX process, and a further decrease in the N-load and temperature led to increase in the discrepancies. The presented model-based approach used for simulation facilitation did not demonstrate strong predictive powers for anticipating the system's dynamic response to nitrogen load and temperature fluctuations in a mainstream ANAMMOX process.

Table 8-2 Experimental and Modelled system performance assessment in the long-term operation of the UASB reactor at mainstream conditions, with different temperature and sulfate levels

Days of Operation	1-17	17-47	47-89	89-525	525-553	553-601	601-649	649-665	665-681
Phase	**I**	**II**	**III**	**IV**	**V**	**VI**	**VII**	**VIII**	**IX**
Duration (Days)	17	31	43	437	29	49	49	17	17
Temp. [°C]	35	35	35	35	35	25	15	15	15
Magnesium sulfate concentration [mg/L]	0	0	0	0	0	0	0	15	30
NLR [KgN/m^3/day]	1.2	0.98	0.6	0.20	0.16	0.20	0.21	0.21	0.20
Experimental pH	8.0	7.6	7.2	7.5	7.8	7.6	7.7	7.8	7.9
Modelled pH	7.3	7.3	7.3	7.4	7.4	7.2	7.2	7.0	7.0
Experimental NRE [KgN/m^3/day]	0.9	0.87	0.7	0.53	0.43	0.31	0.14	0.19	0.26
Modelled NRE [KgN/m^3/day]	0.89	0.88	0.82	0.62	0.66	0.66	0.64	0.64	0.65
Experimental ammonia removal [%]	92.40	90.56	85.4	81.9	77.10	60.01	27.14	28.63	28.39

Modelled ammonia removal [%]	92.43	92.02	91.40	86.87	88.65	88.61	87.96	88.01	88.07
Experimental nitrite removal [%]	95.0	90.75	83.90	85.36	78.70	58.97	18.45	25.01	34.98
Modelled nitrite removal [%]	94.93	93.91	90.21	80.59	85.64	85.41	85.59	85.21	84.17
Experimental specific ANAMMOX activity [gN_2-N/m^2. day]	6.34	6.28	5.91	5.83	5.69	4.50	1.87	1.89	1.81
Modelled specific ANAMMOX activity [gN_2-N/m^2. day]	6.32	6.27	6.01	5.97	5.99	5.99	5.98	5.98	5.98

8.3.4. Addition of trace concentrations of soluble sulfate salt ($MgSO_4 \cdot 7H_2O$)

In confined anaerobic ecosystems such as the UASB system's environment, the hydrogen sulfide produced from sulfate reduction has the propensity to dissolve in the water solution with pH increases, leading to the production of sufficient volumes of dissolved sulfide. Several sulfur sources can function as electron donors for autotrophic denitrification to eliminate nitrate/nitrite (J. Wang et al., 2009). However, linking ANAMMOX and sulfide-dependent autotrophic denitrification has been inadequately investigated, which may play a major part in conditions where sulfur and nitrogen cycles are functional. Table 8-2 shows the time courses of operational phases in the anaerobic reactor system. Nitrite and nitrate concentrations and patterns varied significantly for the different medium conditions from phase VII to IX, yielding a maximum nitrite removal efficiency of 34.98% at 15 ℃ when 30 mg/L of magnesium sulfate was added to the system. Comparing phases VIII and IX with phase VII, it can be understood that autotrophic denitrification occurs in the systems with additional sulfate supplementation and that the addition

of Sulphur could facilitate the denitrification process. There was less nitrite accumulation in the reactor under conditions VIII and IX, as shown in Table 8-2, which means that the rate of autotrophic denitrification in the system under Sulphur addition conditions was higher than phase VII at 15 ℃ and with no additional Sulphur provision. Table 8-2 shows two sequential phases at 15 ℃, distinctly demonstrating the coupling between ANAMMOX and autotrophic denitrification to attain simultaneous oxidation of sulfide and nitrite/nitrate, leading to an improved NRE compared to phase VII. Besides, the drop in nitrate/nitrite concentrations assessed in the process effluent operating under simultaneous ANAMMOX and sulfide-dependent denitrification conditions (phases VIII and IX in Table 8-2) as compared to concentrations examined in the absence of sulfide (phase VII Table 8-2), strengthens the hypothesis that sulfide-dependent autotrophic denitrification was accountable for the diminishing of nitrite/nitrate when the two processes were coupled. A couple of studies have reported the association between ANAMMOX and sulfide-dependent denitrification, playing a substantial role on nitrogen and sulfur fluxes in marine environments (Rios-Del Toro and Cervantes, 2016).

8.4. Conclusion

ANAMMOX bacteria are sustainable and functioning in mainstream municipal wastewater, even at low-level temperatures and substrate concentrations. Nevertheless, attaining a successful ANAMMOX performance at low temperatures continues to be a challenge, for which granular-based strategies with robust aggregates and anaerobic ammonium oxidation coupled with sulfide-dependent autotrophic denitrification for achieving simultaneous removal of ammonium linked to nitrite and nitrate may be a solution. A stable long-term operation with 0.14-0.9 $kgN/m^3/day$ nitrogen removal efficiencies was achieved in a UASB ANAMMOX reactor at mainstream conditions. The system showed a good response during transient N-loads however, shifting the

temperature from 35 to 15 °C majorly affected the process performance. Experiments in the present study indicated that Sulfide-dependent denitrification linked with ANAMMOX during the simultaneous oxidation process could significantly increase the overall NRE by approximately 46% by reducing both nitrite and nitrate available in the system.

CHAPTER 9

Conclusion

ANAMMOX is the process of oxidizing ammonium to dinitrogen gas, with nitrite being the electron acceptor in the absence of oxygen. Unlike any other microbial process involved in the nitrogen cycle, analysis of the ANAMMOX process focused on improving the nitrogen removal procedure from wastewater. On the other hand, the application of ANAMMOX for N-removal has never been easy. The primary hindrance for this process's lab-scale studies and industrial applications is the slow growth rate of the responsible bacterial population. Also, major struggles with low biomass yields and extended doubling times created serious limitations for successful full-scale applications (Kocamemi et al., 2018). To sustain a stable ANAMMOX process, it is crucial to consider microbial stability, diversity and activity improvement. One critical element in stability and effectiveness of procedures coping with slow-growing bacteria is achieving a suitable settlebility to keep the cultivated biomass in the reactor by granulation and achieve rapid startup with improved efficacy (Ye et al., 2018).

This research targeted implementing a sustainable nitrogen removal technology that potentially meets specific levels set for the effluents. Bearing in mind the nitrification's need for aeration and energy supply and the requirement for external carbon for denitrification in the conventional biological nitrogen removal processes, ANAMMOX-based processes pave the path towards reaching an energy-neutral or net energy positive system and reduce the operational costs. On the

other hand, one major challenge In ANAMMOX employment in real-world applications is the bacteria's slow growth rate, leading to extended startup periods and possible biomass washouts. In summary, the research described in this thesis presented the viability of a progressive technology N-removal from both sidestream and mainstream wastewater and developed a robust fundament to effectively shift to a new era where wastewater is more about energy generation rather than energy depletion.

Present research designed an innovative method to cultivate and immobilize ANAMMOX bacterial communities in micro-granules, to enhance the overall NRE in the system by decreasing the biomass washouts, increasing the system's SRT, improving the bacterial interaction. Second, the nitrogen removal performance was investigated using BioWin as a mathematical modeling tool. Development of the presented mathematical models resulted in a better understanding of the process dynamics revealed optimization opportunities, and offered an inclusive reference for improving ANAMMOX process performance.

The initial aim of this study was to upgrade the operative aspects of a laboratory-scale UASB reactor for micro-granular ANAMMOX consortium enrichment from activated sludge with no bioaugmentation. Overcoming the problems linked to seed accessibility plus sludge retention and growth in newly started ANAMMOX reactors were a few of the principal objectives of this research. In the case of ANAMMOX-based systems, there are issues with sludge availability due to the slow bacterial growth rates and yields. As a result, designing a system that would effectively cultivate the ANAMMOX consortium from RAS is very beneficial. The 3-phased experimental analysis completed on the UASB ANAMMOX setup with an average nitrogen loading rate of 0.22 KgN /m^3/day and average SRT of 36 to 72 days, showed nitrogen removal efficiencies of up to 95±2.7% in the final phase of operation. The final operational phase strongly indicated a stable

ANAMMOX process with ammonia removal of 90.3–94.8%, a concurrent diminution of nitrite with nitrite removal rate reaching 96.06%. In parallel, NO_3^- began to accumulate in the effluent, however, the observed nitrate to ammonia ratio was lower than the stoichiometry, signifying autotrophic denitrifiers in the system.

The results attained from the particle size distribution analysis showed a particle diameter of between 253.2–465.7 μm for above 75% of the total sample volume. The cultivated ANAMMOX biomass from RAS had a greater mean particle diameter, by roughly 39.15±2.4%. Granulation is an emergent topic for ANAMMOX-based systems, since the process's efficiency and stability rely on providing adequate HRT and SRT for the slow-growing bacteria. This factor becomes even more critical for full-scale applications since the consequences of biomass loss may be irreparable. The microbial analysis results revealed an increase in the abundance of *Planctomycetes*, being the key phylum liable for anaerobic ammonia removal. Escalation in abundance of *Chloroflexi* (filamentous bacteria) from 0.6 to 6.3%, potentially due to their presence on the ANAMMOX micro-granules' surface was a clear sign of granulation process happening in microbial analysis level. This part of the study effectively cultivated an optimum micro-sized ANAMMOX granular sludge to acquire high nitrogen removal efficiencies with the least biomass washouts. Outcomes of this research deliver a potential substitute and suitable configuration designed for ANAMMOX cultivation. The results validate the efficacy and elevated performance proficiency of micro-sized granules in ANAMMOX-based processes.

As previously discussed ANAMMOX bacteria can successfully treat high ammonia and nitrite concentrations in anoxic environments. However, high ammonia and nitrite concentrations may trigger free ammonia and nitrous acid inhibitions at high pH and temperature conditions (Kalkan Aktan et al., 2012). ANAMMOX bacteria, similar to methanogens, are mesophilic and slow-

growing bacteria identified as bacteria easily affected by environmental conditions. Alternatively, in mainstream environments with depleted nitrogen concentrations, ANAMMOX bacterial populations are suppressed by other bacterial groups due to their low growth rates and bacterial yields (T. R. V Akaboci et al., 2018). Ideal concentrations of ANAMMOX intermediate metabolites including, hydroxylamine (NH_2OH), can stimulate the total nitrogen removal and accelerate the recovery process in a short time (Zekker et al., 2012).

In the second part of this research, the performance and activity of the enriched micro-granular ANAMMOX consortium with the presence of either inhibition or stimulation elements were evaluated. The results indicated that, in experiments with additional ammonium and nitrite concentrations, having a NLR ranging between 2.08 to 4.81 KgN/m^3/day, substrates began to build up in the effluent, causing a major drop in the nitrogen removal efficiency (NRE ~ 0 KgN/m3/day). Alternatively, decreasing the NLR from 1.4 to 0.29 KgN/m^3/day (mimicking mainstream ANAMMOX process conditions) initiated a drop in ANAMMOX activity from 129.8 to 120.7 mgN/d.gVSS. Additional NLR reduction to 0.1 KgN/m^3/day led to an ANAMMOX activity of 103.7, being about 20% lesser than the original control test.

Hydroxylamine supplements at a total level of 30 mgN/L improved the ANAMMOX process. Increasing the hydroxylamine levels from 1.5 to 4.5 mgN/L to 22.5 and 30 mgN/L brought about greater nitrogen removal rates of 1.34 and 1.36 KgN/m^3/day, respectively. The intermediate-based ANAMMOX stimulation approach proposes a potential practice for effective application of the mainstream process. Based on the available results from this study, hydroxylamine can be a recovery factor for previously inhibited ANAMMOX systems in addition to being an enhancing driver for high-temperature mainstream ANAMMOX process employment. Adding hydroxylamine for full-scale ANAMMOX-based process may not be cost-effective, but it can still

help improve the understanding of the metabolic reactions in the electron transport chain of the bacteria.

Although ANAMMOX-based systems are distinguished as one of the most promising approaches for ammonia oxidation to dinitrogen gas, there are significant hurdles that delay the practical applications of the process (Ye et al., 2020). Experimental process analysis is an extremely time-consuming procedure, primarily due to the slow growth rates of the bacterial community (Mattei et al., 2015). Therefore, mathematical modeling is a favorable technique for evaluating different environmental and operational parameters (Hao et al., 2002). Various softwares, including BioWin® (EnviroSim Associates Ltd., Canada), concentrate on modeling the microbiological processes connected with wastewater treatment, which allow for mathematical simulation of ANAMMOX bacterial activity (Dorofeev et al., 2017). BioWin® activated sludge models (ASM) include several functional features such as pH modeling, which simplify complex wastewater treatment systems (Elawwad, 2018).

The third part of our study aimed to evaluate the operation of the lab-scale UASB micro-granular ANAMMOX process in all operational phases, using both mathematical modeling and experimental data. The analysis was used to represent a comparison between the two methods and prove the capacity of BioWin® software to approximate and predict the ANAMMOX process and to represent the long-term active performance of a UASB system setup. Three different model configurations were assessed, in which Model III was capable of predicting the day-to-day nitrogen loading and removal rates in the stabilized operational conditions. Comparably, an equivalent trend was seen in the other two phases among the experimental and modeled NRE, NLR and NRR values, indicating the calibrated model's success to simulate the ANAMMOX UASB. The proposed model is suitable for the stated conditions, however, the methods can be

constructive for all user-specific circumstances and distinctive data assortments. Future developments should focus on the biological perspectives of modeling in which the process efficiency is mathematically combined with the microbial diversity and activity.

Mainstream ANAMMOX is an emerging nitrogen removal process that depends on advanced control strategies to regulate the operational parameters and reach a specific efficiency level. A few of the main obstacles of mainstream ANAMMOX process applications are; depleted nitrogen concentrations, changing nitrogen loading rates, low temperatures, strict effluent standards, process stability, and robustness. The key purpose of this section of the study was to demonstrate a novel and cost-effective method for the gradual conversion of the sidestream ANAMMOX UASB to a mainstream process. After reaching a stable operation with high nitrogen removal rates for over 200 operating days, the nitrogen load was gradually dropped during 550 days to achieve an influent ammonia and nitrite concentrations of 21.8 mgNH_4-N/L and 16.3 mgNO_2-N/L.

Reducing the nitrogen load to less than 0.2 KgN/m^3/day without temperature alteration resulted in a reduction of NRE (from an average of 78% to 51%). considerable effects were recognized on ammonium, nitrite and total nitrogen removals, getting to a level of about 72.6 ± 1.5%, 76.9 ± 3.1% and 50.7 ± 4.8%. Besides the importance of nitrogen loads on ANAMMOX efficiency and stability, the temperature is also a fundamental operating factor distressing the ANAMMOX process kinetics in lowered levels. To understand the impact of temperature drop on ANAMMOX performance, the bacterial activities were initially stabilized at 35 °C, then the microbial activity and process performance were assessed in decreased temperatures of 25 and 15 °C. Based on the assessment outcomes, long-term operation at 15 °C initiated a disruption for ANAMMOX process.

Innovative nitrogen management systems decrease the energy requirements and the removal cost of reactive nitrogen from wastewater. There is a number of promising opportunities for the future

of sidestream and mainstream deammonification. Despite the advantages of the ANAMMOX-based processes, there are also has some limitations. A few of the most important issues are: managing high COD/N ratio; treating low strength wastewater, stable operation at low temperatures and successful retention of microbial populations systems. More research and experimentation are expected in the future, especially focusing on COD concentration, potential energy recovery options, and the ANAMMOX process's integration into a full-scale system treating real municipal wastewater. Therefore, the application of ANAMMOX in municipal wastewater is not yet a mature technology, and it will continue to be a thought-provoking research topic in the future. Based on the reviewed literature and the experience of the authors, future studies should also focus on the inhibition effects of different compounds such as free ammonia, free nitrous acid, hydrazine, hydroxylamine, and the effect of salinity on different microbial communities and provide possible solutions for long startup periods and challenges of biomass retention in ANAMMOX process.

The future developments must principally concentrate on the biological side of modeling, mathematically linking the performance of an ANAMMOX-based system to microbial diversity and activity.

Regarding the strategies investigated in this Thesis, further studies should be conducted:

- To assess the potential of improving the interaction between ANAMMOX and denitrifying bacteria to enhance the NRE in the system by nitrate depletion.
- To better analyze the mixed culture microbial communities involved in N-removal from the sidestream and mainstream systems.
- To investigate the enzymatic reactions in ANAMMOX metabolism to better comprehend the redox reactions.

- To improve microbial activity and performance in decreased temperatures, improve the implementation of the mainstream ANAMMOX process.
- To develop other types of ANAMMOX-based processes, including partial nitritation/ANAMMOX (PNA) and pre-denitrification nitritation ANAMMOX (PDNA).
- To better quantify the microbial species present in outlined models
- To develop models based either on statistical methods or heuristical information.

BIBLIOGRAPHY

Abma, W.R., Driessen, W., Haarhuis, R., Van Loosdrecht, M.C.M., 2010. Upgrading of sewage treatment plant by sustainable and cost-effective separate treatment of industrial wastewater. Water Sci. Technol. 61, 1715–1722. https://doi.org/10.2166/wst.2010.977

Abma, W.R., Schultz, C.E., Mulder, J.W., van der Star, W.R.L., Strous, M., Tokutomi, T., van Loosdrecht, M.C.M., 2007. Full-scale granular sludge Anammox process, in: Water Science and Technology. IWA Publishing, pp. 27–33. https://doi.org/10.2166/wst.2007.238

Ahn, Y.-H., 2006. Sustainable nitrogen elimination biotechnologies: A review. Process Biochem. 41, 1709–1721. https://doi.org/10.1016/J.PROCBIO.2006.03.033

Akaboci, T.R.V., Gich, F., Ruscalleda, M., Balaguer, M.D., Colprim, J., 2018. Effects of extremely low bulk liquid DO on autotrophic nitrogen removal performance and NOB suppression in side- and mainstream one-stage PNA. J. Chem. Technol. Biotechnol. 93, 2931–2941. https://doi.org/10.1002/jctb.5649

Akaboci, T.R. V, Gich, F., Ruscalleda, M., Dolors Balaguer, M., Colprim, J., 2018. Assessment of operational conditions towards mainstream partial nitritation-anammox stability at moderate to low temperature: Reactor performance and bacterial community. Chem. Eng. J. https://doi.org/10.1016/j.cej.2018.05.115

Aktan, C.K., Yapsakli, K., Mertoglu, B., 2012. Inhibitory effects of free ammonia on Anammox bacteria. Biodegradation 23, 751–762. https://doi.org/10.1007/s10532-012-9550-0

Al-Omari, A., Wett, B., Nopens, I., De Clippeleir, H., Han, M., Regmi, P., Bott, C., Murthy, S., 2015. Model-based evaluation of mechanisms and benefits of mainstream shortcut nitrogen removal processes. https://doi.org/10.2166/wst.2015.022

Ali, M., Okabe, S., 2015. Anammox-based technologies for nitrogen removal: Advances in process start-up and remaining issues. Chemosphere 141, 144–153. https://doi.org/10.1016/J.CHEMOSPHERE.2015.06.094

Ali, M., Shaw, D.R., Zhang, L., Haroon, M.F., Narita, Y., Emwas, A.-H., Saikaly, P.E., Okabe, S., 2018. Aggregation ability of three phylogenetically distant anammox bacterial species. Water Res. https://doi.org/10.1016/j.watres.2018.06.007

Allen, M.S., Welch, K.T., Prebyl, B.S., Baker, D.C., Meyers, A.J., Sayler, G.S., 2004. Analysis and glycosyl composition of the exopolysaccharide isolated from the floc-forming wastewater bacterium Thauera sp. MZ1T. Environ. Microbiol. 6, 780–790. https://doi.org/10.1111/j.1462-2920.2004.00615.x

Alphenaar, P.A., Pérez, M.C., Lettinga, G., 1993. The influence of substrate transport limitation on porosity and methanogenic activity of anaerobic sludge granules. Appl. Microbiol. Biotechnol. 39, 276–280. https://doi.org/10.1007/BF00228619

An, W., Guo, F., Song, Y., Gao, N., Bai, S., Dai, J., Wei, H., Zhang, L., Yu, D., Xia, M., Yu, Y., Qi, M., Tian, C., Chen, H., Wu, Z., Zhang, T., Qiu, D., 2016. Comparative genomics analyses on EPS biosynthesis genes required for floc formation of Zoogloea resiniphila and other activated sludge bacteria. Water Res. 102, 494–504.

https://doi.org/10.1016/j.watres.2016.06.058

Anthonisen, A.C., Loehr, R.C., Prakasam, T.B., Srinath, E.G., 1976. Inhibition of nitrification by ammonia and nitrous acid. J. Water Pollut. Control Fed. 48, 835–52.

Aqeel, H., Weissbrodt, D.G., Cerruti, M., Wolfaardt, G.M., Wilén, B.-M., Liss, S.N., 2019. Drivers of bioaggregation from flocs to biofilms and granular sludge. Environ. Sci. Water Res. Technol. 5, 2072–2089. https://doi.org/10.1039/C9EW00450E

Arnaldos, M., Amerlinck, Y., Rehman, U., Maere, T., Van Hoey, S., Naessens, W., Nopens, I., 2015. From the affinity constant to the half-saturation index: Understanding conventional modeling concepts in novel wastewater treatment processes. Water Res. https://doi.org/10.1016/j.watres.2014.11.046

Ashraf, M.A., Batool, S., Ahmad, M., Sarfraz, M., Noor, W.S.A.W.M., 2016. Biopolymers as biofilters and biobarriers, in: Biopolymers and Biotech Admixtures for Eco-Efficient Construction Materials. Elsevier Inc., pp. 387–420. https://doi.org/10.1016/B978-0-08-100214-8.00017-8

Ates, O., 2015. Systems Biology of Microbial Exopolysaccharides Production. Front. Bioeng. Biotechnol. 3. https://doi.org/10.3389/fbioe.2015.00200

Audy, J., Labrie, S., Roy, D., LaPointe, G., 2010. Sugar source modulates exopolysaccharide biosynthesis in Bifidobacterium longum subsp. longum CRC 002. Microbiology 156, 653–664. https://doi.org/10.1099/mic.0.033720-0

Bagchi, S., Biswas, R., Nandy, T., 2010. Start-up and stabilization of an Anammox process from a non-acclimatized sludge in CSTR. J. Ind. Microbiol. Biotechnol. 37, 943–952. https://doi.org/10.1007/s10295-010-0743-4

Bailey, E.L., Bilyk, K., Hanna, A., Wankmuller, D., 2018. Evaluation of Sidestream Deammonification Process Enhancements for Treating High Strength Filtrate at the City of Raleigh's Neuse River Resource Recovery Facility.

Barreto, M., Jedlicki, E., Holmes, D.S., 2005. Identification of a Gene Cluster for the Formation of Extracellular Polysaccharide Precursors in the Chemolithoautotroph Acidithiobacillus ferrooxidans. Appl. Environ. Microbiol. 71, 2902–2909. https://doi.org/10.1128/AEM.71.6.2902-2909.2005

Basuvaraj, M., Fein, J., Liss, S.N., 2015. Protein and polysaccharide content of tightly and loosely bound extracellular polymeric substances and the development of a granular activated sludge floc. Water Res. 82, 104–117. https://doi.org/10.1016/j.watres.2015.05.014

Beech, I.B., Cheung, C.W.S., Johnson, D.B., Smith, J.R., 1996. Comparative studies of bacterial biofilms on steel surface using atomic force microscopy and environmental scanning electron microscopy. Biofouling. https://doi.org/10.1080/08927019609386271

Bemal, S., Anil, A.C., 2018. Effects of salinity on cellular growth and exopolysaccharide production of freshwater Synechococcus strain CCAP1405. J. Plankton Res. 40, 46–58. https://doi.org/10.1093/plankt/fbx064

Berney, M., Weilenmann, H.U., Ihssen, J., Bassin, C., Egli, T., 2006. Specific growth rate

determines the sensitivity of Escherichia coli to thermal, UVA, and solar disinfection. Appl. Environ. Microbiol. 72, 2586–2593. https://doi.org/10.1128/AEM.72.4.2586-2593.2006

Berry, E.D., Foegeding, P.M., 1997. Cold temperature adaptation and growth of microorganisms. J. Food Prot. https://doi.org/10.4315/0362-028X-60.12.1583

Bettazzi, E., Caffaz, S., Vannini, C., Lubello, C., 2010. Nitrite inhibition and intermediates effects on Anammox bacteria: A batch-scale experimental study. Process Biochem. 45, 573–580. https://doi.org/10.1016/J.PROCBIO.2009.12.003

Bhatia, D., Bourven, I., Simon, S., Bordas, F., Van Hullebusch, E.D., Rossano, S., Lens, P.N.L., Guibaud, G., 2013. Fluorescence detection to determine proteins and humic-like substances fingerprints of exopolymeric substances (EPS) from biological sludges performed by size exclusion chromatography (SEC). Bioresour. Technol. https://doi.org/10.1016/j.biortech.2012.12.078

Blackburne, R., Yuan, Z., Keller, J., 2008. Partial nitrification to nitrite using low dissolved oxygen concentration as the main selection factor. Biodegradation 19, 303–312. https://doi.org/10.1007/s10532-007-9136-4

Blanco, Y., Rivas, L.A., González-Toril, E., Ruiz-Bermejo, M., Moreno-Paz, M., Parro, V., Palacín, A., Aguilera, Á., Puente-Sánchez, F., 2019. Environmental parameters, and not phylogeny, determine the composition of extracellular polymeric substances in microbial mats from extreme environments. Sci. Total Environ. 650, 384–393. https://doi.org/10.1016/j.scitotenv.2018.08.440

Boleij, M., 2020. The anammox house : On the extracellular polymeric substances of anammox granular sludge. Delft University of Technology.

Boleij, M., Kleikamp, H., Pabst, M., Neu, T.R., van Loosdrecht, M.C.M., Lin, Y., 2020. Decorating the Anammox House: Sialic Acids and Sulfated Glycosaminoglycans in the Extracellular Polymeric Substances of Anammox Granular Sludge. Environ. Sci. Technol. 54, 5218–5226. https://doi.org/10.1021/acs.est.9b07207

Boleij, M., Pabst, M., Neu, T.R., Van Loosdrecht, M.C.M., Lin, Y., 2018. Identification of Glycoproteins Isolated from Extracellular Polymeric Substances of Full-Scale Anammox Granular Sludge. Environ. Sci. Technol. 52, 13127–13135. https://doi.org/10.1021/acs.est.8b03180

Boleij, M., Seviour, T., Wong, L.L., Van Loosdrecht, M.C.M., Lin, Y., 2019. Solubilization and characterization of extracellular proteins from anammox granular sludge. Water Res. https://doi.org/10.1016/j.watres.2019.114952

Boumann, H.A., Longo, M.L., Stroeve, P., Poolman, B., Hopmans, E.C., Stuart, M.C.A., Sinninghe Damsté, J.S., Schouten, S., 2009. Biophysical properties of membrane lipids of anammox bacteria: I. Ladderane phospholipids form highly organized fluid membranes. Biochim. Biophys. Acta - Biomembr. 1788, 1444–1451. https://doi.org/10.1016/J.BBAMEM.2009.04.008

Bourven, I., Bachellerie, G., Costa, G., Guibaud, G., 2015. Evidence of glycoproteins and sulfated proteoglycan-like presence in extracellular polymeric substance from anaerobic

granular sludge. Environ. Technol. (United Kingdom) 36, 2428–2435. https://doi.org/10.1080/09593330.2015.1034186

Bourven, I., Simon, S., Guibaud, G., 2013. Influence of extraction method on size exclusion chromatography fingerprints of EPS from wastewater sludges. Environ. Technol. (United Kingdom) 34, 321–332. https://doi.org/10.1080/09593330.2012.692722

Bowden, G., Stensel, D., 2016. Technologies for Sidestream Nitrogen Removal.

Bowden, G., Stensel, D., Tsuchihashi, R., 2016. Technologies for Sidestream Nitrogen Removal. IWA Publishing.

Bozkurt, H., Van Loosdrecht, M.C.M., Gernaey, K. V, Sin, G., 2016. Optimal WWTP process selection for treatment of domestic wastewater â€“ A realistic full-scale retrofitting study. Chem. Eng. J. 286, 447–458. https://doi.org/10.1016/j.cej.2015.10.088

Brdjanovic, D., Mithaiwala, M., Moussa, M.S., Amy, G., van Loosdrecht, M.C.M., 2007. Use of modelling for optimization and upgrade of a tropical wastewater treatment plant in a developing country. Water Sci. Technol. 56, 21–31. https://doi.org/10.2166/wst.2007.675

Broda, E., 1977. Two kinds of lithotrophs missing in nature. Z. Allg. Mikrobiol. 17, 491–493. https://doi.org/10.1002/jobm.19770170611

Brun, R., Uhni, M.K., Siegrist, H., Gujer, W., Reichert, P., 2002. Practical identifiability of ASM2d parameters-systematic selection and tuning of parameter subsets, Water Research.

Bura, R., Cheung, M., Liao, B., Finlayson, J., Lee, B.C., Droppo, I.G., Leppard, G.G., Liss, S.N., 1998. Composition of extracellular polymeric substances in the activated sludge floc matrix, in: Water Science and Technology. Elsevier Sci Ltd, pp. 325–333. https://doi.org/10.1016/S0273-1223(98)00125-5

Buthelezi, S.P., 2008. APPLICATION OF BACTERIAL BIOFLOCCULANTS FOR WASTEWATER AND RIVER WATER TREATMENT. University of KWAZULU-NATAL.

Can Der Aa, B.C., Dufrêne, Y.F., 2002. In situ characterization of bacterial extracellular polymeric substances by AFM. Colloids Surfaces B Biointerfaces 23, 173–182. https://doi.org/10.1016/S0927-7765(01)00229-6

Cao, Y., Hong, K.B., Yan, Z., Yu, L., He, J., Chye, C.S., Long, W.Y., Ghani, Y., 2015. Mainstream partial nitritation/anammox nitrogen removal process in the largest water reclamation plant in singapore, in: WEF/IWA Nutrient Removal and Recovery. Beijing University of Technology, pp. 1441–1454. https://doi.org/10.11936/bjutxb2014120074

Cao, Y., Kwok, B.H., Van Loosdrecht, M.C.M., Daigger, G., Png, H.Y., Long, W.Y., Eng, O.K., 2018. The influence of dissolved oxygen on partial nitritation/ anammox performance and microbial community of the 200,000 m3/d activated sludge process at the Changi water reclamation plant (2011 to 2016). Water Sci. Technol. 78, 634–643. https://doi.org/10.2166/wst.2018.333

Cao, Y., van Loosdrecht, M.C.M., Daigger, G.T., 2017. Mainstream partial nitritation–anammox in municipal wastewater treatment: status, bottlenecks, and further studies. Appl. Microbiol.

Biotechnol. https://doi.org/10.1007/s00253-016-8058-7

Capodaglio, A.G., Hlavínek, P., Raboni, M., Capodaglio, A.G., Hlavínek, P., Raboni, M., 2016. Advances in wastewater nitrogen removal by biological processes: state of the art review. Ambient. e Agua - An Interdiscip. J. Appl. Sci. 11, 250. https://doi.org/10.4136/ambi-agua.1772

Carvajal-Arroyo, J.M., Puyol, D., Li, G., Lucero-Acuña, A., Sierra-Álvarez, R., Field, J.A., 2014. Pre-exposure to nitrite in the absence of ammonium strongly inhibits anammox. Water Res. 48, 52–60. https://doi.org/10.1016/J.WATRES.2013.09.015

Carvajal-Arroyo, J.M., Sun, W., Sierra-Alvarez, R., Field, J.A., 2013. Inhibition of anaerobic ammonium oxidizing (anammox) enrichment cultures by substrates, metabolites and common wastewater constituents. Chemosphere 91, 22–27. https://doi.org/10.1016/J.CHEMOSPHERE.2012.11.025

Chamchoi, N., Nitisoravut, S., Schmidt, J.E., 2008. Inactivation of ANAMMOX communities under concurrent operation of anaerobic ammonium oxidation (ANAMMOX) and denitrification. Bioresour. Technol. 99, 3331–3336. https://doi.org/10.1016/J.BIORTECH.2007.08.029

Chan, Y.J., Chong, M.F., Law, C.L., Hassell, D.G., 2009. A review on anaerobic-aerobic treatment of industrial and municipal wastewater. Chem. Eng. J. https://doi.org/10.1016/j.cej.2009.06.041

Chen, H., Hu, H.-Y., Chen, Q.-Q., Shi, M.-L., Jin, R.-C., 2016. Successful start-up of the anammox process: Influence of the seeding strategy on performance and granule properties. Bioresour. Technol. https://doi.org/10.1016/j.biortech.2016.03.139

Chen, J., Ji, Q., Zheng, P., Chen, T., Wang, C., Mahmood, Q., 2010. Floatation and control of granular sludge in a high-rate anammox reactor. Water Res. 44, 3321–3328. https://doi.org/10.1016/j.watres.2010.03.016

Chen, R., Ji, J., Chen, Y., Takemura, Y., Liu, Y., Kubota, K., Ma, H., Li, Y.-Y., 2019a. Successful operation performance and syntrophic micro-granule in partial nitritation and anammox reactor treating low-strength ammonia wastewater. Water Res. 155, 288–299. https://doi.org/10.1016/J.WATRES.2019.02.041

Chen, R., Ji, J., Chen, Y., Takemura, Y., Liu, Y., Kubota, K., Ma, H., Li, Y.-Y., 2019b. Successful operation performance and syntrophic micro-granule in partial nitritation and anammox reactor treating low-strength ammonia wastewater. Water Res. 155, 288–299. https://doi.org/10.1016/J.WATRES.2019.02.041

Chen, T., Zheng, P., Shen, L., Ding, S., Mahmood, Q., 2011. Kinetic characteristics and microbial community of Anammox-EGSB reactor. J. Hazard. Mater.

Chen, W., Qian, C., Zhou, K.G., Yu, H.Q., 2018. Molecular Spectroscopic Characterization of Membrane Fouling: A Critical Review. Chem. https://doi.org/10.1016/j.chempr.2018.03.011

Chen, Z., Meng, Y., Sheng, B., Zhou, Z., Jin, C., Meng, F., 2019. Linking Exoproteome Function and Structure to Anammox Biofilm Development. Environ. Sci. Technol. 53, 1490–1500.

https://doi.org/10.1021/acs.est.8b04397

Chi, Y.-Z., Zhang, Y., Yang, M., Tian, Z., Liu, R.-Y., Yan, F.-Y., Zang, Y.-N., 2018. Start up of anammox process with activated sludge treating high ammonium industrial wastewaters as a favorable seeding sludge source. Int. Biodeterior. Biodegradation 127, 17–25. https://doi.org/10.1016/J.IBIOD.2017.11.007

Cho, S., Kambey, C., Nguyen, V., 2019. Performance of Anammox Processes for Wastewater Treatment: A Critical Review on Effects of Operational Conditions and Environmental Stresses. Water 12, 20. https://doi.org/10.3390/w12010020

Cho, S., Takahashi, Y., Fujii, N., Yamada, Y., Satoh, H., Okabe, S., 2010. Nitrogen removal performance and microbial community analysis of an anaerobic up-flow granular bed anammox reactor. Chemosphere 78, 1129–1135. https://doi.org/10.1016/J.CHEMOSPHERE.2009.12.034

Choi, D., Cho, S., Jung, J., 2018. Key operating parameters affecting nitrogen removal rate in single-stage deammonification. Chemosph. J. https://doi.org/10.1016/j.chemosphere.2018.05.053

Chong, S., Sen, T.K., Kayaalp, A., Ang, H.M., 2012. The performance enhancements of upflow anaerobic sludge blanket (UASB) reactors for domestic sludge treatment - A State-of-the-art review. Water Res. https://doi.org/10.1016/j.watres.2012.03.066

Christensson, M., Ekström, S., Chan, A.A., Le Vaillant, E., Lemaire, R., 2013. Experience from start-ups of the first ANITA Mox Plants. Water Sci. Technol. 67, 2677–2684. https://doi.org/10.2166/wst.2013.156

Christensson, M., Ekström, S., Lemaire, R., Le Vaillant, E., Bundgaard, E., Chauzy, J., Stålhandske, L., Hong, Z., Ekenberg, M., 2011. ANITA^{TM} Mox – A BioFarm Solution for Fast Start-up of Deammonifying MBBRs, in: Proceedings of the Water Environment Federation. Water Environment Federation, pp. 265–282. https://doi.org/10.2175/193864711802639309

Cirpus, I.E.Y., Geerts, W., Hermans, J.H.M., Op Den Camp, J.M., Strous, M., Gijs Kuenen, J., Jetten, M.S.M., 2006. Challenging protein purification from anammox bacteria. Int. J. Biol. Macromol. 39, 88–94. https://doi.org/10.1016/j.ijbiomac.2006.02.018

Clariant/SUD Chemie, 2012. Terra-N performance data, facilities list and operating conditions, provided by personal correspondence.

Cohen-Bazire, G., Pfennig, N., Kunisawa, R., 1964. THE FINE STRUCTURE OF GREEN BACTERIA. J. Cell Biol. 22, 207–25.

Colsen, J., Desloover, J., De Clippeleir, H., Boeckx, P., Laing, G. Du, Verstraete, W., Vlaeminck, S.E., 2010. A retrofitted activated-sludge plant with sequential nitritation and anammox obtains dischargeable effluent.

Comte, S., Guibaud, G., Baudu, M., 2007. Effect of extraction method on EPS from activated sludge: An HPSEC investigation. J. Hazard. Mater. 140, 129–137. https://doi.org/10.1016/j.jhazmat.2006.06.058

Corominas, L., Sin, G., Puig, S., Balaguer, M.D., Vanrolleghem, P.A., Colprim, J., 2011. Modified calibration protocol evaluated in a model-based testing of SBR flexibility. Bioprocess Biosyst. Eng. 34, 205–214. https://doi.org/10.1007/s00449-010-0462-2

Corsino, S.F., Capodici, M., Torregrossa, M., Viviani, G., 2017. Physical properties and Extracellular Polymeric Substances pattern of aerobic granular sludge treating hypersaline wastewater. Bioresour. Technol. 229, 152–159. https://doi.org/10.1016/j.biortech.2017.01.024

Cui, Y.X., Biswal, B.K., Guo, G., Deng, Y.F., Huang, H., Chen, G.H., Wu, D., 2019. Biological nitrogen removal from wastewater using sulphur-driven autotrophic denitrification. Appl. Microbiol. Biotechnol. https://doi.org/10.1007/s00253-019-09935-4

Cuthbertson, L., Mainprize, I.L., Naismith, J.H., Whitfield, C., 2009. Pivotal Roles of the Outer Membrane Polysaccharide Export and Polysaccharide Copolymerase Protein Families in Export of Extracellular Polysaccharides in Gram-Negative Bacteria. Microbiol. Mol. Biol. Rev. 73, 155–177. https://doi.org/10.1128/MMBR.00024-08

Czaczyk, K., Myszka, K., 2006. Biosynthesis of extracellular polymeric substances (EPS) and its role in microbial biofilm formation. Polish J. Environ. Stud.

Dai, W., Xu, X., Liu, B., Yang, F., 2015. Toward energy-neutral wastewater treatment: A membrane combined process of anaerobic digestion and nitritation-anammox for biogas recovery and nitrogen removal. Chem. Eng. J. https://doi.org/10.1016/j.cej.2015.05.036

Daigger, G.T., 2014. Oxygen and Carbon Requirements for Biological Nitrogen Removal Processes Accomplishing Nitrification, Nitritation, and Anammox. Water Environ. Res. 86, 204–209. https://doi.org/10.2175/106143013X13807328849459

Dapena-Mora, A., Campos, J.., Mosquera-Corral, A., Jetten, M.S.., Méndez, R., 2004. Stability of the ANAMMOX process in a gas-lift reactor and a SBR. J. Biotechnol. 110, 159–170. https://doi.org/10.1016/J.JBIOTEC.2004.02.005

Dapena-Mora, A., Fernández, I., Campos, J.L., Mosquera-Corral, A., Méndez, R., Jetten, M.S.M., 2007a. Evaluation of activity and inhibition effects on Anammox process by batch tests based on the nitrogen gas production. Enzyme Microb. Technol. 40, 859–865. https://doi.org/10.1016/J.ENZMICTEC.2006.06.018

Dapena-Mora, A., Fernández, I., Campos, J.L., Mosquera-Corral, A., Méndez, R., Jetten, M.S.M., 2007b. Evaluation of activity and inhibition effects on Anammox process by batch tests based on the nitrogen gas production. Enzyme Microb. Technol. 40, 859–865. https://doi.org/10.1016/j.enzmictec.2006.06.018

Dapena-Mora, A., Vázquez-Padín, J.R., Campos, J.L., Mosquera-Corral, A., Jetten, M., Méndez, R., 2010. Monitoring the stability of an Anammox reactor under high salinity conditions. Biochem. Eng. J. 51, 167–171. https://doi.org/10.1016/j.bej.2010.06.014

De Almeida, N.M., Wessels, H.J.C.T., de Graaf, R.M., Ferousi, C., Jetten, M.S.M., Keltjens, J.T., Kartal, B., 2016. Membrane-bound electron transport systems of an anammox bacterium: A complexome analysis. Biochim. Biophys. Acta - Bioenerg. 1857, 1694–1704. https://doi.org/10.1016/J.BBABIO.2016.07.006

De Mendoza, D., Cronan, J.E., 1983. Thermal regulation of membrane lipid fluidity in bacteria. Trends Biochem. Sci. 8, 49–52. https://doi.org/10.1016/0968-0004(83)90388-2

Degeest, De Vuyst L, 1999. Indication that the nitrogen source influences both amount and size of exopolysaccharides produced by streptococcus thermophilus LY03 and modelling of the bacterial growth and exopolysaccharide production in a complex medium. Appl. Environ. Microbiol. 65, 2863–70.

Di Capua, F., Pirozzi, F., Lens, P.N.L., Esposito, G., 2019. Electron donors for autotrophic denitrification. Chem. Eng. J. 362, 922–937. https://doi.org/10.1016/J.CEJ.2019.01.069

Dietl, A., Ferousi, C., Maalcke, W.J., Menzel, A., De Vries, S., Keltjens, J.T., Jetten, M.S.M., Kartal, B., Barends, T.R.M., 2015. The inner workings of the hydrazine synthase multiprotein complex. Nature 527, 394–397. https://doi.org/10.1038/nature15517

Dignac, M.-F., Urbain, V., Rybacki, D., Bruchet, A., Snidaro, D., Scribe, P., 1998. Chemical description of extracellular polymers: implication on activated sludge floc structure. Water Sci. Technol. 38, 45–53. https://doi.org/10.2166/wst.1998.0789

Dilanji, G.E., Langebrake, J.B., De Leenheer, P., Hagen, S.J., 2012. Quorum activation at a distance: Spatiotemporal patterns of gene regulation from diffusion of an autoinducer signal. J. Am. Chem. Soc. 134, 5618–5626. https://doi.org/10.1021/ja211593q

Ding, C., Adrian, L., Peng, Y., He, J., 2020. 16S rRNA gene-based primer pair showed high specificity and quantification accuracy in detecting freshwater Brocadiales anammox bacteria | FEMS Microbiology Ecology | Oxford Academic. Microbiol. Ecol.

Ding, C., Enyi, F.O., Adrian, L., 2018. Anaerobic Ammonium Oxidation (Anammox) with Planktonic Cells in a Redox-Stable Semicontinuous Stirred-Tank Reactor. Environ. Sci. Technol. https://doi.org/10.1021/acs.est.7b05979

Ding, Z., 2016. Engineering and microbial aspects of Anammox process in wastewater treatment. Paris Est.

Dorofeev, A.G., Nikolaev, Y.A., Kozlov, M.N., Kevbrina, M. V., Agarev, A.M., Kallistova, A.Y., Pimenov, N. V., 2017. Modeling of anammox process with the biowin software suite. Appl. Biochem. Microbiol. 53, 78–84. https://doi.org/10.1134/S0003683817010100

Du, R., Cao, S., Zhang, H., Li, X., Peng, Y., 2020. Flexible Nitrite Supply Alternative for Mainstream Anammox: Advances in Enhancing Process Stability. Environ. Sci. Technol. 54, 6353–6364. https://doi.org/10.1021/acs.est.9b06265

Du, R., Peng, Y., Ji, J., Shi, L., Gao, R., Li, X., 2019. Partial denitrification providing nitrite: Opportunities of extending application for anammox. Environ. Int. https://doi.org/10.1016/j.envint.2019.105001

Egli, K., Fanger, U., Alvarez, P.J.J., Siegrist, H., Van der Meer, J.R., Zehnder, A.J.B., 2001. Enrichment and characterization of an anammox bacterium from a rotating biological contactor treating ammonium-rich leachate. Arch. Microbiol. 175, 198–207. https://doi.org/10.1007/s002030100255

Egli, T., 2010. How to live at very low substrate concentration. Water Res. 44, 4826–4837.

https://doi.org/10.1016/j.watres.2010.07.023

Elawwad, A., 2018. Optimized biological nitrogen removal of high-strength ammonium wastewater by activated sludge modeling. J. Water Reuse Desalin. 8, 393–403. https://doi.org/10.2166/wrd.2017.200

Elawwad, A., Zaghloul, M., Abdel-Halim, H., 2017. Simulation of municipal-industrial full scale WWTP in an arid climate by application of ASM3. J. Water Reuse Desalin. 7, 37–44. https://doi.org/10.2166/wrd.2016.154

Engelbrecht, S., Mozooni, M., Rathsack, K., Böllmann, J., Martienssen, M., 2019. Effect of increasing salinity to adapted and non-adapted Anammox biofilms. Environ. Technol. (United Kingdom) 40, 2880–2888. https://doi.org/10.1080/09593330.2018.1455748

EPA US, 2011. Reactive Nitrogen in the United States: an analysis of inputs, flows, consequences, and management options.

Erdim, E., Özkan, Z.Y., Kurt, H., Kocamemi, A., 2019. Overcoming challenges in mainstream Anammox applications: Utilization of nanoscale zero valent iron (nZVI). Sci. Total Environ. https://doi.org/10.1016/j.scitotenv.2018.09.140

Esparza-Soto, M., Westerhoff, P.K., 2001. Fluorescence spectroscopy and molecular weight distribution of extracellular polymers from full-scale activated sludge biomass, in: Water Science and Technology. IWA Publishing, pp. 87–95. https://doi.org/10.2166/wst.2001.0347

Fajardo, C., Mora, M., Fernández, I., Mosquera-Corral, A., Campos, J.L., Méndez, R., 2014. Cross effect of temperature, pH and free ammonia on autotrophic denitrification process with sulphide as electron donor. Chemosphere 97, 10–15. https://doi.org/10.1016/j.chemosphere.2013.10.028

Fang, F., Yang, M.-M., Wang, H., Yan, P., Chen, Y.-P., Guo, J.-S., 2018. Effect of high salinity in wastewater on surface properties of anammox granular sludge. Chemosphere 210, 366–375. https://doi.org/10.1016/j.chemosphere.2018.07.038

Farrés, J., Caminal, G., López-Santín, J., 1997. Influence of phosphate on rhamnose-containing exopolysaccharide theology and production by Klebsiella I-714. Appl. Microbiol. Biotechnol. 48, 522–527. https://doi.org/10.1007/s002530051090

Felz, S., Al-Zuhairy, S., Aarstad, O.A., van Loosdrecht, M.C.M., Lin, Y.M., 2016. Extraction of structural extracellular polymeric substances from aerobic granular sludge. J. Vis. Exp. 2016. https://doi.org/10.3791/54534

Feng, C., Lotti, T., Lin, Y., Malpei, F., 2019. Extracellular polymeric substances extraction and recovery from anammox granules: Evaluation of methods and protocol development. Chem. Eng. J. https://doi.org/10.1016/j.cej.2019.05.127

Feng, Y., Lu, X., Al-Hamzi, H., Makinia, J., 2017. An overview of the strategies for the deammonification process start-up and recovery after accidental operational failures. Rev. Environ. Sci. Bio/Technology.

Fernández, I., Dosta, J., Fajardo, C., Campos, J.L., Mosquera-Corral, A., Méndez, R., 2012.

Short- and long-term effects of ammonium and nitrite on the Anammox process. J. Environ. Manage. 95, S170–S174. https://doi.org/10.1016/j.jenvman.2010.10.044

Fernández, I., Vázquez-Padín, J.R., Mosquera-Corral, A., Campos, J.L., Méndez, R., 2008. Biofilm and granular systems to improve Anammox biomass retention. Biochem. Eng. J. 42, 308–313. https://doi.org/10.1016/j.bej.2008.07.011

Finore, I., Di Donato, P., Mastascusa, V., Nicolaus, B., Poli, A., 2014. Fermentation technologies for the optimization of marine microbial exopolysaccharide production. Mar. Drugs. https://doi.org/10.3390/md12053005

Flemming, H.-C., Wingender, J., Szewzyk, U., Steinberg, P., Rice, S.A., Kjelleberg, S., 2016. Biofilms: an emergent form of bacterial life. Nat. Rev. Microbiol. https://doi.org/10.1038/nrmicro.2016.94

Flemming, H.C., Wingender, J., 2010. The biofilm matrix. Nat. Rev. Microbiol. https://doi.org/10.1038/nrmicro2415

Flemming, H.C., Wuertz, S., 2019. Bacteria and archaea on Earth and their abundance in biofilms. Nat. Rev. Microbiol. 17, 247–260. https://doi.org/10.1038/s41579-019-0158-9

Freitas, F., Alves, V.D., Reis, M.A.M., 2011. Advances in bacterial exopolysaccharides: from production to biotechnological applications. Trends Biotechnol. https://doi.org/10.1016/j.tibtech.2011.03.008

Frølund, B., Palmgren, R., Keiding, K., Nielsen, P.H., 1996. Extraction of extracellular polymers from activated sludge using a cation exchange resin. Water Res. 30, 1749–1758. https://doi.org/10.1016/0043-1354(95)00323-1

Gaganis, P., 2009. Model calibration/parameter estimation techniques and conceptual model error, in: Uncertainties in Environmental Modelling and Consequences for Policy Making. Springer, Dordrecht, pp. 129–154. https://doi.org/10.1007/978-90-481-2636-1_6

Ganesan, S., Vadivelu, V.M., 2019. Study on the effect of external hydrazine addition on Anammox bacteria during the starvation period, in: AIP Conference Proceedings. American Institute of Physics Inc., p. 020038. https://doi.org/10.1063/1.5117098

Gao, D., Wang, X., Liang, H., Wei, Q., Dou, Y., Li, L., 2018. Anaerobic ammonia oxidizing bacteria: ecological distribution, metabolism, and microbial interactions. Front. Environ. Sci. Eng. https://doi.org/10.1007/s11783-018-1035-x

Ge, S., Peng, Y., Qiu, S., Zhu, A., Ren, N., 2014. Complete nitrogen removal from municipal wastewater via partial nitrification by appropriately alternating anoxic/aerobic conditions in a continuous plug-flow step feed process. Water Res. https://doi.org/10.1016/j.watres.2014.01.058

Gilbert, E.M., Agrawal, S., Brunner, F., Schwartz, T., Horn, H., Lackner, S., 2014a. Response of Different Nitrospira Species To Anoxic Periods Depends on Operational DO. Environ. Sci. Technol. 48, 2934–2941. https://doi.org/10.1021/es404992g

Gilbert, E.M., Agrawal, S., Karst, S.M., Horn, H., Nielsen, P.H., Lackner, S., 2014b. Low temperature partial nitritation/anammox in a moving bed biofilm reactor treating low

strength wastewater. Environ. Sci. Technol. 48, 8784–8792. https://doi.org/10.1021/es501649m

Gilbert, E.M., Agrawal, S., Schwartz, T., Horn, H., Lackner, S., 2015a. Comparing different reactor configurations for Partial Nitritation/ Anammox at low temperatures. Water Res. https://doi.org/10.1016/j.watres.2015.05.022

Gilbert, E.M., Agrawal, S., Schwartz, T., Horn, H., Lackner, S., 2015b. Comparing different reactor configurations for Partial Nitritation/ Anammox at low temperatures. Water Res. 81, 92–100. https://doi.org/10.1016/j.watres.2015.05.022

Gong, W.X., Wang, S.G., Sun, X.F., Liu, X.W., Yue, Q.Y., Gao, B.Y., 2008. Bioflocculant production by culture of Serratia ficaria and its application in wastewater treatment. Bioresour. Technol. 99, 4668–4674. https://doi.org/10.1016/j.biortech.2007.09.077

Gu, J., Zhang, M., Liu, Y., 2020. A review on mainstream deammonification of municipal wastewater: Novel dual step process. Bioresour. Technol. https://doi.org/10.1016/j.biortech.2019.122674

Guibaud, G., Tixier, N., Bouju, A., Baudu, M., 2003. Relation between extracellular polymers' composition and its ability to complex Cd, Cu and Pb. Chemosphere 52, 1701–1710. https://doi.org/10.1016/S0045-6535(03)00355-2

Guo, Jianhua, Peng, Y., Fan, L., Zhang, L., Ni, B.-J., Kartal, B., Feng, X., Jetten, M.S.M., Yuan, Z., 2016. Metagenomic analysis of anammox communities in three different microbial aggregates. Environ. Microbiol. 18, 2979–2993. https://doi.org/10.1111/1462-2920.13132

Guo, Jianbo, Wang, S., Lian, J., Hao Ngo, H., Guo, W., Liu, Y., Song, Y., 2016. Rapid start-up of the anammox process: Effects of five different sludge extracellular polymeric substances on the activity of anammox bacteria. Bioresour. Technol. https://doi.org/10.1016/j.biortech.2016.08.084

Guo, Q., Xing, B.-S., Li, P., Xu, J.-L., Yang, C.-C., Jin, R.-C., 2015. Anaerobic ammonium oxidation (anammox) under realistic seasonal temperature variations: Characteristics of biogranules and process performance. Bioresour. Technol. 192, 765–773. https://doi.org/10.1016/j.biortech.2015.06.049

Guo, X., Wang, X., Liu, J., 2016. Composition analysis of fractions of extracellular polymeric substances from an activated sludge culture and identification of dominant forces affecting microbial aggregation. Sci. Rep. 6. https://doi.org/10.1038/srep28391

Gustavsson, D., Persson, F., Jansen, J. la C., 2014. Manammox – mainstream anammox at Sjölunda WWTP, in: Proceedings from the IWA World Water Congress and Exhibition, September 21-26, Lisbon, Portugal.

Gustavsson, D.J.I., 2010. Biological sludge liquor treatment at municipal wastewater treatment plants-a review.

Güven, D., Dapena, A., Kartal, B., Schmid, M.C., Maas, B., van de Pas-Schoonen, K., Sozen, S., Mendez, R., Op den Camp, H.J.M., Jetten, M.S.M., Strous, M., Schmidt, I., 2005. Propionate oxidation by and methanol inhibition of anaerobic ammonium-oxidizing bacteria. Appl. Environ. Microbiol. 71, 1066–71. https://doi.org/10.1128/AEM.71.2.1066-

1071.2005

Han, M., De Clippeleir, H., Al-Omari, A., Wett, B., Vlaeminck, S.E., Bott, C., Murthy, S., 2016. Impact of carbon to nitrogen ratio and aeration regime on mainstream deammonification. Water Sci. Technol. 74, 375–384. https://doi.org/10.2166/wst.2016.202

Han, M, Vlaeminck, S.E., Al-Omari, A., Wett, B., Bott, C., Murthy, S., De Clippeleir, H., 2016. Uncoupling the solids retention times of flocs and granules in mainstream deammonification: A screen as effective out-selection tool for nitrite oxidizing bacteria. https://doi.org/10.1016/j.biortech.2016.08.115

Hao, X., Heijnen, J.J., Van Loosdrecht, M.C.M., 2002. Model-based evaluation of temperature and inflow variations on a partial nitrification-ANAMMOX biofilm process, Water Research.

He, S., Niu, Q., Ma, H., Zhang, Y., Li, Y.-Y., 2015a. The Treatment Performance and the Bacteria Preservation of Anammox: A Review. Water, Air, Soil Pollut. 226, 163. https://doi.org/10.1007/s11270-015-2394-6

He, S., Niu, Q., Ma, H., Zhang, Y., Li, Y.-Y., 2015b. The Treatment Performance and the Bacteria Preservation of Anammox: A Review. Water, Air, Soil Pollut.

He, S., Zhang, Y., Niu, Q., Ma, H., Li, Y.-Y., 2016. Operation stability and recovery performance in an Anammox EGSB reactor after pH shock. Ecol. Eng. 90, 50–56. https://doi.org/10.1016/j.ecoleng.2016.01.084

Hendrickx, T.L.G., Kampman, C., Zeeman, G., Temmink, H., Hu, Z., Kartal, B., Buisman, C.J.N., 2014. High specific activity for anammox bacteria enriched from activated sludge at 10 °C. Bioresour. Technol. https://doi.org/10.1016/j.biortech.2014.04.025

Hendrickx, T.L.G., Wang, Y., Kampman, C., Zeeman, G., Temmink, H., Buisman, C.J.N., 2012. Autotrophic nitrogen removal from low strength waste water at low temperature. Water Res. https://doi.org/10.1016/j.watres.2012.01.037

Henze, M., Loosdrecht, M., Ekama, G., Brdjanovic, D., 2008. Biological wastewater treatment : principles, modelling and design. IWA Pub.

Hippen, A., Rosenwinkel, K.H., Baumgarten, G., Seyfried, C.F., 1997. Aerobic deammonification: A new experience in the treatment of wastewaters, in: Water Science and Technology. Elsevier Science Ltd, pp. 111–120. https://doi.org/10.1016/S0273-1223(97)00211-4

Hira, D., Toh, H., Migita, C.T., Okubo, H., Nishiyama, T., Hattori, M., Furukawa, K., Fujii, T., 2012. Anammox organism KSU-1 expresses a NirK-type copper-containing nitrite reductase instead of a NirS-type with cytochrome *cd* $_1$. FEBS Lett. 586, 1658–1663. https://doi.org/10.1016/j.febslet.2012.04.041

Hollowed, M., Stec-Uddin, E., Zhao, H., McQuarrie, J., 2013. Evaluation of the Anita-Mox moving bed biofilm reactor process for sidestream deammonification at the Robert W. Hite treatment facility, Denver, Colorado. Proc. water environement Fed. water Assoc. Nutr. Remov. Recover.

Hou, X., Liu, S., Zhang, Z., 2015. Role of extracellular polymeric substance in determining the high aggregation ability of anammox sludge. Water Res. https://doi.org/10.1016/j.watres.2015.02.031

Hu, A., Zheng, P., Mahmood, Q., Zhang, L., Shen, L., Ding, S., 2010. Characteristics of nitrogenous substrate conversion by anammox enrichment. Bioresour. Technol. https://doi.org/10.1016/j.biortech.2010.07.015

Hu, Z., Lotti, T., de Kreuk, M., Kleerebezem, R., van Loosdrecht, M., Kruit, J., Jetten, M.S.M., Kartal, B., 2013. Nitrogen removal by a nitritation-anammox bioreactor at low temperature. Appl. Environ. Microbiol. 79, 2807–12. https://doi.org/10.1128/AEM.03987-12

Huang, P., Hogsett, M., Goel, R., 2011. The Robustness of ANAMMOX Communities Treating Full-Scale Sidestream Municipal Anaerobic Digester Filtrate, in: WEFTEC. https://doi.org/10.2175/193864711802721730

Huang, Q., Du, W.-L., Miao, L.-L., Liu, Y., Liu, Z.-P., 2018. Microbial community dynamics in an ANAMMOX reactor for piggery wastewater treatment with startup, raising nitrogen load, and stable performance. AMB Express 8, 156. https://doi.org/10.1186/s13568-018-0686-0

Hubaux, N., Wells, G., Morgenroth, E., 2014. Impact of coexistence of flocs and biofilm on performance of combined nitritation-anammox granular sludge reactors. Water Res. https://doi.org/10.1016/j.watres.2014.09.036

Hulsbeek, J.J.W., Kruit, J., Roeleveld, P.J., Van Loosdrecht, M.C.M., 2002. A practical protocol for dynamic modelling of activated sludge systems, in: Water Science and Technology. IWA Publishing, pp. 127–136. https://doi.org/10.2166/wst.2002.0100

Hurst, J.K., Lymar, S. V., 1997. Toxicity of Peroxynitrite and Related Reactive Nitrogen Species toward *Escherichia coli*. Chem. Res. Toxicol. 10, 802–810. https://doi.org/10.1021/tx970008v

Ibrahim, M., Yusof, N., Mohd Yusoff, M.Z., Hassan, M.A., 2016. Enrichment of anaerobic ammonium oxidation (anammox) bacteria for short start-up of the anammox process: a review. Desalin. Water Treat. 57, 13958–13978. https://doi.org/10.1080/19443994.2015.1063009

In ’t Zandt, M.H., De Jong, A.E.E., Slomp, C.P., Jetten, M.S.M., 2018. The hunt for the most-wanted chemolithoautotrophic spookmicrobes. FEMS Microbiol. Ecol. 94, 64. https://doi.org/10.1093/femsec/fiy064

Isaka, K., Sumino, T., Tsuneda, S., 2007. High nitrogen removal performance at moderately low temperature utilizing anaerobic ammonium oxidation reactions. J. Biosci. Bioeng. 103, 486–490. https://doi.org/10.1263/JBB.103.486

Iyer, A., Mody, K., Jha, B., 2006. Emulsifying properties of a marine bacterial exopolysaccharide. Enzyme Microb. Technol. 38, 220–222. https://doi.org/10.1016/j.enzmictec.2005.06.007

Izadi, Parin, Izadi, Parnian, Eldyasti, A., 2020a. Influence of microbial population dynamics on accelerated development of anammox micro-granular consortium. J. Water Process Eng. 36,

101384. https://doi.org/10.1016/j.jwpe.2020.101384

Izadi, Parin, Izadi, Parnian, Eldyasti, A., 2020b. Towards mainstream deammonification: Comprehensive review on potential mainstream applications and developed sidestream technologies. J. Environ. Manage. https://doi.org/10.1016/j.jenvman.2020.111615

Janiak, K., Miodonski, S., 2017. Failure of the side-stream deammonification process. Risk of violation of the WWTP effluent quality. Environ. Prot. Eng. https://doi.org/10.37190/epe180212

Jaqaman, K., Danuser, G., 2006. Linking data to models: Data regression. Nat. Rev. Mol. Cell Biol. https://doi.org/10.1038/nrm2030

Jardin, N., Hennerkes, J., 2012. Full-scale experience with the deammonification process to treat high strength sludge water - A case study. Water Sci. Technol. 65, 447–455. https://doi.org/10.2166/wst.2012.867

Jardin, N., Thöle, D., Wett, B., 2006. Treatment of sludge return liquors: Experiences from the operation of full-scale plants, in: Water Environment Federation, WEFTEC.

Jaroszynski, L.W., Cicek, N., Sparling, R., Oleszkiewicz, J.A., 2011. Importance of the operating pH in maintaining the stability of anoxic ammonium oxidation (anammox) activity in moving bed biofilm reactors. Bioresour. Technol. https://doi.org/10.1016/j.biortech.2011.04.069

Jeanningros, Y., Vlaeminck, S.E., Kaldate, A., Verstraete, W., Graveleau, L., 2010. Fast start-up of a pilot-scale deammonification sequencing batch reactor from an activated sludge inoculum. Water Sci. Technol. 61, 1393–1400. https://doi.org/10.2166/wst.2010.019

Jeannotte, R., 2014. Metabolic Pathways: Nitrogen Metabolism, in: Encyclopedia of Food Microbiology: Second Edition. Elsevier Inc., pp. 544–560. https://doi.org/10.1016/B978-0-12-384730-0.00199-3

Jetten, M.S.M., Niftrik, L. van, Strous, M., Kartal, B., Keltjens, J.T., Op den Camp, H.J.M., 2009. Biochemistry and molecular biology of anammox bacteria. Crit. Rev. Biochem. Mol. Biol. 44, 65–84. https://doi.org/10.1080/10409230902722783

Ji, X., Liu, Y., Zhang, J., Huang, D., Zhou, P., Zheng, Z., 2019. Development of model simulation based on BioWin and dynamic analyses on advanced nitrate nitrogen removal in deep bed denitrification filter. Bioprocess Biosyst. Eng. 42, 199–212. https://doi.org/10.1007/s00449-018-2025-x

Jia, F., Yang, Q., Liu, X., Li, X., Li, B., Zhang, L., Peng, Y., 2017. Stratification of Extracellular Polymeric Substances (EPS) for Aggregated Anammox Microorganisms. Environ. Sci. Technol. 51, 3260–3268. https://doi.org/10.1021/acs.est.6b05761

Jia, M., Solon, K., Vandeplassche, D., Venugopal, H., Volcke, E.I.P., 2019. Model-based evaluation of an integrated high-rate activated sludge and mainstream anammox system • Evaluation of an integrated HRAS. Chem. Eng. J. 382, 122878. https://doi.org/10.1016/j.cej.2019.122878

Jin, R.-C., Hu, B.-L., Zheng, P., Qaisar, M., Hu, A.-H., Islam, E., 2007. Quantitative comparison

of stability of ANAMMOX process in different reactor configurations. Bioresour. Technol. https://doi.org/10.1016/j.biortech.2007.04.018

Jin, R.-C., Ma, C., Yu, J.-J., 2013. Performance of an Anammox UASB reactor at high load and low ambient temperature. Chem. Eng. J. https://doi.org/10.1016/j.cej.2013.07.059

Jin, R.-C., Yang, G.-F., Yu, J.-J., Zheng, P., 2012. The inhibition of the Anammox process: A review. Chem. Eng. J. 197, 67–79. https://doi.org/10.1016/j.cej.2012.05.014

Jorand, F., Boue-Bigne, F., Block, J.C., Urbain, V., 1998. Hydrophobic/hydrophilic properties of activated sludge exopolymeric substances. Water Sci. ….

Joss, A., Derlon, N., Cyprien, C., Burger, S., Szivak, I., Traber, J., Siegrist, H., Morgenroth, E., 2011. Combined nitritation-anammox: Advances in understanding process stability. Environ. Sci. Technol. 45, 9735–9742. https://doi.org/10.1021/es202181v

Joss, A., Salzgeber, D., Eugster, J., König, R., Rottermann, K., Burger, S., Fabijan, P., Leumann, S., Mohn, J., Siegrist, H., 2009. Full-Scale Nitrogen Removal from Digester Liquid with Partial Nitritation and Anammox in One SBR. Environ. Sci. Technol. 43, 5301–5306. https://doi.org/10.1021/es900107w

Jung, J.Y., Kang, S.H., Chung, Y.C., Ahn, D.H., 2007. Factors affecting the activity of anammox bacteria during start up in the continuous culture reactor. Water Sci. Technol. 55, 459–468. https://doi.org/10.2166/wst.2007.023

Jung, J Y, Kang, S.H., Chung, Y.C., Ahn, D.H., 2007. Factors affecting the activity of anammox bacteria during start up in the continuous culture reactor. https://doi.org/10.2166/wst.2007.023

Kalkan Aktan, C., Yapsakli, K., Mertoglu, B., 2012. Inhibitory effects of free ammonia on Anammox bacteria. Biodegradation. https://doi.org/10.1007/s10532-012-9550-0

Kallistova, A.Y., Dorofeev, A.G., Nikolaev, Y.A., Kozlov, M.N., Kevbrina, M. V., Pimenov, N. V., 2016. Role of anammox bacteria in removal of nitrogen compounds from wastewater. Microbiology 85, 140–156. https://doi.org/10.1134/S0026261716020089

Kanders, L., 2019. Start-up and operational strategies for deammonification plants : - a study with one-stage moving bed biofilm reactors treating reject water. Mälardalen University.

Kanders, L., 2011. Swedish Experience of the Deammonification Process in a Biofilm System, in: Proceedings of the IWA/Water Environment Federation, Nutrient and Recovery Conference.

Kartal, B., Keltjens, J.T., Jetten, M.S., Kartal, B., Keltjens, J.T., Jetten, M.S., 2008. The Metabolism of Anammox, in: Encyclopedia of Life Sciences. John Wiley & Sons, Ltd, Chichester, UK. https://doi.org/10.1002/9780470015902.a0021315

Kartal, B., Kuypers, M.M.M., Lavik, G., Schalk, J., Op den Camp, H.J.M., Jetten, M.S.M., Strous, M., 2007. Anammox bacteria disguised as denitrifiers: nitrate reduction to dinitrogen gas via nitrite and ammonium. Environ. Microbiol. 9, 635–642. https://doi.org/10.1111/j.1462-2920.2006.01183.x

Kaur, R., Roy, D., Yellapu, S.K., Tyagi, R.D., Drogui, P., Surampalli, R.Y., 2019. Enhanced Composting Leachate Treatment Using Extracellular Polymeric Substances as Bioflocculant. J. Environ. Eng. 145, 04019075. https://doi.org/10.1061/(ASCE)EE.1943-7870.0001584

Kawaguchi, T., Decho, A.W., 2002. In situ analysis of carboxyl and sulfhydryl groups of extracellular polymeric secretions by confocal laser scanning microscopy. Anal. Biochem. 304, 266–267. https://doi.org/10.1006/abio.2002.5615

Kehrein, P., van Loosdrecht, M., Osseweijer, P., Garfí, M., Dewulf, J., Posada, J., 2020. A critical review of resource recovery from municipal wastewater treatment plants – market supply potentials, technologies and bottlenecks. Environ. Sci. Water Res. Technol. 6, 877–910. https://doi.org/10.1039/c9ew00905a

Khramenkov, S. V., Kozlov, M.N., Kevbrina, M. V., Dorofeev, A.G., Kazakova, E.A., Grachev, V.A., Kuznetsov, B.B., Polyakov, D.Y., Nikolaev, Y.A., 2013. A novel bacterium carrying out anaerobic ammonium oxidation in a reactor for biological treatment of the filtrate of wastewater fermented sludge. Microbiol. (Russian Fed. 82, 628–636. https://doi.org/10.1134/S002626171305007X

Khunjar, W.O., Jiang, D., Murthy, S., Wett, B., Chandran, K., 2011. Linking the Nitrogen and One-Carbon Cycles – The Impact of Inorganic Carbon Limitation on Ammonia Oxidation and Nitrogen Oxide Emission Rates in Ammonia Oxidizing Bacteria. Proc. Water Environ. Fed. 2011, 3199–3207. https://doi.org/10.2175/193864711802721848

Kimura, Y., Isaka, K., Kazama, F., Sumino, T., 2010. Effects of nitrite inhibition on anaerobic ammonium oxidation. Appl. Microbiol. Biotechnol. 86, 359–365. https://doi.org/10.1007/s00253-009-2359-z

Kjelleberg, S., Molin, S., 2002. Is there a role for quorum sensing signals in bacterial biofilms? Curr. Opin. Microbiol. https://doi.org/10.1016/S1369-5274(02)00325-9

Klaus, S., Baumler, R., Rutherford, B., Thesing, G., Zhao, H., Bott, C., 2017a. Startup of a Partial Nitritation-Anammox MBBR and the Implementation of pH-Based Aeration Control. Water Environ. Res. 89, 500–508. https://doi.org/10.2175/106143017x14902968254476

Klaus, S., Baumler, R., Rutherford, B., Thesing, G., Zhao, H., Bott, C., 2017b. Startup of a Partial Nitritation-Anammox MBBR and the Implementation of pH-Based Aeration Control. Water Environ. Res. 89, 500–508. https://doi.org/10.2175/106143017X14902968254476@10.1002/(ISSN)1554-7531.BEST-OF-WATER-ENVIRONMENT-RESEARCH

Klotz, M.G., Stein, L.Y., 2008. Nitrifier genomics and evolution of the nitrogen cycle. FEMS Microbiol. Lett. 278, 146–156. https://doi.org/10.1111/j.1574-6968.2007.00970.x

Kocamemi, B.A., Dityapak, D., Semerci, N., Keklik, E., Akarsubası, A., Kumru, M., Kurt, H., 2018. Anammox start-up strategies: the use of local mixed activated sludge seed versus Anammox seed. Water Sci. Technol. 78, 1901–1915. https://doi.org/10.2166/wst.2018.431

Komorowska-Kaufman, M., Majcherek, H., Klaczyński, E., 2006. Factors affecting the

biological nitrogen removal from wastewater. Process Biochem. 41, 1015–1021. https://doi.org/10.1016/j.procbio.2005.11.001

Koncar, V., 2019. Composites and hybrid structures, in: Smart Textiles for In Situ Monitoring of Composites. Woodhead Publishing, pp. 153–215. https://doi.org/10.1016/B978-0-08-102308-2.00002-4

Kostera, J., Youngblut, M.D., Slosarczyk, J.M., Pacheco, A.A., 2008. Kinetic and product distribution analysis of NO• reductase activity in Nitrosomonas europaea hydroxylamine oxidoreductase. J. Biol. Inorg. Chem. 13, 1073–1083. https://doi.org/10.1007/s00775-008-0393-4

Krampe, J., Leak, M., 2012. Strategic planning approach for optimising investment at WWTPs. Water Pract. Technol. https://doi.org/10.2166/wpt.2012.030

Kuai, L., Verstraete, W., 1998. Ammonium removal by the oxygen-limited autotrophic nitrification- denitrification system. Appl. Environ. Microbiol. 64, 4500–4506. https://doi.org/10.1128/aem.64.11.4500-4506.1998

Kuenen, J.G., 2020. Anammox and beyond. Environ. Microbiol. 22, 525–536. https://doi.org/10.1111/1462-2920.14904

Kuenen, J.G., 2008a. Anammox bacteria: from discovery to application. Nat. Rev. Microbiol. 6, 320–326. https://doi.org/10.1038/nrmicro1857

Kuenen, J.G., 2008b. Anammox bacteria: from discovery to application. Nat. Rev. Microbiol. 6, 320–326. https://doi.org/10.1038/nrmicro1857

Kumar, L.R., Zhang, X., Kaur, R., Yellapu, S.K., Tyagi, R.D., Drogui, P., 2020. Techno-economic analysis for extracellular-polymeric substances (EPS) production using activated sludge fortified with crude glycerol as substrate and its application in leachate treatment. Bioresour. Technol. 303, 122954. https://doi.org/10.1016/J.BIORTECH.2020.122954

Kumar, M., Lin, J.-G., 2010. Co-existence of anammox and denitrification for simultaneous nitrogen and carbon removal—Strategies and issues. J. Hazard. Mater. 178, 1–9. https://doi.org/10.1016/J.JHAZMAT.2010.01.077

Kumar Singha, T., 2012. Microbial Extracellular Polymeric Substances: Production, Isolation and Applications. IOSR J. Pharm. 2, 276–281.

Kunacheva, C., Stuckey, D.C., 2014. Analytical methods for soluble microbial products (SMP) and extracellular polymers (ECP) in wastewater treatment systems: A review. Water Re. https://doi.org/10.1016/j.watres.2014.04.044

Kwon, K.D., Green, H., Bjöörn, P., Kubicki, J.D., 2006. Model bacterial extracellular polysaccharide adsorption onto silica and alumina: Quartz crystal microbalance with dissipation monitoring of dextran adsorption. Environ. Sci. Technol. 40, 7739–7744. https://doi.org/10.1021/es061715q

L. G. J. M. van Dongen, M. S. M. Jetten, M.C.M. van L., 2001. The Combined Sharon/Anammox Process. IWA.

Laanbroek, H.J., Gerards, S., 1993. Competition for limiting amounts of oxygen between Nitrosomonas europaea and Nitrobacter winogradskyi grown in mixed continuous cultures. Arch. Microbiol. 159, 453–459. https://doi.org/10.1007/BF00288593

Lackner, S., Gilbert, E.M., Vlaeminck, S.E., Joss, A., Horn, H., van Loosdrecht, M.C.M., 2014. Full-scale partial nitritation/anammox experiences – An application survey. Water Res. 55, 292–303. https://doi.org/10.1016/J.WATRES.2014.02.032

Lackner, S., Thoma, K., Gilbert, E.M., Gander, W., Schreff, D., Horn, H., 2015. Start-up of a full-scale deammonification SBR-treating effluent from digested sludge dewatering. Water Sci. Technol. 71, 553–559. https://doi.org/10.2166/wst.2014.421

Lattner, D., Flemming, H.C., Mayer, C., 2003. 13C-NMR study of the interaction of bacterial alginate with bivalent cations. Int. J. Biol. Macromol. 33, 81–88. https://doi.org/10.1016/S0141-8130(03)00070-9

Laureni, M., Falås, P., Robin, O., Wick, A., Weissbrodt, D.G., Nielsen, J.L., Ternes, T.A., Morgenroth, E., Joss, A., 2016a. Mainstream partial nitritation and anammox: long-term process stability and effluent quality at low temperatures. Water Res. 101, 628–639. https://doi.org/10.1016/j.watres.2016.05.005

Laureni, M., Robin, O., Wick, A., Weissbrodt, D.G., Lund Nielsen, J., Ternes, T.A., Morgenroth, E., Joss, A., 2016b. Mainstream partial nitritation and anammox: long-term process stability and effluent quality at low temperatures. Water Res. 101, 628–639. https://doi.org/10.1016/j.watres.2016.05.005

Laureni, M., Robin, O., Wick, A., Weissbrodt, D.G., Lund Nielsen, J., Ternes, T.A., Morgenroth, E., Joss, A., 2016c. Mainstream partial nitritation and anammox: long-term process stability and effluent quality at low temperatures. Water Res. https://doi.org/10.1016/j.watres.2016.05.005

Laureni, M., Robin, O., Wick, A., Weissbrodt, D.G., Lund Nielsen, J., Ternes, T.A., Morgenroth, E., Joss, A., 2016d. Mainstream partial nitritation and anammox: long-term process stability and effluent quality at low temperatures. Water Res. https://doi.org/10.1016/j.watres.2016.05.005

Laureni, Michele, Weissbrodt, D.G., Sziv Ak, I., Robin, O., Lund Nielsen, J., Morgenroth, E., Joss, A., Laureni, M, 2015. Activity and growth of anammox biomass on aerobically pre-treated municipal wastewater. Water Res. https://doi.org/10.1016/j.watres.2015.04.026

Lauwers, J., Appels, L., Thompson, I.P., Degrève, J., Impe, J.F. Van, Dewil, R., 2013. Mathematical modelling of anaerobic digestion of biomass and waste : Power and limitations. Prog. Energy Combust. Sci. 39, 383–402. https://doi.org/10.1016/j.pecs.2013.03.003

Law, M., Jackson, D., 2016. Residual plots for linear regression models with censored outcome data: A refined method for visualizing residual uncertainty. Commun. Stat. - Simul. Comput. https://doi.org/10.1080/03610918.2015.1076470

Law, Y., Ye, L., Wang, Q., Hu, S., Pijuan, M., Yuan, Z., 2015. Producing free nitrous acid-A green and renewable biocidal agent-From anaerobic digester liquor. Chem. Eng. J.

https://doi.org/10.1016/j.cej.2014.07.138

Le, C., Stuckey, D.C., 2016. Colorimetric measurement of carbohydrates in biological wastewater treatment systems: A critical evaluation. https://doi.org/10.1016/j.watres.2016.03.008

Le, T., Massoudieh, A., Al-Omari, A., Murthy, S., Wett, B., Bott, C., De Clippelier, H., 2016. Controlling competition between anammox bacteria and denitrifiers for nitrite to obtain discharge limits after mainstream deammonification, in: WEFTEC .

Lemaire, R., Thomson, C., Zhao, H., Christensson, M., Veuillet, F., 2016. Mainstream Deammonification Using the ANITA^{TM} Mox Process, in: Proceedings of the Water Environment Federation. Water Environment Federation, pp. 282–292. https://doi.org/10.2175/193864716821125673

Lemaire, R., Webb, R.I., Yuan, Z., 2008. Micro-scale observations of the structure of aerobic microbial granules used for the treatment of nutrient-rich industrial wastewater. ISME J. 2, 528–541. https://doi.org/10.1038/ismej.2008.12

Lettinga, G., 1995. Anaerobic digestion and wastewater treatment systems. Antonie Van Leeuwenhoek 67, 3–28. https://doi.org/10.1007/BF00872193

Lewandowski, Z., Bakke, R., Characklis, W.G., 1987. Nitrification and Autotrophic Denitrification in Calcium Alginate Beads. Water Sci. Technol. 19, 175–182. https://doi.org/10.2166/wst.1987.0199

Li, J., Elliott, D., Nielsen, M., Healy, M.G., Zhan, X., 2011. Long-term partial nitrification in an intermittently aerated sequencing batch reactor (SBR) treating ammonium-rich wastewater under controlled oxygen-limited conditions. Biochem. Eng. J. 55, 215–222. https://doi.org/10.1016/j.bej.2011.05.002

Li, J., Qi, P., Qiang, Z., Dong, H., Gao, D., Wang, D., 2018. Is anammox a promising treatment process for nitrogen removal from nitrogen-rich saline wastewater? Bioresour. Technol. https://doi.org/10.1016/j.biortech.2018.08.115

Li, J., Wang, N., 2012. The gpsX gene encoding a glycosyltransferase is important for polysaccharide production and required for full virulence in Xanthomonas citri subsp. citri. BMC Microbiol. 12, 31. https://doi.org/10.1186/1471-2180-12-31

Li, W., Zheng, P., Wang, L., Zhang, M., Lu, H., Xing, Y., Zhang, J., Wang, R., Song, J., Ghulam, A., 2013. Physical characteristics and formation mechanism of denitrifying granular sludge in high-load reactor. Bioresour. Technol. https://doi.org/10.1016/j.biortech.2013.04.118

Li, X., Klaus, S., Bott, C., He, Z., 2018. Status, Challenges, and Perspectives of Mainstream Nitritation-Anammox for Wastewater Treatment. Water Environ. Res. 90, 634–649. https://doi.org/10.2175/106143017x15131012153112

Li, X., Logan, B.E., 2004. Analysis of bacterial adhesion using a gradient force analysis method and colloid probe atomic force microscopy. Langmuir 20, 8817–8822. https://doi.org/10.1021/la0488203

Li, X., Sun, S., Badgley, B.D., Sung, S., Zhang, H., He, Z., 2016. Nitrogen removal by granular nitritationeanammox in an upflow membrane-aerated biofilm reactor. Water Res. https://doi.org/10.1016/j.watres.2016.02.031

Li, X., Sun, Y., Wang, Z.W., He, Z., 2019. Theoretical understanding of the optimum conditions for a mainstream granular nitritation-anammox reactor coupled with anaerobic pretreatment. Sci. Total Environ. 669, 683–691. https://doi.org/10.1016/j.scitotenv.2019.03.117

Li, X.Y., Yang, S.F., 2007. Influence of loosely bound extracellular polymeric substances (EPS) on the flocculation, sedimentation and dewaterability of activated sludge. Water Res. 41, 1022–1030. https://doi.org/10.1016/j.watres.2006.06.037

Li, Y., Huang, Z., Ruan, W., Ren, H., Zhao, M., 2015. ANAMMOX performance, granulation, and microbial response under COD disturbance. J. Chem. Technol. Biotechnol. 90, 139–148. https://doi.org/10.1002/jctb.4298

Li, Z., Xu, X., Shao, B., Zhang, S., Yang, F., 2014. Anammox granules formation and performance in a submerged anaerobic membrane bioreactor. Chem. Eng. J. https://doi.org/10.1016/j.cej.2014.04.068

Limentani, G.B., Ringo, M.C., Ye, F., Bergquist, M.L., McSorley, E.O., 2005. Beyond the t-test: Statistical equivalence testing. Anal. Chem. https://doi.org/10.1021/ac053390m

Lin, Y.-M., Tay, J.-H., Liu, Y., Hung, Y.-T., 2009. Biological Nitrification and Denitrification Processes, in: Biological Treatment Processes. Humana Press, Totowa, NJ, pp. 539–588. https://doi.org/10.1007/978-1-60327-156-1_13

Lin, Y., Reino, C., Carrera, J., Pérez, J., van Loosdrecht, M.C.M., 2018. Glycosylated amyloid-like proteins in the structural extracellular polymers of aerobic granular sludge enriched with ammonium-oxidizing bacteria. Microbiologyopen 7, e00616. https://doi.org/10.1002/mbo3.616

Lindgren, S.E., Dobrogosz, W.J., 1990. Antagonistic activities of lactic acid bacteria in food and feed fermentations. FEMS Microbiol. Lett. 87, 149–164. https://doi.org/10.1111/j.1574-6968.1990.tb04885.x

Lindsay, D., Brözel, V.S., Mostert, J.F., Von Holy, A., 2000. Physiology of dairy-associated Bacillus spp. over a wide pH range. Int. J. Food Microbiol. 54, 49–62. https://doi.org/10.1016/S0168-1605(99)00178-6

Liu, G., Wang, J., 2012. Probing the stoichiometry of the nitrification process using the respirometric approach. Water Res. 46, 5954–5962. https://doi.org/10.1016/J.WATRES.2012.08.006

Liu, H., Fang, H.H.P., 2002. Extraction of extracellular polymeric substances (EPS) of sludges. J. Biotechnol. 95, 249–256. https://doi.org/10.1016/S0168-1656(02)00025-1

Liu, S., Zhang, Z., Ni, J., 2013. Effects of Ca2+ on activity restoration of the damaged anammox consortium. Bioresour. Technol. 143, 315–321. https://doi.org/10.1016/J.BIORTECH.2013.06.005

Liu, Y., Liu, Q.S., 2006. Causes and control of filamentous growth in aerobic granular sludge

sequencing batch reactors. Biotechnol. Adv. https://doi.org/10.1016/j.biotechadv.2005.08.001

Liu, Y., Ngo, H.H., Guo, W., Peng, L., Pan, Y., Guo, J., Chen, X., Ni, B.J., 2016. Autotrophic nitrogen removal in membrane-aerated biofilms: Archaeal ammonia oxidation versus bacterial ammonia oxidation. Chem. Eng. J. 302, 535–544. https://doi.org/10.1016/j.cej.2016.05.078

Liu, Y., Niu, Q., Wang, S., Ji, J., Zhang, Y., Yang, M., Hojo, T., Li, Y.Y., 2017. Upgrading of the symbiosis of Nitrosomanas and anammox bacteria in a novel single-stage partial nitritation–anammox system: Nitrogen removal potential and Microbial characterization. Bioresour. Technol. 244, 463–472. https://doi.org/10.1016/j.biortech.2017.07.156

Liwarska-Bizukojc, E., Biernacki, R., 2010. Identification of the most sensitive parameters in the activated sludge model implemented in BioWin software. Bioresour. Technol. https://doi.org/10.1016/j.biortech.2010.04.065

Liwarska-Bizukojc, E., Biernacki, R., Gendaszewska, D., Ledakowicz, S., 2013. Improving the operation of the full scale wastewater treatment plant with use of a complex activated sludge model. Environ. Prot. Eng. 39, 183–195. https://doi.org/10.5277/EPE130114

Lotti, T., Carretti, E., Berti, D., Montis, C., Del Buffa, S., Lubello, C., Feng, C., Malpei, F., 2019a. Hydrogels formed by anammox extracellular polymeric substances: Structural and mechanical insights. Sci. Rep. 9, 1–9. https://doi.org/10.1038/s41598-019-47987-8

Lotti, T., Carretti, E., Berti, D., Raffaella Martina, M., Lubello, C., Malpei, F., 2019b. Extraction, recovery and characterization of structural extracellular polymeric substances from anammox granular sludge. J. Environ. Manage. https://doi.org/10.1016/j.jenvman.2019.01.054

Lotti, T., Kleerebezem, R., Hu, Z., Kartal, B., de Kreuk, M.K., van Erp Taalman Kip, C., Kruit, J., Hendrickx, T.L.G., van Loosdrecht, M.C.M., 2015. Pilot-scale evaluation of anammox-based mainstream nitrogen removal from municipal wastewater. Environ. Technol. 36, 1167–1177. https://doi.org/10.1080/09593330.2014.982722

Lotti, T, Kleerebezem, R., Hu, Z., Kartal, B., Jetten, M., Van Loosdrecht, M.C.M., 2014. Simultaneous partial nitritation and anammox at low temperature with granular sludge. Water Res. https://doi.org/10.1016/j.watres.2014.07.047

Lotti, T., Kleerebezem, R., Hu, Z., Kartal, B., Jetten, M.S.M., van Loosdrecht, M.C.M., 2014. Simultaneous partial nitritation and anammox at low temperature with granular sludge. Water Res. 66, 111–121. https://doi.org/10.1016/J.WATRES.2014.07.047

Luo, J., Chen, H., Han, X., Sun, Y., Yuan, Z., Guo, J., 2017. Microbial community structure and biodiversity of size-fractionated granules in a partial nitritation-anammox process. FEMS Microbiol. Ecol. 93, 21. https://doi.org/10.1093/femsec/fix021

Luzi, F., Torre, L., Kenny, J.M., Puglia, D., 2019. Bio- and Fossil-Based Polymeric Blends and Nanocomposites for Packaging: Structure–Property Relationship. Materials (Basel). 12. https://doi.org/10.3390/MA12030471

Lv, Y., Pan, J., Huo, T., Zhao, Y., Liu, S., 2019. Enhanced microbial metabolism in one stage

partial nitritation-anammox system treating low strength wastewater by novel composite carrier. Water Res. https://doi.org/10.1016/j.watres.2019.114872

Ma, B., Peng, Y., Zhang, S., Wang, J., Gan, Y., Chang, J., Wang, Shuying, Wang, Shanyun, Zhu, G., 2013. Performance of anammox UASB reactor treating low strength wastewater under moderate and low temperatures. Bioresour. Technol. 129, 606–611. https://doi.org/10.1016/J.BIORTECH.2012.11.025

Ma, B., Wang, S., Cao, S., Miao, Y., Jia, F., Du, R., Peng, Y., 2016. Biological nitrogen removal from sewage via anammox: Recent advances. Bioresour. Technol. 200, 981–990. https://doi.org/10.1016/j.biortech.2015.10.074

Ma, H., Niu, Q., Zhang, Y., He, S., Li, Y.Y., 2017. Substrate inhibition and concentration control in an UASB-Anammox process. Bioresour. Technol. 238, 263–272. https://doi.org/10.1016/j.biortech.2017.04.017

Ma, W., Li, G., Huang, B., Jin, R., 2020. Advances and challenges of mainstream nitrogen removal from municipal wastewater with anammox-based processes. Water Environ. Res. wer.1342. https://doi.org/10.1002/wer.1342

MacLeod, F.A., Guiot, S.R., Costerton, J.W., 1995. Electron microscopic examination of the extracellular polymeric substances in anaerobic granular biofilms. World J. Microbiol. Biotechnol. 11, 481–485. https://doi.org/10.1007/BF00286356

Makinia, J., 2010. Mathematical Modelling and Computer Simulation of Activated Sludge Systems. IWA Publishing.

Malovanyy, A., Trela, J., Plaza, E., 2015. Mainstream wastewater treatment in integrated fixed film activated sludge (IFAS) reactor by partial nitritation/anammox process. Bioresour. Technol. https://doi.org/10.1016/j.biortech.2015.08.123

Manca, M.C., Lama, L., Improta, R., Esposito, E., Gambacorta, A., Nicolaus, B., 1996. Chemical composition of two exopolysaccharides from Bacillus thermoantarcticus. Appl. Environ. Microbiol. 62, 3265–3269. https://doi.org/10.1128/aem.62.9.3265-3269.1996

Manser, R., Gujer, W., Siegrist, H., 2005. Consequences of mass transfer effects on the kinetics of nitrifiers. Water Res. 39, 4633–4642. https://doi.org/10.1016/J.WATRES.2005.09.020

Mao, N., Ren, H., Geng, J., Ding, L., Xu, · Ke, 2017. Engineering application of anaerobic ammonium oxidation process in wastewater treatment. World J. Microbiol. Biotechnol. 33, 153. https://doi.org/10.1007/s11274-017-2313-7

Marsaglia, G., Tsang, W.W., Wang, J., 2003. Evaluating Kolmogorov's Distribution. J. Stat. Softw. 8.

Massey, F.J., 1951. The Kolmogorov-Smirnov Test for Goodness of Fit. J. Am. Stat. Assoc.

Mattei, M.R., Frunzo, L., D'acunto, B., Esposito, G., Pirozzi, F., 2015. Modelling microbial population dynamics in multispecies biofilms including Anammox bacteria. Ecol. Modell. 304, 44–58. https://doi.org/10.1016/j.ecolmodel.2015.02.007

Mayer, C., Moritz, R., Kirschner, C., Borchard, W., Maibaum, R., Wingender, J., Flemming, H.-

C., 1999. The role of intermolecular interactions: studies on model systems for bacterial biofilms, International Journal of Biological Macromolecules.

Metcalf, L., Eddy, H., Tchobanoglous, G., 2003. Wastewater engineering: treatment, disposal, and reuse.

Miao, L., Yang, G., Tao, T., Peng, Y., 2019. Recent advances in nitrogen removal from landfill leachate using biological treatments – A review. J. Environ. Manage. https://doi.org/10.1016/j.jenvman.2019.01.057

Miao, L., Zhang, Q., Wang, S., Li, B., Wang, Z., Zhang, S., Zhang, M., Peng, Y., 2018. Characterization of EPS compositions and microbial community in an Anammox SBBR system treating landfill leachate. Bioresour. Technol. 249, 108–116. https://doi.org/10.1016/j.biortech.2017.09.151

Miao, Y., Zhang, J., Peng, Y., Wang, S., 2019. An improved start-up strategy for mainstream anammox process through inoculating ordinary nitrification sludge and a small amount of anammox sludge. J. Hazard. Mater. https://doi.org/10.1016/j.jhazmat.2019.121325

Michael T., M., John M., M., Paul V., D., David P., C., 2008. Brock Biology of Microoorganisms.

Mokhtarzadeh, A., Alibakhshi, A., Hejazi, M., Omidi, Y., Ezzati Nazhad Dolatabadi, J., 2016. Bacterial-derived biopolymers: Advanced natural nanomaterials for drug delivery and tissue engineering. TrAC - Trends Anal. Chem. https://doi.org/10.1016/j.trac.2016.06.013

Molina-Ramírez, C., Castro, M., Osorio, M., Torres-Taborda, M., Gómez, B., Zuluaga, R., Gómez, C., Gañán, P., Rojas, O.J., Castro, C., 2017. Effect of different carbon sources on bacterial nanocellulose production and structure using the low pH resistant strain Komagataeibacter medellinensis. Materials (Basel). 10, 639. https://doi.org/10.3390/ma10060639

Molinuevo, B., Garcia, M., Karakashev, D., Angelidaki, I., 2009. Anammox for ammonia removal from pig manure effluents: Effect of organic matter content on process performance. Bioresour. Technol. 100, 2171–2175. https://doi.org/10.1016/j.biortech.2008.10.038

Monfet, E., Aubry, G., Ramirez, A.A., 2018. Nutrient removal and recovery from digestate: a review of the technology. Biofuels. https://doi.org/10.1080/17597269.2017.1336348

Monsan, P., Bozonnet, S., Albenne, C., Joucla, G., Willemot, R.M., Remaud-Siméon, M., 2001. Homopolysaccharides from lactic acid bacteria. Int. Dairy J. 11, 675–685. https://doi.org/10.1016/S0958-6946(01)00113-3

Morales, N., 2014. Novel technologies for WWTP optimization in footprint, nutrients valorization, and energy consumption.

Morales, N., Val Del Río, A., Vázquez-Padín, J.R., Gutiérrez, R., Fernández-González, R., Icaran, P., Rogalla, F., Campos, J.L., Méndez, R., Mosquera-Corral, A., 2015. Influence of dissolved oxygen concentration on the start-up of the anammox-based process: ELAN®. Water Sci. Technol. 72, 520–527. https://doi.org/10.2166/wst.2015.233

More, T T, Yadav, J.S.S., Yan, S., Tyagi, R.D., Surampalli, R.Y., 2014. Extracellular polymeric substances of bacteria and their potential environmental applications. J. Environ. Manage. 144. https://doi.org/10.1016/j.jenvman.2014.05.010

More, T. T., Yadav, J.S.S., Yan, S., Tyagi, R.D., Surampalli, R.Y., 2014. Extracellular polymeric substances of bacteria and their potential environmental applications. J. Environ. Manage. https://doi.org/10.1016/j.jenvman.2014.05.010

More, T.T., Yan, S., Tyagi, R.D., Surampalli, R.Y., 2010. Potential use of filamentous fungi for wastewater sludge treatment. Bioresour. Technol. https://doi.org/10.1016/j.biortech.2010.05.033

Morgan, J.W., Forster, C.F., Evison, L., 1990. A comparative study of the nature of biopolymers extracted from anaerobic and activated sludges. Water Res. 24, 743–750. https://doi.org/10.1016/0043-1354(90)90030-A

Morrison, C., Heitmann, E., Armiger, W., Dodds, D., Koffas, M., 2018. Electrochemical Bioreactor Technology for Biocatalysis and Microbial Electrosynthesis. Adv. Appl. Microbiol. 105, 51–86. https://doi.org/10.1016/BS.AAMBS.2018.07.001

Mota, C.R., Head, M.A., Williams, J.C., Eland, L., Cheng, J.J., de los Reyes, F.L., 2014. Structural integrity affects nitrogen removal activity of granules in semi-continuous reactors. Biodegradation 25, 923–934. https://doi.org/10.1007/s10532-014-9712-3

Moussa, M.S., Rojas, A.R., Hooijmans, C.M., Gijzen, H.J., van Loosdrecht, M.C.M., 2004. Model-based evaluation of nitrogen removal in a tannery wastewater treatment plant. Water Sci. Technol. 50, 251–260. https://doi.org/10.2166/wst.2004.0383

Mulder, A., 1989. Anoxic ammonia oxidation.

Neethling, J., 2014. Deammonification.

Negulescu, M., 2011. Municipal Waste Water Treatment [WWW Document]. Elsevier. URL https://books.google.ca/books?hl=en&lr=&id=DyZMsfSRL-QC&oi=fnd&pg=PP1&dq=Negulescu+M+(2011)+Municipal+Wastewater+Treatment&ots=m2JzAFl75l&sig=-DDYGddryYQ8XHqQ5nQ2t0ul1sA#v=onepage&q=Negulescu M (2011) Municipal Wastewater Treatment&f=false (accessed 4.27.20).

Neu, T., Kuhlicke, U., 2017. Fluorescence Lectin Bar-Coding of Glycoconjugates in the Extracellular Matrix of Biofilm and Bioaggregate Forming Microorganisms. Microorganisms 5, 5. https://doi.org/10.3390/microorganisms5010005

Neu, T.R., Lawrence, J.R., 1999. In Situ Characterization of Extracellular Polymeric Substances (EPS) in Biofilm Systems, in: Microbial Extracellular Polymeric Substances. Springer Berlin Heidelberg, pp. 21–47. https://doi.org/10.1007/978-3-642-60147-7_2

Ni, B.-J., Chen, Y.-P., Liu, S.-Y., Fang, F., Xie, W.-M., Yu, H.-Q., 2009. Modeling a granule-based anaerobic ammonium oxidizing (ANAMMOX) process. Biotechnol. Bioeng. 103, 490–499. https://doi.org/10.1002/bit.22279

Ni, B.J., Hu, B.L., Fang, F., Xie, W.M., Kartal, B., Liu, X.W., Sheng, G.P., Jetten, M., Zheng, P., Yu, H.Q., 2010. Microbial and physicochemical characteristics of compact anaerobic

ammonium-oxidizing granules in an upflow anaerobic sludge blanket reactor. Appl. Environ. Microbiol. 76, 2652–2656. https://doi.org/10.1128/AEM.02271-09

Ni, B.J., Joss, A., Yuan, Z., 2014. Modeling nitrogen removal with partial nitritation and anammox in one floc-based sequencing batch reactor. Water Res. 67, 321–329. https://doi.org/10.1016/j.watres.2014.09.028

Ni, S.Q., Sun, N., Yang, H., Zhang, J., Ngo, H.H., 2015. Distribution of extracellular polymeric substances in anammox granules and their important roles during anammox granulation. Biochem. Eng. J. 101, 126–133. https://doi.org/10.1016/j.bej.2015.05.014

Nifong, A., Nelson, A., Johnson, C., Bott, C.B., 2013. Performance of a Full-Scale Sidestream DEMON® Deammonification Installation, in: 86th Annual Water Environment Federation Technical Exhibition and Conference.

Niftrik, L.A., Fuerst, J.A., Damste, J.S.S., Kuenen, J.G., Jetten, M.S.M., Strous, M., 2004. The anammoxosome: an intracytoplasmic compartment in anammox bacteria. FEMS Microbiol. Lett. 233, 7–13. https://doi.org/10.1016/j.femsle.2004.01.044

Nontembiso, P., Sekelwa, C., Leonard, M. V., Anthony, O.I., 2011. Assessment of Bioflocculant Production by Bacillus sp. Gilbert, a Marine Bacterium Isolated from the Bottom Sediment of Algoa Bay. Mar. Drugs 9, 1232–1242. https://doi.org/10.3390/md9071232

Nsenga Kumwimba, M., Lotti, T., Şenel, E., Li, X., Suanon, F., 2020. Anammox-based processes: How far have we come and what work remains? A review by bibliometric analysis. Chemosphere. https://doi.org/10.1016/j.chemosphere.2019.124627

Nurunnabi, A.A.M., Nasser, M., Imon, A.H.M.R., 2016. Identification and classification of multiple outliers, high leverage points and influential observations in linear regression. J. Appl. Stat. 43, 509–525. https://doi.org/10.1080/02664763.2015.1070806

O'Shaughnessy, Maureen, 2016. Mainstream Deammonification . IWA Publishing.

O'Shaughnessy, M., 2016. Mainstream Deammonification. Water Intell. Online 15, 9781780407852–9781780407852. https://doi.org/10.2166/9781780407852

O'Shaughnessy, M., Sizemore, J., Musabyimana, M., Sanjines, P., Murthy, S., Wett, B., Takács, I., Houweling, D., Love, N.G., Pallansch, K., 2012. OPERATIONS AND PROCESS CONTROL OF THE DEAMMONIFICATION (DEMON) PROCESS AS A SIDESTREAM OPTION FOR NUTRIENT REMOVAL. Proc. Water Environ. Fed. 2008, 6333–6348. https://doi.org/10.2175/193864708788809743

Okutani, K., 1985. Antitumor and immunostimulant activities [to mice] of polysaccharide produced by a marine bacterium of the genus Vibrio. Bull. Japanese Soc. Sci. Fish.

Omoike, A., Chorover, J., 2004. Spectroscopic study of extracellular polymeric substances from Bacillus subtilis: Aqueous chemistry and adsorption effects. Biomacromolecules. https://doi.org/10.1021/bm034461z

Orner, T.G., De Donato, P., El" Ene Ameil, M.-H., Montarges-Pelletier, E., Lartiges, B.S., 2003. Activated sludge exopolymers: separation and identification using size exclusion chromatography and infrared micro-spectroscopy. Water Res. 37, 2388–2393.

https://doi.org/10.1016/S0043-1354(02)00553-5

Ortega-Morales, B.O., Santiago-García, J.L., Chan-Bacab, M.J., Moppert, X., Miranda-Tello, E., Fardeau, M.L., Carrero, J.C., Bartolo-Pérez, P., Valadéz-González, A., Guezennec, J., 2007. Characterization of extracellular polymers synthesized by tropical intertidal biofilm bacteria. J. Appl. Microbiol. 102, 254–264. https://doi.org/10.1111/j.1365-2672.2006.03085.x

Oshiki, M., Ali, M., Shinyako-Hata, K., Satoh, H., Okabe, S., 2016. Hydroxylamine-dependent anaerobic ammonium oxidation (anammox) by " Candidatus Brocadia sinica." Environ. Microbiol. 18, 3133–3143. https://doi.org/10.1111/1462-2920.13355

Oshiki, M., Shimokawa, M., Fujii, N., Satoh, H., Okabe, S., 2011. Physiological characteristics of the anaerobic ammonium-oxidizing bacterium "Candidatus Brocadia sinica." Microbiology 157, 1706–1713. https://doi.org/10.1099/mic.0.048595-0

Papenfort, K., Bassler, B.L., 2016. Quorum sensing signal-response systems in Gram-negative bacteria. Nat. Rev. Microbiol. https://doi.org/10.1038/nrmicro.2016.89

Park, C., Novak, J.T., 2009. Characterization of Lectins and Bacterial Adhesins in Activated Sludge Flocs. Water Environ. Res. 81, 755–764. https://doi.org/10.2175/106143008X370421

Park, H., Rosenthal, A., Jezek, R., Ramalingam, K., Fillos, J., Chandran, K., 2010. Impact of inocula and growth mode on the molecular microbial ecology of anaerobic ammonia oxidation (anammox) bioreactor communities 5. Water Res. https://doi.org/10.1016/j.watres.2010.07.022

Park, H., Sundar, S., Ma, Y., Chandran, K., 2015. Differentiation in the microbial ecology and activity of suspended and attached bacteria in a nitritation-anammox process. Biotechnol. Bioeng. 112, 272–279. https://doi.org/10.1002/bit.25354

Péant, B., LaPointe, G., Gilbert, C., Atlan, D., Ward, P., Roy, D., 2005. Comparative analysis of the exopolysaccharide biosynthesis gene clusters from four strains of Lactobacillus rhamnosus. Microbiology 151, 1839–1851. https://doi.org/10.1099/mic.0.27852-0

Pedrouso, A., Aiartza, I., Morales, N., Vázquez-Padín, J.R., Rogalla, F., Campos, J.L., Mosquera-Corral, A., Val, A., Rio, D., 2018. Pilot-scale ELAN ® process applied to treat primary settled urban wastewater at low temperature via partial nitritation-anammox processes. Sep. Purif. Technol. https://doi.org/10.1016/j.seppur.2018.02.017

Pedrouso, A., Trela, J., Val Del Rio, A., Mosquera-Corral, A., Plaza, E., 2019. Performance of partial nitritation-anammox processes at mainstream conditions in an IFAS system. J. Environ. Manage. https://doi.org/10.1016/j.jenvman.2019.109538

Pereira, A.D., Cabezas, A., Etchebehere, C., Chernicharo, C.A. de L., de Araújo, J.C., 2017. Microbial communities in anammox reactors: a review. Environ. Technol. Rev. 6, 74–93. https://doi.org/10.1080/21622515.2017.1304457

Pereira, A.D., Fernandes, L. de A., Castro, H.M.C., Leal, C.D., Carvalho, B.G.P., Dias, M.F., Nascimento, A.M.A., Chernicharo, C.A. de L., Araújo, J.C. de, 2019. Nitrogen removal from food waste digestate using partial nitritation-anammox process: Effect of different

aeration strategies on performance and microbial community dynamics. J. Environ. Manage. 251, 109562. https://doi.org/10.1016/j.jenvman.2019.109562

Pereira, S.B., Mota, R., Vieira, C.P., Vieira, J., Tamagnini, P., 2015. Phylum-wide analysis of genes/proteins related to the last steps of assembly and export of extracellular polymeric substances (EPS) in cyanobacteria. Sci. Rep. 5, 14835. https://doi.org/10.1038/srep14835

Pérez, J., Lotti, T., Kleerebezem, R., Picioreanu, C., van Loosdrecht, M.C.M., 2014. Outcompeting nitrite-oxidizing bacteria in single-stage nitrogen removal in sewage treatment plants: A model-based study. Water Res. 66, 208–218. https://doi.org/10.1016/J.WATRES.2014.08.028

Pijuan, M., Ribera-Guardia, A., Luís Balcázar, J., Micó, M.M., De La Torre, T., 2020. Effect of COD on mainstream anammox: Evaluation of process performance, granule morphology and nitrous oxide production. Sci. Total Environ. J. https://doi.org/10.1016/j.scitotenv.2019.136372

Plaza, E., Stridh, S., Örnmark, J., Kanders, L., Trela, J., 2011. Swedish Experience of the Deammonification Process in a Biofilm System. Proc. Water Environ. Fed. 2011, 1067–1079. https://doi.org/10.2175/193864711802867397

Polli, E., 2019. Exploring the Conversion of Tertiary Denitrification to Mainstream Deammonification: Pilot Scale Filter Results and Challenges. North Carolina State University.

Qiu, S., Li, Z., Hu, Y., Shi, Lin, Liu, R., Shi, Lei, Chen, L., Zhan, X., 2020. What's the best way to achieve successful mainstream partial nitritation-anammox application? Crit. Rev. Environ. Sci. Technol. 1–33. https://doi.org/10.1080/10643389.2020.1745015

Rattray, J.E., Strous, M., Op den Camp, H.J., Schouten, S., Jetten, M.S., Damsté, J., 2009. A comparative genomics study of genetic products potentially encoding ladderane lipid biosynthesis. Biol. Direct 4, 8. https://doi.org/10.1186/1745-6150-4-8

Rattray, J.E., Van De Vossenberg, J., Hopmans, E.C., Kartal, B., Van Niftrik, L., Rijpstra, W.I.C., Strous, M., Jetten, M.S.M., Schouten, S., Damsté, J.S.S., 2008. Ladderane lipid distribution in four genera of anammox bacteria. Arch. Microbiol. 190, 51–66. https://doi.org/10.1007/s00203-008-0364-8

Regmi, P., Miller, M.W., Holgate, B., Bunce, R., Park, H., Chandran, K., Wett, B., Murthy, S., Bott, C.B., 2014. Control of aeration, aerobic SRT and COD input for mainstream nitritation/denitritation. Water Res. 57, 162–171. https://doi.org/10.1016/J.WATRES.2014.03.035

Rehm, B.H.A., 2010. Bacterial polymers: Biosynthesis, modifications and applications. Nat. Rev. Microbiol. https://doi.org/10.1038/nrmicro2354

Reino, C., Suárez-Ojeda, M.E., Pérez, J., Carrera, J., 2018. Stable long-term operation of an upflow anammox sludge bed reactor at mainstream conditions. Water Res. 128, 331–340. https://doi.org/10.1016/J.WATRES.2017.10.058

Rezania, B., Mavinic, D.S., Kelly, H.G., 2015. Long-term performance of side-stream deammonification in a continuous flow granular-activated sludge process for nitrogen

removal from high ammonium wastewater. Water Sci. Technol. 71, 1241–1248. https://doi.org/10.2166/wst.2015.096

Rikmann, E., Zekker, I., Tenno, Taavo, Saluste, A., Tenno, Toomas, 2017. Inoculum-free start-up of biofilm- and sludge-based deammonification systems in pilot scale. Int. J. Environ. Sci. Technol.

Rios-Del Toro, E.E., Cervantes, F.J., 2016. Coupling between anammox and autotrophic denitrification for simultaneous removal of ammonium and sulfide by enriched marine sediments. Biodegradation 27, 107–118. https://doi.org/10.1007/s10532-016-9759-4

Rosenwinkel, K.-H., Cornelius, A., 2005. Deammonification in the Moving-Bed Process for the Treatment of Wastewater with High Ammonia Content. Chem. Eng. Technol. https://doi.org/10.1002/ceat.200407070

Sandhya, V., Ali, S.Z., 2015. The production of exopolysaccharide by Pseudomonas putida GAP-P45 under various abiotic stress conditions and its role in soil aggregation. Microbiol. (Russian Fed. 84, 512–519. https://doi.org/10.1134/S0026261715040153

Scheuerl, T., Hopkins, M., Nowell, R.W., Rivett, D.W., Barraclough, T.G., Bell, T., 2020. Bacterial adaptation is constrained in complex communities. Nat. Commun. 11, 1–8. https://doi.org/10.1038/s41467-020-14570-z

Schmid, J., Sieber, V., 2015. Enzymatic Transformations Involved in the Biosynthesis of Microbial Exo-Polysaccharides Based on the Assembly of Repeat Units. ChemInform 46, no-no. https://doi.org/10.1002/chin.201528308

Schmid, J., Sieber, V., Rehm, B., 2015. Bacterial exopolysaccharides: Biosynthesis pathways and engineering strategies. Front. Microbiol. https://doi.org/10.3389/fmicb.2015.00496

Sengupta, D., Datta, S., Biswas, D., 2018. Towards a better production of bacterial exopolysaccharides by controlling genetic as well as physico-chemical parameters. Appl. Microbiol. Biotechnol. https://doi.org/10.1007/s00253-018-8745-7

Seviour, T., Derlon, N., Dueholm, M.S., Flemming, H.-C., Girbal-Neuhauser, E., Horn, H., Kjelleberg, S., Van Loosdrecht, M.C.M., Lotti, T., Malpei, M.F., Nerenberg, R., Neu, T.R., Paul, E., Yu, H., Lin, Y., 2019. Extracellular polymeric substances of biofilms: Suffering from an identity crisis. Water Res. https://doi.org/10.1016/j.watres.2018.11.020

Seviour, T., Derlon, N., Dueholm, M.S., Flemming, H.-C., Girbal-Neuhauser, E., Horn, H., Kjelleberg, S., Van Loosdrecht, M.C.M., Lotti, T., Malpei, M.F., Nerenberg, R., Neu, T.R., Paul, E., Yu, H., Lin, Y., 2018. Making Waves Extracellular polymeric substances of biofilms: Suffering from an identity crisis. Water Res. https://doi.org/10.1016/j.watres.2018.11.020

Seyfried, C.F., Rosenwinkel, K.-H., Hippen, A., 2002. DEAMMONIFICATION: A COST-EFFECTIVE TREATMENT PROCESS FOR NITROGEN-RICH WASTEWATERS. Proc. Water Environ. Fed. 2002, 69–84. https://doi.org/10.2175/193864702784900200

Sheng, G.-P., Yu, H.-Q., Li, X.-Y., 2010. Extracellular polymeric substances (EPS) of microbial aggregates in biological wastewater treatment systems: A review. Biotechnol. Adv. https://doi.org/10.1016/j.biotechadv.2010.08.001

Sheng, G.P., Yu, H.Q., 2006. Relationship between the extracellular polymeric substances and surface characteristics of Rhodopseudomonas acidophila. Appl. Microbiol. Biotechnol. 72, 126–131. https://doi.org/10.1007/s00253-005-0225-1

Sheng, G.P., Yu, H.Q., Yu, Z., 2005. Extraction of extracellular polymeric substances from the photosynthetic bacterium Rhodopseudomonas acidophila. Appl. Microbiol. Biotechnol. 67, 125–130. https://doi.org/10.1007/s00253-004-1704-5

Sheng, G.P., Yu, H.Q., Yue, Z., 2006. Factors influencing the production of extracellular polymeric substances by Rhodopseudomonas acidophila. Int. Biodeterior. Biodegrad. 58, 89–93. https://doi.org/10.1016/j.ibiod.2006.07.005

Shi, Y., Wells, G., Morgenroth, E., 2016. Microbial activity balance in size fractionated suspended growth biomass from full-scale sidestream combined nitritation-anammox reactors. Bioresour. Technol. 218, 38–45. https://doi.org/10.1016/j.biortech.2016.06.041

Shimamura, M., Nishiyama, T., Shigetomo, H., Toyomoto, T., Kawahara, Y., Furukawa, K., Fujii, T., 2006. Title: Isolation of a multiheme protein from an anaerobic ammonium-oxidizing enrichment culture with features of a hydrazine-oxidizing enzyme Running title: hydrazine-oxidizing enzyme from an anammox reactor. Appl. Environ. Microbiol. https://doi.org/10.1128/AEM.01978-06

Shu, C.H., Lung, M.Y., 2004. Effect of pH on the production and molecular weight distribution of exopolysaccharide by Antrodia camphorata in batch cultures. Process Biochem. 39, 931–937. https://doi.org/10.1016/S0032-9592(03)00220-6

Siegrist, H., Reithaar, S., Koch, G., Lais, P., 1998. Nitrogen loss in a nitrifying rotating contactor treating ammonium-rich wastewater without organic carbon. Water Sci. Technol. 38, 241–248. https://doi.org/10.1016/S0273-1223(98)00698-2

Sin, G., Kaelin, D., Kampschreur, M.J., Takács, I., Wett, B., Gernaey, K. V., Rieger, L., Siegrist, H., Van Loosdrecht, M.C.M., 2008. Modelling nitrite in wastewater treatment systems: A discussion of different modelling concepts. Water Sci. Technol. 58, 1155–1171. https://doi.org/10.2166/wst.2008.485

Sleytr, U.B., 1997. I. Basic and applied S-layer research: an overview. FEMS Microbiol. Rev. 20, 5–12. https://doi.org/10.1111/j.1574-6976.1997.tb00301.x

Sleytr, U.B., Schuster, B., Egelseer, E.M., Pum, D., 2014. S-layers: Principles and applications. FEMS Microbiol. Rev. 38, 823–864. https://doi.org/10.1111/1574-6976.12063

Sliekers, A.O., Derwort, N., Gomez, J.L.C., Strous, M., Kuenen, J.G., Jetten, M.S.M., 2002. Completely autotrophic nitrogen removal over nitrite in one single reactor. Water Res. 36, 2475–2482. https://doi.org/10.1016/S0043-1354(01)00476-6

SM Jetten, M., Wagner, M., Fuerst, J., Van Loosdrecht, M., Kuenen, G., Strous, M., 2001. Microbiology and application of the anaerobic ammonium oxidation (‘anammox’) process. Curr. Opin. Biotechnol. 12, 283–288. https://doi.org/10.1016/S0958-1669(00)00211-1

Sobotka, D., Czerwionka, K., Makinia, J., 2016. Influence of temperature on the activity of anammox granular biomass. Water Sci. Technol. 73, 2518–2525. https://doi.org/10.2166/wst.2016.103

Sobotka, D., Marcinkowski, M., Makinia, J., 2017. The competition between AOB and NOB as a basic strategy for successful start-up of the partial nitrification process, in: 9th Eastern European YWP "Uniting Europe for Clean Water.

Sobotka, D., Zhai, J., Makinia, J., 2021. Generalized temperature dependence model for anammox process kinetics. Sci. Total Environ. 775, 145760. https://doi.org/10.1016/j.scitotenv.2021.145760

Soliman, M., Eldyasti, A., 2017. Long-term dynamic and pseudo-state modeling of complete partial nitrification process at high nitrogen loading rates in a sequential batch reactor (SBR). Bioresour. Technol. https://doi.org/10.1016/j.biortech.2017.02.108

Sonthiphand, P., Hall, M.W., Neufeld, J.D., 2014. Biogeography of anaerobic ammonia-oxidizing (anammox) bacteria. Front. Microbiol. 5. https://doi.org/10.3389/fmicb.2014.00399

Speth, D.R., Lagkouvardos, I., Wang, Y., Qian, P.Y., Dutilh, B.E., Jetten, M.S.M., 2017. Draft Genome of Scalindua rubra, Obtained from the Interface Above the Discovery Deep Brine in the Red Sea, Sheds Light on Potential Salt Adaptation Strategies in Anammox Bacteria. Microb. Ecol. 74, 1–5. https://doi.org/10.1007/s00248-017-0929-7

Starkey, M., Parsek, M.R., Gray, K.A., Chang, S. Il, 2014. A Sticky Business: the Extracellular Polymeric Substance Matrix of Bacterial Biofilms, in: Microbial Biofilms. American Society of Microbiology, pp. 174–191. https://doi.org/10.1128/9781555817718.ch10

Staudt, C., Horn, H., Hempel, D.C., Neu, T.R., 2004. Volumetric measurements of bacterial cells and extracellular polymeric substance glycoconjugates in biofilm. Biotechnol. Bioeng. 88, 585–592. https://doi.org/10.1002/bit.20241

Stearns, J.C., Davidson, C.J., Mckeon, S., Whelan, F.J., Fontes, M.E., Schryvers, A.B., Bowdish, D.M.E., Kellner, J.D., Surette, M.G., 2015. Culture and molecular-based profiles show shifts in bacterial communities of the upper respiratory tract that occur with age. ISME J. 9, 1246–1259. https://doi.org/10.1038/ismej.2014.250

Straka, L., Summers, A., Stahl, D.A., Winkler, M.K.H., 2019. Kinetic implication of moving warm side-stream Anaerobic ammonium oxidizing bacteria to cold mainstream wastewater. Bioresour. Technol. J. https://doi.org/10.1016/j.biortech.2019.121534

Strous, M, Heijnen, J.J., Kuenen, J.G., Jetten, M.S.M., 1998. The sequencing batch reactor as a powerful tool for the study of slowly growing anaerobic ammonium-oxidizing microorganisms.

Strous, M., Heijnen, J.J., Kuenen, J.G., Jetten, M.S.M., 1998. The sequencing batch reactor as a powerful tool for the study of slowly growing anaerobic ammonium-oxidizing microorganisms. Appl. Microbiol. Biotechnol. 50, 589–596. https://doi.org/10.1007/s002530051340

Strous, M., Kuenen, J.G., Jetten, M.S., 1999. Key physiology of anaerobic ammonium oxidation. Appl. Environ. Microbiol. 65, 3248–50.

Strous, M., Pelletier, E., Mangenot, S., Rattei, T., Lehner, A., Taylor, M.W., Horn, M., Daims, H., Bartol-Mavel, D., Wincker, P., Barbe, V., Fonknechten, N., Vallenet, D., Segurens, B.,

Schenowitz-Truong, C., Médigue, C., Collingro, A., Snel, B., Dutilh, B.E., Op den Camp, H.J.M., van der Drift, C., Cirpus, I., van de Pas-Schoonen, K.T., Harhangi, H.R., van Niftrik, L., Schmid, M., Keltjens, J., van de Vossenberg, J., Kartal, B., Meier, H., Frishman, D., Huynen, M.A., Mewes, H.-W., Weissenbach, J., Jetten, M.S.M., Wagner, M., Le Paslier, D., 2006. Deciphering the evolution and metabolism of an anammox bacterium from a community genome. Nature 440, 790–794. https://doi.org/10.1038/nature04647

Strous, M., Van Gerven, E., Kuenen, J.G., Jetten, M., 1997a. Effects of aerobic and microaerobic conditions on anaerobic ammonium- oxidizing (anammox) sludge. Appl. Environ. Microbiol. 63, 2446–2448. https://doi.org/10.1128/aem.63.6.2446-2448.1997

Strous, M., Van Gerven, E., Zheng, P., Kuenen, J.G., Jetten, M.S.M., 1997b. Ammonium removal from concentrated waste streams with the anaerobic ammonium oxidation (Anammox) process in different reactor configurations. Water Res. 31, 1955–1962. https://doi.org/10.1016/S0043-1354(97)00055-9

Suresh Kumar, A., Mody, K., Jha, B., 2007. Bacterial exopolysaccharides – a perception. J. Basic Microbiol. 47, 103–117. https://doi.org/10.1002/jobm.200610203

Sutherland, Ian W, 2001. The biofilm matrix-an immobilized but dynamic microbial environment, TRENDS in Microbiology.

Sutherland, Ian W., 2001. Microbial polysaccharides from Gram-negative bacteria, in: International Dairy Journal. Elsevier, pp. 663–674. https://doi.org/10.1016/S0958-6946(01)00112-1

Szabó, E., Liébana, R., Hermansson, M., Modin, O., Persson, F., Wilén, B.-M., 2017. Microbial Population Dynamics and Ecosystem Functions of Anoxic/Aerobic Granular Sludge in Sequencing Batch Reactors Operated at Different Organic Loading Rates. Front. Microbiol. 8, 770. https://doi.org/10.3389/fmicb.2017.00770

Tan, C., Saurabh, S., Bruchez, M.P., Schwartz, R., Leduc, P., 2013. Molecular crowding shapes gene expression in synthetic cellular nanosystems. Nat. Nanotechnol. 8, 602–608. https://doi.org/10.1038/nnano.2013.132

Tan, C.H., Koh, K.S., Xie, C., Tay, M., Zhou, Y., Williams, R., Ng, W.J., Rice, S.A., Kjelleberg, S., 2014. The role of quorum sensing signalling in EPS production and the assembly of a sludge community into aerobic granules. ISME J. 8, 1186–1197. https://doi.org/10.1038/ismej.2013.240

Tan, C.H., Oh, H.-S., Sheraton, V.M., Mancini, E., Chye, S., Loo, J., Kjelleberg, S., Sloot, P.M.A., Rice, S.A., 2020. Convection and the Extracellular Matrix Dictate Inter-and Intra-Biofilm Quorum Sensing Communication in Environmental Systems. Environ. Sci. Technol 54, 34. https://doi.org/10.1021/acs.est.0c00716

Tan, F.Y.Y., Tang, C.M., Exley, R.M., 2015. Sugar coating: bacterial protein glycosylation and host-microbe interactions. Trends Biochem. Sci. https://doi.org/10.1016/j.tibs.2015.03.016

Tang, C.-J., He, R., Zheng, P., Chai, L.-Y., Min, X.-B., 2013. Mathematical modeling of high-rate Anammox UASB reactor based on granular packing patterns. J. Hazard. Mater. 250, 1–8. https://doi.org/10.1016/j.jhazmat.2013.01.058

Tang, C.-J., Zheng, P., Hu, B.-L., Chen, J.-W., Wang, C.-H., 2010a. Influence of substrates on nitrogen removal performance and microbiology of anaerobic ammonium oxidation by operating two UASB reactors fed with different substrate levels. J. Hazard. Mater. 181, 19–26. https://doi.org/10.1016/j.jhazmat.2010.04.015

Tang, C.-J., Zheng, P., Wang, C.-H., Mahmood, Q., Zhang, J.-Q., Chen, X.-G., Zhang, L., Chen, J.-W., 2011. Performance of high-loaded ANAMMOX UASB reactors containing granular sludge. Water Res. 45, 135–144. https://doi.org/10.1016/J.WATRES.2010.08.018

Tang, C.-J., Zheng, P., Wang, C.-H., Mahmood, Q., Zhang, J.-Q., Chen, X.-G., Zhang, L., Chen, J.-W., 2010b. Performance of high-loaded ANAMMOX UASB reactors containing granular sludge. Water Res. https://doi.org/10.1016/j.watres.2010.08.018

Tang, C., Zheng, P., Mahmood, Q., Chen, J., 2010. Effect of substrate concentration on stability of anammox biofilm reactors. J. Cent. South Univ. Technol. 17, 79–84. https://doi.org/10.1007/s11771-010-0014-6

Tang, C.J., Zheng, P., Wang, C.H., Mahmood, Q., Zhang, J.Q., Chen, X.G., Zhang, L., Chen, J.W., 2011. Performance of high-loaded ANAMMOX UASB reactors containing granular sludge. Water Res. 45, 135–144. https://doi.org/10.1016/j.watres.2010.08.018

Tay, J.-H., Yan, Y.-G., 1996. Influence of Substrate Concentration on Microbial Selection and Granulation during Start-Up of Upflow Anaerobic Sludge Blanket Reactors. Water Environ. Res. 68, 1140–1150.

Tchobanoglous, G., Burton, F.L. (Franklin L., Stensel, H.D., Metcalf & Eddy., 2003. Wastewater engineering : treatment and reuse. McGraw-Hill.

Thevaranjan, N., Whelan, F.J., Puchta, A., Ashu, E., Rossi, L., Surette, M.G., Bowdish, D.M.E., 2016. Streptococcus pneumoniae colonization disrupts the microbial community within the upper respiratory tract of aging mice. Infect. Immun. 84, 906–916. https://doi.org/10.1128/IAI.01275-15

Third, K.A., Paxman, J., Schmid, M., Strous, M., Jetten, M.S.M., Cord-Ruwisch, R., 2005. Enrichment of anammox from activated sludge and its application in the CANON process. Microb. Ecol. 49, 236–244. https://doi.org/10.1007/s00248-004-0186-4

Tomaszewski, M., Cema, G., Ziembi Nska-Buczy, A., 2017a. Significance of pH control in anammox process performance at low temperature. Chemosphere. https://doi.org/10.1016/j.chemosphere.2017.07.034

Tomaszewski, M., Cema, G., Ziembińska-Buczyńska, A., 2017b. Influence of temperature and pH on the anammox process: A review and meta-analysis. Chemosphere. https://doi.org/10.1016/j.chemosphere.2017.05.003

Trojanowicz, K., Plaza, E., Trela, J., 2016. Pilot scale studies on nitritation-anammox process for mainstream wastewater at low temperature. Water Sci. Technol. 73, 761–768. https://doi.org/10.2166/wst.2015.551

Trojanowicz, K., Trela, J., Plaza, E., 2019. Possible mechanism of efficient mainstream partial nitritation/anammox (PN/A) in hybrid bioreactors (IFAS). Environ. Technol. (United Kingdom). https://doi.org/10.1080/09593330.2019.1650834

Tsuchihashi, Ryujiro, 2015. Technologies for Sidestream Nitrogen Removal.

Val del Río, Á., Campos Gómez, J.L., Mosquera Corral, A., 2016. Technologies for the treatment and recovery of nutrients from industrial wastewater, Technologies for the Treatment and Recovery of Nutrients from Industrial Wastewater. IGI Global. https://doi.org/10.4018/978-1-5225-1037-6

Val Del Rio, A., Campos, J.L., Da Silva, C., Pedrouso, A., Mosquera-Corral, A., 2019. Determination of the intrinsic kinetic parameters of ammonia-oxidizing and nitrite-oxidizing bacteria in granular and flocculent sludge. Sep. Purif. Technol. https://doi.org/10.1016/j.seppur.2018.12.048

van de Graaf, A.A., de Bruijn, P., Robertson, L.A., Jetten, M.S.M., Kuenen, J.G., 1997. Metabolic pathway of anaerobic ammonium oxidation on the basis of 15N studies in a fluidized bed reactor. Microbiology 143, 2415–2421. https://doi.org/10.1099/00221287-143-7-2415

van de Graaf, A.A., de Bruijn, P., Robertson, L.A., Jetten, M.S.M., Kuenen, J.G., 1996. Autotrophic growth of anaerobic ammonium-oxidizing micro-organisms in a fluidized bed reactor. Microbiology 142, 2187–2196. https://doi.org/10.1099/13500872-142-8-2187

van den Berg, D., Robijn, G.W., Janssen, A.C., Giuseppin, M., Vreeker, R., Kamerling, J.P., Vliegenthart, J., Ledeboer, A.M., Verrips, C.T., 1995. Production of a Novel Extracellular Polysaccharide by Lactobacillus sake 0-1 and Characterization of the Polysaccharide. Appl. Environ. Microbiol. 61.

van der Star, W.R.L., Abma, W.R., Blommers, D., Mulder, J.-W., Tokutomi, T., Strous, M., Picioreanu, C., van Loosdrecht, M.C.M., 2007a. Startup of reactors for anoxic ammonium oxidation: Experiences from the first full-scale anammox reactor in Rotterdam. Water Res. 41, 4149–4163. https://doi.org/10.1016/J.WATRES.2007.03.044

van der Star, W.R.L., Abma, W.R., Blommers, D., Mulder, J.W., Tokutomi, T., Strous, M., Picioreanu, C., van Loosdrecht, M.C.M., 2007b. Startup of reactors for anoxic ammonium oxidation: Experiences from the first full-scale anammox reactor in Rotterdam. Water Res. 41, 4149–4163. https://doi.org/10.1016/j.watres.2007.03.044

van der Star, Wouter R.L., Miclea, A.I., van Dongen, U.G.J.M., Muyzer, G., Picioreanu, C., van Loosdrecht, M.C.M., 2008. The membrane bioreactor: A novel tool to grow anammox bacteria as free cells. Biotechnol. Bioeng. 101, 286–294. https://doi.org/10.1002/bit.21891

van der Star, Wouter R L, van de Graaf, M.J., Kartal, B., Picioreanu, C., Jetten, M.S.M., van Loosdrecht, M.C.M., 2008. Response of anaerobic ammonium-oxidizing bacteria to hydroxylamine. Appl. Environ. Microbiol. 74, 4417–26. https://doi.org/10.1128/AEM.00042-08

Van Dongen, U., Jetten, M.S.M., Van Loosdrecht, M.C.M., 2001. The SHARON®-Anammox® process for treatment of ammonium rich wastewater, in: Water Science and Technology. IWA Publishing, pp. 153–160. https://doi.org/10.2166/wst.2001.0037

Van Hulle, S.W.H., Vandeweyer, H.J.P., Meesschaert, B.D., Vanrolleghem, P.A., Dejans, P., Dumoulin, A., 2010. Engineering aspects and practical application of autotrophic nitrogen

removal from nitrogen rich streams. Chem. Eng. J. 162, 1–20. https://doi.org/10.1016/J.CEJ.2010.05.037

Van Loosdrecht, M.C.M., Lopez-Vazquez, C.M., Meijer, S.C.F., Hooijmans, C.M., Brdjanovic, D., 2015. Twenty-five years of ASM1: Past, present and future of wastewater treatment modelling. J. Hydroinformatics 17, 697–718. https://doi.org/10.2166/hydro.2015.006

Van Loosdrecht, M.C.M., Nielsen, P.H., Lopez Vazquez, C.M., Brdjanovic, D., 2016. Experimental Methods in Wastewater Treatment | IWA Publishing.

Van Niftrik, L., 2013. Cell biology of unique anammox bacteria that contain an energy conserving prokaryotic organelle. Antonie van Leeuwenhoek, Int. J. Gen. Mol. Microbiol. 104, 489–497. https://doi.org/10.1007/s10482-013-9990-5

van Niftrik, L., Jetten, M.S.M., 2012. Anaerobic ammonium-oxidizing bacteria: unique microorganisms with exceptional properties. Microbiol. Mol. Biol. Rev. 76, 585–96. https://doi.org/10.1128/MMBR.05025-11

van Teeseling, M.C.F., Maresch, D., Rath, C.B., Figl, R., Altmann, F., Jetten, M.S.M., Messner, P., Schäffer, C., van Niftrik, L., 2016. The S-layer protein of the anammox bacterium Kuenenia stuttgartiensis is heavily O-glycosylated. Front. Microbiol. 7. https://doi.org/10.3389/fmicb.2016.01721

van Teeseling, M.C.F., Neumann, S., van Niftrik, L., 2013. The anammoxosome organelle is crucial for the energy metabolism of anaerobic ammonium oxidizing bacteria. J. Mol. Microbiol. Biotechnol. 23, 104–17. https://doi.org/10.1159/000346547

Vanhooren, P.T., Vandamme, E.J., 2000. Microbial production of clavan, an L-fucose rich exopolysaccharide. Prog. Biotechnol. 17, 109–114. https://doi.org/10.1016/S0921-0423(00)80057-X

Vanrolleghem, P.A., Insel, G., Petersen, B., Sin, G., De Pauw, D., Nopens, I., Dovermann, H., Weijers, S., Gernaey, K., 2003. A COMPREHENSIVE MODEL CALIBRATION PROCEDURE FOR ACTIVATED SLUDGE MODELS, in: WEFTEC.

Vázquez-Padín, J., Mosquera-Corral, A., Campos, J.L., Méndez, R., Revsbech, N.P., 2010. Microbial community distribution and activity dynamics of granular biomass in a CANON reactor. Water Res. 44, 4359–4370. https://doi.org/10.1016/J.WATRES.2010.05.041

Vázquez-Padín, J.R., Morales, N., Gutiérrez, R., Fernández, R., Rogalla, F., Barrio, J.P., Campos, J.L., Mosquera-Corral, A., Méndez, R., 2014. Implications of full-scale implementation of an anammox-based process as post-treatment of a municipal anaerobic sludge digester operated with co-digestion. Water Sci. Technol. 69, 1151–1158. https://doi.org/10.2166/wst.2013.795

Veuillet, F., Lacroix, S., Bausseron, A., Gonidec, E., Ochoa, J., Christensson, M., Lemaire, R., 2014. Integrated fixed-film activated sludge ANITA^{TM}Mox process - A new perspective for advanced nitrogen removal. Water Sci. Technol. 69, 915–922. https://doi.org/10.2166/wst.2013.786

Vlaeminck, S.E., De Clippeleir, H., Verstraete, W., 2012. Microbial resource management of one-stage partial nitritation/anammox. Microb. Biotechnol. 5, 433–448.

https://doi.org/10.1111/j.1751-7915.2012.00341.x

Vu, B., Chen, M., Crawford, R., Ivanova, E., 2009. Bacterial Extracellular Polysaccharides Involved in Biofilm Formation. Molecules 14, 2535–2554. https://doi.org/10.3390/molecules14072535

Wagner, M., Ivleva, N.P., Haisch, C., Niessner, R., Horn, H., 2009. Combined use of confocal laser scanning microscopy (CLSM) and Raman microscopy (RM): Investigations on EPS - Matrix. Water Res. 43, 63–76. https://doi.org/10.1016/j.watres.2008.10.034

Waki, M., Tokutomi, T., Yokoyama, H., Tanaka, Y., 2007. Nitrogen removal from animal waste treatment water by anammox enrichment. Bioresour. Technol. 98, 2775–2780. https://doi.org/10.1016/J.BIORTECH.2006.09.031

WAKI, M., TOKUTOMI, T., YOKOYAMA, H., TANAKA, Y., 2007. Nitrogen removal from animal waste treatment water by anammox enrichment. Bioresour. Technol. 98, 2775–2780. https://doi.org/10.1016/j.biortech.2006.09.031

Wang, C., Liu, S., Xu, X., Zhang, C., Wang, D., Yang, F., 2018. Achieving mainstream nitrogen removal through simultaneous partial nitrification, anammox and denitrification process in an integrated fixed film activated sludge reactor. Chemosphere. https://doi.org/10.1016/j.chemosphere.2018.04.016

Wang, D., Wang, Q., Laloo, A., Xu, Y., Bond, P.L., Yuan, Z., 2016. Achieving Stable Nitritation for Mainstream Deammonification by Combining Free Nitrous Acid-Based Sludge Treatment and Oxygen Limitation. Nature 6, 1–10. https://doi.org/10.1038/srep25547

Wang, J., Lu, H., Chen, G.H., Lau, G.N., Tsang, W.L., van Loosdrecht, M.C.M., 2009. A novel sulfate reduction, autotrophic denitrification, nitrification integrated (SANI) process for saline wastewater treatment. Water Res. 43, 2363–2372. https://doi.org/10.1016/j.watres.2009.02.037

Wang, Q., Wang, Y., Lin, J., Tang, R., Wang, W., Zhan, X., Hu, Z.-H., 2018. Selection of seeding strategy for fast start-up of Anammox process with low concentration of Anammox sludge inoculum. Bioresour. Technol. 268, 638–647. https://doi.org/10.1016/J.BIORTECH.2018.08.056

Wang, S., Liu, Y., Niu, Q., Ji, J., Hojo, T., Li, Y.-Y., 2017. Nitrogen removal performance and loading capacity of a novel single-stage nitritation-anammox system with syntrophic micro-granules. Bioresour. Technol. 236, 119–128. https://doi.org/10.1016/J.BIORTECH.2017.03.164

Wang, T., Zhang, H., Yang, F., Liu, S., Fu, Z., Chen, H., 2009. Start-up of the Anammox process from the conventional activated sludge in a membrane bioreactor. Bioresour. Technol. 100, 2501–2506. https://doi.org/10.1016/J.BIORTECH.2008.12.011

Wang, W., Yan, Y., Zhao, Y., Shi, Q., Wang, Y., 2019. Characterization of stratified EPS and their role in the initial adhesion of anammox consortia. Water Res. https://doi.org/10.1016/j.watres.2019.115223

Wang, X., Gao, D., 2017. The transformation from anammox granules to deammonification granules in micro-aerobic system by facilitating indigenous ammonia oxidizing bacteria.

Bioresour. Technol. J. https://doi.org/10.1016/j.biortech.2017.11.046

Wang, Y.-P., Chen, F.-Y., Nie1, J.-L., Ning, P., 2016. Formation and Stability of Nitrifying Granules under High Loading Rates. Int. Proc. Chem. Biol. Environ. Eng. https://doi.org/10.7763/IPCBEE

Wang, Y., Lin, Z., He, L., Huang, W., Zhou, J., He, Q., 2020. Simultaneous partial nitrification, anammox and denitrification (SNAD) process for nitrogen and refractory organic compounds removal from mature landfill leachate: Performance and metagenome-based microbial ecology. Bioresour. Technol. 294, 122166. https://doi.org/10.1016/j.biortech.2019.122166

Wang, Z., Zhang, S., Zhang, L., Wang, B., Liu, W., Ma, S., Peng, Y., 2018. Restoration of real sewage partial nitritation-anammox process from nitrate accumulation using free nitrous acid treatment. Bioresour. Technol. 251, 341–349. https://doi.org/10.1016/j.biortech.2017.12.073

Wang, Zichao, Gao, M., Wang, Zhe, She, Z., Chang, Q., Sun, C., Zhang, J., Ren, Y., Yang, N., 2013. Effect of salinity on extracellular polymeric substances of activated sludge from an anoxic-aerobic sequencing batch reactor. Chemosphere. https://doi.org/10.1016/j.chemosphere.2013.09.038

Ward, B.B., 2008. Nitrification in Marine Systems, in: Nitrogen in the Marine Environment. Elsevier Inc., pp. 199–261. https://doi.org/10.1016/B978-0-12-372522-6.00005-0

Water Environment Federation, 2005. Biological Nutrient Removal (BNR) Operation in Wastewater Treatment Plants. McGraw Hill Professional.

Weissbrodt, D.G., Shani, N., Holliger, C., 2014. Linking bacterial population dynamics and nutrient removal in the granular sludge biofilm ecosystem engineered for wastewater treatment. FEMS Microbiol. Ecol. 88, 579–595. https://doi.org/10.1111/1574-6941.12326

Weissenbacher, N., Wett, B., 2018. Deammonifikation auf Kläranlagen – Verfahrensentwicklung aus Österreich in alle WeltDeammonification at wastewater treatment plants—process development from Austria to the world. Österreichische Wasser- und Abfallwirtschaft 70, 570–578. https://doi.org/10.1007/s00506-018-0521-5

Wen, R., Jin, Y., Zhang, W., 2020. Application of the Anammox in China—A Review. Int. J. Environ. Res. Public Health 17, 1090. https://doi.org/10.3390/ijerph17031090

Wett, B., 2007. Development and implementation of a robust deammonification process. Water Sci. Technol. 56, 81–88. https://doi.org/10.2166/wst.2007.611

Wett, B., 2006. Solved upscaling problems for implementing deammonification of rejection water, in: Water Science and Technology. pp. 121–128. https://doi.org/10.2166/wst.2006.413

Wett, B., Johnson, C., 2012. Results of the Large-Scale Pilot Investigation of the DEMON® Nitrogen Removal System in Pierce County, in: Proceedings of the Water Environment Federation. https://doi.org/10.2175/193864712811740774

Wett, B., Murthy, S., Takács, I., Hell, M., Bowden, G., Deur, A., O'shaughnessy, M., 2007. Key

Parameters for Control of DEMON Deammonification Process. Water Pract. • 1. https://doi.org/10.2175/193317707X257017

Wett, B., Nyhuis, G., Takács, I., Murthy, S., 2012. Development of Enhanced Deammonification Selector. Proc. Water Environ. Fed. 2010, 5917–5926. https://doi.org/10.2175/193864710798194139

Wett, B., Omari, A., Podmirseg, S.M., Han, M., Akintayo, O., Gómez Brandón, M., Murthy, S., Bott, C., Hell, M., Takács, I., Nyhuis, G., O'Shaughnessy, M., 2013. Going for mainstream deammonification from bench to full scale for maximized resource efficiency. Water Sci. Technol. 68, 283–289. https://doi.org/10.2166/wst.2013.150

Wett, B., Podmirseg, S.M., Gómez-Brandón, M., Hell, M., Nyhuis, G., Bott, C., Murthy, S., 2015. Expanding DEMON Sidestream Deammonification Technology Towards Mainstream Application. Water Environ. Res. 87, 2084–2089. https://doi.org/10.2175/106143015X14362865227319

Wett, B., Rauch, W., 2003. The role of inorganic carbon limitation in biological nitrogen removal of extremely ammonia concentrated wastewater. Water Res. 37, 1100–1110. https://doi.org/10.1016/S0043-1354(02)00440-2

Wiesmann, U., 1994. Biological nitrogen removal from wastewater. Adv. Biochem. Eng. Biotechnol. https://doi.org/10.1007/bfb0008736

Wilson, K.N., 2017. Piloting of a deammonification moving bed biofilm reactor for mainstream industrial wastewater application. The University of Manitoba.

Winkler, M.-K.H., Kleerebezem, R., van Loosdrecht, M.C.M., 2012. Integration of anammox into the aerobic granular sludge process for main stream wastewater treatment at ambient temperatures. Water Res. 46, 136–144. https://doi.org/10.1016/j.watres.2011.10.034

Winkler, M.K., Straka, L., 2019. New directions in biological nitrogen removal and recovery from wastewater. Curr. Opin. Biotechnol. https://doi.org/10.1016/j.copbio.2018.12.007

Wong, L.L., Natarajan, G., Boleij, M., Thi, S.S., Winnerdy, F.R., Mugunthan, S., Lu, Y., Lee, J.-M., Lin, Y., Loosdrecht, M. van, Law, Y., Kjelleberg, S., Seviour, T.W., 2019. Isolation of a putative S-layer protein from anammox biofilm extracellular matrix using ionic liquid extraction. bioRxiv 705566. https://doi.org/10.1101/705566

Wong, L.L., Natarajan, G., Boleij, M., Thi, S.S., Winnerdy, F.R., Mugunthan, S., Lu, Y., Lee, J.M., Lin, Y., van Loosdrecht, M., Law, Y., Kjelleberg, S., Seviour, T., 2020. Extracellular protein isolation from the matrix of anammox biofilm using ionic liquid extraction. Appl. Microbiol. Biotechnol. 104, 3643–3654. https://doi.org/10.1007/s00253-020-10465-7

Wu, D., Li, G.-F., Shi, Z.-J., Zhang, Q., Huang, B.-C., Fan, N.-S., Jin, R.-C., 2019. Co-inhibition of salinity and Ni(II) in the anammox-UASB reactor. Sci. Total Environ. https://doi.org/10.1016/j.scitotenv.2019.03.130

Xiang, T., Gao, D., Wang, X., 2020. Performance and microbial community analysis of two sludge type reactors in achieving mainstream deammonification with hydrazine addition. Sci. Total Environ. https://doi.org/10.1016/j.scitotenv.2019.136377

Xie, B., Jin, C., Parker, W.J., 2019. Impact of mixing intensity on dissolved oxygen half-velocity constants in a sidestream deammonification environment. Water Qual. Res. J. https://doi.org/10.2166/wqrj.2019.009

Xing, B.-S., Guo, Q., Zhang, Z.-Z., Zhang, J., Wang, H.-Z., Jin, R.-C., 2014. Optimization of process performance in a granule-based anaerobic ammonium oxidation (anammox) upflow anaerobic sludge blanket (UASB) reactor. Bioresour. Technol. 170, 404–412. https://doi.org/10.1016/J.BIORTECH.2014.08.026

Xu, G., Xu, X., Yang, F., Liu, S., Gao, Y., 2012. Partial nitrification adjusted by hydroxylamine in aerobic granules under high DO and ambient temperature and subsequent Anammox for low C/N wastewater treatment. Chem. Eng. J. 213, 338–345. https://doi.org/10.1016/J.CEJ.2012.10.014

Xu, G., Zhou, Y., Yang, Q., Lee, Z.M.-P., Gu, J., Lay, W., Cao, Y., Liu, Y., 2015a. The challenges of mainstream deammonification process for municipal used water treatment. Appl. Microbiol. Biotechnol. 99, 2485–2490. https://doi.org/10.1007/s00253-015-6423-6

Xu, G., Zhou, Y., Yang, Q., Lee, Z.M.P., Gu, J., Lay, W., Cao, Y., Liu, Y., 2015b. The challenges of mainstream deammonification process for municipal used water treatment. Appl. Microbiol. Biotechnol. https://doi.org/10.1007/s00253-015-6423-6

Yang, S.F., Tay, J.H., Liu, Y., 2004. Inhibition of free ammonia to the formation of aerobic granules. Biochem. Eng. J. 17, 41–48. https://doi.org/10.1016/S1369-703X(03)00122-0

Yang, W., Young, S., Munoz, A., Palmarin, M.J., 2019. Dynamic modeling of a full-scale anaerobic mesophilic digester start-up process for the treatment of primary sludge. J. Environ. Chem. Eng. https://doi.org/10.1016/j.jece.2019.103091

Yang, Y., Zhang, L., Cheng, J., Zhang, S., Li, X., Peng, Y., 2018. Microbial community evolution in partial nitritation/anammox process: From sidestream to mainstream. Bioresour. Technol.

Ye, J., Liu, J., Ye, M., Ma, X., Li, Y.Y., 2020. Towards advanced nitrogen removal and optimal energy recovery from leachate: A critical review of anammox-based processes. Crit. Rev. Environ. Sci. Technol. 50, 612–653. https://doi.org/10.1080/10643389.2019.1631989

Ye, L., Li, D., Zhang, J., Zeng, H., 2018. Fast start-up of anammox process with mixed activated sludge and settling option. Environ. Technol. 39, 3088–3095. https://doi.org/10.1080/09593330.2017.1375016

Yin, C., Meng, F., Chen, G.-H., 2015. Spectroscopic characterization of extracellular polymeric substances from a mixed culture dominated by ammonia-oxidizing bacteria. Water Res. https://doi.org/10.1016/j.watres.2014.10.046

Yin, X., Qiao, S., Zhou, J., Quan, X., 2015. Using three-bio-electrode reactor to enhance the activity of anammox biomass. Bioresour. Technol. 196, 376–382. https://doi.org/10.1016/j.biortech.2015.07.096

Yongzhen, P., Shouyou, G., Shuying, W., Lu, B., Peng, Y., Gao, S., Wang, S., Bai, L., Yongzhen, P., Shouyou, G., Shuying, W., Lu, B., 2007. Partial Nitrification from Domestic Wastewater by Aeration Control at Ambient Temperature. Chinese J. Chem. Eng. 15, 115–

121. https://doi.org/10.1016/S1004-9541(07)60043-3

Yu, H.-Q., 2020. Molecular Insights into Extracellular Polymeric Substances in Activated Sludge. Environ. Sci. Technol. 54, 7750. https://doi.org/10.1021/acs.est.0c00850

Yu, Y.C., Gao, D.W., Tao, Y., 2013. Anammox start-up in sequencing batch biofilm reactors using different inoculating sludge. Appl. Microbiol. Biotechnol. 97, 6057–6064. https://doi.org/10.1007/s00253-012-4427-z

Zekker, I., Kroon, K., Rikmann, E., Tenno, Toomas, Tomingas, M., Vabamäe, P., Vlaeminck, S.E., Tenno, Taavo, 2012. Accelerating effect of hydroxylamine and hydrazine on nitrogen removal rate in moving bed biofilm reactor. Biodegradation 23, 739–749. https://doi.org/10.1007/s10532-012-9549-6

Zekker, I., Raudkivi, M., Artemchuk, O., Rikmann, E., Priks, H., Jaagura, M., Tenno, T., 2020. Mainstream-sidestream wastewater switching promotes anammox nitrogen removal rate in organic-rich, low-temperature streams. Environ. Technol. 42, 3073–3082. https://doi.org/10.1080/09593330.2020.1721566

Zekker, I., Rikmann, E., Kroon, K., Mandel, A., Mihkelson, J., Tenno, T., Tenno, T., 2017. Ameliorating nitrite inhibition in a low-temperature nitritation–anammox MBBR using bacterial intermediate nitric oxide. Int. J. Environ. Sci. Technol. 14, 2343–2356. https://doi.org/10.1007/s13762-017-1321-3

Zhang, J., Miao, Y., Zhang, Q., Sun, Y., Wu, L., Peng, Y., 2020. Mechanism of stable sewage nitrogen removal in a partial nitrification-anammox biofilm system at low temperatures: Microbial community and EPS analysis. Bioresour. Technol. 297, 122459. https://doi.org/10.1016/j.biortech.2019.122459

Zhang, Jianhua, Zhang, L., Miao, Y., Sun, Y., Zhang, Q., Wu, L., Peng, Y., 2019. Enhancing sewage nitrogen removal via anammox and endogenous denitrification: Significance of anaerobic/oxic/anoxic operation mode. Bioresour. Technol. 289, 121665. https://doi.org/10.1016/j.biortech.2019.121665

Zhang, Jing, Zhang, Y.Z., Zhao, B.H., Zhang, K., Liang, D.B., Wei, J., Wang, X.J., Li, J., Chen, G.H., 2019. Effects of pH on AHL signal release and properties of ANAMMOX granules with different biomass densities. Environ. Sci. Water Res. Technol. 5, 1723–1735. https://doi.org/10.1039/c9ew00581a

Zhang, L., Liu, M., Zhang, S., Yang, Y., Peng, Y., 2015. Integrated fixed-biofilm activated sludge reactor as a powerful tool to enrich anammox biofilm and granular sludge. Chemosphere. https://doi.org/10.1016/j.chemosphere.2015.02.001

Zhang, L., Zheng, P., Tang, C. jian, Jin, R. cun, 2008. Anaerobic ammonium oxidation for treatment of ammonium-rich wastewaters. J. Zhejiang Univ. Sci. B. https://doi.org/10.1631/jzus.B0710590

Zhang, M., Wang, S., Ji, B., Liu, Y., 2019. Towards mainstream deammonification of municipal wastewater: Partial nitrification-anammox versus partial denitrification-anammox. Sci. Total Environ. https://doi.org/10.1016/j.scitotenv.2019.07.293

Zhang, P., Shen, Y., Guo, J.S., Li, C., Wang, H., Chen, Y.P., Yan, P., Yang, J.X., Fang, F., 2015.

Extracellular protein analysis of activated sludge and their functions in wastewater treatment plant by shotgun proteomics. Sci. Rep. 5, 1–11. https://doi.org/10.1038/srep12041

Zhang, Q., De Clippeleir, H., Su, C., Al-Omari, A., Wett, B., Vlaeminck, S.E., Murthy, S., 2016. Deammonification for digester supernatant pretreated with thermal hydrolysis: overcoming inhibition through process optimization. Appl. Microbiol. Biotechnol. 100, 5595–5606. https://doi.org/10.1007/s00253-016-7368-0

Zhang, Q., Fan, N.S., Fu, J.J., Huang, B.C., Jin, R.C., 2020. Role and application of quorum sensing in anaerobic ammonium oxidation (anammox) process: A review. Crit. Rev. Environ. Sci. Technol. https://doi.org/10.1080/10643389.2020.1738166

Zhang, T., Fang, H.H.P., 2001. Quantification of extracellular polymeric substances in biofilms by confocal laser scanning microscopy. Biotechnol. Lett. 23, 405–409. https://doi.org/10.1023/A:1005620730265

Zhang, X., Yu, B., Zhang, N., Zhang, Haojing, Wang, C., Zhang, Hongzhong, 2016. Effect of inorganic carbon on nitrogen removal and microbial communities of CANON process in a membrane bioreactor. Bioresour. Technol. https://doi.org/10.1016/j.biortech.2015.11.083

Zhang, Y., Ma, H., Niu, Q., Chen, R., Hojo, T., Li, Y.Y., 2016. Effects of substrate shock on extracellular polymeric substance (EPS) excretion and characteristics of attached biofilm anammox granules. RSC Adv. 6, 113289–113297. https://doi.org/10.1039/C6RA20097D

Zhang, Y., Wang, F., Yang, X., Gu, C., Kengara, F.O., Hong, Q., Lv, Z., Jiang, X., 2011. Extracellular polymeric substances enhanced mass transfer of polycyclic aromatic hydrocarbons in the two-liquid-phase system for biodegradation. Appl. Microbiol. Biotechnol. 90, 1063–1071. https://doi.org/10.1007/s00253-011-3134-5

Zhao, Y., Feng, Y., Li, J., Guo, Y., Chen, L., Liu, S., 2018. Insight into the Aggregation Capacity of Anammox Consortia during Reactor Start-Up. Environ. Sci. Technol. 52, 3685–3695. https://doi.org/10.1021/acs.est.7b06553

Zheng, Y., Hou, L., Liu, M., Yin, G., 2019. Dynamics and environmental importance of anaerobic ammonium oxidation (anammox) bacteria in urban river networks. Environ. Pollut. 254, 112998. https://doi.org/10.1016/j.envpol.2019.112998

Zhou, X., Song, J., Wang, G., Yin, Z., Cao, X., Gao, J., 2020. Unravelling nitrogen removal and nitrous oxide emission from mainstream integrated nitrification-partial denitrification-anammox for low carbon/nitrogen domestic wastewater. J. Environ. Manage. 270, 110872. https://doi.org/10.1016/j.jenvman.2020.110872

Zhu, A., Guo, J., Ni, B.J., Wang, S., Yang, Q., Peng, Y., 2015. A novel protocol for model calibration in biological wastewater treatment. Sci. Rep. 5, 1–10. https://doi.org/10.1038/srep08493

Zhu, G., Wang, S., Ma, B., Wang, X., Zhou, J., Zhao, S., Liu, R., 2018. Anammox granular sludge in low-ammonium sewage treatment: Not bigger size driving better performance. Water Res. 142, 147–158. https://doi.org/10.1016/J.WATRES.2018.05.048

Zhu, G, Peng, Y, Guo, J, Li, B, Yang, Q, Wang, S, Zhu, Guibing, Peng, Yongzhen, Li, Baikun, Guo, Jianhua, Yang, Qing, Wang, Shuying, 2008. Biological Removal of Nitrogen from

Wastewater.

Zhu, P., Long, G., Ni, J., Tong, M., 2009. Deposition kinetics of extracellular polymeric substances (EPS) on silica in monovalent and divalent salts. Environ. Sci. Technol. 43, 5699–5704. https://doi.org/10.1021/es9003312

Zinatizadeh, A.A., Rahimi, Z., Younesi, H., 2020. Sludge Blanket Height (SBH) as a Process Stability Indicator in UASFF Reactor: Relationship Between SBH and Sludge Concentration at Different Operating Conditions. Waste and Biomass Valorization 11, 4003–4012. https://doi.org/10.1007/s12649-019-00708-8

Zouboulis, A.I., Chai, X.L., Katsoyiannis, I.A., 2004. The application of bioflocculant for the removal of humic acids from stabilized landfill leachates. J. Environ. Manage. 70, 35–41. https://doi.org/10.1016/j.jenvman.2003.10.003

APPENDICES

Appendice A. [UASB reactor chemical analysis]

The UASB was developed and operated for 317 days. The experimental analysis was studied in three main phases that coincides with different feeding medium and subsequent inhibition effects, in which

- Phase I (~55 days) is the startup and initial ANAMMOX activity observation stage.
- Phase II (~63 days) points out the effect of high influent ammonia concentration on the process.
- Phase III (~200 days) specifies a stable ANAMMOX process with high ammonia and nitrite removal rates.

The detailed data collected from the UASB during experiment for approximately 320 days of operation are presented in the following table.

Table 0-1 UASB reactor chemical analysis results

	Date	**days**	**Ammonia in (mgN/l)**	**Nitrite in (mgN/l)**	**Ammonia eff (mgN/l)**	**Nitrate eff (mgN/l)**	**Nitrite eff (mgN/l)**	**pH eff**	**Alkalinity eff (mgCaCO3/l)**	**Fraction of unoinized ammonia**	**Ammonia removal (%)**	**Nitrite removal (%)**
Phase I	07-Feb	1	50.1	66.1	36.1	1.2	16.1	9.0	3290	0.529	27.9	75.7
	08-Feb	2	51.0	67.3	29.2	1.0	8.0	9.0	2780	0.529	42.7	88.1
	09-Feb	3	52.3	69.0	26.3	1.6	6.1	9.5	2655	0.780	49.8	91.2
	10-Feb	4	54.0	71.3	26.3	1.6	6.1	9.5	2655	0.780	51.4	91.5
	12-Feb	5	55.1	72.7	19.9	1.1	12.6	9.0	2215	0.529	63.8	82.7
	13-Feb	6	56.0	73.9	19.9	1.1	12.6	9.0	2215	0.529	64.4	83.0

	14-Feb	7	54.3	71.7	14.0	1.4	14.7	9.0	1400	0.529	74.3	79.5
	16-Feb	9	55.1	72.7	11.9	1.0	29.5	9.0	1180	0.529	78.4	59.4
	17-Feb	10	52.3	69.0	12.0	1.0	29.5	9.0	1180	0.529	77.0	57.2
	18-Feb	11	54.1	71.4	12.3	1.0	29.5	9.0	1180	0.529	77.3	58.7
	19-Feb	12	50.2	66.3	11.8	1.0	29.5	9.0	1180	0.529	76.5	55.5
	20-Feb	13	50.4	66.5	11.4	0.6	21.9	8.7	1175	0.360	77.5	67.1
	21-Feb	14	56.1	74.1	10.2	0.6	17.8	8.2	1430	0.157	81.7	76.0
	23-Feb	16	50.1	66.1	11.7	4.4	10.8	8.0	955	0.099	76.6	83.7
	26-Feb	19	49.5	65.3	20.3	2.6	9.8	7.8	860	0.061	59.0	85.0
	27-Feb	20	49.9	65.9	11.2	2.8	17.8	7.8	770	0.065	77.6	73.0
	01-Mar	22	48.0	63.4	11.5	2.8	10.8	8.2	510	0.154	75.9	83.0
	02-Mar	23	50.1	66.1	11.5	2.9	11.1	8.2	511	0.154	77.1	83.2
	03-Mar	24	51.2	67.6	11.9	2.8	11.2	8.2	510	0.154	76.8	83.4
	04-Mar	25	50.9	67.2	11.5	2.7	10.9	8.2	512	0.154	77.4	83.8
	05-Mar	26	50.4	66.5	11.5	2.8	10.8	8.2	500	0.154	77.1	83.8

	06-Mar	27	50.3	66.4	11.0	2.2	11.2	8.2	415	0.148	78.2	83.1
	08-Mar	29	52.0	68.6	11.4	4.4	10.9	8.2	530	0.163	78.2	84.1
	13-Mar	34	50.4	66.5	11.5	4.1	11.2	8.4	675	0.228	77.1	83.2
	14-Mar	35	51.0	67.3	11.5	4.2	11.2	8.4	676	0.228	77.5	83.4
	15-Mar	36	54.0	71.3	11.7	4.0	11.5	8.4	675	0.228	78.4	83.9
	16-Mar	37	55.0	72.6	11.8	4.2	11.4	8.4	671	0.228	78.5	84.3
	17-Mar	38	56.0	73.9	11.5	4.0	11.9	8.4	677	0.228	79.4	83.9
	19-Mar	40	52.0	68.6	17.3	4.4	18.3	8.0	700	0.103	66.7	73.4
	21-Mar	42	53.0	70.0	18.8	4.6	11.8	8.6	660	0.290	64.5	83.1
	26-Mar	46	54.0	71.3	12.7	1.8	11.5	8.5	405	0.276	76.5	83.9
	28-Mar	48	51.0	67.3	18.6	0.2	9.5	8.7	360	0.355	63.5	85.8
	29-Mar	49	52.0	68.6	18.6	0.3	9.8	8.7	361	0.355	64.3	85.7
	30-Mar	50	53.0	70.0	19.0	0.5	9.4	8.7	363	0.355	64.1	86.6
	31-Mar	51	50.0	66.0	19.8	0.1	9.6	8.7	365	0.355	60.4	85.5
	01-Apr	52	50.1	66.1	20.0	0.4	9.1	8.7	361	0.355	60.1	86.2

	02-Apr	53	52.0	68.6	18.6	0.2	9.4	8.7	360	0.355	64.2	86.3
	03-Apr	54	50.1	66.1	18.1	0.2	9.5	8.7	366	0.355	63.9	85.6
Phase II	04-Apr	55	71.5	60.8	6.0	2.4	11.4	8.2	620	0.160	91.549	87.894
	06-Apr	58	71.5	60.8	19.8	0.0	18.4	7.9	1510	0.087	72.241	80.495
	09-Apr	61	72.1	61.3	16.0	4.0	27.3	7.8	1131	0.065	77.778	71.320
	13-Apr	66	73.0	62.1	17.0	5.4	13.6	7.8	1135	0.065	76.742	85.837
	14-Apr	67	71.5	60.8	16.4	5.5	12.6	7.8	1125	0.065	77.063	86.650
	15-Apr	68	70.9	60.3	17.0	5.6	13.1	7.8	1123	0.065	76.053	86.002
	16-Apr	69	70.8	60.2	16.2	4.8	13.8	7.8	1135	0.065	77.105	85.234
	17-Apr	70	72.0	61.2	23.4	4.8	10.3	8.1	1124	0.114	67.452	89.146
	18-Apr	71	73.0	62.1	22.9	4.6	10.6	8.1	1110	0.114	68.630	89.000
	19-Apr	72	71.0	60.4	23.4	4.5	10.4	8.1	1119	0.114	67.042	88.903
	20-Apr	73	73.0	62.1	23.9	4.2	10.3	8.1	1120	0.114	67.260	89.295
	23-Apr	76	70.6	60.0	29.4	4.6	21.4	8.0	1315	0.099	58.338	77.011
	24-Apr	77	71.0	60.4	29.0	4.3	21.5	8.0	1316	0.099	59.141	77.059

	25-Apr	78	72.5	61.6	30.2	4.6	21.6	8.0	1315	0.099	58.345	77.429
	26-Apr	79	73.6	62.6	30.1	6.0	21.8	8.0	1316	0.099	59.103	77.561
	27-Apr	80	70.9	60.3	29.5	6.5	21.4	8.0	1317	0.099	58.392	77.108
	30-Apr	83	70.6	60.0	27.3	5.9	25.1	7.9	1211	0.075	61.387	73.094
	01-May	84	70.5	59.9	28.0	6.0	25.6	7.9	1210	0.075	60.258	72.483
	02-May	85	71.0	60.4	27.5	5.5	25.4	7.9	1212	0.075	61.268	72.898
	03-May	86	72.0	61.2	27.4	6.0	24.9	7.9	1209	0.075	61.944	73.801
	04-May	87	73.0	62.1	27.5	10.8	25.1	7.9	1210	0.075	62.329	73.952
	07-May	91	71.0	60.4	28.0	10.6	50.3	7.8	1321	0.063	60.549	46.323
	08-May	92	72.0	61.2	29.0	10.5	50.4	7.8	1318	0.063	59.708	46.970
	09-May	93	73.0	62.1	28.4	9.9	50.2	7.8	1320	0.063	61.096	47.904
	10-May	94	74.0	62.9	27.5	10.8	50.8	7.8	1328	0.063	62.838	47.993
	11-May	95	70.2	59.7	27.6	10.8	51.0	7.8	1329	0.063	60.684	44.952
	12-May	97	70.3	59.8	27.0	9.2	51.1	7.8	1321	0.063	61.607	44.944
	13-May	99	70.4	59.8	28.3	9.2	50.6	7.8	1320	0.063	59.801	45.549

	14-May	102	70.5	59.9	27.6	9.5	50.0	7.8	1317	0.063	60.851	46.239
	15-May	106	70.6	60.0	30.8	9.0	37.3	7.7	1170	0.058	56.306	59.982
	16-May	108	70.0	59.5	33.7	9.3	30.3	8.4	1310	0.224	51.832	67.196
	17-May	110	70.8	60.2	32.9	9.4	30.4	8.4	1319	0.224	53.531	67.471
	18-May	112	71.5	60.8	34.0	9.2	30.6	8.4	1316	0.224	52.434	67.578
	19-May	113	71.9	61.1	33.7	12.6	30.9	8.4	1320	0.224	53.199	67.442
	20-May	116	72.0	61.2	33.0	12.0	31.0	8.4	1324	0.224	54.194	67.361
	28-May	118	73.0	62.1	30.9	12.6	30.9	8.4	1320	0.224	57.671	67.933
Phase III	29-May	120	70.9	93.59	34.10	12.8	30.6	8.41	1320	0.224	51.904	67.304
	30-May	122	71.5	94.38	33.50	12.4	30.7	8.41	1321	0.224	53.147	67.472
	31-May	124	74.0	97.68	32.59	7.8	30.3	8.41	1323	0.224	55.959	68.969
	05-Jun	126	50.1	66.13	17.77	7.9	14.9	7.4	925	0.027	64.528	77.422
	06-Jun	128	50.1	66.13	18.01	7.5	14.5	7.4	915	0.027	64.052	78.074
	07-Jun	130	50.1	66.13	17.40	7.6	14.6	7.4	912	0.027	65.269	77.878
	08-Jun	132	50.1	66.13	17.50	12.4	14.9	7.4	915	0.027	65.070	77.422

	09-Jun	134	51.1	67.45	10.80	12.5	13.7	7.6	1122	0.043	78.868	79.763
	10-Jun	136	51.1	67.45	10.80	12.8	13.6	7.6	1125	0.043	78.868	79.778
	11-Jun	138	51.1	67.45	10.65	12.6	13.2	7.6	1121	0.043	79.159	80.416
	20-Jun	141	51.1	67.45	9.90	12.7	13.7	7.6	1129	0.043	80.626	79.763
	29-Jun	150	52.1	68.77	6.10	26.9	3.1	6.81	540	0.007	88.292	95.565
	30-Jun	152	52.1	68.77	5.16	26.1	3.1	6.81	5402	0.007	90.094	95.559
	03-Jul	154	53.1	70.09	4.84	26.0	2.6	6.84	440	0.008	90.887	96.241
	04-Jul	155	53.1	70.09	4.59	24.9	2.4	6.84	439	0.008	91.356	96.576
	06-Jul	157	54.1	71.41	0.41	25.0	2.8	6.9	345	0.009	99.245	96.105
	07-Jul	160	55.1	72.73	0.42	25.4	3.1	7.77	660	0.062	99.245	95.774
	11-Jul	162	55.1	72.73	0.49	23.4	3.1	7.77	663	0.062	99.111	95.774
	12-Jul	163	56.1	74.05	7.62	22.9	24.7	7.37	445	0.026	86.415	66.579
	13-Jul	165	56.1	74.05	8.01	23.4	24.7	7.37	444	0.026	85.722	66.579
	14-Jul	167	56.1	74.05	8.10	12.8	25.1	7.37	445	0.026	85.561	66.105
	18-Jul	169	56.1	74.05	7.50	12.5	26.0	7.37	449	0.026	86.631	64.876
	19-Jul	171	56.1	74.05	7.90	12.4	24.5	7.37	446	0.026	85.918	66.915
	20-Jul	173	56.1	74.05	7.80	1.0	24.7	7.37	445	0.026	86.096	66.579
	24-Jul	175	57.1	75.37	5.54	1.9	3.3	7.38	710	0.026	90.299	95.594

	25-Jul	177	57.1	75.37	5.36	2.0	3.6	7.38	709	0.026	90.613	95.210
	26-Jul	179	57.1	75.37	5.48	1.5	3.3	7.38	700	0.026	90.403	95.688
	27-Jul	181	57.1	75.37	4.98	0.6	3.3	7.38	711	0.026	91.278	95.594
	31-Jul	183	53.6	70.75	2.80	0.9	3.0	8.49	1070	0.258	94.776	95.730
	02-Aug	186	56.5	74.62	3.27	1.0	3.0	8.42	1001	0.228	94.216	96.013
	03-Aug	188	56.5	74.62	3.56	1.5	3.0	8.42	1001	0.228	93.702	96.013
	04-Aug	191	56.5	74.62	3.47	1.6	2.6	8.42	1021	0.228	93.862	96.516
	05-Aug	193	56.5	74.62	3.21	0.8	2.5	8.42	1001	0.228	94.321	96.596
	10-Aug	194	56.5	74.62	3.56	0.9	3.6	8.32	1211	0.190	93.702	95.187
	11-Aug	196	56.5	74.62	3.48	1.0	3.7	8.32	1201	0.190	93.844	95.108
	12-Aug	198	56.5	74.62	3.69	0.6	3.2	8.32	1203	0.190	93.472	95.711
	13-Aug	200	56.5	74.62	3.80	0.8	3.4	8.32	1201	0.190	93.284	95.443
	18-Aug	202	51.2	67.58	3.92	0.9	3.1	8.56	1148	0.290	92.351	95.460
	19-Aug	204	51.2	67.58	3.65	1.0	3.1	8.56	1149	0.290	92.871	95.460
	20-Aug	207	51.2	67.58	3.24	0.7	3.6	8.56	1138	0.290	93.672	94.673
	21-Aug	208	51.2	67.58	2.99	0.8	3.4	8.56	1148	0.290	94.160	94.969

	22-Aug	211	51.2	67.58	3.90	0.9	3.0	8.56	1151	0.290	92.383	95.531
	23-Aug	213	51.2	67.58	3.87	1.0	3.1	8.56	1148	0.290	92.441	95.460
	24-Aug	215	51.2	67.58	3.48	0.9	3.9	8.56	1150	0.290	93.203	94.229
	25-Aug	217	51.2	67.58	3.69	0.9	4.0	8.56	1148	0.290	92.793	94.067
	07-Sep	222	52.3	69.08	3.42	1.2	3.1	8.12	1185	0.129	93.470	95.440
	08-Sep	225	52.3	69.08	3.33	1.0	3.1	8.12	1195	0.129	93.637	95.440
	09-Sep	227	52.3	69.08	3.45	1.6	3.3	8.12	1196	0.129	93.407	95.281
	10-Sep	228	52.3	69.08	2.99	1.1	3.5	8.12	1190	0.129	94.286	94.919
	13-Sep	229	51.4	67.90	3.87	1.0	3.0	8.23	1421	0.160	92.477	95.582
	14-Sep	230	51.4	67.90	3.65	1.5	3.5	8.23	1428	0.160	92.905	94.829
	15-Sep	232	51.4	67.90	3.56	1.6	3.6	8.23	1423	0.160	93.080	94.698
	16-Sep	234	51.4	67.90	3.84	1.5	3.6	8.23	1411	0.160	92.537	94.713
	20-Sep	236	50.6	66.73	3.15	2.0	3.5	8.24	1121	0.163	93.769	94.810
	21-Sep	238	50.6	66.73	3.40	1.5	3.3	8.24	1122	0.163	93.284	95.055
	22-Sep	240	50.6	66.73	3.55	2.1	3.3	8.24	1126	0.163	92.978	95.115

	23-Sep	242	50.6	66.73	3.36	2.0	3.7	8.24	1121	0.163	93.354	94.530
	27-Sep	243	49.7	65.56	3.45	2.5	3.0	8.34	1230	0.197	93.054	95.354
	28-Sep	246	49.7	65.56	3.21	2.3	3.0	8.34	1239	0.197	93.537	95.354
	29-Sep	249	49.7	65.56	3.80	2.4	3.1	8.34	1240	0.197	92.349	95.272
	05-Oct	251	48.8	64.39	3.17	2.0	3.3	8.13	1296	0.132	93.506	94.937
	06-Oct	253	48.8	64.39	3.45	1.8	3.5	8.13	1299	0.132	92.928	94.642
	07-Oct	255	48.8	64.39	3.78	2.1	3.4	8.13	1293	0.132	92.251	94.745
	12-Oct	258	47.9	63.22	2.82	2.0	2.6	8.1	1329	0.124	94.106	95.935
	13-Oct	261	47.9	63.22	2.56	2.6	2.1	8.1	1319	0.124	94.655	96.757
	17-Oct	263	47.0	62.05	3.19	3.2	3.6	7.94	1259	0.089	93.220	94.165
	18-Oct	265	47.0	62.05	3.69	3.4	4.0	7.94	1269	0.089	92.150	93.586
	19-Oct	269	47.0	62.05	3.45	3.5	3.7	7.94	1255	0.089	92.661	94.118
	24-Oct	270	53.1	70.09	3.59	2.6	3.5	7.87	1248	0.077	93.239	95.078
	25-Oct	273	53.1	70.09	3.78	3.0	3.3	7.87	1238	0.077	92.881	95.349
	30-Oct	276	50.8	67.08	4.87	3.1	4.4	7.71	1302	0.055	90.414	93.458

	31-Oct	278	50.8	67.08	4.59	3.2	4.3	7.71	1312	0.055	90.968	93.649
	01-Nov	281	50.8	67.08	4.87	3.2	4.3	7.71	1303	0.055	90.417	93.604
	05-Nov	282	51.3	67.75	4.78	3.5	4.2	7.91	1225	0.084	90.687	93.786
	06-Nov	284	51.3	67.75	4.80	3.6	4.3	7.91	1265	0.084	90.654	93.720
	07-Nov	287	51.3	67.75	4.56	4.0	4.3	7.91	1255	0.084	91.116	93.638
	14-Nov	291	51.8	68.42	4.68	3.0	5.0	7.84	1149	0.072	90.977	92.678
	15-Nov	293	51.8	68.42	4.69	3.0	4.1	7.84	1140	0.072	90.952	93.988
	16-Nov	295	51.8	68.42	4.89	3.0	4.1	7.84	1143	0.072	90.566	93.988
	17-Nov	297	51.8	68.42	4.79	3.0	4.2	7.84	1149	0.072	90.759	93.818
	18-Nov	301	51.8	68.42	4.98	2.6	4.5	7.84	1142	0.072	90.393	93.409
	19-Nov	303	52.3	69.09	4.07	2.8	3.8	7.94	1112	0.089	92.218	94.520
	20-Nov	309	52.3	69.09	4.01	3.4	3.5	7.94	1100	0.089	92.339	94.978
	04-Dec	311	52.3	69.09	3.99	3.0	3.2	7.94	1103	0.089	92.377	95.441
	05-Dec	313	52.3	69.09	3.89	2.5	3.2	7.94	1102	0.089	92.568	95.383
	06-Dec	315	52.3	69.09	4.10	2.4	3.8	7.94	1120	0.089	92.167	94.442

	07-Dec	316	52.3	69.09	4.20	3.0	3.5	7.94	1102	0.089	91.976	94.876
	10-Dec	317	52.9	69.77	3.84	3.0	3.7	7.89	1205	0.080	92.742	94.650

Appendice B. [Nitrogen fate analysis in the UASB reactor]

Table 0-2 Nitrogen fate analysis results for the UASB reactor

		THEORETICAL VALUES (100% EFFICIENCY)				THEORETICAL VALUES (Based on observed ammonia removal efficiency)					DENITRIFICATION POSSIBLE CONTRIBUTION ESTIMATION BASED ON ALKALINITY							
	Time (days)	Nitrate out (mgN/L)	Alkalinity out (mgCaCO3/L)	Nitrogen gas (mgN/L)	N in cells (mgN/L)	Ammonia removal (%)	Nitrate out (mgN/L)	Alkalinity out (mgCaCO3/L)	Nitrogen gas (mgN/L)	N in cells (mgN/L)5	Alkalinity in (mgCaCO3/L)	Alkalinity out (mgCaCO3/L)	Alkalinity out (mgCaCO3/L)Based on observed ammonia removal efficiency)	Difference in observed and expected alkalinity (mg CaCO3/L)	Conversion of CaCO3 to CO2 (mg/L)	Conversion of CO2 to nitrite and nitrate removal mgN/L	Free ammonia (mgN/L)	Free nitrous oxide (mgN/L)
PHASE I	1	10.1816129	3486.55316	39.8295	0.392900415	27.88104089	2.838739657	3496.250881	11.10487925	0.109544725	3500	3290	3496.250881	206.250881	121.7218314	967.4922344	19.59839311	0.000106736
	2	10.3645161 3	3486.3116	40.545	0.399958506	42.66564618	4.422087778	3494.159756	17.29878625	0.170644881	3500	2780	3494.159756	714.1597557	421.4713312	3350.017291	15.86055525	5.32289E-05
	3	10.6287090 68	3485.96268	41.5785	0.410153527	49.78853768	5.291879122	3493.011024	20.70132714	0.204209443	3500	2655	3493.011024	838.0110236	494.5638828	3930.985185	22.91292341	1.27222E-05
	4	10.9741935 5	3485.5064	42.93	0.423485477	51.36926899	5.637362993	3492.554744	22.05282714	0.217541394	3500	2655	3492.554744	837.5547436	494.2946028	3928.844843	22.91292341	1.27222E-05
	5	11.1977419 4	3485.21116	43.8045	0.432112033	63.83257207	7.147806691	3490.559903	27.96153903	0.275828225	3500	2215	3490.559903	1275.559903	752.7819451	5983.461959	10.80942 3	8.3557E-05
	6	11.3826774 2	3484.9669 16	44.52795	0.439248548	64.42018784	7.332742175	3490.315659	28.68498903	0.282964774	3500	2215	3490.315659	1275.315659	752.6405307	5982.316246	10.80942 3	8.3557E-05
	7	11.0351612 9	3485.42588	43.1685	0.425838174	74.27550371	8.196421633	3489.174999	32.06362082	0.316293449	3500	1400	3489.174999	2089.174999	1232.955737	9800.009472	7.57669 8367	9.7792 7E-05
	9	11.1977419 4	3485.21116	43.8045	0.432112033	78.36714591	8.775350761	3488.410408	34.32833643	0.338633868	3500	1180	3488.410408	2308.410408	1362.340569	10828.4102	6.46549273	0.000196204
	10	10.6287090 68	3485.96268	41.5785	0.410153527	77.03632887	8.187967742	3489.186164	32.03055	0.315967222	3500	1180	3489.186164	2309.186164	1362.798392	10832.04915	6.51442811 6	0.000196204

	11	10.99451613	3485.47956	43.0095	0.42426971	77.26432532	8.4948387 1	3488.78088	33.231	0.327809129	3500	1180	3488.78088	2308.78088	1362.559208	10830.14803	6.671729045	0.000196204
	12	10.20193548	3486.52632	39.909	0.3936846 47	76.4940239	7.8038709 68	3489.69344	30.528	0.3011452 28	3500	1180	3489.69344	2309.69344	1363.097768	10834.42871	6.4005205 47	0.000196204
	13	10.24258065	1441.47264	40.068	0.3952531 12	77.4583997 2	7.9337390 57	1444.5219 23	31.0360316	0.3061567 35	1455	1175	1444.5219 23	269.52192 34	159.06211 87	1264.28729 2	3.9739806 46	0.000290213
	14	11.40096774	1439.94276	44.5995	0.4399543 57	81.7406516 5	9.3192253 27	1442.6921 14	36.4559219 3	0.3596215 58	1455	1430	1442.6921 14	12.6921139	7.4904278 77	59.5368202 9	1.4696416 2	0.000712325
	16	10.1816129	1441.55316	39.8295	0.3929004 15	76.5799256 5	7.7970715 91	1444.7024 2	30.5014014 9	0.3008828 46	1455	955	1444.7024 2	489.70241 99	289.00470 68	2297.12128 3	1.0418773 88	0.000734682
	19	10.05967742	1441.7142	39.3525	0.3881950 21	58.9883969 8	5.9340424 51	1447.1629 2	23.2134089 2	0.2289900 2	1455	860	1447.1629 2	587.16291 96	346.52237 88	2754.29400 4	1.0943605 05	0.001129339
	20	10.14096774	1441.60684	39.6705	0.3913319 5	77.6057691 6	7.8699760 16	1444.6061 35	30.7865965 5	0.3036961 7	1455	770	1444.6061 35	674.60613 52	398.12821 09	3164.47713 5	0.6434405 7	0.001917209
	22	9.7548387 1	1442.1168	38.16	0.3764315 35	75.9433085 5	7.4081472 6	1445.2160 72	28.9799665 4	0.2858745 62	1455	510	1445.2160 72	935.21607 17	551.93079 64	4386.95962	1.6233420 59	0.000442693
	23	10.1816129	941.55316	39.8295	0.3929004 15	77.1457085 8	7.8546774 19	944.62634	30.7267 5	0.3031058 09	955	510	944.62634	434.62634	256.50079 08	2038.76757 6	1.6096757 16	0.000454896
	24	10.40516129	941.25792	40.704	0.4015269 71	76.7578125	7.9867741 94	944.45188	31.2435	0.3082033 2	955	510	944.45188	434.45188	256.39783 08	2037.94921	1.6729380 8	0.000458994
	25	10.34419355	941.33844	40.4655	0.3991742 74	77.4066796 76	8.0070967 74	944.42504	31.323	0.3089875 52	955	510	944.42504	434.42504	256.38199 08	2037.82330 8	1.6167048 67	0.000404467
	26	10.24258065	941.47264	40.068	0.3952531 12	77.0888652 9	7.8958891 95	944.57191 17	30.8879665 4	0.3046961 39	955	510	944.57191 17	434.57191 17	256.46866 92	2038.51226 1	1.6233420 59	0.000442693
	27	10.22225806	941.49948	39.9885	0.3944688 8	78.1541235 9	7.9891162 01	944.44878 69	31.2526617 1	0.3082936 96	955	415	944.44878 69	529.44878 69	312.46157 92	2483.56558 4	1.4829935 35	0.000481459
	29	10.56774194	901.0432	41.34	0.4078008 3	78.1519874 2	8.2589003 48	904.09248 34	32.3080316	0.3187044 53	915	530	904.09248 34	374.09248 34	220.77589 19	1754.81225	1.6973327 57	0.000416885
	34	10.24258065	948.47264	40.068	0.3952531 12	77.0888652 9	7.8958891 95	951.57191 17	30.8879665 4	0.3046961 39	962	675	951.57191 17	276.57191 17	163.22276 75	1297.35773 9	2.4559496 94	0.000282376

	35	10.36451613	967.3116	40.545	0.399958506	77.54901961	8.037580645	970.38478	31.44225	0.3101639	981	675	970.38478	295.38478	174.3254439	1385.606109	2.435273922	0.000282376
	36	10.97419355	1321.5064	42.93	0.423485477	78.42592593	8.606612903	1324.633266	33.66825	0.3321224	1336	675	1324.633266	649.63326	383.3901207	3047.333088	2.477811457	0.000290596
	37	11.17741935	1435.238	43.725	0.431327801	78.54545455	8.779354839	1438.405128	34.344	0.3387883	1450	675	1438.405128	763.40512	450.5341692	3581.010997	2.509714609	0.000288069
	38	11.38064516	1354.9696	44.52	0.439170124	79.37997876	9.033953711	1358.068872	35.33996654	0.3486131	1370	675	1358.068872	683.06887117	403.1226128	3204.174574	2.455949694	0.000300703
	40	10.56774194	1606.0432	41.34	0.407800833	66.69073492	7.047704761	1610.692108	27.56994981	0.2719653	1620	700	1610.692108	910.69210775	537.4576372	4271.921349	1.604962441	0.001185489
	42	10.77096774	1000.7748	42.135	0.415643154	64.50796074	6.948131667	1005.823614	27.18042937	0.2681229	1015	660	1005.823614	345.8236135	204.0926244	1622.207182	5.177701029	0.000216838
	46	10.97419355	1255.5064	42.93	0.423485477	76.54688145	8.400402926	1258.905601	32.86157621	0.3241649	1270	405	1258.905601	853.90560123	503.9442892	4005.544286	3.303280868	0.000225378
	48	10.36451613	736.3116	40.545	0.399958506	63.48130333	6.579529992	741.3104253	25.73849442	0.2538988	750	360	741.3104253	381.3104253	225.0356608	1788.670543	6.408450333	0.000129531
	49	10.56774194	636.0432	41.34	0.407800833	64.30769231	6.795870968	641.0247044	26.5848	0.2622473	650	360	641.0247044	281.0247044	165.8506457	1318.245127	6.386244602	0.000132999
	50	10.77096774	415.7748	42.135	0.415643154	64.13207547	6.907645161	420.8770884	27.02205	0.2665605	430	360	420.8770884	60.877084	35.92745941	285.5653548	6.541083507	0.000127562
	51	10.16129032	416.58	39.75	0.392116183	60.4	6.137419355	421.89432	24.009	0.2368381	430	360	421.89432	61.89432	36.52779541	290.3370577	6.812911806	0.000130276
	52	10.18161296	416.55316	39.8295	0.392900415	60.07984032	6.117096774	421.92116	23.9295	0.2360539	430	360	421.92116	61.92116	36.54363541	290.4629602	6.817290797	0.000123491
	53	10.56774194	416.0432	41.34	0.407800833	64.18358593	6.782755726	421.0420253	26.53349442	0.2617411	430	360	421.0420253	61.04202528	36.02480188	286.3390698	6.408450333	0.000127562
	54	10.18161296	416.55316	39.8295	0.392900415	63.87225549	6.503225806	421.4112	25.44	0.2509543	430	360	421.4112	61.4112	36.24267541	288.0708136	6.227964833	0.000129531
PHASE II	55	14.53064516	935.8094	56.8425	0.560726141	91.54929577	13.30270332	937.4311408	52.03890845	0.5133408	955	620	937.4311408	317.4311408	187.3364111	1489.022312	0.884644254	0.000471485

	58	14.530645 16	935.8094	56.8425	0.560726141	72.24080268	10.4970547	941.1365565	41.06347826	0.4050730 65	955	630	941.1365565	311.1365565	183.6215743	1459.495352	1.5496048 48	0.0014374 99
	61	14.652580 65	895.6483 6	57.3195	0.565431535	77.77844781	11.3965497 9	899.9485948	44.58221739	0.4397838 72	915	600	899.9485948	299.9485948	177.0188428	1407.014286	0.9225319 17	0.0029422 13
	66	14.835483 87	942.4068	58.035	0.572489627	76.7421084	11.3850631 1	946.9637652	44.53728261	0.4393406 1	962	580	946.9637652	366.9637652	216.5687795	1721.372492	0.9776084 49	0.0014711 07
	67	14.530645 16	961.8094	56.8425	0.560726141	77.06293706	11.1977419 4	966.2116	43.8045	0.4321120 33	981	610	966.2116	356.2116	210.2229797	1670.933619	0.9443121 82	0.0013581 61
	68	14.408709 68	952.2704 4	56.3655	0.560207 47	76.05322867	10.9582889 2	956.8274052	42.86778261	0.4228717 3	971.3	520	956.8274052	436.8274052	257.7997801	2049.092446	0.9776084 49	0.0014120 56
	69	14.388387 1	958.19728	56.286	0.552365 15	77.10451977	11.0940967 7	962.5480444	43.39905	0.4281124 48	977.2	550	962.5480444	412.5480444	243.4709768	1935.20157	0.9333719 8	0.0014875 09
	70	14.632258 06	963.7752	57.24	0.564647303	67.45169082	9.8697054 7	970.0650957	38.60934783	0.3808641 53	983.1	621	970.0650957	349.0650957	206.0056302	1637.412493	2.4139727 19	0.0005971 25
	71	14.835483 87	969.4068	58.035	0.572489627	68.63013699	10.1816129	975.55316	39.8295	0.3929004 15	989	612	975.55316	363.55316	214.5596 33	1705.37385	2.3588857 72	0.0006136 11
	72	14.429032 26	975.8436	56.445	0.568049 79	67.04225352	9.6735483 87	982.12416	37.842	0.3732946 06	994.9	700	982.12416	282.12416	166.4995043	1323.402511	2.4103898 28	0.0006020 33
	73	14.835483 87	981.2068	58.035	0.572489627	67.26027397	9.9783870 97	987.62156	39.0345	0.3850580 91	1000.8	621.6	987.62156	366.02156	216.0127239	1716.952748	2.4618938 84	0.0005971 25
	76	14.347741 94	987.75096	56.127	0.536680 5	58.33846533	8.3702524 54	995.6454209	32.74363043	0.3230014 43	1006.7	624.7454545	995.6454209	370.8999663	218.8917834	1739.836627	2.6117438 6	0.0014570 84
	77	14.429032 26	993.5436	56.445	0.568049 79	59.14084507	8.5334516 13	1001.329884	33.38205	0.3292991 7	1012.6	627.8909091	1001.329884	373.4389749	220.3902147	1751.746739	2.5759554 41	0.0014622 59
	78	14.733870 97	999.041	57.6375	0.568568465	58.34482759	8.5964516 13	1007.146684	33.6285	0.3317302 9	1018.5	631.0363636	1007.146684	376.1103164	221.9667441	1764.276045	2.6816220 03	0.0014690 6
	79	14.957419 35	1004.64576	58.512	0.577195021	59.10326087	8.8403225 81	1012.7246	34.5825	0.3411410 79	1024.4	634.1818182	1012.7246	378.5427818	223.4022975	1775.687939	2.6727424 6	0.0014826 62
	80	14.408709 68	1011.27044	56.3655	0.560207 47	58.39210155	8.4135483 87	1019.188824	32.913	0.3246721 99	1030.3	637.3272727	1019.188824	381.8609673	225.3605708	1791.253053	2.6194652 02	0.0014570 84

	83	14.34774194	1017.2509 6	56.127	0.5536680 5	61.386870 3	8.8076297 34	1024.5 67777	34.4546087	0.3398794 88	1036.2	640.47 27273	1024.5 67777	384.09 50501	226.67 9046	1801.73 2804	1.8 290 454 96	0.0 023 004 08
	84	14.32335484	1023.1 831 68	56.031 6	0.5527 269 71	60.258 229 28	8.631	1030.7 010 52	33.763 65	0.3330 634 85	1042.1	643.61 818 18	1030.7 010 52	387.08 287 02	228.44 234 96	1815.74 822 4	1.8 793 077 83	0.0 023 486 74
	85	14.42903226	1028.9 436	56.445	0.5568 049 79	61.267 605 63	8.8403 225 81	1036.3 246	34.582 5	0.3411 410 79	1048	646.76 363 64	1036.3 246	389.56 096 36	229.90 483 1	1827.37 259 2	1.8 450 897 55	0.0 023 303 25
	86	14.63225806	1034.5 752	57.24	0.5646 473 03	61.944 444 44	9.0638 709 68	1041.9 293 6	35.457	0.3497 676 35	1053.9	649.90 909 09	1041.9 293 6	392.02 026 91	231.35 622 44	1838.90 882 9	1.8 383 803 37	0.0 022 844 52
	87	14.83548387	1040.2 068	58.035	0.5724 896 27	62.328 767 12	9.2467 741 94	1047.5 878	36.172 5	0.3568 257 26	1059.8	653.05 454 55	1047.5 878	394.53 325 45	232.83 929 78	1850.69 687	1.8 450 897 55	0.0 023 028 01
	91	14.42903226	1046.6 436	56.445	0.5568 049 79	60.549 295 77	8.7366 774 19	1054.1 614 84	34.177 05	0.3371 414 94	1065.7	656.2	1054.1 614 84	397.96 148 4	234.86 251 51	1866.77 818 5	1.5 778 069 94	0.0 055 488 71
	92	14.63225806	1052.2 752	57.24	0.5646 473 03	59.708 333 33	8.7366 774 19	1060.0 614 84	34.177 05	0.3371 414 94	1071.6	659.34 545 45	1060.0 614 84	400.71 602 95	236.48 814 85	1879.69 934 8	1.6 341 371 26	0.0 055 591 82
	93	14.83548387	1057.9 068	58.035	0.5724 896 27	61.095 890 41	9.0638 709 68	1065.5 293 6	35.457	0.3497 676 35	1077.5	662.49 090 91	1065.5 293 6	403.03 845 09	237.85 875 79	1890.59 348 2	1.5 997 757 46	0.0 055 371 21
	94	15.03870968	1063.5 384	58.83	0.5803 319 5	62.837 837 84	9.45	1070.9 194	36.9675	0.3646 680 5	1083.4	665.63 636 36	1070.9 194	405.28 303 64	239.18 343 13	1901.12 249 9	1.5 490 786 27	0.0 056 033 02
	95	14.26645161	1070.4 583 2	55.809	0.5505 311 2	60.683 760 68	8.6574 193 55	1077.8 661 6	33.867	0.3340 829 88	1089.3	668.78 181 82	1077.8 661 6	409.08 434 18	241.42 682 47	1918.95 385 8	1.5 547 116 4	0.0 056 264 65
	97	14.28677419	1076.3 314 8	55.8885	0.5513 153 53	61.607 396 87	8.8017 096 77	1083.5 755 96	34.431 45	0.3396 510 37	1095.2	671.92 727 27	1083.5 755 96	411.64 832 33	242.93 999 41	1930.98 111 4	1.5 203 502 6	0.0 056 352 9
	99	14.30709677	1082.2 046 4	55.968	0.5520 995 85	59.801 136 36	8.5558 064 52	1089.8 003 6	33.469 5	0.3301 618 26	1101.1	675.07 272 73	1089.8 003 6	414.72 763 27	244.75 729 14	1945.42 569 7	1.5 941 427 33	0.0 055 812 42
	102	14.32741935	1088.0 778	56.047 5	0.5528 838 17	60.851 063 83	8.7183 870 97	1095.4 856 4	34.105 5	0.3364 356 85	1107	678.21 818 18	1095.4 856 4	417.26 745 82	246.25 620 48	1957.33 964 1	1.5 547 116 4	0.0 055 183 7
	106	14.34774194	1093.9 509 6	56.127	0.5536 680 5	56.306 195 34	8.0786 676 02	1102.2 305 17	31.602 978 26	0.3117 494 14	1112.9	681.36 363 64	1102.2 305 17	420.86 688 02	248.38 045 39	1974.22 399 5	1.5 912 618 54	0.0 045 103 67
	108	14.22580645	1100.0 12	55.65	0.5489 626 56	51.832 298 14	7.3735 624 12	1109.0 617 48	28.844 673 91	0.2845 399 6	1118.8	684.50 909 09	1109.0 617 48	424.55 265 69	250.55 566 64	1991.51 342 6	7.0 360 884 88	0.0 007 837 72

	110	14.388387 1	1105.6972 8	56.286	0.5552365 15	53.531073 45	7.7022580 65	1114.5276 4	30.1305	0.2972240 66	1124.7	687.65454 55	1114.5276 4	426.87309 45	251.92510 5	2002.39825 4	6.8655166 46	0.0007860 77
	112	14.530645 16	1111.4094	56.8425	0.5607261 41	52.433566 43	7.6189354 84	1120.5376 84	29.80455	0.2940087 14	1130.6	690.8	1120.5376 84	429.73768 4	253.61568 24	2015.83561 7	7.0971495 78	0.0007912 48
	113	14.611935 48	1117.2020 4	57.1605	0.5638630 71	53.198887 34	7.7733870 97	1126.2337	30.40875	0.2999688 8	1136.5	693.94 54545	1126.2337	432.28 82455	255.12 09317	2027.79 9922	7.0220 25384	0.0007 99005
	116	14.632258 06	1123.0752	57.24	0.5646473 03	54.194444 44	7.9298 70968	1131.9270 32	31.0209	0.3060074 69	1142.4	697.09 09091	1131.9270 32	434.83 61229	256.62 45971	2039.75 1637	6.8822 10911	0.0008 02108
	118	14.835483 87	1128.7068	58.035	0.5724896 27	57.671232 88	8.5558 06452	1137.0 0036	33.4695	0.3301618 26	1148.3	700.23 63636	1137.0 0036	436.76 39964	257.76 23585	2048.79 5004	6.4481 60011	0.0007 99005
	120	14.408709 68	1135.1 7044	56.3655	0.5560207 47	51.904090 27	7.4787 09677	1144.3 2288	29.256	0.2885975 1	1154.2	703.38 18182	1144.3 2288	440.94 10618	260.22 75119	2068.38 8998	7.1159 30627	0.0007 91248
	122	14.530645 16	1316.8094	56.8425	0.5607261 41	53.146853 15	7.7225 80645	1325.8008	30.21	0.2980082 99	1336	706.52 72727	1325.8008	619.27 35273	365.47 29013	2904.92 0093	6.9907 23636	0.0007 93834
	124	15.038709 68	1430.1384	58.83	0.5803319 5	55.959459 46	8.4155 80645	1438.8 85556	32.92095	0.3247506 22	1450	709.67 27273	1438.8 85556	729.21 28287	430.35 5112	3420.62 902	6.8008 26367	0.0007 83772
PHASE III	126	10.181612 9	1356.5531 6	39.8295	0.3929004 15	64.528301 89	6.5700 21911	1361.3 22982	25.7013	0.2535319 66	1370	589.6	1361.3 22982	771.72 29825	455.44 30716	3620.03 7834	0.4289 14239	0.0039 50471
	128	10.181612 9	1606.5531 6	39.8295	0.3929004 15	64.051896 21	6.5215 16129	1611.3 87044	25.511 55	0.2516601 66	1620	690.23	1611.3 87044	921.15 7044	543.63 36653	4321.01 0811	0.4346 74809	0.0038 3644
	130	10.181612 9	1001.5531 6	39.8295	0.3929004 15	65.269461 08	6.6454 83871	1006.2 2332	25.9965	0.2564439 83	1015	545.23	1006.2 2332	460.99 332	272.06 16315	2162.45 1161	0.4199 52342	0.0038 70835
	132	10.181612 9	1256.5531 6	39.8295	0.3929004 15	65.069860 28	6.6251 6129	1261.2 5016	25.917	0.2556597 51	1270	641.3	1261.2 5016	619.95 016	365.87 22256	2908.09 4077	0.4223 65861	0.0039 50471
	134	10.384838 71	736.28 476	40.6245	0.4007427 39	78.867924 53	8.1903 06756	739.18 30749	32.0397	0.3160574 81	750	720.6	739.18 30749	18.583 07487	10.967 06058	87.1704 4279	0.4083 13843	0.0022 78797
	136	10.384838 71	714.28 476	40.6245	0.4007427 39	78.867924 53	8.1903 06756	717.18 30749	32.0397	0.3160574 81	728	559.4	717.18 30749	157.78 30749	93.117 88025	740.136 9579	0.4083 13843	0.0022 77128
	138	10.384838 71	1606.2 8476	40.6245	0.4007427 39	79.158 51272	8.2204 83871	1609.1 4322	32.157 75	0.3172219 92	1620	524.87	1609.1 4322	1084.2 7322	639.89 89495	5086.16 4554	0.4026 99099	0.0022 05341

	141	10.38483871	1001.28476	40.6245	0.400742739	80.62622309	8.372903226	1003.94192	32.754	0.3231037 34	1015	584.87	1003.94192	419.07192	247.32113 31	1965.804103	0.3743400 08	0.0022787 97
	150	10.58806452	1256.01636	41.4195	0.4085850 62	88.29174664	9.348387097	1257.6536	36.57	0.3607468 88	1270	649.2	1257.6536	608.4536	359.08737 05	2854.165422	0.0384097 69	0.0031387 83
	152	10.58806452	937.68302 67	41.4195	0.4085850 62	90.09433962	9.539246805	939.06819 86	37.316625	0.3681120 14	951.66666 67	741.2	939.06819 86	197.86819 86	116.77467 46	928.1703165	0.0324962 33	0.0031434 04
	154	10.79129032	762.41462 67	42.2145	0.4164273 86	90.88679245	9.807857638	763.71344 47	38.367405	0.3784774 94	776.66666 67	623.48	763.71344 47	140.23344 47	82.76072143	657.8142504	0.0326374 79	0.0025305 03
	155	10.79129032	1355.74796	42.2145	0.4164273 86	91.35593 22	9.858483871	1356.9799 16	38.56545	0.3804311 2	1370	645.08545 45	1356.9799 16	711.89446 15	420.13443 63	3339.391132	0.0309573 31	0.0023050 57
	157	10.99451613	1605.47956	43.0095	0.4242697 1	99.24528302	10.91153865	1605.589148	42.6849	0.4210676 74	1620	648.50909 09	1605.589148	957.08005 73	564.83413 22	4489.520328	0.0031591 84	0.0023267 61
	160	11.19774194	1855.21116	43.8045	0.4321120 33	99.24528302	11.11323068	1855.322774	43.4739	0.4288508 1	1870	651.93272 73	1855.322774	1203.390047	710.19740 46	5644.923887	0.0229158 16	0.0003469 27
	162	11.19774194	1635.21116	43.8045	0.4321120 33	99.11070 78	11.09816129	1635.342676	43.4149 5	0.4282692 95	1650	655.35636 36	1635.342676	979.98631 24	578.35257 78	4596.970167	0.0270019 85	0.0003469 27
	163	11.40096774	1414.94276	44.5995	0.4399543 57	86.41509434	9.852157033	1416.988272	38.5407	0.3801869 73	1430	658.78	1416.988272	758.20827 18	447.46717 68	3556.642335	0.1718884 84	0.0070163 66
	165	11.40096774	1324.94276	44.5995	0.4399543 57	85.72192513	9.773129032	1327.092644	38.23155	0.3771373 44	1340	662.20363 64	1327.092644	664.88900 76	392.39351 27	3118.895533	0.1806590 87	0.0070163 66
	167	11.40096774	1034.94276	44.5995	0.4399543 57	85.56149733	9.754838 71	1037.1168	38.16	0.3764315 35	1050	665.62727 27	1037.1168	371.48952 73	219.23972 1	1742.60217	0.1826889 64	0.0071159 3
	169	11.40096774	894.94276	44.5995	0.4399543 57	86.63101604	9.876774194	896.95576	38.637	0.3811369 29	910	669.05090 91	896.95576	227.90485 09	134.50122 35	1069.067789	0.1691564 48	0.0073739 18
	171	11.40096774	1134.94276	44.5995	0.4399543 57	85.91800357	9.795483871	1137.0631 2	38.319	0.378	1150	672.47454 55	1137.0631 2	464.58857 45	274.18342 1	2179.315966	0.1781781 25	0.0069458 28
	173	11.40096774	948.27609 33	44.5995	0.4399543 57	86.09625668	9.815806452	950.36961 33	38.3985	0.3787842 32	963.33333 33	675.89818 18	950.36961 33	274.47143 15	161.98313 99	1287.504699	0.1759227 06	0.0070163 66
	175	11.60419355	865.34102 67	45.3945	0.4477966 8	90.29850746	10.47841358	866.82784 25	40.99055597	0.4043537 19	880.66666 67	679.32181 82	866.82784 25	187.50602 43	110.65929 3	879.5628969	0.1277950 7	0.0009201 3

	177	11.604193555	782.67436	45.3945	0.4779668	90.61295972	10.51490323	784.112984	41.13333	0.405761826	798	682.74545	784.112984	101.36752	59.82346001	475.5000176	0.1236528	0.0010001
	179	11.604193555	700.00769	45.3945	0.4779668	90.40280021	10.49051613	701.47852	41.0379	0.404820747	715.33333	686.16909	701.47852	15.30943442	9.035076054	71.81428192	0.1264	0.0009
	181	11.604193555	617.34102	45.3945	0.4779668	91.27845884	10.59212903	618.67765	41.4354	0.408741909	632.66667	689.59	618.67765	-70.91506861	-41.85151559	-332.6520489	0.1148	0.0009
	183	10.89290323	1230.61376	42.612	0.4203485	94.77611	10.32387097	1231.36528	40.386	0.3983900	1245	693.01	1231.36528	538.34	317.71	2525.31	0.6	6.4
	186	11.48806452	1310.827731	44.94021429	0.4433153	94.21641791	10.82364287	1311.752	42.3410601	0.4176758	1326	696.44	1311.752	615.26	363.10	2886.11	0.6	7.5
	188	11.48806452	1238.8	44.94021429	0.4433153	93.70229972	10.76458065	1239.7	42.1100142	0.4153966	1254	642.3	1239.7	597.48	352.61	2802.70	0.7	7.5
	191	11.48806452	1353.8	44.94021429	0.4433153	93.86151125	10.78287097	1354.7	42.1815642	0.4161024	1369	590.1	1354.7	764.65	451.27	3586.90	0.7	6.5
	193	11.48806452	1358.3	44.94021429	0.4433153	94.32145565	10.83570968	1359.1	42.3882642	0.4181414	1373.5	536.60	1359.1	822.58	485.45	3858.61	0.6	6.4
	194	11.48806452	1388.3	44.94021429	0.4433153	93.70229972	10.76458065	1389.2	42.1100142	0.4153966	1403.5	483.43	1389.2	905.84	534.59	4249.19	0.6	0.0
	196	11.48806452	1418.3	44.94021429	0.4433153	93.84382108	10.78083871	1419.2	42.1736142	0.4160240	1433.5	430.26	1419.2	988.99	583.66	4639.22	0.6	0.0
	198	11.48806452	634.82773	44.94021429	0.4433153	93.47232752	10.73816129	635.81812	42.0066642	0.4143771	650	377.09	635.81812	258.72	152.68	1213.62	0.6	0.0
	200	11.48806452	414.82773	44.94021429	0.4433153	93.28358209	10.71647809	415.84	41.9218416	0.4135404	430	323.92	415.84	91.92009	54.24792	431.1835	0.6	0.0
	202	10.40516129	726.25792	40.704	0.4015269	92.35074627	9.609244102	727.30908	37.5904477	0.3708131	740	270.75	727.30908	456.55	269.44	2141.61	1.0	5.6
	204	10.40516129	636.25792	40.704	0.4015269	92.87109375	9.663387097	637.23758	37.80225	0.3729024	650	217.58	637.23758	419.65	247.66	1968.52	1.0	5.6
	207	10.40516129	796.25792	40.704	0.4015269	93.671875	9.746709677	797.12753	38.1282	0.3761178	810	359.4	797.12753	437.72753	258.33100	2053.31	0.8	6.5

	208	10.405161629	1136.2579 2	40.704	0.4015269 71	94.160156 25	9.7975161 29	1137.0604 36	38.32695	0.3780784 23	1150	389.4	1137.0604 36	747.6604 36	441.24222 45	3507.16400 4	0.8230028 49	6.2402402E-05
	211	10.405161629	1107.2579 2	40.704	0.4015269 71	92.382812 5	9.6125806 45	1108.3046 8	37.6035	0.3709419 09	1121	400.5	1108.3046 8	707.80468	417.72079 48	3320.20657 5	1.0734819 76	5.5284E-05
	213	10.405161629	1187.2579 2	40.704	0.4015269 71	92.441406 25	9.6186774 19	1188.2966 28	37.62735	0.3711771 78	1201	424.2	1188.2966 28	764.09662 8	450.94227 23	3584.26373 8	1.0652244 23	5.6167E-05
	215	10.405161629	1342.7579 2	40.704	0.4015269 71	93.203125	9.6979354 84	1343.6919 52	37.9374	0.3742356 85	1356.5	444.75	1343.6919 52	898.94195 2	530.52311 92	4216.80311 5	0.9578762 25	7.1393 2E-05
	217	10.405161629	1457.1579 2	40.704	0.4015269 71	92.792968 75	9.6552580 65	1458.1483 16	37.77045	0.3725887 97	1470.9	465.3	1458.1483 16	992.84831 6	585.94326 85	4657.30391 4	1.0156791 01	7.3406 9E-05
	222	10.634806 45	725.95 4628	41.60235	0.4103887 97	93.470149 25	9.9403694 63	726.87 17698	38.88577864	0.3835910 21	740	485.85	726.87 17698	241.02 17698	142.24 2356	1130.59 7307	0.3991179 51	0.0001587 97
	225	10.634806 45	635.95 4628	41.60235	0.4103887 97	93.636537 36	9.9580645 16	636.84 84	38.955	0.3842738 59	650	506.4	636.84 84	130.44 84	76.985940 98	611.914059 9	0.3889479 67	0.0001587 97
	227	10.634806 45	795.95 4628	41.60235	0.4103887 97	93.407223 39	9.9336774 19	796.88 0608	38.8596	0.3833327 8	810	526.95	796.88 0608	269.93 0608	159.30 330 96	1266.20 437 1	0.4029641 1	0.0001643 64
	228	10.634806 45	1135.9 54628	41.60235	0.4103887 97	94.286260 27	10.027161 29	1136.7 57144	39.2253	0.3869402 49	1150	463.2	1136.7 57144	673.55 7144	397.50 913 42	3159.55 6473	0.3492 35562	0.0001769 68
	229	10.454516 13	1171.1 927 37	40.897071 43	0.4034315 35	92.477089 7	9.6680322 58	1172.2 31445	37.82042143	0.3730817 43	1185	500.2	1172.2 31445	672.03 14451	396.60 872 17	3152.39 964 6	0.5666 053 65	0.0001174 12
	230	10.454516 13	1310.1 927 37	40.897071 43	0.4034315 35	92.904748 68	9.7127419 35	1311.1 723 97	37.99532143	0.3748070 54	1324	532.52	1311.1 723 97	778.65 23971	459.53 256 22	3652.54 268 8	0.5343 952 41	0.0001374 12
	232	10.454516 13	1449.1 927 37	40.897071 43	0.4034315 35	93.079700 08	9.7310322 58	1450.1 48241	38.06687143	0.3755128 63	1463	545.58 27273	1450.1 48241	904.56 55139	533.84 194 26	4243.18 240 8	0.5212 183 72	0.0001408 94
	234	10.454516 13	1581.1 927 37	40.897071 43	0.4034315 35	92.537313 43	9.6743283 58	1589.2 2313	37.84505117	0.3733247 04	1602	558.64 54545	1589.2 2313	1030.5 77675	608.20 977 56	4834.28 673 3	0.5620 694 75	0.0001405 02
	236	10.274225 81	796.43 08463	40.191792 86	0.3964742 74	93.769250 33	9.6340645 16	797.27 63063	37.68754286	0.3717709 54	810	571.70 818 18	797.27 63063	225.56 812 45	133.12 217 18	1058.10 655 3	0.4706 112 08	0.0001324 62
	238	10.274225 81	1136.4308 46	40.191792 86	0.3964742 74	93.283582 09	9.5841658 64	1137.3 422 07	37.49234408	0.3698454 05	1150	584.77 090 91	1137.3 422 07	552.57 129 83	326.10 765 14	2592.02 984 9	0.5072 939 39	0.0001262 13

	240	10.27422581	1171.430846	40.19179286	0.396474274	92.97804402	9.552774194	1172.383666	37.36954286	0.368634025	1185	597.8336364	1172.383666	574.5500299	339.0787062	2695.128813	0.5303713	0.000124683
	242	10.27422581	1022.430846	40.19179286	0.396474274	93.35386702	9.591387097	1023.332667	37.52059286	0.370124066	1036	610.8963636	1023.332667	412.4363066	243.4050334	1934.677427	0.5019852	0.000139599
	243	10.09393548	1192.668955	39.48651429	0.389517012	93.05395766	9.392806452	1193.549435	36.74376429	0.362460996	1206	623.9590909	1193.549435	569.6358445	336.1785312	2672.0771	0.6288560	9.2530E-05
	246	10.09393548	1291.668955	39.48651429	0.389517012	93.53716061	9.441580645	1292.530519	36.93456429	0.364343154	1305	637.0218182	1292.530519	655.5087012	386.8575942	3074.89391	0.5851095	9.2530E-05
	249	10.09393548	1407.668955	39.48651429	0.389517012	92.34928677	9.321677419	1408.688875	36.46551429	0.359716183	1421	650.0845455	1408.688875	758.6043300	447.7009161	3558.500184	0.6926530	9.4178E-05
	251	9.913645161	1295.907065	38.78123571	0.382559751	93.50649351	9.269901969	1296.757255	36.26297365	0.357718209	1309	663.1472727	1296.757255	633.6099825	373.9337601	2972.170274	0.3777540	0.000160622
	253	9.913645161	1418.907065	38.78123571	0.382559751	92.92763644	9.212516129	1419.833045	36.03848571	0.355503734	1432	600.5418182	1419.833045	819.2912264	483.5161336	3843.173397	0.4114285	0.000169984
	255	9.913645161	1348.907065	38.78123571	0.382559751	92.25114914	9.145451613	1349.921617	35.77613571	0.352915768	1362	602.1472727	1349.921617	747.7743438	441.3094488	3507.698329	0.4507825	0.000166722
	258	9.733354839	1332.145174	38.07595714	0.375602499	94.10646388	9.159716055	1332.902778	35.83193685	0.353466221	1345	603.7527273	1332.902778	729.1500503	430.3180625	3420.335453	0.3162213	0.000135663
	261	9.733354839	1315.145174	38.07595714	0.375602499	94.65489471	9.213096774	1315.832278	36.04075714	0.355526141	1328	588.8396364	1315.832278	726.9926414	429.0448375	3410.218445	0.2867949	0.000108228
	263	9.530645516	1238.383283	37.37067857	0.368645228	93.22033898	8.905399125	1239.238654	34.83707324	0.343652331	1251	578.1892727	1239.238654	661.0493808	390.1275034	3100.884414	0.2542318	0.000276308
	265	9.530645516	1384.716616	37.37067857	0.368645228	92.15012916	8.803161229	1385.707012	34.43712857	0.339707054	1397.333333	567.5389091	1385.707012	818.1681031	482.8533067	3837.904993	0.2943638	0.000303716
	269	9.530645516	1402.504495	37.37067857	0.368645228	92.66068986	8.851935484	1403.475075	34.62792857	0.341589212	1415.212212	556.8854545	1403.475075	846.5419295	499.5985158	3971.002396	0.2752182	0.000278534
	270	10.79129032	1418.657051	42.2145	0.416427386	93.23917137	10.06170968	1419.620707	39.36045	0.388273444	1432.909091	546.2318182	1419.620707	873.3824251	515.4388083	4096.907173	0.2461618	0.000309316
	273	10.79129032	1436.449493	42.2145	0.416427386	92.88135593	10.02309677	1437.459482	39.2094	0.386783402	1450.696697	535.5878182	1437.459482	901.8716635	532.2521293	4230.543595	0.2591898	0.000292281

	276	10.32729677	1454.845604	40.39940143	0.3985222441	90.41353383	9.337273963	1456.153126	36.52652648	0.3603180841	1468.484848	524.93745	1456.153126	931.215671	549.5699042	436	8.194335	0.2351887878
	278	10.32729677	1472.633483	40.39940143	0.3985222441	90.96756419	9.394490323	1473.865439	36.75035143	0.3625259575	1486.272727	514.28709	1473.865439	959.57834	566.3085332	450	1.239438	0.2215965
	281	10.32729677	1490.421362	40.39940143	0.3985222441	90.41656593	9.337587097	1491.728477	36.52775143	0.3603301024	1504.060606	503.63672	1491.728477	988.09174	583.1361102	463	4.991534	0.2351143
	282	10.43070968	1508.072663	40.80394286	0.4025128463	90.68692941	9.459290323	1509.355615	37.00384286	0.3650265556	1521.848485	492.98636	1509.355615	1016.3692	599.8244763	476	7.637128	0.3574328
	284	10.43070968	1525.860542	40.80394286	0.4025128463	90.65420561	9.455876997	1527.148002	36.99049025	0.3648948438	1539.636364	482.336	1527.148002	1044.812002	616.6103618	490	1.057843	0.3586888
	287	10.43070968	1543.648421	40.80394286	0.4025128463	91.11556446	9.504	1544.872325	37.17874286	0.3667518467	1557.424242	471.68563	1544.872325	1073.186688	633.3560784	503	4.159281	0.3409
	291	10.53412258	1561.299722	41.20848429	0.4065034585	90.97744361	9.583675431	1562.549765	37.49042555	0.3698264791	1575.212121	461.03527	1562.549765	1101.519704	650.0772021	516	7.065245	0.3004106
	293	10.53412258	1579.087601	41.20848429	0.4065034585	90.95198461	9.580993548	1580.346397	37.47993429	0.3697229288	1593	450.38490	1580.346397	1129.961488	666.8625175	530	0.481429	0.3012582
	295	10.53412258	1181.087601	41.20848429	0.4065034585	90.56614174	9.540348387	1182.400077	37.32093429	0.3681545523	1195	439.73454	1182.400077	742.6655316	438.2944121	348	3.733651	0.3141051
	297	10.53412258	1134.087601	41.20848429	0.4065034585	90.75906317	9.560670968	1135.732337	37.40043429	0.3689387551	1148	429.08418	1135.732337	706.2890552	416.8263277	331	3.097004	0.3076817
	301	10.53412258	1146.087601	41.20848429	0.4065034585	90.39251244	9.522058065	1147.424233	37.24938429	0.3674487114	1160	418.43381	1147.424233	728.9904148	430.2238514	341	9.585709	0.3198862
	303	10.63753548	1237.951024	41.61302571	0.4104941008	92.21789883	9.809711711	1239.044329	38.37465795	0.3785490441	1252	407.78345	1239.044329	831.2608748	490.5801884	389	9.321239	0.3249504
	309	10.63753548	1272.156906	41.61302571	0.4104941008	92.33905743	9.8226	1273.233319	38.42507571	0.3790463	1286.205882	397.13309	1273.233319	876.1000992	517.0426815	410	9.655378	0.3198913
	311	10.63753548	1276.362788	41.61302571	0.4104941008	92.37726662	9.826664516	1277.433704	38.44097571	0.3792032037	1290.411765	386.48272	1277.433704	890.9509772	525.8071341	417	9.318648	0.3182958
	313	10.63753548	1280.568671	41.61302571	0.4104941008	92.56831257	9.846987097	1281.634747	38.52047571	0.3799874069	1294.617647	375.83236	1281.634747	905.7803832	534.5589147	424	8.881181	0.3103185

	315	10.637535 48	1319.6821 16	41.613025 71	0.4104941 08	92.167116 08	9.8043096 77	1320.7825 56	38.353525 71	0.3783405 81	1333.7310 92	582.2	1320.7825 56	738.58255 62	435.88478 73	3464.58101 9	0.3270709 25	0.0002930 33
	316	10.637535 48	1345.0350 57	41.613025 71	0.4104941 08	91.976070 13	9.7839870 97	1346.1623 37	38.274025 71	0.3775563 49	1359.0840 34	526.8	1346.1623 37	819.36233 74	483.55810 08	3843.50696 9	0.3350482 65	0.0002701 39
	317	10.740948 39	1370.2514 21	42.017567 14	0.4144847 3	92.741935 48	9.9613634 24	1371.2810 18	38.967905 01	0.3844011 61	1384.4369 75	624.65863 64	1371.2810 18	746.62238 16	440.62960 22	3502.29464 5	0.2746986 78	0.0003195 87

Appendice C. [Particle size distribution analysis]

Table 0-3 Particle size distribution analysis results

RAS		ANAMMOX	
Channel diameter (μm)	Differential volume (%)	Channel diameter (μm)2	Differential volume (%)2
0.375	0	0.375	0
0.412	0	0.412	0
0.452	0	0.452	0
0.496	0	0.496	0
0.545	0	0.545	0
0.598	0	0.598	0
0.657	0	0.657	0
0.721	0	0.721	0
0.791	0	0.791	0
0.869	0	0.869	0
0.954	0	0.954	0
1.047	0	1.047	0
1.149	0	1.149	0
1.261	0	1.261	0
1.385	0	1.385	0
1.52	0	1.52	0
1.669	0	1.669	0
1.832	0	1.832	0
2.011	0	2.011	0
2.208	0	2.208	0
2.423	0	2.423	0
2.66	0	2.66	0
2.92	0.00014	2.92	0
3.206	0.0014	3.206	0
3.519	0.0075	3.519	0.0002
3.863	0.019	3.863	0.0021
4.241	0.039	4.241	0.0099
4.656	0.061	4.656	0.023
5.111	0.088	5.111	0.039
5.611	0.12	5.611	0.054
6.159	0.15	6.159	0.072
6.761	0.19	6.761	0.093
7.422	0.22	7.422	0.12
8.148	0.26	8.148	0.14
8.944	0.3	8.944	0.16
9.819	0.35	9.819	0.19

10.78	0.39	10.78	0.22
11.83	0.44	11.83	0.25
12.99	0.49	12.99	0.29
14.26	0.55	14.26	0.33
15.65	0.61	15.65	0.38
17.18	0.69	17.18	0.43
18.86	0.77	18.86	0.5
20.71	0.87	20.71	0.58
22.73	0.98	22.73	0.67
24.95	1.1	24.95	0.76
27.39	1.23	27.39	0.86
30.07	1.36	30.07	0.97
33.01	1.51	33.01	1.11
36.24	1.68	36.24	1.28
39.78	1.91	39.78	1.52
43.67	2.17	43.67	1.83
47.94	2.47	47.94	2.21
52.63	2.77	52.63	2.63
57.77	3.04	57.77	3.06
63.42	3.26	63.42	3.46
69.62	3.43	69.62	3.82
76.43	3.58	76.43	4.11
83.9	3.73	83.9	4.34
92.1	3.9	92.1	4.49
101.1	4.09	101.1	4.54
111	4.28	111	4.48
121.8	4.42	121.8	4.3
133.7	4.48	133.7	4.02
146.8	4.45	146.8	3.65
161.2	4.31	161.2	3.27
176.9	4.1	176.9	2.9
194.2	3.82	194.2	2.59
213.2	3.5	213.2	2.37
234.1	3.17	234.1	2.25
256.9	2.85	256.9	2.2
282.1	2.54	282.1	2.21
309.6	2.24	309.6	2.22
339.9	1.94	339.9	2.2
373.1	1.63	373.1	2.11
409.6	1.3	409.6	1.94
449.7	0.96	449.7	1.69

493.6	0.63	493.6	1.4
541.9	0.34	541.9	1.11
594.9	0.14	594.9	0.85
653	0.035	653	0.65
716.9	0.0044	716.9	0.51
786.9	0.00016	786.9	0.43
863.9	0	863.9	0.39
948.3	0	948.3	0.4
1041	0	1041	0.43
1143	0	1143	0.49
1255	0	1255	0.55
1377	0	1377	0.62
1512	0	1512	0.69
1660	0	1660	0.74
1822	0	1822	0.81
2000	0	2000	0.81

Appendice D. [Microbial analysis]

The RNA extraction was performed using RNeasy Mini Kit QIAGEN from kit's protocol in "Purification of Total RNA from Bacterial Lysate." The steps are demonstrated as following, 10 ml of RNAprotect Bacteria Reagent was added to 5 ml of bacterial suspension then mixed by vortexing for 5 seconds. The mix was incubated at room temperature at 22 °C for 5 minutes, after that the mix was centrifuged for 10 mins at 5000 rpm. The resulting supernatant was decanted and then, 200 µl of TE Buffer was added containing Lysozyme to lyse all of the cell debris and cell wall. Next, 10 seconds of vortex every 2 mins during incubation at room temperature for 5 mins. Followed by the addition of 700 µl of RLT Buffer with β-mercaptoethanol for RNA stabilization, then the mixture was vortexed for 10 seconds. 500 µL of 96% ethanol was then added and mixed. For RNA purification, 700 µl of Lysate was transferred to an RNeasy Mini spin column placed in a 2-ml collection tube then centrifuged for 15 seconds at 10000 rpm. The flow through was then discarded. Then, 700 of µl RW1 Buffer was added to the RNeasy Mini spin column followed by 15 seconds centrifugation at 10000rpm, the flow through was then discarded and collected in a tube. The RNeasy mini spin column was placed in a new collection tube where 500 µl of RPE buffer was added to the column and centrifuged for another 15 seconds afterwards the flow through was discarded then the collection tube was reused and 500 µl of RPE Buffer was added to the column then centrifuged for 2 mins. To wash the spin column membrane at the same speed. The RNeasy mini spin column was placed in a new 1.5 ml collection tube. Then 40 µl of RNase free water was placed directly to the spin column membrane then subjected to 1 min centrifugation at the same speed to elute the RNA.

Samples preparation was performed using one step RT-PCR QIAGEN kit following the instructor's protocol. The reaction mix was prepared and contained the following components

added in the following order; 22 µl RNase-free water, 10 µl QIAGEN OneStep RT-PCR Buffer (5x), 10 µl 5x of Q-Solution, 2 µl dNTP mix, 1.5 µl ANAMMOX Primer as shown in the following table (van der Star et al., 2007b), 2 µl QIAGEN One Step RT-PCR Enzyme Mix except for the 1 µg template RNA which was added directly to the PCR tubes. The thermal cycler was programmed according to the manufacturer's instructions with the melting temperature (T_m=50ºC) adjusted according to the employed primers containing the 50 µL master mix PCR tubes. The target DNA was amplified using RT-PCR which confirms the presence of ANAMMOX then products were separated for visualization using gel electrophoresis.

Briefly, 150 ml of 1% TAE buffer was prepared. Then, 1.5 g of agarose was dissolved in the TAE buffer with 3 µl of ethidium bromide before decanting the mix into the gel mold for 20 mins to dry. The gels were examined for fluorescent bands using an alpha imager amended with 2 µl dye (Eva green). In the first lane, 12 µl of RNA sample including 2 µl dye were injected 10 µl of 1 kb ladder then a current of 100 A and 50 v was implied for 1 hour at 60ºC before taking the images.

Table 0-4 The primer sets used in this study for PCR identification (van der Star et al., 2007b)

Target Organism	**Name**	**Sequence 5'–3'**
Planctomyctales	Pla46F	GGATTAGGCATGCAAGTC
ANAMMOX	AMX667R	ACCAGAAGTTCCACTCTC
ANAMMOX	AMX361	AGAATCTTTCGCAATGCCCG-F
Most ANAMMOX	AMX381	L-AAGGGTGACGAAGCGACGCC
Kuenenia and Brocadia	AMX382	L-AAGGTGACGAAGCGACGCC

Appendice E. [Experimental and modeling data]

Table 0-5 Experimental and BioWin modeling results

Experimental NRR (KgN/m3/day)	Model I NRR (KgN/m3/day)	Model II NRR (KgN/m3/day)	Model III NRR (KgN/m3/day)	Experimental NRE (%)	Model I NRE (%)	Model II NRE (%)	Model III NRE (%)	Experimental pH	Experimental Alkalinity out (mgCaCO3/L)	Model I pH	Model I Alkalinity out (mgCaCO3/L)	Model II pH	Model II Alkalinity out (mgCaCO3/L)	Model III pH	Model III Alkalinity out (mgCaCO3/L)
0.11097472	0.12615694	0.06900785	0.12615694	58.13817311	58.765979	32.1449906	58.76598	9	3290	8.80894594	3619	9.51366163	4704.7	9.09	3619
0.12954516	0.10484010	0.05734753	0.10484010	66.66932311	54.924328	30.0436076	54.92433	9	2780	8.86049009	3058	9.56932929	3975.4	9.09	3058
0.13883366	0.10727253	0.05867807	0.10727253	69.67357893	56.198645	30.7406589	56.19865	9.5	2655	8.90806330	2920.5	9.62070836	3796.65	9.595	2920.5
0.14531066	0.10965417	0.05998083	0.10965417	70.62829960	57.446355	31.4231567	57.44636	9.5	2655	8.95206178	2920.5	9.68226731	3796.65	9.595	2920.5
0.14981541	0.11198403	0.06125526	0.11198403	71.36412356	58.666936	32.0908145	58.66694	9	2215	8.99293623	2436.5	9.71237113	3167.45	9.09	2436.5
0.15328251	0.11425607	0.06249807	0.11425607	71.82937348	59.857225	32.7419026	59.85723	9	2215	9.03107195	2436.5	9.75355770	3167.45	9.09	2436.5
0.15028544	0.11646917	0.06370864	0.11646917	72.64272462	61.016643	33.3761038	61.01664	9	1400	9.06679005	1540	9.79213325	2002	9.09	1540

0.14097564 1	0.11 8620 071	0.06 488 517 9	0.11 862 007 1	67.1 533 224 2	62. 14 34 67 1	33. 99 24 76 5	62 .1 43 47	9	1180	9.11 713 261 8	129 8	9.8 465 032 27	168 7.4	9.09	1298
0.130 21734 4	0.12 0709 393	0.06 602 803 8	0.12 070 939 3	65.3 494 848	63. 23 80 34 6	34. 59 12 04 9	63 .2 38 03	9	1180	9.15 997 436 6	125 0.8	9.8 927 723 15	162 6.0 4	9.09	1250 .8
0.136 78534 4	0.12 2735 107	0.06 713 610 4	0.12 273 510 7	66.3 616 729 4	64. 29 92 79 2	35. 17 17 05 7	64 .2 99 28	9	1180	9.20 281 611 5	125 0.8	9.9 390 414 04	162 6.0 4	9.09	1250 .8
0.122 42634 4	0.12 4699 821	0.06 821 080 2	0.12 469 982 1	64.0 097 582 8	65. 32 85 66 7	35. 73 47 26	65 .3 28 57	9	1180	9.24 565 786 3	125 0.8	9.9 853 104 92	162 6.0 4	9.00 9	1250 .8
0.131 66343 7	0.12 6603 286	0.06 925 199 7	0.12 660 328 6	68.5 661 359 1	66. 32 57 66 2	36. 28 01 94 1	66 .3 25 77	8.7	1175	8.89 133 901 2	124 5.5	9.6 026 461 33	161 9.1 5	8.70 87	1245 .5
0.158 59530 7	0.12 8453 75	0.07 026 420 1	0.12 845 375	74.1 997 589 2	67. 29 51 99 6	36. 81 04 74 2	67 .2 95 2	8.22	1430	8.43 986 246 7	151 5.8	9.1 150 514 64	197 0.5 4	8.22 822	1515 .8
0.137 42954 5	0.13 0247 75	0.07 124 551 9	0.13 024 775	71.9 974 982 5	68. 23 50 52 2	37. 32 45 73 6	68 .2 35 05	7.99	955	8.58 676 809 8	101 2.3	9.2 737 095 46	131 5.9 9	7.99 799	1012 .3
0.129 40060 8	0.13 1989 214	0.07 219 81	0.13 198 921 4	68.6 129 578 4	69. 14 73 82	37. 82 36 18	69 .1 47 38	7.76	860	8.33 475 227 8	911. 6	9.0 015 324 6	118 5.0 8	7.76 776	911. 6
0.131 84208	0.13 3681 321	0.07 312 368 3	0.13 368 132 1	69.3 471 351 9	70. 03 38 54 3	38. 30 85 18 3	70 .0 33 85	7.79	770	8.18 246 682 1	816. 2	8.8 370 641 66	106 1.0 6	7.79 779	816. 2
0.131 21479	0.13 5325 643	0.07 402 312 7	0.13 532 564 3	71.7 491 196 3	70. 89 52 92 3	38. 77 97 24 9	70 .8 95 29	8.21	510	8.03 018 136 3	511. 02	8.6 725 958 73	664 .32 6	8.21 821	511. 02
0.138 91523 2	0.13 6926 607	0.07 489 885 4	0.13 692 660 7	72.7 758 301 6	71. 73 40 16	39. 23 85 06 8	71 .7 34 02	8.21	510	7.09 022 535 3	511. 02	7.6 574 433 81	664 .32 6	8.21 821	511. 02

0.14265623 2	0.13 8486 071	0.07 575 188 1	0.13 848 607 1	73.1 300 403 8	72. 55 09 98 5	39. 68 53 96 2	72 .5 51	8.21	510	7.10 999 052 2	511. 02	7.6 787 897 64	664 .32 6	8.21 821	511. 02
0.14231323 2	0.14 0004 643	0.07 658 254	0.14 000 464 3	73.3 841 933 7	73. 34 65 57 7	40. 12 05 67 1	73 .3 46 56	8.21	510	7.12 886 100 9	511. 02	7.6 991 698 9	664 .32 6	8.21 821	511. 02
0.140 35879	0.14 1678 152	0.07 749 794 9	0.14 167 815 2	73.0 943 996 5	74. 22 32 87	40. 60 01 38	74 .2 23 29	8.21	510	7.14 691 167	511. 02	7.7 186 646 04	664 .32 6	8.21 821	511. 02
0.140 719336	0.14 3280 791	0.07 837 459 3	0.14 328 079 1	73.4 278 509 8	75. 06 28 88	41. 05 93 99 7	75 .0 62 89	8.19	415	7.16 421 019 5	415. 83	7.7 373 470 1	540 .57 9	8.19 819	415. 83
0.144 943266	0.13 1989 214	0.07 219 81	0.13 198 921 4	73.1 593 306 2	69. 14 73 82	37. 82 36 18	69 .1 47 38	8.24	530	7.18 081 559 7	531. 06	7.7 552 808 45	690 .37 8	8.24 824	531. 06
0.138 686299	0.13 3681 321	0.07 312 368 3	0.13 368 132 1	72.2 234 196 1	70. 03 38 54 3	38. 30 85 18 3	70 .0 33 85	8.42	675	7.19 677 941	676. 35	7.7 725 217 63	879 .25 5	8.42 842	676. 35
0.140 969511	0.13 5325 643	0.07 402 312 7	0.13 532 564 3	72.5 487 680 4	70. 89 52 92 3	38. 77 97 24 9	70 .8 95 29	8.42	675	7.21 214 86	742. 5	7.7 891 204 88	965 .25	8.42 842	742. 5
0.152 064232	0.13 6926 607	0.07 489 885 4	0.13 692 660 7	73.9 108 741	71. 73 40 16	39. 23 85 06 8	71 .7 34 02	8.42	675	7.22 696 401 4	742. 5	7.8 051 211 35	891	8.42 842	742. 5
0.155 634232	0.13 8486 071	0.07 575 188 1	0.13 848 607 1	74.2 706 907	72. 55 09 98 5	39. 68 53 96 2	72 .5 51	8.42	675	7.24 126 297 5	742. 5	7.8 205 640 13	891	8.42 842	742. 5
0.159 39702	0.12 8453 75	0.07 026 420 1	0.12 845 375	74.7 080 148 4	67. 29 51 99 6	36. 81 04 74 2	67 .2 95 2	8.42	675	7.25 507 677 9	742. 5	7.8 354 829 21	891	8.42 842	742. 5
0.131 63137	0.13 0247 75	0.07 124 551 9	0.13 024 775	66.4 402 230 5	68. 23 50 52 2	37. 32 45 73 6	68 .2 35 05	8.01	700	7.26 843 408 1	770	7.8 499 088 07	924	8.01 801	770

0.14015824 7	0.13 1798 75	0.07 209 391 6	0.13 179 875	69.4 093 236 4	69. 04 76 00 3	37. 76 90 37 4	69 .0 47 6	8.56	660	7.28 135 994	726	7.8 638 687 35	871 .2	8.56 856	726
0.153 26954 8	0.13 1351 639	0.07 184 934 7	0.13 135 163 9	74.4 967 183 6	68. 81 33 64 9	37. 64 09 10 6	68 .8 13 36	8.53	405	7.29 387 671 5	445. 5	7.8 773 868 52	534 .6	8.53 853	445. 5
0.139 42462 3	0.13 0904 528	0.07 160 477 7	0.13 090 452 8	71.7 537 042 4	68. 57 91 29 4	37. 51 27 83 8	68 .5 79 13	8.69	360	7.30 600 549 9	396	7.8 904 859 39	475 .2	8.69 869	396
0.142 94423 2	0.13 0457 417	0.07 136 020 7	0.13 045 741 7	72.1 503 292 8	68. 34 48 94	37. 38 46 57	68 .3 44 89	8.69	360	7.31 776 090 6	396	7.9 031 817 79	475 .2	8.69 869	396
0.146 50423 2	0.13 0010 306	0.07 111 563 7	0.13 001 030 6	72.5 519 894 8	68. 11 06 58 5	37. 25 65 30 2	68 .1 10 66	8.69	360	7.32 915 983	396	7.9 154 926 16	475 .2	8.69 869	396
0.134 48423 2	0.12 9563 195	0.07 087 106 8	0.12 956 319 5	70.5 953 975 7	67. 87 64 23 1	37. 33 20 32 7	67 .8 76 42	8.69	360	7.34 021 416 8	396	7.9 274 313 01	475 .2	8.69 869	396
0.134 86523 2	0.13 5325 643	0.07 402 312 7	0.13 532 564 3	70.6 540 893 9	70. 89 52 92 3	38. 99 24 10 8	70 .8 95 29	8.69	360	7.35 093 487 5	378	7.9 390 096 65	453 .6	8.78 559	378
0.143 37969 7	0.13 6926 607	0.07 489 885 4	0.13 692 660 7	72.3 701 277 3	71. 73 40 16	39. 45 37 08 8	71 .7 34 02	8.69	360	7.36 133 437 1	378	7.9 502 411 2	453 .6	8.78 559	378
0.136 52015 8	0.13 8486 071	0.07 575 188 1	0.13 848 607 1	71.5 210 827 8	72. 55 09 98 5	39. 90 30 49 2	72 .5 51	8.69	360	7.37 141 734 6	378	7.9 611 307 34	453 .6	8.78 559	378
0.225 31589 2	0.20 7536 071	0.11 393 730 3	0.21 350 050 8	82.9 281 898 7	79. 84 27 55	43. 91 35 15 2	82 .1 37 38	8.23	620	7.38 119 239 1	682	7.9 716 877 82	818 .4	8.32 053	682
0.206 92771 1	0.18 7503 75	0.10 293 955 9	0.18 509 393 8	76.1 603 646	75. 02 22 06 1	41. 26 22 13 4	74 .0 58 02	7.93	630	7.69 282 895 8	693	8.3 082 552 74	831 .6	8.01 723	693

0.20014684 1	0.20929775	0.11490446 5	0.19602400 8	73.0516245 9	77.5375003	42.6456252	72.620 04	7.79	600	7.69499490 6	660	8.3105944 98	792	7.87569	660
0.21485814 5	0.21084875	0.11575596 4	0.20732660 4	77.4542701 5	78.1120916	42.9616504	76.807 26	7.79	580	7.69713126 3	638	8.3129017 64	765.6	7.87569	638
0.21068423 2	0.21540163 9	0.11825 55	0.21385421 7	77.5429637	78.3475268	43.0911398	77.784 69	7.79	610	7.69924 04	671	8.3151796 32	805.2	7.87569	671
0.20722597 1	0.21995452 8	0.12075503 6	0.21767477 7	76.9155858 9	78.5745516	43.2160034	77.760 15	7.79	520	7.70132048 1	572	8.3174261 2	686.4	7.87569	572
0.20771423 2	0.21450741 7	0.11776457 2	0.21354390 7	77.2057063 5	78.0222736	42.9122505	77.671 82	7.79	550	7.70337290 5	605	8.3196427 37	726	7.87569	605
0.20853423 2	0.21906030 6	0.12026410 8	0.21480016 7	76.2186521 8	78.2551079	43.0403094	76.733 25	8.06	621	7.70539777 1	683.1	8.3218295 93	819.72	8.14866	683.1
0.21278423 2	0.21361319 5	0.11727364 4	0.21025061 7	76.7066644 69	77.6970204	42.7333612	76.473 96	8.06	612	7.70739660 6	648.72	8.3239883 35	778.464	8.14866	648.72
0.20498423 2	0.22370897 6	0.12281622 8	0.21438375	75.9763648 5	80.1065333	44.0585933	76.767 32	8.06	700	7.70898982	742	8.3257090 05	890.4	8.14866	742
0.21246901 5	0.22630994	0.12424415 7	0.21526841 7	76.5930118 9	80.7487481	44.4118114	76.809 07	8.06	621.6	7.71076788 2	658.896	8.3276293 13	790.6752	8.14866	658.896
0.18632727 6	0.22886940 5	0.12564930 3	0.19922965 6	69.4525405 7	81.3716414	44.7544028	70.833 6	7.99	624.7454545	7.71255547 7	662.2301818	8.3295599 15	794.6762182	8.07789	662.2301818
0.18847423 2	0.22623625 2	0.12420370 2	0.20085724	69.8570171 9	80.1504 92	44.0827706	71.159 27	7.99	627.8909091	7.71432504 5	665.5643636	8.3314710 49	798.6772364	8.07789	665.5643636

0.19258423 2	0.217572448	0.11944727 4	0.19026565	69.9035326 2	79.6197752	43.7908764	69.626 96	7.99	631.0363636	7.71607246 9	668.898545 5	8.3333582 67	802.67825 45	8.07789	668.8985455
0.19525423 2	0.218908644	0.12018084 6	0.18975414	69.8134412 1	79.8166665	43.8991657	69.1 8659	7.99	634.1818182	7.71779639	672.232727 3	8.3352201 02	739.456	8.07789	672.2327273
0.18548031 9	0.220244 84	0.12091441 7	0.19124071 3	68.8443023 2	80.0121 2422	43.8466 44	69.4753	7.99	637.3272727	7.71949819 3	675.566909 1	8.3370580 48	743.12 36	8.07789	675.5669091
0.18352945	0.22 1581 036	0.12164798 9	0.19142903 3	68.4096651 8	80.2061 683	43.9529 802	69.2 9198	7.86	640.4727273	7.72117769 9	641.753 672 7	8.3388719 15	705.92 904	7.94646	641.7536727
0.18168823 2	0.22 2917 232	0.12238156 1	0.18931971 5	67.8386673 2	80.3988 128	44.0585 494	68.2 8131	7.86	643.6181818	7.72283395 7	644.905 418 2	8.3406606 73	709.39 596	7.94646	644.9054182
0.18490423 2	0.22 4253 428	0.12311513 2	0.19158575 5	68.5338148 1	80.5900 727	44.1633 598	68.8 5027	7.86	646.7636364	7.72447139 9	648.057 163 6	8.3424291 11	712.86 288	7.94646	648.0571636
0.18878423 2	0.22 5589 625	0.12384870 4	0.19266743 5	69.0000849 3	80.7799 628	44.2674 196	68.9 9106	7.86	649.9090909	7.72608577 8	651.208 909 1	8.3441726 4	716.32 98	7.94646	651.2089091
0.18748423 2	0.22 0059 587	0.12081271 3	0.18159410 1	67.5862409 4	80.4905 328	44.1088 12	66.4 2113	7.86	653.0545455	7.72768127 6	654.360 654 5	8.3458957 78	719.79 672	7.94646	654.3606545
0.15436771 1	0.22 0395 783	0.12121768 1	0.15554173 3	57.2156080 9	80.6135 022	44.1761 992	56.8 9203	7.78	656.2	7.72925499 8	657.512 4	8.3475953 98	723.26 364	7.86558	657.5124
0.15717423 2	0.22 2731 979	0.12250258 9	0.15652739 1	57.4467223 6	80.8763 675	44.3202 494	56.8 3677	7.78	659.3454545	7.73080866 5	660.664 145 5	8.3492733 58	726.73 056	7.78778	660.6641455
0.16238423 2	0.22 5068 176	0.12378749 7	0.15996700 1	58.5379352 4	81.1354 424	44.4622 224	57.6 6694	7.78	662.4909091	7.73234259 7	663.815 890 9	8.3509300 05	730.19 748	7.78778	663.8158909

0.16554423 2	0.227404372	0.12507240 4	0.16131356 1	58.8706374	81.3908082	44.6021629	57.7361	7.78	665.6363636	7.73385789	732.2	8.3525665 22	805.42	7.78778	732.2
0.15083423 2	0.229740568	0.12635731 2	0.16303789 1	56.5430470 7	81.6425 44	44.7401141	57.93852	7.78	668.7818182	7.73535357	735.66	8.3541818 56	809.22 6	7.78778	735.66
0.15334423 2	0.212076764	0.11664222	0.14835057 9	57.4021982 4	80.5156771	44.1225911	56.32181	7.78	671.9272727	7.73683049 8	739.12	8.3557769 38	813.03 2	7.78778	739.12
0.15290423 2	0.219443707	0.12069403 9	0.15752155 9	57.1561873 4	80.2652641	43.9853648	57.616 19	7.78	675.0727273	7.73828883 2	742.58	8.3573519 38	816.83 8	7.78778	742.58
0.15425423 2	0.214488071	0.11796843 9	0.15198712 9	57.5790341	80.3678284	44.0415 7	56.94897	7.78	678.2181818	7.73972968 1	746.04	8.3589080 55	820.64 4	7.78778	746.04
0.16463292 8	0.215349885	0.11844243 7	0.16659077 7	61.3660832	79.3542261	43.4861159	61.38699	7.74	681.3636364	7.74115194 8	749.5	8.3604441 04	824.45	7.74774	749.5
0.16615597 1	0.217428531	0.11958569 2	0.17217810 4	62.4646509 4	79.6090362	43.6257518	63.0411	8.41	684.5090909	7.74255739 2	752.96	8.3619619 84	828.25 6	8.41841	752.96
0.16982423 2	0.219507177	0.12072894 8	0.17455572 6	63.1222986 8	79.8606156	43.7636174	63.50648	8.41	687.6545455	7.74394445 4	756.42	8.3634600 1	832.06 2	8.41841	756.42
0.17137423 2	0.221585824	0.12187220 3	0.17517596 6	63.0748002 8	80.1090254	43.8997459	63.33066	8.41	690.8	7.74739773 6	759.88	8.3671895 55	835.86 8	8.41841	759.88
0.16955423 2	0.223664 47	0.12301545 8	0.17354167 6	62.0577675	80.3543252	44.0341702	62.34707	8.41	693.9454545	7.74909856 1	763.34	8.3690264 46	839.67 4	8.41841	763.34
0.17109423 2	0.219393899	0.12066664 4	0.17010766 9	62.5344416 5	80.1465 25	43.9202957	62.14183	8.41	697.0909091	7.75079938 6	766.8	8.3708633 37	843.48	8.41841	766.8

0.17648423 2	0.219730 095	0.12085 1552	0.17171 5159	63.620848	80.26 9340 4	43.98 7598 5	62 .7 2906	8.41	700. 2363 636	7.75 250 021	735. 248 181 8	8.3 727 002 27	808 .77 3	8.41 841	735. 2481 818
0.16540423 2	0.219090 928	0.12050 001	0.16876 723 4	61.3 927 074 3	79. 98 14 50 4	43. 82 98 34 8	61 .6 10 26	8.41	703. 3818 182	7.75 420 103 5	738. 550 909 1	8.3 745 371 18	812 .40 6	8.41 841	738. 5509 091
0.16858423 2	0.218534 779	0.12019 412 9	0.16916 632 9	62.0 479 324 1	79. 92 74 67 1	43. 80 02 52	61 .8 71 32	8.41	706. 5272 727	7.75 590 186	741. 853 636 4	8.3 763 740 09	816 .03 9	8.41 841	741. 8536 364
0.18398336 3	0.217978 631	0.11988 824 7	0.17461 954 5	65.4 279 384 1	79. 87 32 81 7	43. 77 05 58 4	63 .9 85 34	8.41	709. 6727 273	7.75 760 268 5	780. 64	8.3 782 108 99	858 .70 4	8.41 841	780. 64
0.12326192 3	0.13 5908 722	0.07 474 979 7	0.12 302 462 5	64.7 452 061 5	71. 20 07 59 8	39. 01 80 16 4	64 .4 50 95	7.4	589. 6	7.16 421 019 5	648. 56	7.7 373 470 1	713 .41 6	7.40 74	648. 56
0.12385423 2	0.13 5863 379	0.07 472 485 8	0.12 362 344 9	65.0 563 254 4	71. 17 70 05	39. 00 49 98 7	64 .7 64 67	7.4	690. 23	7.18 081 559 7	759. 253	7.7 552 808 45	911 .10 36	7.40 74	759. 253
0.12423423 2	0.13 5818 035	0.07 469 992	0.12 400 762 9	65.2 559 262 3	71. 15 32 50 2	38. 99 19 81 1	64 .9 65 94	7.4	545. 23	7.19 677 941	599. 753	7.7 725 217 63	719 .70 36	7.40 74	599. 753
0.11903324 4	0.13 5772 692	0.07 440 343 5	0.11 874 943	62.5 240 278 5	71. 12 94 95 4	38. 97 89 63 5	62 .2 11 24	7.4	641. 3	7.21 214 86	705. 43	7.7 891 204 88	846 .51 6	7.40 74	705. 43
0.13071574 2	0.13 5727 349	0.07 437 858 7	0.12 671 863 5	67.3 167 894 7	71. 10 57 40 6	39. 10 81 57 3	66 .3 86 2	7.6	720. 6	7.22 696 401 4	792. 66	7.8 051 211 35	951 .19 2	7.60 76	792. 66
0.13042574 2	0.13 1989 214	0.07 233 008 9	0.12 642 544 5	67.1 674 435 1	69. 14 73 82	38. 03 10 60 1	66 .2 32 6	7.6	559. 4	7.24 126 297 5	615. 34	7.8 205 640 13	738 .40 8	7.60 76	615. 34
0.13120423 2	0.13 3681 321	0.07 325 736 4	0.12 721 249 9	67.5 683 553 2	70. 03 38 54 3	38. 51 86 19 9	66 .6 44 92	7.6	524. 87	7.25 507 677 9	577. 357	7.8 354 829 21	692 .82 84	7.60 76	577. 357

0.131414232	0.135325643	0.074158452	0.127424809	67.6765024	70.8952923	38.9924108	66.756615	7.6	584.87	7.26843408 1	619.9622	7.849908807	743.95464	7.6076	619.9622
0.135434232	0.136926607	0.075035781	0.127647229	68.4080373 6	71.7340 16	39.4537 088	66.872 67	6.81	649.2	7.28135 994	688.152	7.8 638 687 35	825.7824	6.81 681	688.152
0.137 14889 3	0.13 84486 071	0.07 589 036 7	0.12 938 075 1	69.2 741 151 2	72.55 09 98 5	39.90 30 49 2	67.7 80 84	6.81	741.2	7.29 387 671 5	785.672	7.8 773 868 52	942.8064	6.81 681	785.672
0.141 80038 6	0.140 0004 643	0.07 672 254 4	0.13 024 161 1	70.2 747 479 1	73.34 65 57 7	40.34 06 06 8	68.2 31 84	6.84	623.48	7.30 600 549 9	660.888 8	7.8 904 859 39	793.06656	6.84 684	660.8888
0.143 37423 2	0.14 1485 857	0.07 753 425	0.13 183 276 9	71.0 547 290 9	74.12 25 46 1	40.76 74 00 3	69.0 65 42	6.84	645.0854 545	6.99 359 865 6	683.790 581 8	7.5 530 865 49	820.54869 82	6.84 684	683.7905 818
0.150 87451 8	0.14 2931 214	0.07 832 630 5	0.13 557 375 8	73.3 896 867 6	74.87 97 49 3	41.18 38 62 1	71.0 25 28	6.9	648.5090 909	6.99 533 488 9	687.419 636 4	7.5 549 616 81	824.90356 36	6.90 69	687.4196 364
0.153 97470 8	0.14 4341 821	0.07 909 931 8	0.13 486 625	73.5 384 028 7	75.61 87 47 5	41.59 03 11 1	70.6 54 62	7.77	651.9327 273	6.99 703 332 9	691.048 690 9	7.5 567 959 95	829.25842 91	7.77 9324	691.0486 909
0.155 90055 7	0.14 5718 786	0.07 985 389 5	0.13 681 328 3	74.4 581 894 1	76.34 01 20 7	41.98 70 66 4	71.6 74 65	7.77	655.3563 636	6.99 869 993 6	694.677 745 5	7.5 585 959 31	833.61329 45	7.77 9324	694.6777 455
0.131 39429 2	0.14 7064 071	0.08 059 111 1	0.10 819 564 9	61.6 353 746 2	77.04 48 97 8	42.37 46 93 8	56.6 82 25	7.37	658.78	7.00 033 041 6	660.097 56	7.5 603 568 5	792.11707 2	7.37 8844	660.0975 6
0.130 50542 4	0.14 8378	0.08 131 114 4	0.10 729 700 3	61.2 184 181	77.73 32 47 4	42.75 32 86 1	56.2 11 46	7.37	662.2036 364	7.00 192 944 5	695.313 818 2	7.5 620 838 01	834.37658 18	7.37 8844	695.3138 182
0.140 66423 2	0.14 9662 714	0.08 201 516 7	0.11 756 755 9	65.9 837 847 7	78.40 62 92	43.12 34 60 6	61.5 92 07	7.37	665.6272 727	7.00 349 684 5	698.908 636 4	7.5 637 765 93	838.69036 36	7.37 8844	698.9086 364

0.14065423 2	0.150917214	0.08270263 3	0.11755744 9	65.9790938 9	79.0635078	43.4849293	61.586877	7.37	669.0509091	7.00503233 8	735.956	7.5654349 25	883.1472	7.378844	735.956
0.14186423 2	0.152143286	0.08337452 1	0.11878075 9	66.5466893 5	79.7058302	43.8382066	62.227 65	7.37	672.4745455	7.00653834 5	739.722	7.5670614 13	887.6664	7.378844	739.722
0.15309542 4	0.153342286	0.08403157 3	0.13013549 3	71.8150969 6	80.3339702	44.1836836	68.176 24	7.37	675.8981818	7.00801376 5	743.488	7.5686548 66	892.1856	7.378844	743.488
0.17970351 6	0.154514321	0.08436482	0.15319447 5	82.8203134 5	80.9479784	44.5213912	80.256 53	7.38	679.3218182	7.00946159 1	747.254	7.5702185 18	896.7048	7.388856	747.254
0.17949423 2	0.155660707	0.08499074 6	0.15298288 9	82.7238604 3	81.5485602	44.8517081	80.145 69	7.38	682.7454545	7.01087925	751.02	7.5717495 9	901.224	7.388856	751.02
0.18023423 2	0.156780354	0.08560207 3	0.15373102 9	83.0649056 9	82.1351279	45.1743204	80.537 63	7.38	686.1690909	7.01226951 6	754.786	7.5732510 78	905.7432	7.388856	754.786
0.18154600 4	0.157876364	0.08620049 5	0.15505723	83.6694643 2	82.7093133	45.4901223	81.232 41	7.38	689.5927273	7.01363359 5	758.552	7.5747242 82	910.2624	7.388856	758.552
0.17044296 1	0.158947489	0.08678532 9	0.15727835 4	83.6817367 6	83.2704613	45.7987537	82.396 02	8.49	693.0163636	7.60734105 3	762.318	8.2159283 37	914.7816	8.500188	762.318
0.18101816 9	0.159995639	0.08735761 9	0.15671890 3	84.2695278 8	83.8195731	46.1007652	82.102 93	8.42	696.44	7.61207764 6	738.2264	8.2210438 57	885.8716 8	8.430104	738.2264
0.18025754 5	0.161025 7	0.08792003 2	0.15594991 3	83.9154341 6	84.3592081	46.3975645	81.700 07	8.42	642.3	7.61277178 9	680.838	8.2217935 32	885.0894	8.430104	680.838
0.18062280 4	0.162032386	0.08846968 3	0.15631918 9	84.0854732 2	84.8865973	46.6876285	81.893 53	8.42	590.1	7.61557312	625.506	8.2248189 7	813.1578	8.430104	625.506

0.18177380 4	0.16 3017 346	0.08 900 747 1	0.15 748 285	84.6 212 991 3	85. 40 26 05	46. 97 14 32 7	82 .5 03 16	8.42	536. 6066 667	7.61 864 392 1	568. 803 066 7	8.2 281 354 34	739 .44 398 67	8.43 0104	568. 8030 667
0.180 24157 4	0.16 3980 914	0.08 953 357 9	0.15 593 376 5	83.9 079 989 4	85. 90 74 05 3	47. 24 90 72 9	81 .6 91 61	8.32	483. 4366 667	7.62 170 4	512. 442 866 7	8.2 314 403 21	666 .17 572 67	8.32 9984	512. 4428 667
0.180 16280 4	0.16 4922 429	0.09 004 764 6	0.15 585 412 9	83.8 713 290 6	86. 40 06 52	47. 52 03 58 6	81 .6 49 89	8.32	430. 2666 667	7.62 471 108 5	456. 082 666 7	8.2 346 879 72	592 .90 746 67	8.32 9984	456. 0826 667
0.180 84280 4	0.16 5827 811	0.09 054 198 5	0.15 654 160 9	84.1 878 899 9	86. 87 49 69 6	47. 78 12 33 3	82 .0 10 05	8.32	377. 0966 667	7.62 715 107 9	399. 722 466 7	8.2 373 231 65	519 .63 920 67	8.32 9984	399. 7224 667
0.180 28210 9	0.16 4204 393	0.08 965 559 9	0.15 597 474 6	83.9 268 691 6	86. 02 44 82 7	47. 31 34 65 5	81 .7 13 08	8.32	323. 9266 667	7.62 990 947	343. 362 266 7	8.2 403 022 27	446 .37 094 67	8.32 9984	343. 3622 667
0.160 15957 9	0.16 2486 45	0.08 871 760 2	0.15 610 217 5	82.3 188 626 4	85. 12 44 75 5	46. 81 84 61 5	81 .7 79 84	8.56	270. 7566 667	7.63 266 786	271. 298 18	8.2 432 812 89	352 .68 763 4	8.57 0272	271. 2981 8
0.160 32599 7	0.16 0789 114	0.08 779 085 6	0.15 627 042 3	82.4 043 981 7	84. 23 52 64	45. 99 24 54 1	81 .8 67 98	8.56	217. 5866 667	7.63 542 625 1	228. 466	8.2 462 603 51	297 .00 58	8.57 8832	228. 466
0.160 51423 2	0.15 9110 929	0.08 687 456 7	0.15 646 072 9	82.5 011 473 9	83. 35 60 85	45. 51 24 22 4	81 .9 67 68	8.56	359. 4	7.63 818 464 1	377. 37	8.2 492 394 13	490 .58 1	8.57 8832	377. 37
0.160 84023 2	0.15 7450 154	0.08 596 778 4	0.15 679 031 5	82.6 687 049 6	82. 48 60 27 2	45. 03 73 70 8	82 .1 40 35	8.56	389. 4	7.64 094 303 2	428. 34	8.2 522 184 75	556 .84 2	8.57 8832	428. 34
0.160 23423 2	0.15 5807 357	0.08 522 662 4	0.15 617 764 9	82.3 572 329 2	81. 62 53 88 1	44. 56 74 61 9	81 .8 19 38	8.56	400. 5	7.64 370 142 3	440. 55	8.2 551 975 37	572 .71 5	8.57 8832	440. 55
0.160 10599 7	0.15 4181 357	0.08 433 720 2	0.15 604 800 3	82.2 913 225 1	80. 77 35 48 5	44. 10 23 57 5	81 .7 51 46	8.56	424. 2	7.64 645 981 3	466. 62	8.2 581 765 99	606 .60 6	8.57 8832	466. 62

0.159752232	0.152570964	0.08345631 7	0.155690347	82.1094944 3	79.9298853	43.6417174	81.564 09	8.56	444.75	7.64921820 4	489.225	8.2611556 6	635.9925	8.578832	489.225
0.159432232	0.150978214	0.08258508 3	0.155366827	81.9450207 5	79.0954649	43.1861238	81.3946	8.56	465.3	7.65197659 5	511.83	8.2641347 22	665.379	8.578832	511.83
0.164571571	0.149662714	0.08186550 5	0.156221465	82.7600005 3	78.4062 92	42.8098354	81.842 33	8.12	485.85	7.29387671 5	534.435	7.8773868 52	694.7655	8.137864	534.435
0.164822642	0.150917214	0.08255171 6	0.156475297	82.8862594 4	79.0635078	43.1686752	81.975 31	8.12	506.4	7.30600549 9	557.04	7.8904859 39	724.152	8.137864	557.04
0.164028232	0.152143286	0.08322237 7	0.155672149	82.4867653 5	79.7058302	43.5193833	81.5 5455	8.12	526.95	7.31776090 6	579.645	7.9031817 79	753.5385	8.137864	579.645
0.164778232	0.153342286	0.08387823	0.156430399	82.8639264 8	80.3339702	43.8623477	81.951 779	8.12	463.2	7.32915983	490.992	7.9154926 16	638.2896	8.137864	490.992
0.161061 09	0.154514321	0.08451933 4	0.156080593	82.3914136 8	80.9479784	44.1975993	81.768 53	8.23	500.2	7.34021416 8	530.212	7.9274313 01	689.2756	8.248106	530.212
0.160285052	0.155660707	0.08514640 7	0.155296019	81.9944287 8	81.5485602	44.5255139	81.357 5	8.23	532.52	7.35093487 5	564.4712	7.9390096 65	733.81256	8.248106	564.4712
0.160207 09	0.156780354	0.08575885 3	0.155217199	81.9545467 3	82.1351279	44.8457799	81.316 21	8.23	545.5827273	7.36133437 1	578.3176909	7.9502411 2	751.8129982	8.248106	578.3176909
0.160088807	0.157876364	0.08635837 1	0.155096871	81.8936620 1	82.7093133	45.1592851	81.253 17	8.23	558.6454545	7.37141734 6	592.1641818	7.9611307 34	740.2052273	8.248106	592.1641818
0.157032 56	0.158947489	0.08694427 7	0.155415975	81.7402314 2	83.2704613	45.4656719	81.420 35	8.24	571.7081818	7.38119239 1	606.0106727	7.9716877 82	757.5133409	8.258128	606.0106727

0.157379414	0.159995639	0.087517615	0.155766644	81.92077937	83.819573 1	46.184584 8	81.604 06	8.24	584.7709091	7.390668034	619.8571636	7.9819214 77	774.82145 45	8.258128	619.8571636
0.156725947	0.161025 7	0.088081058	0.155105989	81.58062991	84.359 2081	46.481923 7	81.257 95	8.24	597.8336364	7.399847124	633.7036545	7.9918348 93	792.12 95682	8.258128	633.7036545
0.156575947	0.162032386	0.088631715	0.154954339	81.50255034	84.886 5973	46.772 5151	81.178 5	8.24	610.8963636	7.40873645	641.4411818	8.0014353 66	801.80 14773	8.258128	641.4411818
0.153229049	0.163017346	0.089659541	0.154978851	81.18500847	85.402 6605	47.056 8353	81.191 34	8.34	623.9590909	7.41734280 7	655.1570455	8.0107302 32	818.94 63068	8.358348	655.1570455
0.153669049	0.163980914	0.090189503	0.155423691	81.41813 27	85.907 4053	47.334 98033	81.424 39	8.34	637.0218182	7.42567 291	700.724	8.0197267 43	875.90 5	8.358348	700.724
0.152924804	0.164922429	0.090707336	0.154671259	81.02381096	86.400 6652	47.606 7593	81.030 2	8.34	650.0845455	7.43373 3569	715.093	8.0284322 55	893.86 625	8.358348	715.093
0.150458036	0.165827811	0.091205296	0.155585582	81.16658549	86.874 96966	47.868 10822	81.509 2	8.13	663.1472727	7.44153 3491	729.462	8.0368561 7	911.82 75	8.147886	729.462
0.150153661	0.164204393	0.090312416	0.155277859	81.00238647	86.024 4827	47.394 99	81.347 99	8.13	600.5418182	7.44908 3709	660.596	8.0450104 05	825.74 5	8.147886	660.596
0.149589863	0.162486 45	0.089367548	0.154707 86	80.69823844	85.124 4755	46.903 5386	81.049 38	8.13	602.1472727	7.46462 4704	662.362	8.0617946 81	827.95 25	8.147886	662.362
0.148049204	0.160789114	0.088434013	0.156558478	81.34648269	84.235 2364	46.413 63035	82.018 89	8.1	603.7527273	7.47429 8598	664.128	8.0722424 86	830.16	8.11782	664.128
0.148272518	0.159110929	0.087511011	0.156784249	81.46918 39	83.356 085	45.929 20228	82.137 17	8.1	588.8396364	7.48397 2492	647.7236	8.0826902 92	809.65 45	8.11782	647.7236

0.142 14361 1	0.15 7450 154	0.08 659 758 4	0.15 399 614 9	79.5 755 943 4	82. 48 60 27 2	45. 44 98 01	80 .6 76 52	7.94	578. 1892 727	7.73 910 913	636. 008 2	8.3 582 378 61	795 .01 025	7.95 7468	636. 0082
0.141 04137 5	0.15 5807 357	0.08 569 404 6	0.15 288 178 9	78.9 585 350 6	81. 62 53 88 1	44. 97 55 88 9	80 .0 92 72	7.94	567. 5389 091	7.73 810 639 5	601. 591 243 6	8.3 571 549 06	751 .98 905 45	7.95 7468	601. 5912 436
0.141 51137 5	0.15 4181 357	0.08 479 974 6	0.15 335 695 9	79.2 216 529 7	80. 77 35 48 5	44. 50 62 25 2	80 .3 41 66	7.94	556. 8885 455	7.73 719 063	590. 301 858 2	8.3 561 658 81	737 .87 732 27	7.95 7468	590. 3018 582
0.165 63423 2	0.15 2570 964	0.08 391 403	0.15 433 762 9	82.0 865 459 2	79. 92 98 85 3	44. 04 13 66 8	80 .8 55 42	7.87	546. 2381 818	7.73 629 658 5	579. 012 472 7	8.3 552 003 12	723 .76 559 09	7.88 7314	579. 0124 727
0.165 27423 2	0.15 0978 214	0.08 303 801 8	0.15 397 366 9	81.9 081 337 9	79. 09 54 64 9	43. 58 16 01 1	80 .6 64 74	7.87	535. 5878 182	7.73 541 160 1	567. 723 087 3	8.3 542 445 29	709 .65 385 91	7.88 7314	567. 7230 873
0.154 20852 7	0.14 9402 464	0.08 217 135 5	0.15 155 761 9	79.8 577 353 5	78. 26 99 50 5	43. 12 67 42 7	79 .3 99 01	7.71	524. 9374 545	7.73 453 283 1	556. 433 701 8	8.3 532 954 57	695 .54 212 73	7.72 6962	556. 4337 018
0.154 58829	0.14 7842 321	0.08 131 327 7	0.15 194 155 9	80.0 543 975 1	77. 45 26 12 6	42. 67 63 89 5	79 .6 00 15	7.71	514. 2870 909	7.73 366 224 5	545. 144 316 4	8.3 523 552 24	681 .43 039 55	7.72 6962	545. 1443 164
0.154 26829	0.15 0917 214	0.08 300 446 8	0.15 161 803 9	79.8 886 837 4	79. 06 35 07 8	43. 16 86 75 2	79 .4 30 66	7.71	503. 6367 273	7.73 279 781	533. 854 930 9	8.3 514 216 35	667 .31 866 36	7.72 6962	533. 8549 309
0.155 99194 7	0.15 2143 286	0.08 367 880 7	0.15 140 572 9	79.9 804 013 4	79. 70 58 30 2	43. 51 93 83 3	79 .3 19 43	7.91	492. 9863 636	7.73 193 928 2	517. 635 681 8	8.3 504 944 24	647 .04 460 23	7.92 7402	517. 6356 818
0.155 89013 1	0.15 3342 286	0.08 433 825 7	0.15 130 279 3	79.9 281 982	80. 33 39 70 2	43. 86 23 47 7	79 .2 65 51	7.91	482. 336	7.73 108 868 4	506. 452 8	8.3 495 757 78	633 .06 6	7.92 7402	506. 4528
0.155 70194 7	0.15 4514 321	0.08 498 287 7	0.15 111 253 9	79.8 317 121 5	80. 94 79 84	44. 19 75 99 3	79 .1 65 84	7.91	471. 6856 364	7.73 024 402 6	518. 854 2	8.3 486 635 48	648 .56 775	7.92 7402	518. 8542

0.1577488	0.155660707	0.085613389	0.151226981	80.08717166	81.5485602	44.5255139	79.22579	7.84	461.0352727	7.72940487	507.1388	8.347757259	608.56656	7.857248	507.1388
0.158641794	0.156846225	0.085794885	0.152129797	80.54053395	82.1696371	44.8646219	79.69876	7.84	450.3849091	7.728573777	495.4234	8.346859679	594.50808	7.857248	495.4234
0.158451794	0.158018655	0.086436204	0.151937707	80.44407323	82.7838575	45.1999862	79.59813	7.84	439.7345455	7.727749256	483.708	8.345969197	580.4496	7.857248	483.708
0.158445604	0.155807357	0.085226624	0.151931449	80.4409304	81.6253881	44.5674619	79.59485	7.84	429.0841818	7.726929208	471.9926	8.345083545	566.39112	7.857248	471.9926
0.158365604	0.154181357	0.084337202	0.151850569	80.40031536	80.7735485	44.1023575	79.55248	7.84	418.4338182	7.726116728	460.2772	8.344206066	552.33264	7.857248	460.2772
0.161729227	0.152570964	0.083456317	0.153296265	81.30977288	79.9298853	43.6417174	80.30986	7.94	407.7834545	7.725311726	448.5618	8.343336664	538.27416	7.957468	448.5618
0.161509261	0.150978214	0.082585083	0.153073879	81.1991844	79.0954649	43.1861238	80.19336	7.94	397.1330909	7.72451101	436.8464	8.342471891	524.21568	7.957468	436.8464
0.162262261	0.149360018	0.08169993	0.153835162	81.57775703	78.2477134	42.7232515	80.59218	7.94	386.4827273	7.723717042	409.6716909	8.341614406	491.6060291	7.957468	409.6716909
0.162809261	0.150917214	0.082551716	0.154388179	81.85276265	79.0635078	43.1686752	80.8819	7.94	375.8323636	7.722929211	398.3823055	8.340763548	478.0587665	7.957468	398.3823055
0.162049261	0.152143286	0.083222377	0.153619819	81.47067075	79.7058302	43.5193833	80.47937	7.94	582.2	7.722149166	617.132	8.3399211	740.5584	7.957468	617.132
0.161662261	0.153342286	0.08387823	0.153228562	81.27610554	80.3339702	43.8623477	80.27439	7.94	526.8	7.721372159	558.408	8.339081932	670.0896	7.957468	558.408

0.16372631 5	0.154514321	0.08451933 4	0.15336039 3	81.5213035 5	80.947984	44.19759 93	80.343 46	7.89	624.6586364	7.72060425 2	662.1381545	8.3382525 93	794.56578 55	7.907358